Multi-enzymatic routes for the targeted synthesis of enantiopure vicinal amino alcohols

Corrado, M.L.

Publication date
2020

Document Version
Final published version

License
Other

MULTI-ENZYMATIC ROUTES FOR THE TARGETED SYNTHESIS OF ENANTIOPURE VICINAL AMINO ALCOHOLS

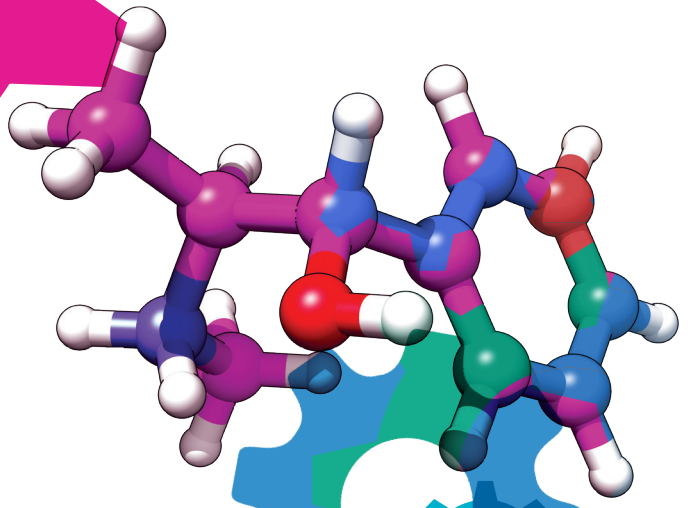

Maria Luisa Corrado

Multi-enzymatic routes for the targeted synthesis of enantiopure vicinal amino alcohols

Multi-enzymatic routes for the targeted synthesis of enantiopure vicinal amino alcohols

ACADEMISCH PROEFSCHRIFT

ter verkrijging van de graad van doctor aan de Universiteit van Amsterdam

op gezag van de Rector Magnificus

prof. dr. ir. K.I.J. Maex

ten overstaan van een door het College voor Promoties ingestelde

commissie, in het openbaar te verdedigen

op woensdag 24 Juni 2020, te 10:00 uur

door

Maria Luisa Corrado

geboren te Soriano Calabro

Promotiecommissie:

Promotores:	Dr. F. Mutti	Universiteit van Amsterdam
	Prof. Dr. J. H. van Maarseveen	Universiteit van Amsterdam
Overige leden:	Prof. Dr. H. J. Bouwmeester	Universiteit van Amsterdam
	Prof. Dr. P. Timmerman	Universiteit van Amsterdam
	Prof. Dr. W.J.H. van Berkel	Wageningen University&Research
	Prof. Dr. F. Hollmann	Technische Universiteit Delft
	Dr. M. A. Fernández Ibáñez	Universiteit van Amsterdam
	Dr. J. C. Slootweg	Universiteit van Amsterdam

Faculteit der Natuurwetenschappen, Wiskunde en Informatica

This project was financed by the Nederlandse Organisatie voor Wetenschappelijk Onderzoek (NWO), grant ECHO Chemistry in Relation to Technology and Sustainability 2013 CW, project number 717.014.007.

Netherlands Organisation for Scientific Research

Cover design: Marcelo F. Masman & Maria L. Corrado

To my beloved parents

"Above all, don't fear difficult moments. The best comes from them."

Rita Levi-Montalcini (1909-2012)
Italian Nobel Laureate (1986)

"Soprattutto, non temete i momenti difficili. Il meglio viene da lì."

Rita Levi-Montalcini (1909-2012)
Premio Nobel per la medicina (1986)

Table of content

List of Abbreviations

ADH	Alcohol dehydrogenase
AlaDH	Alanine dehydrogenase
AmDH	Amine dehydrogenase
BDHA	2,3-butanediol dehydrogenase
CH_2Cl_2	Dichloromethane
CIP	Cahn-Ingold-Prelog
DABCO	1,4-Diazabicyclo[2.2.2]octane
DBU	1,8-Diazabicyclo[5.4.0]undec-7-ene
DCPK	Dicyclopropyl ketone
de	Diastereomeric excess
DMF	Dimethylformamide
dr	Diasteromeric ratio
ee	Enantiomeric excess
EH	Epoxide hydrolase
er	Enantiomeric ratio
EtOAc	Ethyl acetate
FAD	Flavin adenine dinucleotide
FDH	Formate dehydrogenase
Fus-SMO	N-His_6-StyA-linker-StyB
GDH	Glucose dehydrogenase
GITC	2,3,4,6-Tetra-O-acetyl-β-D-glucopyranosyl isothiocyanate
HCOONa	Sodium formate
$HCOONH_4$	Ammonium formate
K_2CO_3	Potassium carbonate
K_2HPO_4	Dipotassium phosphate
KF	Potassium fluoride
KH_2PO_4	Monopotassium phosphate
KPi	Potassium phosphate buffer
LB	Luria-Bertani broth
LDH	Lactate dehydrogenase

mCPBA	meta-Chloroperoxybenzoic acid
MTBE	Tert-butyl methyl ether
n.a.	Not applicable
n.c.	No conversion
n.d.	Not detected
n.m.	Not measured
$NAD(P)^+$	Nicotinamide adenine dinucleotide (phosphate)
NE	Norephedrine
NOx	NADH-dependent oxidase
NPE	Nor(pseudo)ephedrine
NP-HPLC	Normal-phase HPLC
o.n.	Overnight
PE	Petroleum ether
PEG-PLL	Poly(ethylene glycol)- Poly-L-Lysine
PLL	Poly-L-Lysine
PLP	Pyridoxal 5'-phosphate
PPA	Phenylpropanolamine
rr	Regioisomeric ratio
RP-HPLC	Reverse-phase HPLC
SDS-PAGE	Polyacrylamide gel electrophoresis
SMO	Styrene monooxygenase bi-enzymatic system (StyA and StyB)
StyA	Epoxidase enzymatic unit of SMO
StyB	Reductase enzymatic unit of SMO
TA	Transaminase
TB	Terrific-Broth
THF	Tetrahydrofuran
TMSCN	Trimethylsilyl cyanide
Tris-HCl	Tris(hydroxymethyl)aminomethane buffer
UHP	Urea hydrogen peroxide
YcnD	NADPH-dependent oxidase

Chapter 1

Biocatalysis for a green and sustainable economy: general introduction

This chapter is based on a literature review.

1.1 The concept of green and sustainable development: towards a circular economy

The need to overcome the dependency on fossil fuels causes a change in the way of thinking about the production of platform, commodity and fine chemicals, active pharmaceutical ingredients (APIs), and materials such as plastics and fibers. Chemical industries and processes have had a strong impact on society during the last two centuries, thus leading to a considerable increase in human lifestyle and comfort. Nevertheless, many chemical processes require the use of hazardous chemicals which have considerable consequences on our health and our planet, considering that the produced waste needs to be disposed of properly. The production of large amount of hazardous waste is common in the chemical industry. A model example reported by Sheldon *et al*. is the manufacturing of phloroglucinol, a highly demanded pharmaceutical intermediate, of which the synthesis started from 2,4,6-trinitrotoluene.[1] In this case study, the process leads to forty kg of waste for each kg of product, although the overall yield was 90% over three steps. Based on the sole yield, this process was considered a selective and efficient route. In contrast, the large production of chromium containing waste as well as the formation of other by-products make this process completely unsustainable if one considers the E-factor and atom efficiency (see below for definitions). Indeed, the manufacturing process was abandoned in the 1980s due to the high costs for disposing the toxic waste products. In general, the primary cause of waste in the chemicals manufacture originates from obsolete methodologies which require (supra)-stoichiometric quantities of reagents such oxidants, reductants, acids and bases as well organic solvents such as chlorinated hydrocarbons.[2,3] The obvious solution is the application of greener catalytic options[4, 5] in combination with the use of more environmentally friendly solvents (e.g., aqueous system).[6-14] Ideally, a catalytic process should not generate any waste. Therefore, the establishment of new catalytic routes for the manufacture of pharmaceutical active compounds (APIs) and other chemicals is one of the fundamental solutions for minimizing waste generation.

The following parameters are used in green chemistry:[15] process mass intensity,[16,17] reaction mass efficiency,[18,19] effective mass yield,[20] and C(arbon) factor.[21] Nevertheless, Sheldon and Trost reported the most popular and accepted metrics for environmental assessment of a process: the Environmental factor (E-factor)[15, 22] and atom economy (AE).[23,24] The former is the ratio between produced waste and formed product, which also entails solvents, auxiliary materials and the waste

derived from work-up procedures. Conversely, the simplified E-factor (sEF) does not consider solvents and water. **Equation 1.1** shows the most accepted formulas for calculating the E-factor.[14]

$$\text{A)} \quad sEF = \frac{\Sigma m(raw\ materials) + \Sigma m(reagents) - m(product)}{m\ (product)}$$

$$\text{B)} \quad cEF = \frac{\Sigma m(raw\ materials) + \Sigma m(reagents) + \Sigma m(solvents) + m(water) - m(product)}{m\ (product)}$$

$$\text{C)} \quad atom\ economy = \frac{MW\ product\ x\ 100}{\Sigma\ MW(raw\ materials) + \Sigma MW(reagents)}$$

Equation 1.1. Formula for the calculations of: **(A)** simplified E-factor (sEF); **(B)** complete E-factor (cEF) and **(C)** Atom economy.

In 1992, Sheldon and co-workers illustrated the relevance of the waste production in chemical manufacturing (**Table 1.1**), thereby demonstrating the need for "greener" synthetic methodologies.[25] They showed that industries with a relatively small plant capacity, such as the pharmaceutical sector, produce even greater amount of waste. The main concern stands in the application of traditional technologies and the major challenge remains the development of green, catalytic alternatives.[4,5]

Table 1.1. Waste contributions in different sectors of the chemical industry (adapted from ref.[14]).

Industry section	E-factor	Plant capacity [tons]
Oil refinery	<0.1	10^6-10^8
Bulky chemicals	<1-5	10^4-10^6
Fine chemicals	5-50	10^2-10^4
Pharmaceutical	25->100	10-10^3

The atom economy is calculated as the ratio of the product molecular mass over the total molecular masses of reagents contributing to the stoichiometry of the reaction.[23,24] Indeed, the latter allows the prediction *a priori* of the minimum amount of waste expected from a certain reaction. Nevertheless, the AE assumes the stoichiometric use of reagents as well as theoretical yields while excluding solvents and other auxiliaries that do not show up in the stoichiometric equation.[15] In a real process, the actual yield is usually not quantitative. Moreover, reagents

and auxiliaries—applied in large excess—contribute tremendously to the E-factor. Nevertheless, the use of both metrics is pivotal for the design of greener processes.[15] A typical example of high atom economical process is the catalytic aerobic (ideally by using air) oxidation of secondary alcohols (in this case α-methylbenzyl alcohol as a model substrate).[26] Traditionally, for this transformation stoichiometric oxidants such as the Dess-Martin periodinane are used (**Scheme 1.1**).[14]

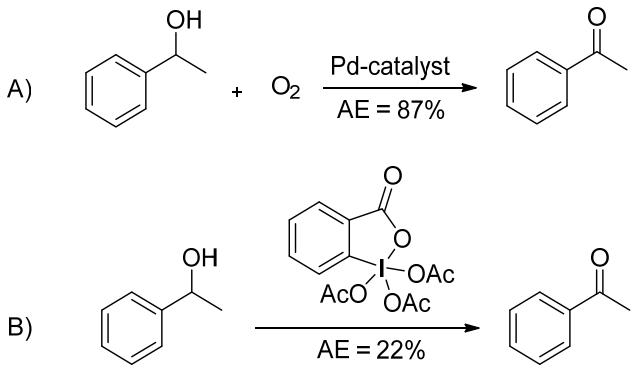

Scheme 1.1. Comparison of the atom economy of **A)** catalytic aerobic oxidation[27] and **B)** stoichiometric oxidation using Dess-Martin periodinane.[28]

Nowadays, the main focus is on the establishment of more sustainable chemical productions that start from renewable feedstocks rather than fossil resources, and eliminate and/or reduce waste production by circumventing the need for stoichiometric amounts of unsafe materials. Hence, a general solution relies on the application of the green chemistry parameters.[29] Although greener catalytic approaches have been embraced already by the bulk chemical industries, the transition process in the pharmaceutical sector proceeds at slower pace.[29]

Anastas and colleagues defined the concept of Green Chemistry in the 1990s, setting the ground for a new era in chemical manufacture.[30,31] In general, the 12 principles of green chemistry deal with the environmental footprint of chemical processes, and an overview is given in **Table 1.2**.[32, 33]

Table 1.2. The 12 principles of green chemistry

Entry	Principle	Description
1	Waste prevention	Waste prevention rather the disposal or treatment after the process occurred
2	Atom economy	Chemical routes that boost atom efficiency
3	Avoid unsafe chemical synthesis	Use of substances which have no critical consequences on society
4	Safer chemicals	Products design retaining high efficacy but less harmful
5	Safer reagents	Eliminate solvents and auxiliaries whenever possible and/or use innocuous substances
6	Power-efficient processes	Decrease energy demand in regard of economic and ecological impact
7	Application of renewable feedstock	Renewable feedstocks in alternative to limited resources
8	Avoid derivatization	Minimize protection/deprotection methods
9	Catalysis	Catalytic reagents in alternative to stoichiometric ones
10	Materials degradation	Design materials that decompose
11	Pollution prevention	Real-time analytics for preventing evolution of dangerous chemicals
12	Preventing accidents	Choose safer chemical processes

Ten out of the twelve principles relate directly to the manufacturing process itself, while two principles (*i.e.* 4 and 10) refer to the properties of the target product. Hence, the green chemistry parameters integrate well with the idea of sustainability and bio-based circular economy.

Brundtland proposed that the sustainable development model must take into equal consideration the necessities of current and future communities on our planet.[34] People, planet and profit are the three main segments that build up the general idea of sustainability which can be illustrated by a Venn diagram (**Figure 1.1**).[35-37]

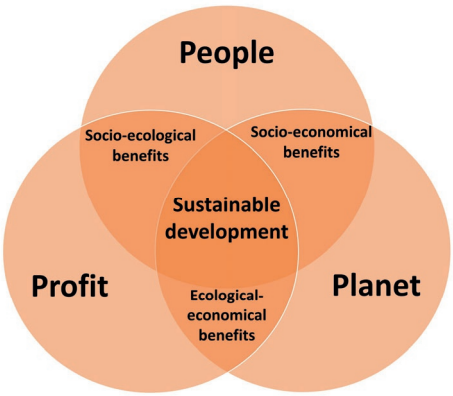

Figure 1.1. Venn diagram to visually illustrate the concept of sustainable development (adapted from ref.[15,37]).

Two main requirements must be fulfilled for a process or technology to be considered sustainable:[38] *i*) the utilization of natural resources should not lead to diminish stocks; *ii*) the produced residues should be promptly incorporated back into natural environmental processes.[15,39] Last but not least, sustainable technologies must be cost effective over the long term, which may vary depending on the geographical location. Both chemo- and bio-catalysts have a central function in designing greener processes; in particular, the contribution of biocatalysis will be discussed in more details for the scope of this thesis.

Next, the focus will be redirected to the valorization of renewable feedstock as substitute of fossil supplies.[40] The use of biomass would reduce our society's carbon footprint. Furthermore, the substitution of current products with environmentally benign alternatives such as biocompatible and biodegradable plastics is another advantage.[41]

The need for a waste-free circular economy emerged in the last decade and it is at the core of green manufacturing towards prevention of waste generation. For example, the valorization of lignocellulose waste is particularly appealing and adapts with the current tendency towards a circular economy business model. The concept of circular economy is based on the incorporation of recycling idea already during process design, such that humankind could potentially harness the highest value from any raw material.[42,43] This results in the elimination and/or valorization of waste by-products, and considers resources efficiency and recyclability during processes design as mentioned above.[15] It is undeniable that the linear route of production has largely contributed to several global crises—for instance climate change and reduced biodiversity—through the consumption of limited resources and the discard of potentially valuable material as waste. In general, a circular economy targets the replacement of this linear "take–make–use–dispose" approach with circular manufacturing processes,[43,44] by turning discarded goods into renewable resources for other applications.[42] Research on waste as raw material, comprising municipal waste, industrial by-products and waste biomass, has led to an important progress in the valorization of renewable resources.[45] In this context, green chemistry principles provide a skeleton for performing sustainable chemistry and developing cleaner products and processes.[30,45,46]

1.1.1 The potential of lignocellulose biomass as renewable feedstock for a bio-based economy

The seventh principle of green chemistry implicitly asserts that humankind must make use of renewable feedstock at any time that is practically and financially viable.[29] However, the modern chemical industry is still largely based on processes that rely on finite carbon fossil resources.[47] During the past decade, the progressive depletion of petroleum supplies have spurred both industry and academy to undertake research projects aimed at finding alternative routes from renewable resources. In particular, the valorization of waste biomass has received much attention. Nevertheless, as Sheldon has pointed out, the move towards a bio-based economy, in which biomass is also used as feedstock, represents one of the biggest challenges.[40,48] This transition is hampered mostly because of economic reasons not only related to the production itself but also on the availability and development of suitable technologies and infrastructures. Regarding the economical part, the well-established fossil-based "take-make-use-dispose" chain should also take into account the costs for waste disposal, resource depletion and environmental pollution, which are at the moment always considered aside of the process itself. This misleads to the wrong concept that fossil-based feedstocks are more economically viable than bio-based ones. Furthermore, the transition will require the development of efficient technologies that are able to convert lignocellulose biomass to its main sugar constituents and further to liquid fuels and chemicals.[49] This requires hybrid research between biotechnology and chemical engineering.[50,51]

First generation biomass (e.g. corn) is not considered a sustainable resource due to the competition with food supplies. The ideal scenario of using second generation feedstock implies the valorization of lignocellulose coming from agricultural (e.g., rice and wheat straw, corn stover, etc.) and forestry residues.[52,53] Lignocellulose biomass residues comprise the largest source of carbohydrates and lignin whose global annual production is estimated to exceed 2×10^{11} tons (**Table 1.3**). This puts the basis for the second-generation bio-based economy, which would lead eventually from feeding bio-refineries with agriculture biomass to the production of bio-fuels, bio-materials as well as commodity chemicals by applying resource-efficient catalytic processes (Table 1.3).[14,54-56]

Table 1.3. Examples of ideal scenario of using second generation biomass feedstocks derived from agriculture waste (adapted from ref.[14,29]).

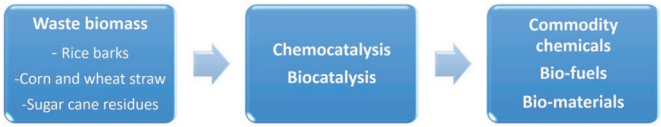

Agricultural residues from	Global manufacturing Tons/annum[14,29]
Rice	730 x 10^6
Wheat	354 x 10^6
Sugar cane	180 x 10^6
Corn	128 x 10^6

The food supply chain waste (FSCW), for instance cooking oil, fruits, vegetables peels and other food residues that are rich in fats, carbohydrates and proteins, as bio-refineries feedstock received very recently great attention.[57,58] In fact, the processing and consumption of agricultural products, for instance in the manufacture of food and beverages, result in large volumes of organic waste which is usually discarded in landfills.[59, 60] Although the main focus of green chemistry is indeed based on preventing waste generation, there is a great demand for novel technologies enabling the valorization of unavoidable waste, such as agriculture residues. This is relevant in the current trend of a circular economy model.

Lignocellulose is the primary constituent of second-generation feedstock. Cellulose (ca. 40%), hemicellulose (ca. 25%) and lignin (ca. 20%) are the largest portions.[45,61] The remaining 15% is made up of triglycerides, proteins and other vegetable extracts such as waxes and terpenes. Compared with sucrose or starch, lignocellulose biomass requires more processing. First of all, it needs to be depolymerized and partially deoxygenated. This can be accomplished via either thermochemical processing (e.g., pyrolysis and gasification) or hydrolytic pre-treatments.[61, 62] In the thermochemical processing, pyrolysis of lignocellulose waste biomass would lead to pyrolysis oils and charcoal, which can be further hydrogenated to yield lower olefins and/or benzene, toluene and xylenes (BTX). Furthermore, gasification of the lignocellulose affords synthesis gas (syngas), a blend of CO and H_2. This is further transformed either to methanol and subsequently to lower olefins, via methanol synthesis, or to liquid fuels via the well-established Fischer-Tropsch process.[63,64] More recently, for instance microbial

fermentation technologies (e.g., acetogenic bacteria)[65] have been commercialized for bio-fuels and platform compounds from syngas waste derived from steel mills.[65-67] An overview for the thermochemical processing of lignocellulose is depicted in **Figure 1.2**.

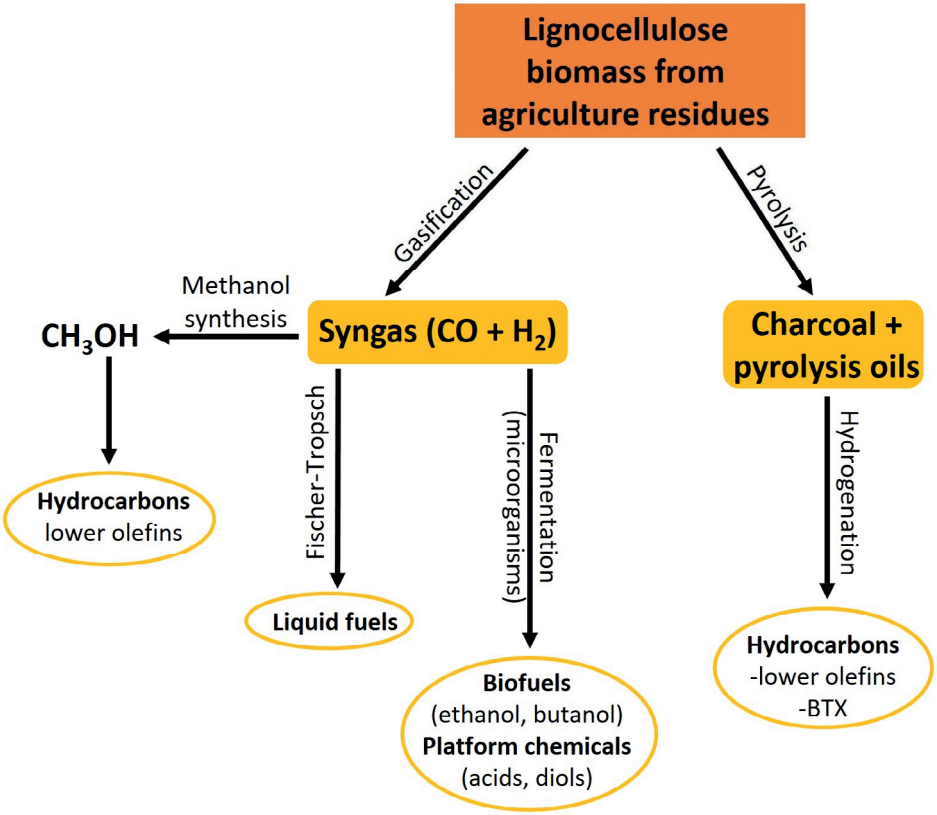

Figure 1.2. Overview of the two pathways for the thermochemical processing of lignocellulose biomass from agriculture waste to high valuable chemicals. (Scheme is based on ref.[45,68]).

The alternative hydrolytic methodologies to break down the complex lignocellulose structure, thus leading to a mixture of cellulose, hemicellulose, lignin and other residues, require some form of biomass pre-treatment that is usually catalyzed by diluted mineral acids (or solid acids catalysts as greener solution)[69, 70] at elevated temperatures. A well-known process is for example the Organosolv technology in which the lignocellulose biomass is heated up in a mixture of H_2O:EtOH, usually under acidic conditions. Cellulose is then removed by filtration while distillation of the EtOH leads to lignin precipitation allowing removal by filtration. The remaining filtrate contains hemicellulose and other residues.[71-73] After these hydrolytic pre-

treatments, the further hydrolysis of cellulose and hemicellulose affords the monosaccharide building blocks pentose and hexose (C5 and C6 sugars).[74] Another strategy for the hydrolytic conversion of lignocellulose biomass entails still some types of pre-treatment methods,[75] ammonia fiber expansion or steam explosion, in order to loosen the material's complex structure and provide more accessibility to ether and ester bonds.[76] In the next step, cellulose and hemicellulose are hydrolyzed by a mixture of enzymes[77] to a blend of C6 and C5 monomers (process known as saccharification).[78,79] These biomass-derived monosaccharide building blocks (C5 and C6) can be converted further to biofuels as well as to commodity/platform chemicals via fermentation processes, chemo-and bio-catalytic methods or a combination thereof.[41, 51, 80-87] For example, hexose and pentose can be converted to ethanol (biofuel), propanol and butanol by fermentation and further dehydrated to the reciprocal hydrocarbons (ethylene, propylene, butenes etc.). Bio-ethanol can also be transformed in other commodity chemicals such as acetone, acetaldehyde, ethylacetate etc.[88-90] Furthermore, biomass-derived C5 and C6 monomers can be converted directly to hydrocarbons.[91] For instance, isobutene[92] or isoprene[93] can be accessed through fermentation using metabolic engineering (e.g., genetically modified yeast).[94-96] Alternatively, the application of a chemocatalytic process (e.g., aqueous phase reforming)[97] would yield a mixture of gasoline, kerosene and aromatic hydrocarbons (BTX) over several steps. Other relevant chemicals can be accessed by fermentation of biomass-derived sugars such as adipic acid,[87, 98] lactic acid,[99] succinic acid,[100] citric acid,[101] 3-hydroxypropionic acid (3-HPA),[102] 1,3-propanediol (1,3-PDO),[103,104] 2,3-butanediol (2,3-BDO) and 1,4-butanediol (1,4-BDO),[105] which can undergo further conversion to higher valued chemicals.[106,107] Moreover, the acid-catalyzed hydrolysis of the C5 and C6 fractions leads to the formation of furfural[108] and hydroxymethylfurfural (HMF).[54,109-111] The latter can undergo either oxidation to furan-2,5-dicarboxylic acid (FDCA), by chemo-and bio-catalysis methods,[112-116] or acidic conversion to levulinic acid (LA).[117] Both FDCA and LA are highly promising building blocks for various biopolymers and bioplastics, with Avantium PEF pioneering the field.[49,84,118-120] An overview of the hydrolytic processing of lignocellulose is given in **Figure 1.3**.

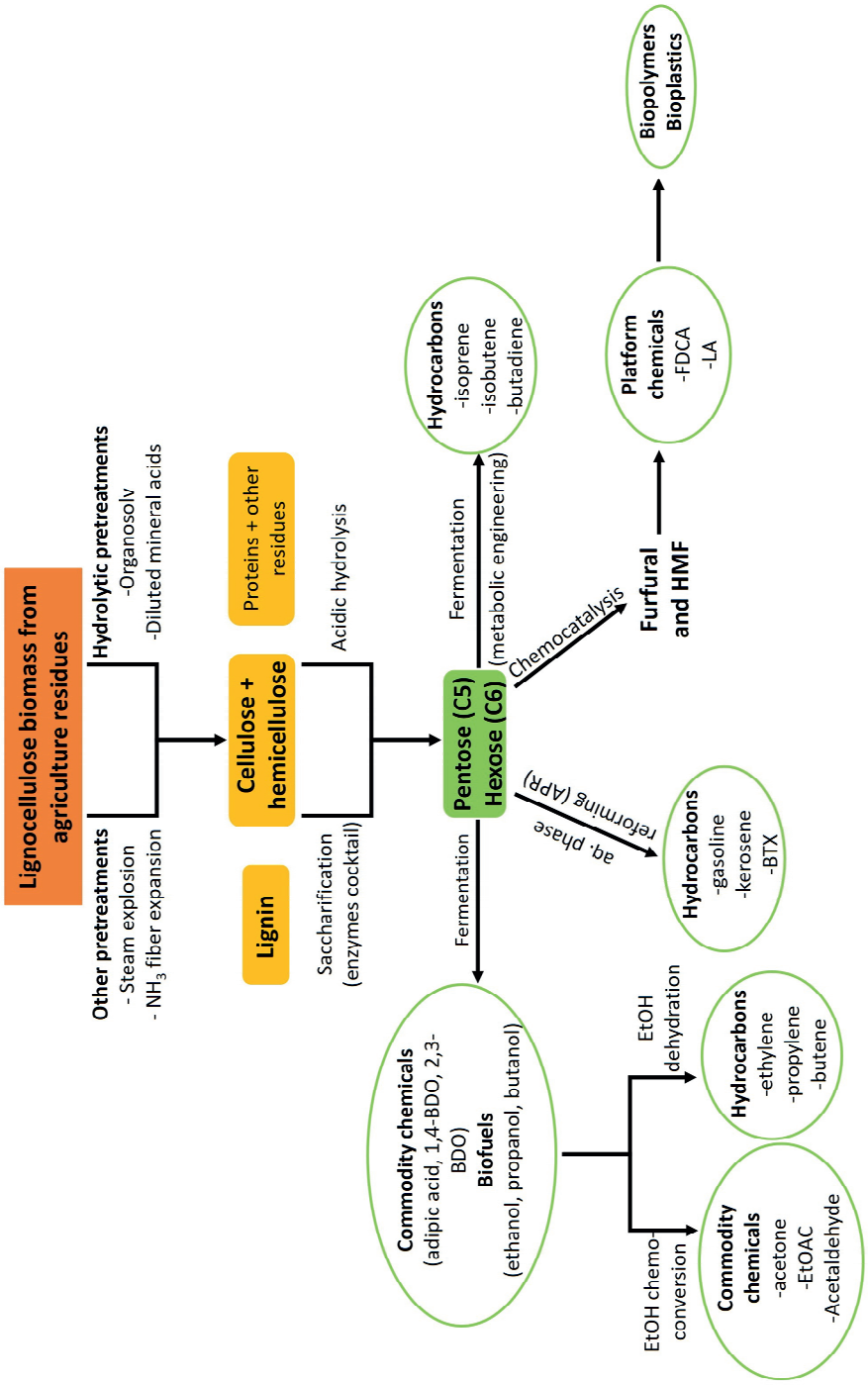

Figure 1.3. Overview of hydrolytic chemo-enzymatic processing for the deconstruction of lignocellulose biomass into the two main components (lignin and cellulose/hemicellulose) and subsequent treatments of cellulose to high value added chemicals. (Scheme is based on ref.[45,68]).

Hence, the sugar monomers (C5 and C6), coming from the conversion of lignocellulose biomass, are the major source for replacing fossil-based hydrocarbons. Apart from the BTX aromatic fractions—that can also be obtained from such sugars—there is still a pressing need for chemo- and biocatalytic methods affording aromatic platform chemicals from waste lignocellulose biomass. In this regard, lignin is the most prominent aromatic polymer in nature.[54,121] The paper manufacturing process produces tons of lignin as waste.[122,123] Moreover, in the processing of lignocellulose biomass, lignin is obtained in large portions as co-product. Nevertheless, this remaining lignin is usually burnt for energy recovery. It is estimated that the bio-refineries could produce 60 times more lignin than the amount required to supply energy to the infrastructure itself. Only a single bio-ethanol production plant could generate ca. 60 x 10^6 tons per year in the USA by 2022.[121]

Lignin is an amorphous polymer, providing structural integrity to the plants. Coniferyl alcohol*, p*-coumaryl alcohol and sinapyl alcohol are the three principal monolignol units followed by the correspondent subunits *p*-guaiacyl, hydroxyphenyl and syringyl. These lignin monomers arrange in a random polymeric network with no repetitive units and different bonding pattern depending on the plant species (**Figure 1.4**).[68]

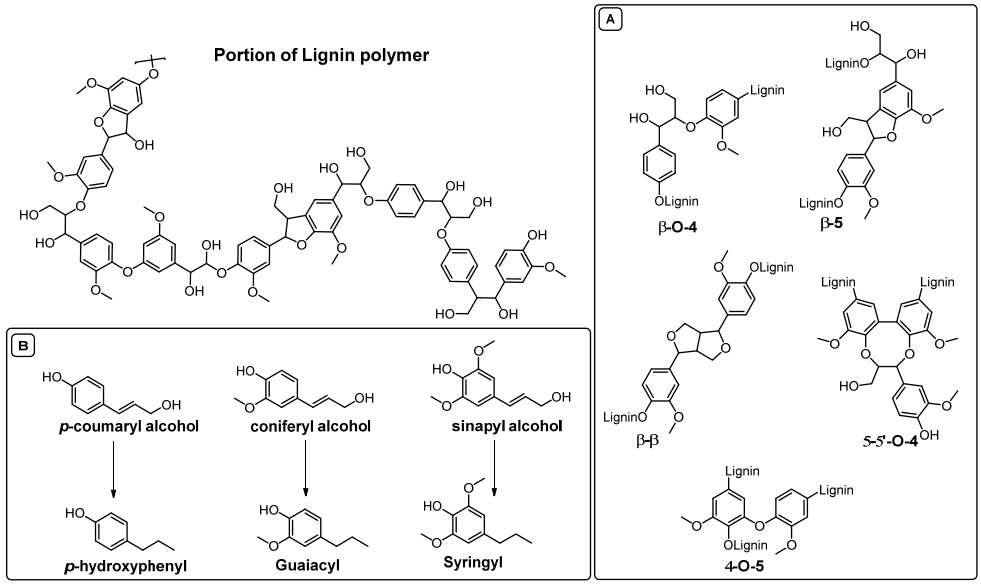

Figure 1.4. Portion of lignin polymer (top); **(A)** main bonding pattern present in lignin; **(B)** primary monolignol units that compose the polymeric structure of lignin and the correspondent subunits (adapted from ref.[68]).

The different distribution of these units that build up the complex lignin structure in the various species of plants, either naturally occurring or from genetic modifications of biosynthetic pathways in plants, gives rise to distinct polymeric structures of lignin, as shown in **Figure 1.5**.[121, 124-132] The greatest challenge in the valorization of lignin relates to the establishment of new methodologies for the degradation of these polymeric structures (not discussed in this thesis). Three important developments occurred in the last decades, which can significantly contribute in finding (bio)catalytic strategies for the controlled degradation of this high valuable natural polymer: *i*) engineering plants feedstock for production of more homogeneous lignin structures[133] (interruption of monolignol biosynthesis in order to modify the subunits ratio),[128, 134-138] *ii*) advances in computational modelling and analytical techniques to elucidate lignin structure for improvements in genetic engineering,[139-147] *iii*) upgraded biomass pre-treatments for easier recovery and follow-up conversion of lignin.[121]

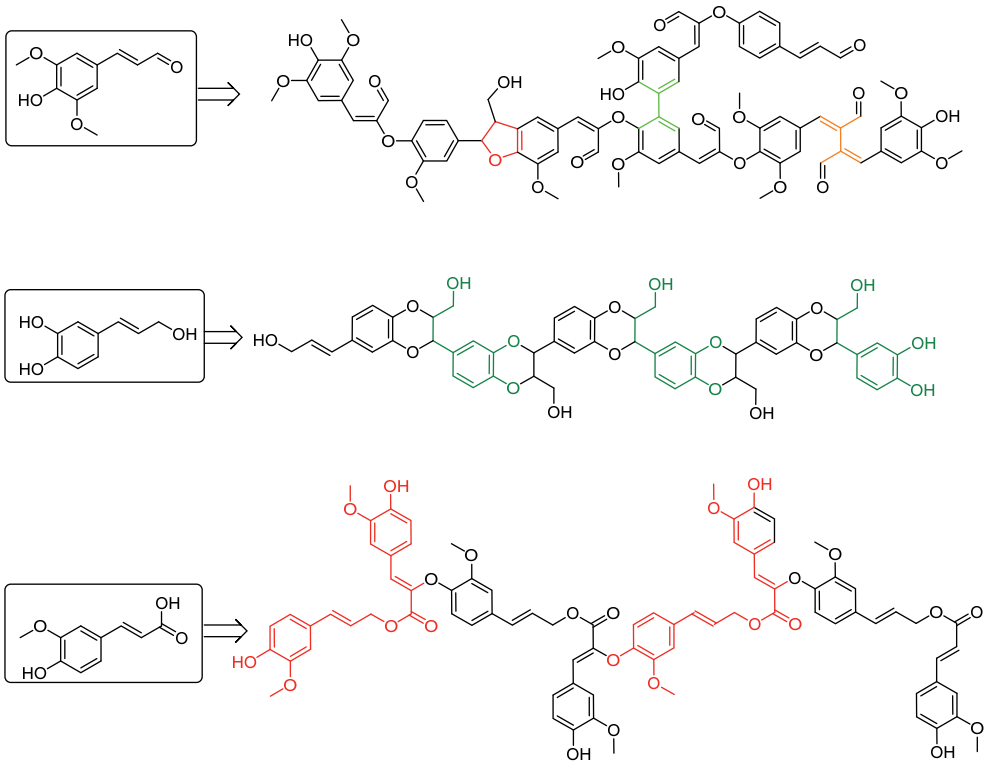

Figure 1.5. Portions of distinct polymeric structures of lignin depending on the distribution of the primary monolignol units in the various plant species (adapted from ref.[121]).

Nevertheless, the main challenge remains the controlled deconstruction of this complex polymer.[148,149] For example, oxidative depolymerization of lignin can be accomplished by homogeneous or heterogeneous catalysis.[150-152] Moreover, thermal treatment such as catalytic pyrolysis can also be a viable methodology for disruption of the complex lignin structure. First, a bio-oil consisting of a blend of oxygenated monomers and oligomers is obtained followed by further processing to yield the targeted aromatic products.[153-155] Gasification of lignin to syngas is also a viable route for the valorization of this high-value bio-refineries co-product.[148] In nature, lignin depolymerization occurs via the concerted action of several oxidative enzymes, such as laccases, lignin peroxidase and other promiscuous peroxidases. These enzymes are predominantly produced by white-rot fungi, but they are also found in brown-rot fungi and some bacteria (e.g., glyoxal oxidase and aryl alcohol oxidases). Recombinant enzymatic processes for unlocking lignin value have also been reported.[156-166]

The ability to modulate the composition of the lignin monomers is advantageous as it facilitates lignin extraction during pre-treatment of lignocellulose biomass, and enables the development of efficient biotechnological, chemical and thermal methods to accomplish depolymerization of this cross-linked phenolic biopolymer and the further upgrade to high-valued chemicals.[156, 163, 167, 168] However, lignin coming from the paper industry or bio-refineries is very challenging to valorize due to the harsh conditions used in processing the lignocellulosic biomass that alter the lignin structure. Nonetheless, a plausible solution can be the initial extraction of lignin from lignocellulose (e.g. by reductive catalytic fractionation RCF)[169] before performing the pre-treatment for the separation of cellulose and hemicellulose.[170] Also alternative strategies have been reported to overcome this challenge.[171, 172] Basically, lignin valorization can occur by either direct utilization of its monomers or by catalytic upgrading of lignin co-product coming from lignocellulose bio-refineries.[151] The aromatic nature of lignin provides a broad variety of potential uses (**Figure 1.6**):[148] for instance, as precursor for bio-based carbon fibers synthesis,[173-175] for the manufacture of bio-plastics and bio-polymers,[176, 177] adhesives and binders as well as aromatic compounds, APIs precursors [178] and many other high valued chemicals.[148,176,177,179,180] Moreover, it can be a source of phenolic derivatives[150, 181] and a typical example is the industrial production of vanillin.[182] However, with respect to the developments achieved for the valorization of bio-based monosaccharide C6 and C5 to high valued chemicals, more research is needed for the development of highly efficient technologies (combination of

biotechnology, (bio)chemistry and engineering) for the integration of lignin valorization in the bio-refineries.

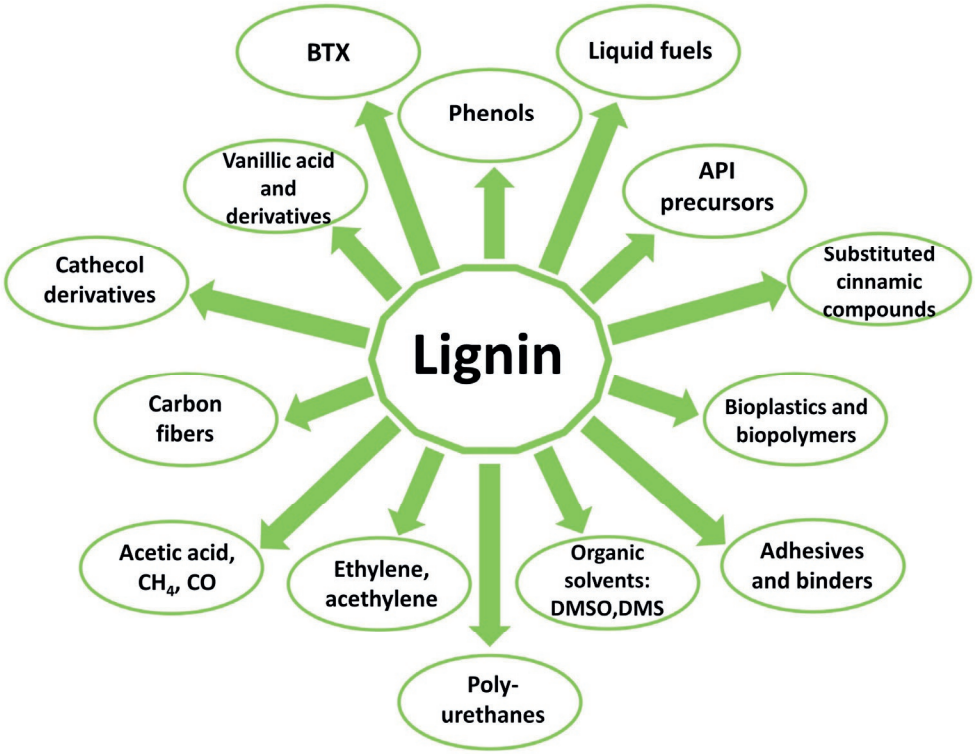

Figure 1.6. Overview of potential lignin-derived chemicals and value-added products.

1.2 The role of biocatalysis for a green and sustainable chemistry

Based on the needs for greener processes and to meet a sustainable development, the use of catalytic methods are good substitutes to the traditional use of stoichiometric reagents in chemical synthesis. In this regard, biocatalysis has even more benefits to offer in both environmental and economic terms.[183,184] Interestingly, five green chemistry principles are fulfilled by the intrinsic elevated chemo-, regio- and stereoselectivity of enzymes. In general, biocatalysis is considered safe, sustainable and selective. By principle, enzymes are non-hazardous and non-toxic for both environment and people and are renewable and biodegradable by nature.[185] Biocatalytic reactions are commonly run in aqueous solutions and less harsh conditions. Moreover, highly selective enzymes can afford products in elevated purity, hence reducing the amount of solvents conventionally used for further purifications (e.g., column chromatography). Biocatalysts do not

usually require activating agents, protection/deprotection steps, thus leading to processes with greater step economy and more energy utilization than conventional routes. This translates to less waste along with precluding toxic metals, auxiliaries and (supra) stoichiometric amount of other reagents.[29,184] Furthermore, the use of biocatalytic processes complies with the concept of waste lignocellulose biomass valorization; as described earlier, enzymes can transform biological feedstocks (cellulose and lignin) in high valuable compounds.[186] It is expected that the establishment of a bio-based economy will further broaden the scope of biocatalysis by discovering new enzymatic activities to enable the performance of new chemical transformations. Although enzymes' potential in organic synthesis has been known for a long time, their broad utilization began just in the 1980s. A major hurdle was the scarce availability of commercialized enzymes, mainly hydrolases (lipases, esterases and glycosidases).[14] Nowadays, the enzymes toolbox is expanding continuously thus covering much of the known chemical reactions used in many synthetic pathways. For instance, oxidoreductases (e.g., dehydrogenases, oxidases, peroxidases) and (amino)-transferases are two of the most studied and applied enzymes classes in both academia and industry, and many examples can be found throughout the literature.[187-189] Many enzymes display substrate promiscuity. Even more relevant, these superb catalysts often show catalytic promiscuity thereby being able to perform different reactions besides their native catalytic activity.[190,191] This peculiar trait provides the fundamentals for subsequent developments as exemplified by directed evolution.[192] Indeed, as a result of advances in modern biotechnology (e.g., recombinant DNA technology, protein engineering techniques, high-throughput screening),[193-195] "tailor-made" biocatalysts can be designed to meet specific requirements such as substrate specificity, activity, stability and selectivity,[196, 197] thus broadening the availability of enzymatic reactions for applications in organic synthesis.[198-200] As a consequence, more enzymes are available on the market because they are also produced at more competitive prices compared to twenty years ago. Moreover, these biotechnology advances will allow the discovery and generation of new enzymes performing unnatural transformations.[201]

Biocatalytic processes can be performed with *i*) growing cells (fermentation), in which the metabolic pathways of growing cells is used; *ii*) whole resting cells, and *iii)* isolated enzymes.[202] Fermentation processes were already used in ancient times mainly for the production of food as well as beverages (e.g. bread, beer and wine). Later on, fermentation processes were applied in the preparation of amino acids,

alcohols, vitamins, hormones and many other bioactive molecules. More recently, overproduction of metabolites was performed by engineering organism metabolism for performing unnatural reactions.[203] However, the use of growing cells for carrying out conversion of external substrates can result in lower reaction rates due to limitation in substrate diffusion through the cell walls, for instance. Moreover, the development of fermentation processes requires large financial investments and time while pharmaceutical industries tend to favor catalysts that can be stored, and therefore easier to handle.[187,204] In general, biocatalytic transformations are preferentially carried out by using recombinant microorganisms (GMOs, e.g. *E.coli*) in the form of whole resting cells (fresh and frozen cells, lyophilized powders, free-cell extract), which produce the desired overexpressed enzyme.[205] Alternatively, the isolated enzymes can also be applied by performing extraction from the host organism followed by purification.[202] The use of whole cells provides some advantages compared with isolated enzymes; for instance, protection of the overexpressed enzyme within the cell walls, avoidance of enzyme purification, easy removal of the cells debris and the aid of cell metabolism for coenzymes regeneration.[202,206] In this case, substrate diffusion can be overcome since cell membrane becomes more permeable due to pre-treatments such as freeze/thaw or lyophilization.[207] The major downsides can derive from side reactions due to the presence of other enzymes coming from the host organisms; however, this can be mitigated by overexpression of the desired enzyme and suppression of the undesired ones.[210] On the other hand, one of the main advantages of isolated/purified enzymes is the exclusion of contamination from other enzymes that are present in the host organisms. Nevertheless, whole cells are ca. 10% cheaper than the purified enzymes. The main costs are associated with the purification step as well as the need of external cofactor regeneration.[207] Nonetheless, many efficient cofactor recycling systems were reported in literature especially in regard of NAD(P)H-dependent enzymes: for instance, formate/FDH and glucose/GDH.[201,211,212] Moreover, the use of orthogonal cofactor regeneration systems enables the removal of byproducts formed during the reactions, thereby favoring the product formation. An example is the asymmetric synthesis of optically active amines with aminotransferases, in which alanine is commonly used as amino donor, hence generating pyruvate as by-product (**Figure 1.7**).[213-217] Another alternative is the use of surface display of the desired enzyme in engineered cells; this does not require the substrate to cross the cell membrane, however, this

technology may not be generally applicable especially for cofactor dependent-enzymes.[208, 209]

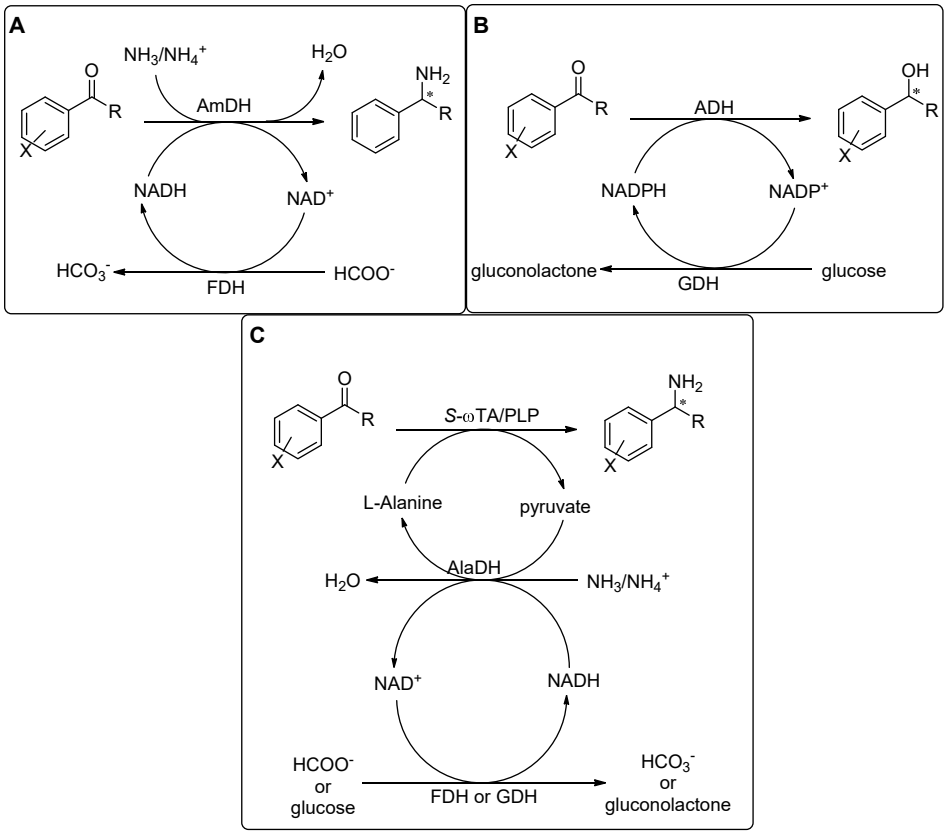

Figure 1.7. Examples of internal and orthogonal co-enzyme/co-substrate recycling systems

Nevertheless, for a truly economic and sustainable process, the enzyme needs to be recovered and re-used. This can be accomplished by immobilization techniques of either purified enzymes or the whole host organism carrying the desired overexpressed biocatalyst. Examples are solid cross-linked enzyme aggregates (CLEAs), enzymes bound to a carrier materials or encapsulated in polymeric hydrogels.[187, 218,219] The immobilization of enzymes can reduce catalytic activities. However, higher stability is often achieved.[184] Furthermore, the coupling of immobilization strategies with continuous flow processes is a further improvement in regard to the reusability of the biocatalyst. However, this technology requires more research in order to find full applicability in industrial biocatalysis.[220-222]

1.2.1 Biocatalytic cascade reactions

The fact that enzymes are often compatible and can operate simultaneously at the same temperature, pressure, pH and reaction media is of high relevance in asymmetric organic synthesis. This property enables the implementation of multiple-step processes.[223,224] It also results in the minimization of solvents consumption as well as reduction of reaction volumes, by avoiding intermediate isolation and purification. Moreover, cascade reactions have the advantages of cutting down operation time and costs as well as enabling higher space time yields.[225] In addition, the removal of the *in situ* formed intermediates or coproducts—which may inhibit and/or deactivate the biocatalysts—by applying orthogonal systems permits to achieve product formation by shifting the thermodynamic equilibrium.[187,216, 226-229] Finally, the *in situ* formation of unstable or highly toxic intermediates, which are then directly converted in the follow-up step, confers to these one-pot enzymatic processes a further improvement compared to conventional multi-step organic synthesis.[230] Another trend concerns the development of chemoenzymatic cascade reactions,[225,231] wherein the key step is usually performed by enzymes due to their exquisite chemo-, regio- and stereoselectivity, followed by chemocatalytic steps such as hydrogenation using molecular hydrogen.[232,233] Because of the enormous amount of artificial cascade reactions that are continuously reported, classifications of these multi-step processes have been proposed, which sometimes lead to ambiguity.[216,225,229,230,233,234] An interesting and linear classification was described by Rudroff's group.[233] One-pot cascade reactions consist of any system in which two or more transformations take place in the same pot involving at least one catalyst.[229] Accordingly, cascades can be performed in two main mode, namely: sequential and concurrent reactions. The first refers to systems in which two or more transformations are carried out in the same pot but are separated in time. Conversely, in the concurrent mode the product of the first reaction is subsequently converted in the follow up reaction thereby both reactions occur in the same pot and at the same time. Concurrent cascade reactions can further be classified in domino and tandem reactions wherein the first are intended when an unstable intermediate, formed by the initial catalyzed step, undergoes spontaneous reactions before converting into the most stable product. On the other hand, tandem (or linear) cascades relate to multiple catalyzed transformations, concerning enzymes that usually perform individually but are instead combined in the same pot (**Figure 1.8**). Nevertheless, systems in which an additional orthogonal

reaction is used for shifting the reaction equilibrium or for regeneration of a cofactor, cannot be classified as cascades since only one desired transformation is effectively occurring. Examples of such orthogonal systems are shown in **Figure 1.7**.

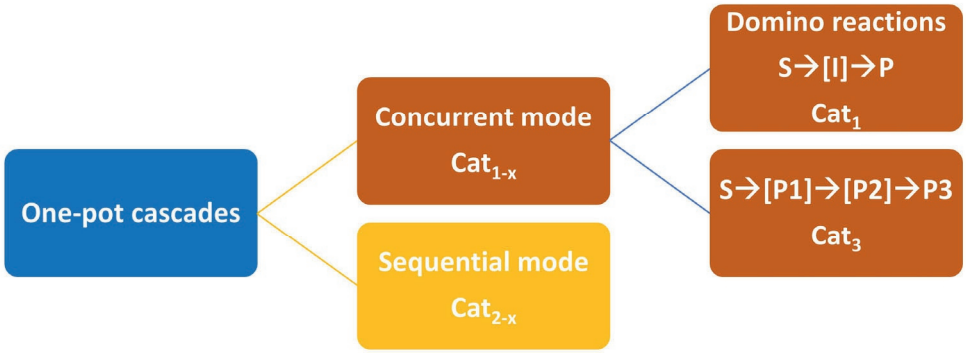

Figure 1.8. Tentative classification of one-pot cascade reactions based on the definitions reported by Rudroff *et al.*;[233] Cat = catalyst; 1-x = number of catalyst involved from 1 to x; S = substrate; I = intermediate; P = product; squared brackets indicate an intermediate which is not isolated.

Many multi-enzymatic cascade reactions are reported, which involve a large variety of enzymes, such as amine dehydrogenases, monooxygenases, peroxidases, hydrolases, aminotransferases, alcohol dehydrogenases, imine reductases etc. For instance, Li and coworkers developed a network of whole cells enzymatic transformations of alkenes to highly valuable chemicals by engineering *E. coli* strains co-expressing the required biocatalysts in modules.[235-247] A smart way to perform multi-step enzymatic one-pot conversions is via the so called hydrogen-borrowing cascades which uses the first oxidative step for providing the required reducing equivalent in the second reductive step through interconnected coenzyme regeneration.[248-252] Mutti and coworkers described the application of these enzymatic redox-neutral processes in the synthesis of amines[211, 253-255] and nor(pseudo)ephedrine isomers.[256] A large number of one-pot biocatalytic reactions have been reported throughout these years for the synthesis of high valuable compounds.[187,213,216,224,229-231,234,242,249,257-266] Examples are shown in **Figure 1.9**.

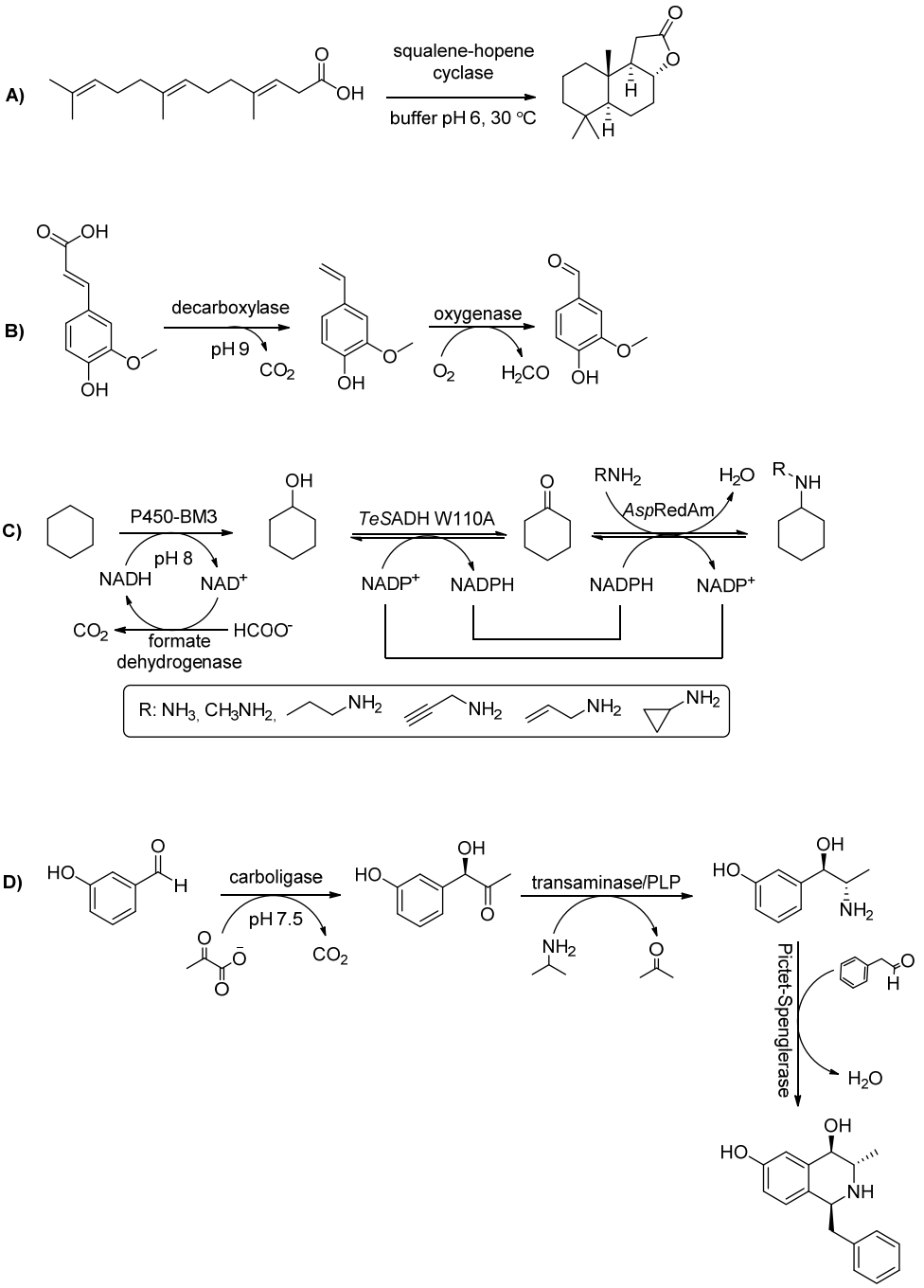

Figure 1.9. Examples of one-pot multi-enzymatic reactions for the synthesis of high valuable compounds: A) concurrent mode domino cascade;[267, 268] B) concurrent mode cofactor-free tandem cascade;[269] C) concurrent mode tandem cascade (TeSADH = alcohol dehydrogenase variant; AspRedAm = reductive aminase);[270, 271] D) sequential mode cascade.[272] (Schemes were adapted from ref.[230, 234]).

1.3 Biocatalysis in APIs synthesis

The FDA regulations, which oblige the exclusive commercialization of one active enantiomer as drug, favored the breakthrough towards implementation of asymmetric enzymatic synthesis for stereoselective processes.[273,274] In the last decades, biocatalysis has been integrated into synthetic routes, in particular, in the pharmaceutical industry in order to perform key steps as the introduction of stereogenic centers.[14,275-281] Another contribution for this escalation to the use of enzymes in the pharmaceutical industry came from the possibility to perform biocatalytic processes in organic media, or more in general in non-aqueous solvent system,[282] at elevated temperatures[283] allowing higher substrates solubility and easier recovery of products. The ACS Institute of Green Chemistry has released a guide of crucial research areas aimed to incorporate the green chemistry principles in the manufacture of pharmaceuticals.[284] Sheldon *et al.* gave an integrated outline of enzymes within these processes.[187] As shown in **Table 1.4**, biocatalysis integrates very well in the process of developing greener methodologies but much more still needs to be investigated. The enzymatic synthesis of optically active amines, by reductive amination of prochiral ketones or by functional group manipulation starting from alcohols, and the synthesis of chiral alcohols, by reduction of the correspondent carbonyl compounds, are particularly popular due to the abundant presence of these functionalities in APIs. Many enzymes involved in these transformations have been amply studied, such as transaminases and alcohol dehydrogenases but also amine dehydrogenases, monoamine oxidases and other related enzymes. Furthermore, kinetic resolution has been extensively incorporated in the manufacture of APIs.[285,286,287,288] Some examples of enzymatic key steps involved in the synthesis of pharmaceuticals as well as enzymatic routes leading to valuable building blocks and drugs intermediates are depicted in **Figure 1.10**.[14,187,202,285,289-293]

Table 1.4. Key research areas in the pharmaceutical industry and biocatalysis contribution (adapted from ref. 187 and 284)

Key research areas for greener processes in the pharmaceutical industry	**Class of enzymes related to research area**
Versatile methods which use non-precious and sustainable metals	Enzymes sometime use cheap and sustainable metals
Catalytic methodologies for amide and/or peptide formation	Proteases, lipases; nitrile hydratases
Predictable site-selective C-H activation employing greener oxidants	Oxidoreductases
Reduction of amide bond without using $LiAlH_4$ and diborane	Amide reductases are unknown (yet)
Functionalization of alcohols	Hydrogen-borrowing enzymatic cascades
Catalytic immobilization techniques avoiding significant loss of activity	Enzymes immobilization techniques
Asymmetric hydrogenation of unfunctionalized compounds (olefins,enamines,imines)	Ene-reductases; Imine reductases
Improvement of fluorination/trifluoromethoxylation methods	Known C-H fluorination enzymes but not yet commonly applicable
Methods which avoid the use of Ph_3PO in the Wittig reaction	Enzymatic carbonyl olefination
Greener oxidative processes for C-O and C-N bonds	Peroxygenases, Cytochrome P450

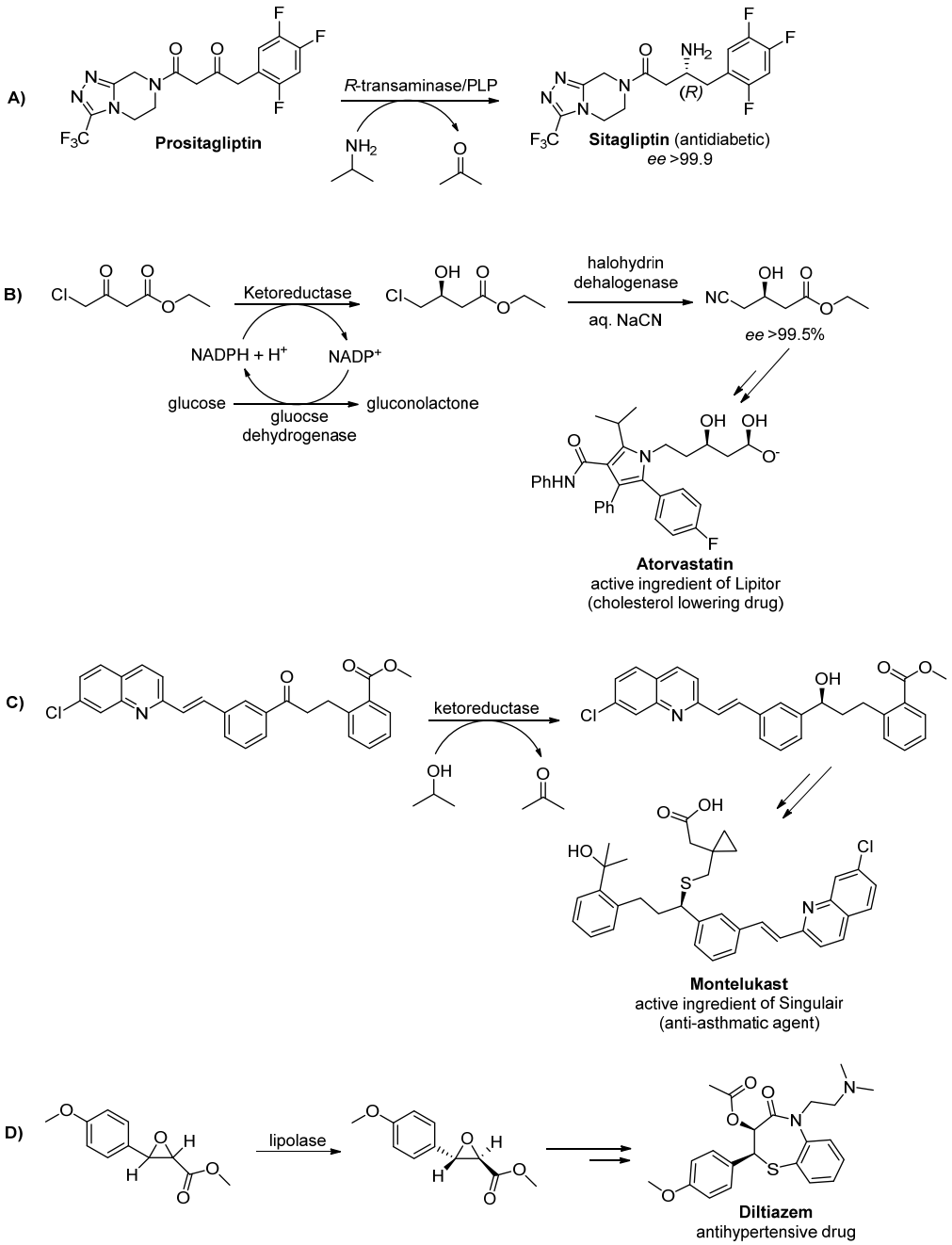

Figure 1.10. Examples of enzymes as key steps in the synthesis of APIs, valuable chiral building blocks and drugs intermediates; A) Sitagliptin;[294] B) Atorvastatin;[295] C) Montelukast;[296] D) Diltiazem[297]

1.3.1 Vicinal amino alcohols

Among the various functionality present in APIs, amino alcohols constitute the active core of several natural products and pharmaceutical active compounds such as alkaloids, neurotransmitters (e.g., ephedrine, pseudoephedrine, norephedrine, epinephrine), sphingosine derivatives as sulfobacin B, HIV protease inhibitors as saquinavir, ritonavir and lopinavir, aminopeptidase inhibitor as bestatin, antibiotics such as chloroamphenicol, anisomycin etc. (**Figure 1.11**).[298-302] Furthermore, vicinal amino alcohols are extensively used in organic chemistry as ligands and chiral auxiliaries as well as they find applications as chiral building blocks.[302, 303]

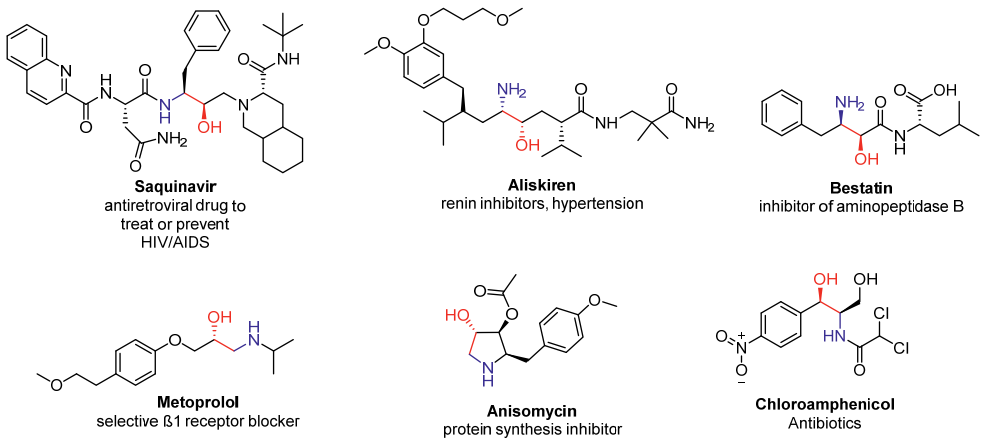

Figure 1.11. Bioactive molecules with vicinal amino alcohol functionalities.

A variety of chemical methods are known for the synthesis of amino alcohols. The most acknowledged routes being the Sharpless asymmetric aminohydroxylation of olefins[304,305] and the selective nucleophilic opening of epoxides and/or aziridines.[301,302,306,307] Many more strategies have been reported in the literature which can mainly be divided in *i*) direct transformation of substrates carrying the two heteroatoms (e.g., nucleophilic addition to an α-amino carbonyl[308-310] or to an α-hydroxy imine;[311-313] reduction of a chiral α-amino acids,[314] α-amino ketones[315, 316] or α-hydroxy imines[317]); *ii*) coupling reactions of two molecules each carrying one heteroatom (e.g., aldol-type reactions;[318-320] pinacol-type reactions[321]) and *iii*) single heteroatom addition to a molecule already carrying the other heteroatom (e.g., alkoxide to α,β-unsaturated amines;[324-326] nitrogen to electrophilic carbons.[322,323]).[302,327,328] Nevertheless, toxic and expensive metals associated with stoichiometric amounts of reagents and hazardous solvent systems are often required. Moreover, protection/deprotection steps are very often present in these types of synthetic routes which result then in lengthy and tedious syntheses.

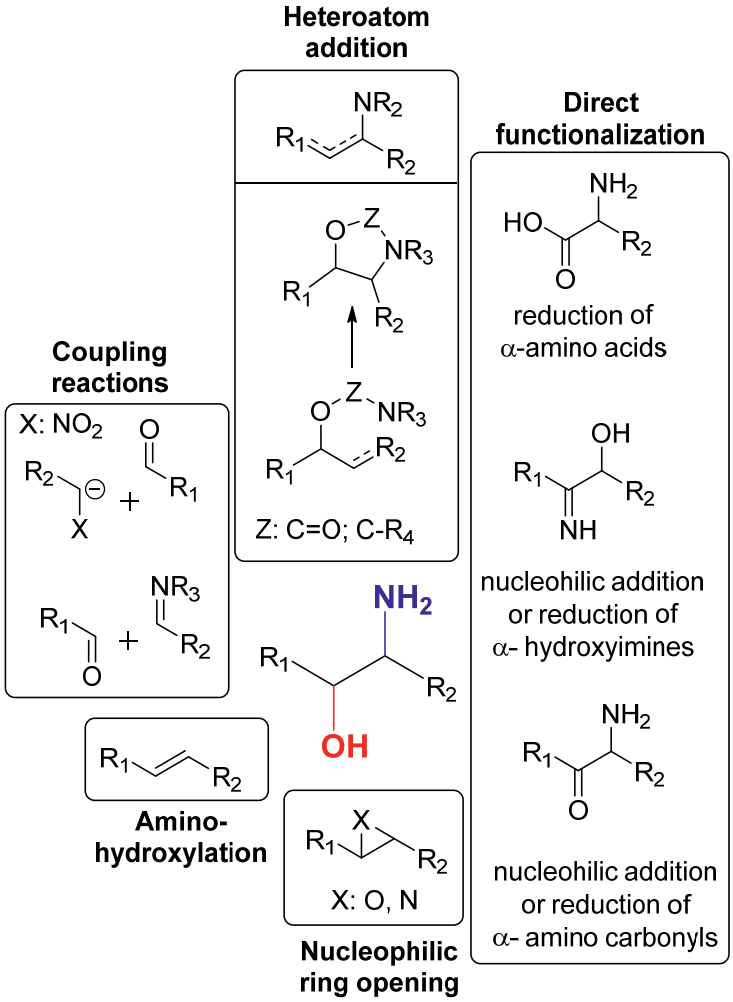

Figure 1.12. Classification of chemical approaches for the asymmetric synthesis of chiral amino alcohols (adapted from ref. [302,329]).

On the other hand, a comprehensive classification for the enzymatic methods for amino alcohols synthesis cannot be drawn yet. In fact, most of the literature covers the preparation of targeted amino alcohol structures rather than describing general synthetic approaches. Anyway, it is possible to give an overview of the enzymes involved in such transformations and a recent review about biocatalysts for amino alcohols synthesis was published by Gupta *et al.*[327] Transaminases or aminotransferases are the most employed enzymes; they perform the transfer of an amino group to a prochiral ketone via PLP coenzyme.[214] This class of enzymes was applied in the asymmetric amination of α-hydroxyketones[213,330,331] and in the

resolution of racemic amino alcohols.[332,333] Nevertheless, many kinetic resolution strategies were reported employing hydrolases, mainly lipases.[334,335] Moreover, transaminases were also coupled with alcohol dehydrogenases for the asymmetric amino hydroxylation of diketone compounds[336] as well as with transketolase starting from glycolaldehyde and hydroxypyruvate.[337,338] Reductive amination of α-hydroxyketones can also be performed with amine dehydrogenases[339] while alcohol dehydrogenases were used in the reduction of amino/azido carbonyls. When starting from azido ketones, a chemical hydrogenation step is often used in combination with an ADH.[232,340] Other applied approaches comprise amino acids decarboxylation (enzymatically prepared by aldolases)[341] and the selective opening of epoxide catalyzed either by halohydrine dehalogenases with an azide source[342] or by lipases with an amino compound.[343] Furthermore, enzymes involved in the formation of C-C bonds (e.g., hydroxynitrile lyases and promiscuous hydrolases) were also integrated in chemoenzymatic approaches for the preparation of amino alcohols.[344-346] Overall, there is still not a versatile enzymatic methodology to yield amino alcohols, for instance through direct asymmetric aminohydroxylation of alkenes. Li's group published the asymmetric aminohydroxylation of aromatic terminal olefins by an engineered *E. coli* strain co-expressing four enzymes, namely: styrene monooxygenase, epoxide hydrolase, alcohol dehydrogenase and transaminase.[235,237,241] Few years later, Arnold and colleagues described the use of an engineered hemoprotein for the direct aminohydroxylation of alkenes.[347] Nevertheless, both approaches were applied on targeted products and limited to aromatic terminal alkenes. A general overview of some chemical and enzymatic approaches for amino alcohols synthesis is depicted in **Figure 1.12-1.13**. More details on certain chemical and enzymatic routes will be discussed in the next chapters of this thesis.

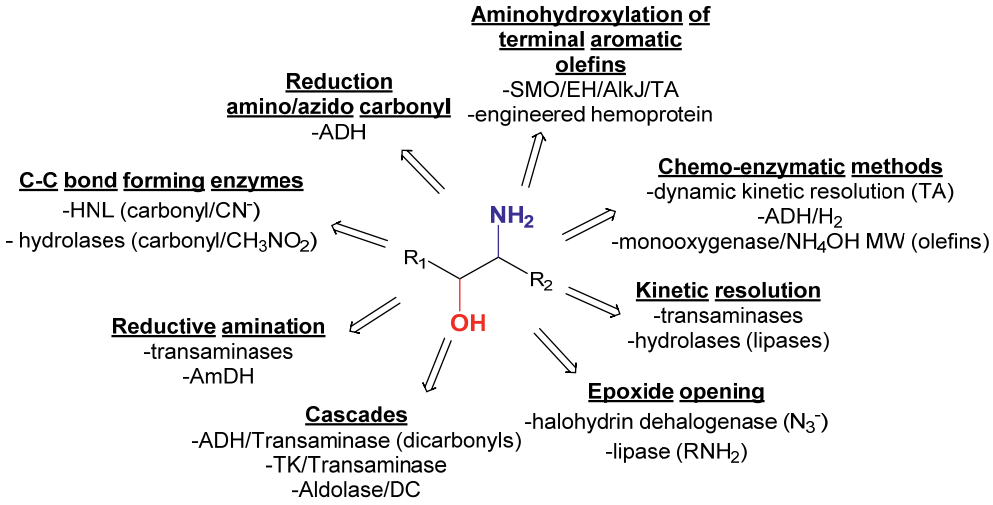

Figure 1.13. Overview of enzymatic approaches for the preparation of amino alcohols; SMO = styrene monooxygenase; TA = transaminase; ADH = alcohol dehydrogenase; TK = transketolase; AmDH = amine dehydrogenase; EH = epoxide hydrolase; HNL = hydroxynitrile lyase; AlKJ = alcohol dehydrogenase.

1.4 Thesis outline

The aim of this thesis is the development of biocatalytic cascade reactions for optically active vicinal amino alcohol's synthesis with a focus on phenylpropanolamine scaffolds (nor(pseudo)ephedrine) and phenylethanolamine isomers. The goal was pursued through the testing of several one-pot cascades towards the synthesis of the target amino alcohol products and starting from aromatic olefins. The thesis entails two independent sequential cascades: *i*) the asymmetric enzymatic one-pot synthesis of diol substrates starting from aromatic alkenes and *ii)* the multi-enzymatic transformation of chiral diols to targeted amino alcohols. Apart from **Chapter 1**, which consists in a conceptual road map on the role of biocatalysis in modern organic chemistry, this thesis comprises five more chapters. **Chapter 2** describes the work on the engineering of a styrene monooxygenase. The two units of the catalytic system, StyB (the reductase domain) and StyA (the epoxidation domain) were genetically fused by a 30 amino acids linker to generate the chimeric Fus-SMO. The enzyme's catalytic performance and applicability for the asymmetric synthesis of targeted epoxides were both evaluated. In **Chapter 3,** the formal regio-, chemo- and stereoselective synthesis of two isomers of nor(pseudo)ephedrine was accomplished via the so called hydrogen-borrowing (HB) cascade. Optically active diols were transformed to the targeted compounds by coupling alcohol dehydrogenases (ADHs) and amine

dehydrogenases (AmDHs) in a one-pot fashion. Moreover, the 1,2-phenylpropanediol substrates could also be enzymatically synthesized starting from β-methylstyrene via a one pot cascade catalyzed by the above-mentioned engineered Fus-SMO combined with two stereocomplementary epoxide hydrolases (EHs). Thus, we were able to obtain all the four diol isomers in enantiomeric pure form. Due to the lack of (*S*)-selective AmDHs, the enzymatic synthesis of the other two isomers of nor(pseudo)ephedrine could be achieved by coupling ADHs with stereocomplementary ω-transaminases (ωTAs), as described in detail in **Chapter 4**. Similarly, to the HB-bioamination, which is a redox-neutral cascade because of the internal recycling of the NAD^+ coenzyme catalyzed by ADH and AmDH, the ADH/TA system regenerated the required oxidized NAD^+ coenzyme via an alanine dehydrogenase (AlaDH). Simultaneously, the pyruvate side product was converted back to alanine that re-entered the cycle as amino donor in the aminotransfer reaction. **Chapter 5** deals with an extension of the one-pot cascade reported in chapter 4. In this case, another class of amino alcohol structures were targeted, namely phenylethanolamine isomers. Both α- and β-amino alcohols could be obtained, starting from chiral 1,2-phenylethanediol, by either the one-pot cascade described in chapter 4 or via an orthogonal bioamination cascade. In this latter case, an alcohol oxidase was combined with an amine dehydrogenase. The latter enzyme was also part of an orthogonal enzymatic system whereby the NADH coenzyme, required in the reductive amination step, was recycled. Finally, **Chapter 6** is a proof of principle to show the high potential of the cascades discussed so far. The overall perspective of this work is to show the possibility to further expand the applicability of these one-pot cascades for giving access to other amino alcohols structures (e.g., adrenaline and derivatives thereof). Moreover, these cascades may be further improved by sourcing the olefins substrates—which ultimately are the starting material to obtain the amino alcohols—from renewable resources (e.g., caffeic acids). Nevertheless, no conclusive evaluations can be drawn, yet since more tests and analysis of the cascade processes are necessary. However, the engineering of a toolbox of better biocatalysts through the integration of computational methods and directed evolution is critical in order to enhance the overall catalytic performance of these cascades.

1.5 References

1. R. A. Sheldon, *Chem. Soc. Rev.*, 2012, 41, 1437-1451.
2. R. A. Sheldon, *Green Chem.*, 2005, 7, 267.
3. D. J. C. Constable, C. Jimenez-Gonzalez and R. K. Henderson, *Org. Process Res. Dev.*, 2007, 11, 133-137.
4. R. A. Sheldon, *Chem. Ind.-London*, 1997, 12-15.
5. R. A. Sheldon, *J. Chem. Technol. Biotechnol.*, 1997, 68, 381-388.
6. A. D. Curzons, D. C. Constable and V. L. Cunningham, *Clean Technol. Envir.*, 1999, 1, 82-90.
7. C. Jimenez-Gonzalez, A. D. Curzons, D. J. C. Constable and V. L. Cunningham, *Clean Technol. Envir.*, 2004, 7, 42-50.
8. R. K. Henderson, C. Jiménez-González, D. J. C. Constable, S. R. Alston, G. G. A. Inglis, G. Fisher, J. Sherwood, S. P. Binks and A. D. Curzons, *Green Chem.*, 2011, 13, 854.
9. C. M. Alder, J. D. Hayler, R. K. Henderson, A. M. Redman, L. Shukla, L. E. Shuster and H. F. Sneddon, *Green Chem.*, 2016, 18, 3879-3890.
10. D. Prat, O. Pardigon, H.-W. Flemming, S. Letestu, V. Ducandas, P. Isnard, E. Guntrum, T. Senac, S. Ruisseau, P. Cruciani and P. Hosek, *Org. Process Res. Dev.*, 2013, 17, 1517-1525.
11. K. Alfonsi, J. Colberg, P. J. Dunn, T. Fevig, S. Jennings, T. A. Johnson, H. P. Kleine, C. Knight, M. A. Nagy, D. A. Perry and M. Stefaniak, *Green Chem.*, 2008, 10, 31-36.
12. J. P. Adams, C. M. Alder, I. Andrews, A. M. Bullion, M. Campbell-Crawford, M. G. Darcy, J. D. Hayler, R. K. Henderson, C. A. Oare, I. Pendrak, A. M. Redman, L. E. Shuster, H. F. Sneddon and M. D. Walker, *Green Chem.*, 2013, 15, 1542.
13. F. I. McGonagle, D. S. MacMillan, J. Murray, H. F. Sneddon, C. Jamieson and A. J. B. Watson, *Green Chem.*, 2013, 15, 1159.
14. R. A. Sheldon, *Green Chem.*, 2017, 19, 18-43.
15. R. A. Sheldon, *ACS Sustain. Chem. Eng.*, 2017, 6, 32-48.
16. C. Jimenez-Gonzalez, C. S. Ponder, Q. B. Broxterman and J. B. Manley, *Org. Process Res. Dev.*, 2011, 15, 912-917.
17. C. Jiménez-González, C. Ollech, W. Pyrz, D. Hughes, Q. B. Broxterman and N. Bhathela, *Org. Process Res. Dev.*, 2013, 17, 239-246.
18. A. D. Curzons, D. N. Mortimer, D. J. C. Constable and V. L. Cunningham, *Green Chem.*, 2001, 3, 1-6.
19. D. J. C. Constable, A. D. Curzons and V. L. Cunningham, *Green Chem.*, 2002, 4, 521-527.
20. T. Hudlicky, D. A. Frey, L. Koroniak, C. D. Claeboe and L. E. Brammer, *Green Chem.*, 1999, 1, 57-59.
21. B. Voss, S. I. Andersen, E. Taarning and C. H. Christensen, *ChemSusChem*, 2009, 2, 1152-1162.
22. R. A. Sheldon, *Green Chem.*, 2007, 9, 1273.
23. B. M. Trost, *Science*, 1991, 254, 1471-1477.
24. B. M. Trost, *Acc. Chem. Res.*, 2002, 35, 695-705.
25. R. A. Sheldon, *Chem. Ind.-London*, 1992, 903-906.
26. R. A. Sheldon, *Catal. Today*, 2015, 247, 4-13.
27. G. J. ten Brink, I. W. Arends and R. A. Sheldon, *Science*, 2000, 287, 1636-1639.
28. D. B. Dess and J. C. Martin, *J. Org. Chem.*, 1983, 48, 4155-4156.
29. R. A. Sheldon, *J. R. Soc. Interface*, 2016, 13, 20160087.
30. P. Anastas and J. Warner, *Green chemistry: theory and practice*, Oxford University Press, Oxford, UK, 1998.
31. K. Wilson, *Appl. Organomet. Chem.*, 2007, 21, 1002.
32. P. T. Anastas and J. C. Warner, *Org. Process Res. Dev.*, 2000, 4, 437-438.
33. P. Anastas and N. Eghbali, *Chem. Soc. Rev.*, 2010, 39, 301-312.

34. G. H. Brundtland, *Our Common Future:The Report of the World Commission on Environment and Development*, Oxford University Press, Oxford & New York, 1987.
35. A. Azapagic and S. Perdan, *Process Saf. Environ.*, 2000, 78, 243-261.
36. A. Azapagic, A. Millington and A. Collett, *Chem. Eng. Res. Des.*, 2006, 84, 439-452.
37. S. K. Sikdar, *AlChE J.*, 2003, 49, 1928-1932.
38. T. E. Graedel, in *Handbook of green chemistry and technology*, eds. J. Clark and D. J. Macquarrie, Wiley,New York, 2002, ch. 4, pp. 56-61.
39. J. M. Köhler, *Green Process Synth.*, 2014, 3, 33-45.
40. R. A. Sheldon, *Green Chem.*, 2014, 16, 950-963.
41. E. de Jong, A. Higson, P. Walsh and M. Wellisch, *Biofuel, Bioprod. Bior.*, 2012, 6, 606-624.
42. W. R. Stahel, *Nature*, 2016, 531, 435-438.
43. T. Keijer, V. Bakker and J. C. Slootweg, *Nat. Chem.*, 2019, 11, 190-195.
44. J. H. Clark, T. J. Farmer, L. Herrero-Davila and J. Sherwood, *Green Chem.*, 2016, 18, 3914-3934.
45. H. C. Erythropel, J. B. Zimmerman, T. M. de Winter, L. Petitjean, F. Melnikov, C. H. Lam, A. W. Lounsbury, K. E. Mellor, N. Z. Janković, Q. Tu, L. N. Pincus, M. M. Falinski, W. Shi, P. Coish, D. L. Plata and P. T. Anastas, *Green Chem.*, 2018, 20, 1929-1961.
46. A. E. Marteel-Parrish and M. A. Abraham, *Green Chemistry and Engineering: A Pathway to Sustainability* Wiley, 2013.
47. R. Noyori, *Nat. Chem.*, 2009, 1, 5-6.
48. R. Höfer and J. Bigorra, *Green Chem. Lett. Rev.*, 2008, 1, 79-97.
49. P. Gallezot, *Chem. Soc. Rev.*, 2012, 41, 1538-1558.
50. H. Kawaguchi, T. Hasunuma, C. Ogino and A. Kondo, *Curr. Opin. Biotechnol.*, 2016, 42, 30-39.
51. A. J. Straathof, *Chem. Rev.*, 2014, 114, 1871-1908.
52. S. Shackley, S. Carter, T. Knowles, E. Middelink, S. Haefele, S. Sohi, A. Cross and S. Haszeldine, *Energy Policy*, 2012, 42, 49-58.
53. A. Demirbas, *Energy Convers. Manage.*, 2011, 52, 1280-1287.
54. C. O. Tuck, E. Perez, I. T. Horvath, R. A. Sheldon and M. Poliakoff, *Science*, 2012, 337, 695-699.
55. J. K. Saini, R. Saini and L. Tewari, *3 Biotech*, 2015, 5, 337-353.
56. Z. Anwar, M. Gulfraz and M. Irshad, *J. Radiat. Res. Appl. Sc.*, 2019, 7, 163-173.
57. L. A. Pfaltzgraff, M. De bruyn, E. C. Cooper, V. Budarin and J. H. Clark, *Green Chem.*, 2013, 15, 307.
58. C. S. K. Lin, L. A. Pfaltzgraff, L. Herrero-Davila, E. B. Mubofu, S. Abderrahim, J. H. Clark, A. A. Koutinas, N. Kopsahelis, K. Stamatelatou, F. Dickson, S. Thankappan, Z. Mohamed, R. Brocklesby and R. Luque, *Energy Environ. Sci.*, 2013, 6, 426.
59. S. M. Andler and J. M. Goddard, *NPJ Sci. Food*, 2018, 2, 19.
60. M. Bilal and H. M. N. Iqbal, *Food Res. Int.*, 2019, 123, 226-240.
61. J.-P. Lange, *Biofuel, Bioprod. Bior.*, 2007, 1, 39-48.
62. S. Haghighi Mood, A. Hossein Golfeshan, M. Tabatabaei, G. Salehi Jouzani, G. H. Najafi, M. Gholami and M. Ardjmand, *Renew. Sust. Energ. Rev.*, 2013, 27, 77-93.
63. A. F. Kirkels and G. P. J. Verbong, *Renew. Sust. Energ. Rev.*, 2011, 15, 471-481.
64. R. A. Sheldon, *Chemicals from Synthesis Gas: Catalytic Reactions of CO and H2*, Springer, Dordrecht, 1983.
65. J. Daniell, M. Köpke and S. Simpson, *Energies*, 2012, 5, 5372-5417.
66. A. M. Henstra, J. Sipma, A. Rinzema and A. J. Stams, *Curr. Opin. Biotechnol.*, 2007, 18, 200-206.
67. P. C. Munasinghe and S. K. Khanal, *Bioresour. Technol.*, 2010, 101, 5013-5022.
68. R. A. Sheldon, *J. Mol. Catal. A: Chem.*, 2016, 422, 3-12.
69. J. M. Thomas, J. C. Hernandez-Garrido and R. G. Bell, *Top. Catal.*, 2009, 52, 1630-1639.

70. R. Rinaldi and F. Schüth, *Energy Environ. Sci.*, 2009, 2, 610-626.
71. X. Zhao, K. Cheng and D. Liu, *Appl. Microbiol. Biotechnol.*, 2009, 82, 815-827.
72. J. Wildschut, A. T. Smit, J. H. Reith and W. J. Huijgen, *Bioresour. Technol.*, 2013, 135, 58-66.
73. J. Viell, A. Harwardt, J. Seiler and W. Marquardt, *Bioresour. Technol.*, 2013, 150, 89-97.
74. P. L. Dhepe and A. Fukuoka, *ChemSusChem*, 2008, 1, 969-975.
75. P. Kumar, D. M. Barrett, M. J. Delwiche and P. Stroeve, *Ind. Eng. Chem. Res.*, 2009, 48, 3713-3729.
76. P. Bajpai, *Pretreatment of Lignocellulosic Biomass for Biofuel Production*, Springer, 2016.
77. V. Menon and M. Rao, *Prog. Energy Combust. Sci.*, 2012, 38, 522-550.
78. U. Bornscheuer, K. Buchholz and J. Seibel, *Angew. Chem. Int. Ed.*, 2014, 53, 10876-10893.
79. P. Alvira, E. Tomas-Pejo, M. Ballesteros and M. J. Negro, *Bioresour. Technol.*, 2010, 101, 4851-4861.
80. C. Chatterjee, F. Pong and A. Sen, *Green Chem.*, 2015, 17, 40-71.
81. J. S. Luterbacher, D. Martin Alonso and J. A. Dumesic, *Green Chem.*, 2014, 16, 4816-4838.
82. X. Tong, Y. Ma and Y. Li, *Appl. Catal. A-Gen.*, 2010, 385, 1-13.
83. P. Y. Dapsens, C. Mondelli and J. Pérez-Ramírez, *ACS Catal.*, 2012, 2, 1487-1499.
84. J. J. Bozell and G. R. Petersen, *Green Chem.*, 2010, 12, 539.
85. T. M. Carole, J. Pellegrino and M. D. Paster, *Appl. Biochem. Biotechnol.*, 2004, 113-116, 871-885.
86. T. J. Schwartz, B. J. O'Neill, B. H. Shanks and J. A. Dumesic, *ACS Catal.*, 2014, 4, 2060-2069.
87. R. Beerthuis, G. Rothenberg and N. R. Shiju, *Green Chem.*, 2015, 17, 1341-1361.
88. J. Rass-Hansen, H. Falsig, B. Jørgensen and C. H. Christensen, *J. Chem. Technol. Biotechnol.*, 2007, 82, 329-333.
89. J. A. Posada, A. D. Patel, A. Roes, K. Blok, A. P. Faaij and M. K. Patel, *Bioresour. Technol.*, 2013, 135, 490-499.
90. J. M. R. Gallo, J. M. C. Bueno and U. Schuchardt, *J. Braz. Chem. Soc.*, 2014.
91. N. Ladygina, E. G. Dedyukhina and M. B. Vainshtein, *Process Biochem.*, 2006, 41, 1001-1014.
92. B. N. van Leeuwen, A. M. van der Wulp, I. Duijnstee, A. J. van Maris and A. J. Straathof, *Appl. Microbiol. Biotechnol.*, 2012, 93, 1377-1387.
93. J. Yang, G. Zhao, Y. Sun, Y. Zheng, X. Jiang, W. Liu and M. Xian, *Bioresour. Technol.*, 2012, 104, 642-647.
94. J. D. Keasling, *Metab. Eng.*, 2012, 14, 189-195.
95. J. M. Clomburg and R. Gonzalez, *Appl. Microbiol. Biotechnol.*, 2010, 86, 419-434.
96. V. G. Yadav, M. De Mey, C. G. Lim, P. K. Ajikumar and G. Stephanopoulos, *Metab. Eng.*, 2012, 14, 233-241.
97. J. N. Chheda and J. A. Dumesic, *Catal. Today*, 2007, 123, 59-70.
98. T. Polen, M. Spelberg and M. Bott, *J. Biotechnol.*, 2013, 167, 75-84.
99. N. Thongchul, in *Bioprocessing Technologies in Biorefinery for Sustainable Production of Fuels, Chemicals, and Polymers*, eds. S. T. Yang, H. A. El-Enshasy and N. Thongchul, 2013, ch. 16, pp. 293-316.
100. A. Cukalovic and C. V. Stevens, *Biofuel, Bioprod. Bior.*, 2008, 2, 505-529.
101. K. Zhang, B. Zhang and S.-T. Yang, in *Bioprocessing Technologies in Biorefinery for Sustainable Production of Fuels, Chemicals, and Polymers*, eds. S. T. Yang, H. A. El-Enshasy and N. Thongchul, 2013, ch. 20, pp. 375-398.
102. K. N. Valdehuesa, H. Liu, G. M. Nisola, W. J. Chung, S. H. Lee and S. J. Park, *Appl. Microbiol. Biotechnol.*, 2013, 97, 3309-3321.
103. R. K. Saxena, P. Anand, S. Saran and J. Isar, *Biotechnol. Adv.*, 2009, 27, 895-913.
104. G. Kaur, A. K. Srivastava and S. Chand, *Biochem. Eng. J.*, 2012, 64, 106-118.
105. A. P. Zeng and W. Sabra, *Curr. Opin. Biotechnol.*, 2011, 22, 749-757.
106. V. C. Ghantani, S. T. Lomate, M. K. Dongare and S. B. Umbarkar, *Green Chem.*, 2013, 15, 1211.

107. J. Le Notre, S. C. Witte-van Dijk, J. van Haveren, E. L. Scott and J. P. Sanders, *ChemSusChem*, 2014, 7, 2712-2720.
108. J. P. Lange, E. van der Heide, J. van Buijtenen and R. Price, *ChemSusChem*, 2012, 5, 150-166.
109. R.-J. van Putten, A. S. Dias and E. de Jong, in *Catalytic Process Development for Renewable Materials*, eds. P. Imhof and J. C. v. d. Waal, 2013, ch. 4, pp. 81-117.
110. R. J. van Putten, J. C. van der Waal, E. de Jong, C. B. Rasrendra, H. J. Heeres and J. G. de Vries, *Chem. Rev.*, 2013, 113, 1499-1597.
111. S. P. Simeonov, J. A. Coelho and C. A. Afonso, *ChemSusChem*, 2012, 5, 1388-1391.
112. O. Casanova, S. Iborra and A. Corma, *ChemSusChem*, 2009, 2, 1138-1144.
113. E. Taarning, I. S. Nielsen, K. Egeblad, R. Madsen and C. H. Christensen, *ChemSusChem*, 2008, 1, 75-78.
114. B. Liu, Y. Ren and Z. Zhang, *Green Chem.*, 2015, 17, 1610-1617.
115. W. P. Dijkman, C. Binda, M. W. Fraaije and A. Mattevi, *ACS Catal.*, 2015, 5, 1833-1839.
116. M. Sajid, X. Zhao and D. Liu, *Green Chem.*, 2018, 20, 5427-5453.
117. M. Mascal and E. B. Nikitin, *Green Chem.*, 2010, 12, 370-373.
118. S. K. Burgess, R. M. Kriegel and W. J. Koros, *Macromolecules*, 2015, 48, 2184-2193.
119. G. J. M. Gruter and F. Dautzenberg, *Eur. Pat 1834950A1 and Eur. Pat 1834951A1*, 2007.
120. G. J. M. Gruter and F. Dautzenberg, *EP Pat. 1834950 and EP Pat. 1834951*, 2007.
121. A. J. Ragauskas, G. T. Beckham, M. J. Biddy, R. Chandra, F. Chen, M. F. Davis, B. H. Davison, R. A. Dixon, P. Gilna, M. Keller, P. Langan, A. K. Naskar, J. N. Saddler, T. J. Tschaplinski, G. A. Tuskan and C. E. Wyman, *Science*, 2014, 344, 1246843.
122. J. Gierer, *Wood Sci. Technol.*, 1980, 14, 241-266.
123. F. S. Chakar and A. J. Ragauskas, *Ind. Crops Prod.*, 2004, 20, 131-141.
124. F. Chen, Y. Tobimatsu, L. Jackson, J. Nakashima, J. Ralph and R. A. Dixon, *Plant J.*, 2013, 73, 201-211.
125. J. K. Weng, H. Mo and C. Chapple, *Plant J.*, 2010, 64, 898-911.
126. N. D. Bonawitz, J. I. Kim, Y. Tobimatsu, P. N. Ciesielski, N. A. Anderson, E. Ximenes, J. Maeda, J. Ralph, B. S. Donohoe, M. Ladisch and C. Chapple, *Nature*, 2014, 509, 376-380.
127. F. Chen, Y. Tobimatsu, D. Havkin-Frenkel, R. A. Dixon and J. Ralph, *Proc. Natl. Acad. Sci. U.S.A.*, 2012, 109, 1772-1777.
128. A. Eudes, A. George, P. Mukerjee, J. S. Kim, B. Pollet, P. I. Benke, F. Yang, P. Mitra, L. Sun, O. P. Cetinkol, S. Chabout, G. Mouille, L. Soubigou-Taconnat, S. Balzergue, S. Singh, B. M. Holmes, A. Mukhopadhyay, J. D. Keasling, B. A. Simmons, C. Lapierre, J. Ralph and D. Loque, *Plant Biotechnol. J.*, 2012, 10, 609-620.
129. Y. Tobimatsu, F. Chen, J. Nakashima, L. L. Escamilla-Trevino, L. Jackson, R. A. Dixon and J. Ralph, *Plant Cell*, 2013, 25, 2587-2600.
130. C. Lapierre, B. Pollet, M. Petit-Conil, G. Toval, J. Romero, G. Pilate, J. C. Leple, W. Boerjan, V. V. Ferret, V. De Nadai and L. Jouanin, *Plant Physiol.*, 1999, 119, 153-164.
131. S. E. Sattler, A. J. Saathoff, E. J. Haas, N. A. Palmer, D. L. Funnell-Harris, G. Sarath and J. F. Pedersen, *Plant Physiol*, 2009, 150, 584-595.
132. Q. Zhao, Y. Tobimatsu, R. Zhou, S. Pattathil, L. Gallego-Giraldo, C. Fu, L. A. Jackson, M. G. Hahn, H. Kim, F. Chen, J. Ralph and R. A. Dixon, *Proc. Natl. Acad. Sci. U.S.A.*, 2013, 110, 13660-13665.
133. L. Li, Y. Zhou, X. Cheng, J. Sun, J. M. Marita, J. Ralph and V. L. Chiang, *Proc. Natl. Acad. Sci. U.S.A.*, 2003, 100, 4939-4944.
134. R. Franke, M. R. Hemm, J. W. Denault, M. O. Ruegger, J. M. Humphreys and C. Chapple, *Plant J.*, 2002, 30, 47-59.
135. A. Ziebell, K. Gracom, R. Katahira, F. Chen, Y. Pu, A. Ragauskas, R. A. Dixon and M. Davis, *J. Biol. Chem.*, 2010, 285, 38961-38968.
136. R. Van Acker, R. Vanholme, V. Storme, J. C. Mortimer, P. Dupree and W. Boerjan, *Biotechnol. Biofuels*, 2013, 6, 46.

137. R. Vanholme, V. Storme, B. Vanholme, L. Sundin, J. H. Christensen, G. Goeminne, C. Halpin, A. Rohde, K. Morreel and W. Boerjan, *Plant Cell*, 2012, 24, 3506-3529.
138. C. G. Wilkerson, S. D. Mansfield, F. Lu, S. Withers, J. Y. Park, S. D. Karlen, E. Gonzales-Vigil, D. Padmakshan, F. Unda, J. Rencoret and J. Ralph, *Science*, 2014, 344, 90-93.
139. S. Jung, M. Foston, U. C. Kalluri, G. A. Tuskan and A. J. Ragauskas, *Angew. Chem. Int. Ed.*, 2012, 51, 12005-12008.
140. C. Zhou, Q. Li, V. L. Chiang, L. A. Lucia and D. P. Griffis, *Anal. Chem.*, 2011, 83, 7020-7026.
141. Y. Tobimatsu, A. Wagner, L. Donaldson, P. Mitra, C. Niculaes, O. Dima, J. I. Kim, N. Anderson, D. Loque, W. Boerjan, C. Chapple and J. Ralph, *Plant J.*, 2013, 76, 357-366.
142. S. Kiyoto, A. Yoshinaga, N. Tanaka, M. Wada, H. Kamitakahara and K. Takabe, *Planta*, 2013, 237, 705-715.
143. L. Tetard, A. Passian, S. Jung, A. J. Ragauskas and B. H. Davison, *Ind. Biotechnol. (New Rochelle NY)*, 2012, 8, 245-249.
144. M. Li, C. Foster, S. Kelkar, Y. Pu, D. Holmes, A. Ragauskas, C. M. Saffron and D. B. Hodge, *Biotechnol. Biofuels*, 2012, 5, 38.
145. K. M. Holtman, H. M. Chang, H. Jameel and J. F. Kadla, *J. Agric. Food. Chem.*, 2003, 51, 3535-3540.
146. L. Petridis, R. Schulz and J. C. Smith, *J. Am. Chem. Soc.*, 2011, 133, 20277-20287.
147. S. E. Harton, S. V. Pingali, G. A. Nunnery, D. A. Baker, S. H. Walker, D. C. Muddiman, T. Koga, T. G. Rials, V. S. Urban and P. Langan, *ACS Macro Lett.*, 2012, 1, 568-573.
148. V. K. Ponnusamy, D. D. Nguyen, J. Dharmaraja, S. Shobana, J. R. Banu, R. G. Saratale, S. W. Chang and G. Kumar, *Bioresour. Technol.*, 2019, 271, 462-472.
149. W. Schutyser, T. Renders, S. Van den Bosch, S. F. Koelewijn, G. T. Beckham and B. F. Sels, *Chem. Soc. Rev.*, 2018, 47, 852-908.
150. J. Zakzeski, P. C. Bruijnincx, A. L. Jongerius and B. M. Weckhuysen, *Chem. Rev.*, 2010, 110, 3552-3599.
151. S. Van den Bosch, S. F. Koelewijn, T. Renders, G. Van den Bossche, T. Vangeel, W. Schutyser and B. F. Sels, *Top. Curr. Chem.*, 2018, 376, 36.
152. L. Das, P. Kolar and R. Sharma-Shivappa, *Biofuels*, 2014, 3, 155-166.
153. P. R. Patwardhan, R. C. Brown and B. H. Shanks, *ChemSusChem*, 2011, 4, 1629-1636.
154. W. Mu, H. Ben, A. Ragauskas and Y. Deng, *Bioenergy Res.*, 2013, 6, 1183-1204.
155. D. J. Nowakowski, A. V. Bridgwater, D. C. Elliott, D. Meier and P. de Wild, *J. Anal. Appl. Pyrolysis*, 2010, 88, 53-72.
156. D. L. Gall, W. S. Kontur, W. Lan, H. Kim, Y. Li, J. Ralph, T. J. Donohue and D. R. Noguera, *Appl. Environ. Microbiol.*, 2018, 84.
157. V. Hamalainen, T. Gronroos, A. Suonpaa, M. W. Heikkila, B. Romein, P. Ihalainen, S. Malandra and K. R. Birikh, *Front. Bioeng. Biotechnol.*, 2018, 6, 20.
158. M. U. Khan and B. K. Ahring, *Biomass Bioenergy*, 2019, 128, 105325.
159. A. T. Martinez, M. Speranza, F. J. Ruiz-Duenas, P. Ferreira, S. Camarero, F. Guillen, M. J. Martinez, A. Gutierrez and J. C. del Rio, *Int. Microbiol.*, 2005, 8, 195-204.
160. T. D. Bugg, M. Ahmad, E. M. Hardiman and R. Singh, *Curr. Opin. Biotechnol.*, 2011, 22, 394-400.
161. D. Salvachua, A. Prieto, M. Lopez-Abelairas, T. Lu-Chau, A. T. Martinez and M. J. Martinez, *Bioresour. Technol.*, 2011, 102, 7500-7506.
162. M. Monrroy, I. Ortega, M. Ramirez, J. Baeza and J. Freer, *Enzyme Microb. Technol.*, 2011, 49, 472-477.
163. Z. Sun, B. Fridrich, A. de Santi, S. Elangovan and K. Barta, *Chem. Rev.*, 2018, 118, 614-678.
164. G. de Gonzalo, D. I. Colpa, M. H. Habib and M. W. Fraaije, *J. Biotechnol.*, 2016, 236, 110-119.
165. M. E. Brown and M. C. Chang, *Curr. Opin. Chem. Biol.*, 2014, 19, 1-7.
166. G. Janusz, A. Pawlik, J. Sulej, U. Swiderska-Burek, A. Jarosz-Wilkolazka and A. Paszczynski, *FEMS Microbiol. Rev.*, 2017, 41, 941-962.

167. C. Xu, R. A. Arancon, J. Labidi and R. Luque, *Chem. Soc. Rev.*, 2014, 43, 7485-7500.
168. G. T. Beckham, C. W. Johnson, E. M. Karp, D. Salvachua and D. R. Vardon, *Curr. Opin. Biotechnol.*, 2016, 42, 40-53.
169. W. Lan and J. S. Luterbacher, *Chimia*, 2019, 73, 591-598.
170. W. Lan and J. S. Luterbacher, *ACS Cent. Sci*, 2019, 5, 1642-1644.
171. W. Lan, M. T. Amiri, C. M. Hunston and J. S. Luterbacher, *Angew. Chem. Int. Ed.*, 2018, 57, 1356-1360.
172. Z. Sun, G. Bottari, A. Afanasenko, M. C. A. Stuart, P. J. Deuss, B. Fridrich and K. Barta, *Nat. Catal.*, 2018, 1, 82-92.
173. D. A. Baker and T. G. Rials, *J. Appl. Polym. Sci.*, 2013, 130, 713-728.
174. I. Norberg, Y. Nordström, R. Drougge, G. Gellerstedt and E. Sjöholm, *J. Appl. Polym. Sci.*, 2013, 128, 3824-3830.
175. M. Foston, G. A. Nunnery, X. Meng, Q. Sun, F. S. Baker and A. Ragauskas, *Carbon*, 2013, 52, 65-73.
176. J. Rajesh Banu, S. Kavitha, R. Yukesh Kannah, T. Poornima Devi, M. Gunasekaran, S. H. Kim and G. Kumar, *Bioresour. Technol.*, 2019, 290, 121790.
177. H. Chung and N. R. Washburn, *Green Mater.*, 2013, 1, 137-160.
178. S. Elangovan, A. Afanasenko, J. Haupenthal, Z. Sun, Y. Liu, A. K. H. Hirsch and K. Barta, *ACS Cent. Sci*, 2019, 5, 1707-1716.
179. J. L. C. Iara F. Demuner, Antonio J. Demuner, and Carolina M. Jardim, *BioResources*, 2019, 14, 7543-7581.
180. Y. Yang, W. Y. Song, H. G. Hur, T. Y. Kim and S. Ghatge, *Int. J. Biol. Macromol.*, 2019, 124, 200-208.
181. M. P. Pandey and C. S. Kim, *Chem. Eng. Technol.*, 2011, 34, 29-41.
182. J. D. P. Araújo, C. A. Grande and A. E. Rodrigues, *Chem. Eng. Res. Des.*, 2010, 88, 1024-1032.
183. R. de Regil and G. Sandoval, *Biomolecules*, 2013, 3, 812-847.
184. R. A. Sheldon and J. M. Woodley, *Chem. Rev.*, 2018, 118, 801-838.
185. J. L. Tucker and M. M. Faul, *Nature*, 2016, 534, 27-29.
186. S. Heux, I. Meynial-Salles, M. J. O'Donohue and C. Dumon, *Biotechnol. Adv.*, 2015, 33, 1653-1670.
187. R. A. Sheldon and D. Brady, *ChemSusChem*, 2019, 12, 2859-2881.
188. S. E. Milner and A. R. Maguire, *Arkivoc*, 2012, 2012, 321-382.
189. R. Wohlgemuth, *Curr. Opin. Biotechnol.*, 2010, 21, 713-724.
190. J. Vilim, T. Knaus and F. G. Mutti, *Angew. Chem. Int. Ed.*, 2018, 57, 14240-14244.
191. A. Peracchi, *Trends Biochem. Sci*, 2018, 43, 984-996.
192. S. D. Copley, *Curr. Opin. Struct. Biol.*, 2017, 47, 167-175.
193. N. J. Turner, *Nat. Chem. Biol.*, 2009, 5, 567-573.
194. M. T. Reetz, *J. Am. Chem. Soc.*, 2013, 135, 12480-12496.
195. C. A. Tracewell and F. H. Arnold, *Curr. Opin. Chem. Biol.*, 2009, 13, 3-9.
196. U. T. Bornscheuer, G. W. Huisman, R. J. Kazlauskas, S. Lutz, J. C. Moore and K. Robins, *Nature*, 2012, 485, 185-194.
197. A. Illanes, A. Cauerhff, L. Wilson and G. R. Castro, *Bioresour. Technol.*, 2012, 115, 48-57.
198. M. T. Reetz, *J. Org. Chem.*, 2009, 74, 5767-5778.
199. S. Luetz, L. Giver and J. Lalonde, *Biotechnol. Bioeng.*, 2008, 101, 647-653.
200. J. M. Woodley, *Curr. Opin. Chem. Biol.*, 2013, 17, 310-316.
201. V. Tseliou, T. Knaus, M. F. Masman, M. L. Corrado and F. G. Mutti, *Nat. Commun.*, 2019, 10, 3717.
202. R. A. Sheldon and D. Brady, *Chem. Commun.*, 2018, 54, 6088-6104.
203. S. Aslan, E. Noor and A. Bar-Even, *Biochem. J.*, 2017, 474, 3935-3950.
204. M. D. Truppo, *ACS Med. Chem. Lett.*, 2017, 8, 476-480.

205. F. Garzon-Posse, L. Becerra-Figueroa, J. Hernandez-Arias and D. Gamba-Sanchez, *Molecules*, 2018, 23.
206. J. Wachtmeister and D. Rother, *Curr. Opin. Biotechnol.*, 2016, 42, 169-177.
207. P. r. Tufvesson, J. Lima-Ramos, M. Nordblad and J. M. Woodley, *Org. Process Res. Dev.*, 2011, 15, 266-274.
208. J. Schuurmann, P. Quehl, G. Festel and J. Jose, *Appl. Microbiol. Biotechnol.*, 2014, 98, 8031-8046.
209. J. K. Sakkos, L. P. Wackett and A. Aksan, *Sci. Rep.*, 2019, 9, 3158.
210. B. Lin and Y. Tao, *Microb. Cell Fact.*, 2017, 16, 106.
211. J. A. Houwman, T. Knaus, M. Costa and F. G. Mutti, *Green Chem.*, 2019, 21, 3846-3857.
212. T. Knaus, W. Böhmer and F. G. Mutti, *Green Chem.*, 2017, 19, 453-463.
213. T. Sehl, H. C. Hailes, J. M. Ward, R. Wardenga, E. von Lieres, H. Offermann, R. Westphal, M. Pohl and D. Rother, *Angew. Chem. Int. Ed.*, 2013, 52, 6772-6775.
214. F. Guo and P. Berglund, *Green Chem.*, 2017, 19, 333-360.
215. M. Fuchs, J. E. Farnberger and W. Kroutil, *Eur. J. Org. Chem.*, 2015, 2015, 6965-6982.
216. R. C. Simon, N. Richter, E. Busto and W. Kroutil, *ACS Catal.*, 2013, 4, 129-143.
217. N. Richter, J. E. Farnberger, D. Pressnitz, H. Lechner, F. Zepeck and W. Kroutil, *Green Chem.*, 2015, 17, 2952-2958.
218. R. A. Sheldon and S. van Pelt, *Chem. Soc. Rev.*, 2013, 42, 6223-6235.
219. M. P. Thompson, S. R. Derrington, R. S. Heath, J. L. Porter, J. Mangas-Sanchez, P. N. Devine, M. D. Truppo and N. J. Turner, *Tetrahedron*, 2019, 75, 327-334.
220. J. Britton, S. Majumdar and G. A. Weiss, *Chem. Soc. Rev.*, 2018, 47, 5891-5918.
221. W. Bohmer, T. Knaus, A. Volkov, T. K. Slot, N. R. Shiju, K. Engelmark Cassimjee and F. G. Mutti, *J. Biotechnol.*, 2019, 291, 52-60.
222. M. P. Thompson, I. Peñafiel, S. C. Cosgrove and N. J. Turner, *Org. Process Res. Dev.*, 2018, 23, 9-18.
223. J. M. Sperl and V. Sieber, *ACS Catal.*, 2018, 8, 2385-2396.
224. R. A. Sheldon, in *Multi-Step Enzyme Catalysis: Biotransformations and Chemoenzymatic Synthesis*, ed. E. Garcia-Junceda, Wiley-VCH, 2008, ch. 6, pp. 109-135.
225. A. Bruggink, R. Schoevaart and T. Kieboom, *Org. Process Res. Dev.*, 2003, 7, 622-640.
226. R. A. Sheldon and P. C. Pereira, *Chem. Soc. Rev.*, 2017, 46, 2678-2691.
227. R. Abu and J. M. Woodley, *ChemCatChem*, 2015, 7, 3094-3105.
228. A. Bruggink, A. J. Straathof and L. A. van der Wielen, *Adv. Biochem. Eng. Biotechnol.*, 2003, 80, 69-113.
229. E. Ricca, B. Brucher and J. H. Schrittwieser, *Adv. Synth. Catal.*, 2011, 353, 2239-2262.
230. J. H. Schrittwieser, S. Velikogne, M. Hall and W. Kroutil, *Chem. Rev.*, 2018, 118, 270-348.
231. V. Kohler, Y. M. Wilson, M. Durrenberger, D. Ghislieri, E. Churakova, T. Quinto, L. Knorr, D. Haussinger, F. Hollmann, N. J. Turner and T. R. Ward, *Nat. Chem.*, 2013, 5, 93-99.
232. J. H. Schrittwieser, F. Coccia, S. Kara, B. Grischek, W. Kroutil, N. d'Alessandro and F. Hollmann, *Green Chem.*, 2013, 15, 3318.
233. F. Rudroff, M. D. Mihovilovic, H. Gröger, R. Snajdrova, H. Iding and U. T. Bornscheuer, *Nat. Catal.*, 2018, 1, 12-22.
234. S. Gandomkar, A. Żądło-Dobrowolska and W. Kroutil, *ChemCatChem*, 2018, 11, 225-243.
235. S. Wu, Y. Zhou and Z. Li, *Chem. Commun.*, 2019, 55, 883-896.
236. Y. Zhou, S. Wu and Z. Li, *Angew. Chem. Int. Ed.*, 2016, 55, 11647-11650.
237. Z. Li, S. Wu and J. Liu, *Synlett*, 2016, 27, 2644-2658.
238. S. Wu, Y. Chen, Y. Xu, A. Li, Q. Xu, A. Glieder and Z. Li, *ACS Catal.*, 2014, 4, 409-420.
239. S. Wu and Z. Li, *ChemCatChem*, 2018, 10, 2164-2178.
240. S. Wu, J. Liu and Z. Li, *ACS Catal.*, 2017, 7, 5225-5233.
241. S. Wu, Y. Zhou, T. Wang, H. P. Too, D. I. Wang and Z. Li, *Nat. Commun.*, 2016, 7, 11917.
242. J. Zhang, S. Wu, J. Wu and Z. Li, *ACS Catal.*, 2014, 5, 51-58.

243. B. S. Sekar, B. R. Lukito and Z. Li, *ACS Sustain. Chem. Eng.*, 2019.
244. B. R. Lukito, B. S. Sekar, S. Wu and Z. Li, *Adv. Synth. Catal.*, 2019, 361, 3560-3568.
245. Y. Zhou, S. Wu and Z. Li, *Adv. Synth. Catal.*, 2017, 359, 4305-4316.
246. S. Wu, Y. Zhou, D. Seet and Z. Li, *Adv. Synth. Catal.*, 2017, 359, 2132-2141.
247. A. Li, S. Wu, J. P. Adams, R. Snajdrova and Z. Li, *Chem. Commun.*, 2014, 50, 8771.
248. E. Tassano and M. Hall, *Chem. Soc. Rev.*, 2019, 48, 5596-5615.
249. J. H. Schrittwieser, J. Sattler, V. Resch, F. G. Mutti and W. Kroutil, *Curr. Opin. Chem. Biol.*, 2011, 15, 249-256.
250. T. Knaus, F. G. Mutti, L. D. Humphreys, N. J. Turner and N. S. Scrutton, *Org. Biomol. Chem.*, 2015, 13, 223-233.
251. T. Knaus and F. G. Mutti, *Chim. Oggi-Chem. Today*, 2017, 35, 34-37.
252. M. H. S. A. Hamid, P. A. Slatford and J. M. J. Williams, *Adv. Synth. Catal.*, 2007, 349, 1555-1575.
253. F. G. Mutti, T. Knaus, N. S. Scrutton, M. Breuer and N. J. Turner, *Science*, 2015, 349, 1525-1529.
254. W. Bohmer, T. Knaus and F. G. Mutti, *ChemCatChem*, 2018, 10, 731-735.
255. M. P. Thompson and N. J. Turner, *ChemCatChem*, 2017, 9, 3833-3836.
256. M. L. Corrado, T. Knaus and F. G. Mutti, *Green Chem.*, 2019, 21, 6246-6251.
257. R. C. Simon, N. Richter and W. Kroutil, in *Cascade Biocatalysis: Integrating Stereoselective and Environmentally Friendly Reactions*, eds. S. Riva and W. D. Fessner, 2014, ch. 4, pp. 65-86.
258. J. Dong, E. Fernandez-Fueyo, F. Hollmann, C. E. Paul, M. Pesic, S. Schmidt, Y. Wang, S. Younes and W. Zhang, *Angew. Chem. Int. Ed.*, 2018, 57, 9238-9261.
259. E. García-Junceda, I. Lavandera, D. Rother and J. H. Schrittwieser, *J. Mol. Catal. B: Enzym.*, 2015, 114, 1-6.
260. S. P. France, L. J. Hepworth, N. J. Turner and S. L. Flitsch, *ACS Catal.*, 2016, 7, 710-724.
261. L. Leemans, L. van Langen, F. Hollmann and A. Schallmey, *Catalysts*, 2019, 9, 522.
262. L. Huang, G. V. Sayoga, F. Hollmann and S. Kara, *ACS Catal.*, 2018, 8, 8680-8684.
263. F. Hollmann, S. Kara, D. J. Opperman and Y. Wang, *Chem. Asian J.*, 2018, 13, 3601-3610.
264. M. Pesic, S. J. Willot, E. Fernandez-Fueyo, F. Tieves, M. Alcalde and F. Hollmann, *Z. Naturforsch. C: Biosci.*, 2019, 74, 101-104.
265. J. I. Ramsden, R. S. Heath, S. R. Derrington, S. L. Montgomery, J. Mangas-Sanchez, K. R. Mulholland and N. J. Turner, *J. Am. Chem. Soc.*, 2019, 141, 1201-1206.
266. F. Parmeggiani, A. Rué Casamajo, C. J. W. Walton, J. L. Galman, N. J. Turner and R. A. Chica, *ACS Catal.*, 2019, 9, 3482-3486.
267. M. Seitz, J. Klebensberger, S. Siebenhaller, M. Breuer, G. Siedenburg, D. Jendrossek and B. Hauer, *J. Mol. Catal. B: Enzym.*, 2012, 84, 72-77.
268. M. Seitz, P. O. Syren, L. Steiner, J. Klebensberger, B. M. Nestl and B. Hauer, *ChemBioChem*, 2013, 14, 436-439.
269. T. Furuya, M. Kuroiwa and K. Kino, *J. Biotechnol.*, 2017, 243, 25-28.
270. M. Tavanti, J. Mangas-Sanchez, S. L. Montgomery, M. P. Thompson and N. J. Turner, *Org. Biomol. Chem.*, 2017, 15, 9790-9793.
271. A. Pennec, F. Hollmann, M. S. Smit and D. J. Opperman, *ChemCatChem*, 2015, 7, 236-239.
272. V. Erdmann, B. R. Lichman, J. Zhao, R. C. Simon, W. Kroutil, J. M. Ward, H. C. Hailes and D. Rother, *Angew. Chem. Int. Ed.*, 2017, 56, 12503-12507.
273. S. C. Stinson, *Chem. Eng. News*, 1992, 70, 46-79.
274. S. W. Smith, *Toxicol. Sci.*, 2009, 110, 4-30.
275. K. Faber, in *Biotransformations in Organic Chemistry*, Springer, 7th edn., 2018, ch. 1, pp. 1-30.
276. H. Gröger and Y. Asano, in *Enzyme Catalysis in Organic Synthesis*, eds. K. Drauz, H. Gröger and O. May, Wiley-VCH, 2012, ch. 1, pp. 1-42.

277. W. L. J. Wang, in *Chiral Drugs: Chemistry and Biological Action*, eds. G. Q. Lin, Q. D. You and J. F. Cheng, John Wiley & Sons, Inc., 2011, ch. 3, pp. 77–136.
278. A. Schmid, J. S. Dordick, B. Hauer, A. Kiener, M. Wubbolts and B. Witholt, *Nature*, 2001, 409, 258-268.
279. J. M. Choi, S. S. Han and H. S. Kim, *Biotechnol. Adv.*, 2015, 33, 1443-1454.
280. G. W. Huisman and S. J. Collier, *Curr. Opin. Chem. Biol.*, 2013, 17, 284-292.
281. P. Hoyos, V. Pace, M. Hernaiz and A. Alcantara, *Curr. Green Chem.*, 2014, 1, 155-181.
282. R. A. Sheldon, *Chem. Eur. J.*, 2016, 22, 12984-12999.
283. A. Zaks and A. M. Klibanov, *Science*, 1984, 224, 1249-1251.
284. M. C. Bryan, P. J. Dunn, D. Entwistle, F. Gallou, S. G. Koenig, J. D. Hayler, M. R. Hickey, S. Hughes, M. E. Kopach, G. Moine, P. Richardson, F. Roschangar, A. Steven and F. J. Weiberth, *Green Chem.*, 2018, 20, 5082-5103.
285. H. Sun, H. Zhang, E. L. Ang and H. Zhao, *Bioorg. Med. Chem.*, 2018, 26, 1275-1284.
286. L. A. H. a. J. H. Roskam, *Eur. Pat. Appl, EP343714A119891129*, 1989.
287. R. A. Sheldon, *J. Chem. Technol. Biotechnol.*, 1996, 67, 1-14.
288. R. Fernandez-Lafuente, *J. Mol. Catal. B: Enzym.*, 2010, 62, 197-212.
289. E. M. M. Abdelraheem, H. Busch, U. Hanefeld and F. Tonin, *React. Chem. Eng.*, 2019, 4, 1878-1894.
290. K. Rosenthal and S. Lütz, *Curr. Opin. Green Sustain. Chem.*, 2018, 11, 58-64.
291. R. N. Patel, *Bioorg. Med. Chem.*, 2018, 26, 1252-1274.
292. R. C. Simon, F. G. Mutti and W. Kroutil, *Drug Discov. Today Technol.*, 2013, 10, e37-44.
293. A. P. Green and N. J. Turner, *Perspect. Sci.*, 2016, 9, 42-48.
294. C. K. Savile, J. M. Janey, E. C. Mundorff, J. C. Moore, S. Tam, W. R. Jarvis, J. C. Colbeck, A. Krebber, F. J. Fleitz, J. Brands, P. N. Devine, G. W. Huisman and G. J. Hughes, *Science*, 2010, 329, 305-309.
295. S. K. Ma, J. Gruber, C. Davis, L. Newman, D. Gray, A. Wang, J. Grate, G. W. Huisman and R. A. Sheldon, *Green Chem.*, 2010, 12, 81-86.
296. J. Liang, J. Lalonde, B. Borup, V. Mitchell, E. Mundorff, N. Trinh, D. A. Kochrekar, R. Nair Cherat and G. G. Pai, *Org. Process Res. Dev.*, 2010, 14, 193-198.
297. S.-i. Yamada, I. Tsujioka, T. Shibatani and R. Yoshioka, *Chem. Pharm. Bull.*, 1999, 47, 146-150.
298. Y. Ohta and I. Shinkai, *Biorg. Med. Chem.*, 1997, 5, 465-466.
299. H. Umezawa, T. Aoyagi, H. Suda, M. Hamada and T. Takeuchi, *J. Antibiot.*, 1976, 29, 97-99.
300. M. E. Jung and S. W. Yi, *Tetrahedron Lett.*, 2012, 53, 4216-4220.
301. O. K. Karjalainen and A. M. Koskinen, *Org. Biomol. Chem.*, 2012, 10, 4311-4326.
302. S. C. Bergmeier, *Tetrahedron*, 2000, 56, 2561-2576.
303. D. J. Ager, I. Prakash and D. R. Schaad, *Chem. Rev.*, 1996, 96, 835-876.
304. J. A. Bodkin and M. D. McLeod, *J. Chem. Soc., Perkin Trans. 1*, 2002, 2733-2746.
305. O. R. Dmitry Nilov, *Adv. Synth. Catal.*, 2002, 344, 1169-1173.
306. D. S. Bhagavathula, G. Boddeti and R. Venu, *R.R.J.Chem.*, 2017, 6, 27-46.
307. T. J. Donohoe, C. K. Callens, A. Flores, A. R. Lacy and A. H. Rathi, *Chem. Eur. J.*, 2011, 17, 58-76.
308. C. Liu, J. Weng, Z.-H. Lin, W.-J. Huang, J. Guo, L.-J. Huang and G. Lu, *Tetrahedron: Asymmetry*, 2017, 28, 41-46.
309. G. Veeresha and A. Datta, *Tetrahedron Lett.*, 1997, 38, 5223-5224.
310. T. Laïb, J. Chastanet and J. Zhu, *J. Org. Chem.*, 1998, 63, 1709-1713.
311. O. Schwardt, *Synthesis*, 1999, 1999, 1473-1490.
312. G. K. Friestad, *Org. Lett.*, 1999, 1, 1499-1501.
313. N. A. Petasis and I. A. Zavialov, *J. Am. Chem. Soc.*, 1998, 120, 11798-11799.
314. S. C. Bergmeier and P. P. Seth, *J. Org. Chem.*, 1997, 62, 2671-2674.
315. M. R. Paleo, M. I. Calaza and F. J. Sardina, *J. Org. Chem.*, 1997, 62, 6862-6869.

316. S.-K. Chung and J.-M. Lee, *Tetrahedron: Asymmetry*, 1999, 10, 1441-1444.
317. M. Haddad, C. Botuha and M. Larchevêque, *Synlett*, 1999, 1999, 1118-1120.
318. H. Sasai, T. Tokunaga, S. Watanabe, T. Suzuki, N. Itoh and M. Shibasaki, *J. Org. Chem.*, 1995, 60, 7388-7389.
319. M. Horikawa, J. Busch-Petersen and E. J. Corey, *Tetrahedron Lett.*, 1999, 40, 3843-3846.
320. S. Kobayashi, H. Ishitani and M. Ueno, *J. Am. Chem. Soc.*, 1998, 120, 431-432.
321. F. Machrouhi and J.-L. Namy, *Tetrahedron Lett.*, 1999, 40, 1315-1318.
322. S.-K. Kang, T.-G. Baik and Y. Hur, *Tetrahedron*, 1999, 55, 6863-6870.
323. S. T. Masanari Kimura, and Yoshinao Tamaru, *J. Org. Chem*, 1995, 60, 3764-3772.
324. R. A. T. M. Van Benthem, H. Hiemstra and W. N. Speckamp, *J. Org. Chem.*, 1992, 57, 6083-6085.
325. H. G. Brunker and W. Adam, *J. Am. Chem. Soc.*, 1995, 117, 3976-3982.
326. W. Adam and H.-G. Brünker, *Synthesis*, 1995, 1995, 1066-1068.
327. P. Gupta and N. Mahajan, *New J. Chem.*, 2018, 42, 12296-12327.
328. L. Keinicke, P. Fristrup, P. O. Norrby and R. Madsen, *J. Am. Chem. Soc.*, 2005, 127, 15756-15761.
329. T. Sehl, Z. Maugeri and D. Rother, *J. Mol. Catal. B: Enzym.*, 2015, 114, 65-71.
330. X. Wu, M. Fei, Y. Chen, Z. Wang and Y. Chen, *Appl. Microbiol. Biotechnol.*, 2014, 98, 7399-7408.
331. K. Smithies, M. E. B. Smith, U. Kaulmann, J. L. Galman, J. M. Ward and H. C. Hailes, *Tetrahedron: Asymmetry*, 2009, 20, 570-574.
332. E. Liardo, N. Ríos-Lombardía, F. Morís, F. Rebolledo and J. González-Sabín, *ACS Catal.*, 2017, 7, 4768-4774.
333. H. Yun, J. Kim, K. Kinnera and B. G. Kim, *Biotechnol. Bioeng.*, 2006, 93, 391-395.
334. V. Recuero, G. de Gonzalo, R. Brieva and V. Gotor, *Eur. J. Org. Chem.*, 2006, 2006, 4224-4230.
335. N. M. T. Lourenço, S. Barreiros and C. A. M. Afonso, *Green Chem.*, 2007, 9, 734-736.
336. T. Sehl, H. C. Hailes, J. M. Ward, U. Menyes, M. Pohl and D. Rother, *Green Chem.*, 2014, 16, 3341-3348.
337. C. U. Ingram, M. Bommer, M. E. Smith, P. A. Dalby, J. M. Ward, H. C. Hailes and G. J. Lye, *Biotechnol. Bioeng.*, 2007, 96, 559-569.
338. L. Rios-Solis, P. Morris, C. Grant, A. O. O. Odeleye, H. C. Hailes, J. M. Ward, P. A. Dalby, F. Baganz and G. J. Lye, *Chem. Eng. Sci.*, 2015, 122, 360-372.
339. F.-F. Chen, S. C. Cosgrove, W. R. Birmingham, J. Mangas-Sanchez, J. Citoler, M. P. Thompson, G.-W. Zheng, J.-H. Xu and N. J. Turner, *ACS Catal.*, 2019, 9, 11813-11818.
340. J. S. Yadav, P. T. Reddy, S. Nanda and A. B. Rao, *Tetrahedron: Asymmetry*, 2002, 12, 3381-3385.
341. J. Steinreiber, M. Schurmann, M. Wolberg, F. van Assema, C. Reisinger, K. Fesko, D. Mink and H. Griengl, *Angew. Chem. Int. Ed.*, 2007, 46, 1624-1626.
342. G. Hasnaoui-Dijoux, M. Majeric Elenkov, J. H. Lutje Spelberg, B. Hauer and D. B. Janssen, *ChemBioChem*, 2008, 9, 1048-1051.
343. P. Gupta, S. Bhatia, A. Dhawan, S. Balwani, S. Sharma, R. Brahma, R. Singh, B. Ghosh, V. S. Parmar and A. K. Prasad, *Bioorg. Med. Chem.*, 2011, 19, 2263-2268.
344. H. Buhler, F. Effenberger, S. Forster, J. Roos and H. Wajant, *ChemBioChem*, 2003, 4, 211-216.
345. T. Purkarthofer, K. Gruber, M. Gruber-Khadjawi, K. Waich, W. Skranc, D. Mink and H. Griengl, *Angew. Chem. Int. Ed.*, 2006, 45, 3454-3456.
346. F. Xu, J. Wang, B. Liu, Q. Wu and X. Lin, *Green Chem.*, 2011, 13, 2359.
347. I. Cho, C. K. Prier, Z. J. Jia, R. K. Zhang, T. Görbe and F. H. Arnold, *Angew. Chem. Int. Ed.*, 2019, 131, 3170-3174.

Chapter 2

A Chimeric Styrene Monooxygenase with Increased Efficiency in Asymmetric Biocatalytic Epoxidation

This chapter is based on the following publication:

Maria L. Corrado, Tanja Knaus and Francesco G. Mutti, A Chimeric Styrene Monooxygenase with Increased Efficiency in Asymmetric Biocatalytic Epoxidation, *ChemBioChem*., **2018**, 19 (7), 679-686

Supporting information is available under DOI: 10.1002/cbic.201800119

Abstract. *The styrene monooxygenase (SMO) system from Pseudomonas sp. is constituted by the two enzymes StyA and StyB. StyB catalyzes the reduction of FAD at the expense of NADH. After the transfer of $FADH_2$ from StyB to StyA, reaction with O_2 generates FAD-OOH that is the epoxidizing agent. The waste of redox equivalents due to a partial diffusive transfer of $FADH_2$, the insolubility of recombinant StyB and the impossibility to express StyA and StyB in a 1:1 molar ratio reduce the catalytic efficiency of the natural system. Herein, we present a chimeric SMO (Fus-SMO) that was obtained by genetic fusion of StyA and StyB with a flexible linker. E. coli cells expressing Fus-SMO possess ca. 50% higher activity for the epoxidation of styrene derivatives than E. coli cells expressing separated StyA and StyB as a combination of: i) balanced and improved expression levels of reductase and epoxidase units; ii) intrinsic higher specific epoxidation activity of Fus-SMO in some cases. The epoxidation activity of purified Fus-SMO was up to 3-fold higher than two-component StyA-StyB (1:1, molar ratio) and up to 110-fold higher than natural fused SMO. Determination of coupling efficiency and study on the influence of O_2 pressure were also performed. Finally, Fus-SMO and formate dehydrogenase were coexpressed in E. coli and applied as self-sufficient biocatalytic system for the epoxidation above 500 mg scale.*

2.1 Introduction

Chiral epoxides are important building blocks in organic synthesis because of their high versatility and reactivity towards a variety of reagents. Indeed, they can undergo S_N2 reactions with a large variety of nucleophiles. Furthermore, epoxides find large applications as intermediates for the synthesis of active pharmaceutical ingredients, natural products, flavors and fragrances, other fine chemicals and advanced polymeric materials.[1-22] Moreover, epoxide moieties are also found in naturally occurring APIs, such as epothilones,[23] a class of potential cancer drugs (**Figure 2.1**).

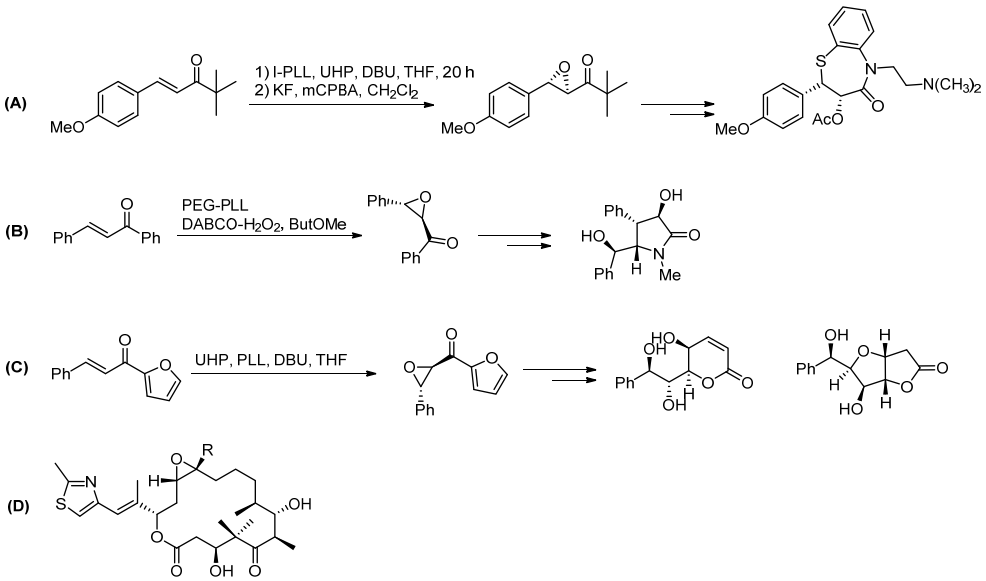

Figure 2.1. Examples of chemical synthesis involving chiral epoxide as key intermediate **(A-C)**; natural bioactive compound carrying an epoxide moiety **(D)**

Chiral epoxides are classically synthesized *via* asymmetric epoxidation of alkenes using Ti(O-*i*Pr)$_4$ (*i.e*. Katsuki-Sharpless)[24] or salen-Mn(III) complexes (*i.e*. Jacobsen),[25] which require stoichiometric amounts of a chemical oxidant. Hydrolytic kinetic resolution of racemic epoxides is also possible using chemical methods[2,8,26] as well as biocatalytic methods involving hydrolases.[3,27-31] Other more recent methodologies involve iron-based catalysts with hydrogen peroxide[32-34] or organocatalysts with an oxidant such as hydrogen peroxide, oxone, hypochlorite salts, peroxides (e.g. TBHP, mCPBA) or trichloroisocyanuric acid, etc.[35-40] Despite of significant research efforts and progresses in the field of chemocatalytic and organocatalytic asymmetric epoxidation of terminal alkenes such as styrene and derivatives, achieving elevated stereoselectivity (99% *ee* or higher) remains still a

challenge.[35,36,38,41-51] Hence, the biocatalytic counterpart of this reaction has been investigated during the past fifteen years using either flavin (FAD) or iron-dependent monooxygenases.[52] Enzymatic epoxidation is particularly attractive as epoxides are usually obtained with elevated enantiomeric excess (>99%) using molecular oxygen as oxidant. Among the others, the bi-enzymatic system of the FAD-dependent styrene monooxygenase (SMO) from *Pseudomonas* sp. has been exploited for the production of enantiopure styrene oxide (and derivatives thereof) in laboratory and pilot-scale production employing fermenting or resting recombinant *E. coli* cells[53-56] as well as crude enzyme preparations.[57] A thorough comparison between the SMO enzymatic process and different chemical epoxidation processes has shown that the former is the most advantageous when economic profitability and environmental impact are concomitantly considered.[58] The potential of SMOs in chemical synthesis has also been demonstrated in the production of chiral vicinal diols, amino-alcohols, α-hydroxy-carboxylic acids and α-aminoacids through one-pot, concurrent multi-step cascades.[59-62]

The current drawback regarding the use of the natural SMO enzymatic system, as in *Pseudomonas* sp., is the requirement of two separated enzymes (StyA and StyB) in order to promote the efficient epoxidation activity.[63] Hence, both enzymes are usually coexpressed in *E. coli*.[53] StyB catalyzes the reduction of FAD to $FADH_2$ at the expense of NADH, whereas StyA utilizes $FADH_2$ and O_2 to generate FAD-OOH in its active site. The final epoxidation of the styrene substrate, performed by StyA, regenerates the oxidized FAD upon dehydration (**Figure 2.2**). The actual mechanism of this bi-enzymatic process is still matter of debate. Early studies have reported a pure diffusive transfer of $FADH_2$ from StyB to StyA.[64] Nonetheless, subsequent in-depth studies strongly support the existence of a molecular interaction during the catalytic cycle between StyB and StyA from *Pseudomonas* sp. as well as other SMOs.[65-67] Published kinetic data show: *i)* the existence of two competitive mechanisms (diffusive and channeling) for the transfer of $FADH_2$ from StyB to StyA;[65-67] *ii)* a variation of the epoxidation activity of StyA in presence of different types of StyB, wherein the highest rate was observed in combination with the natural partner.[67]

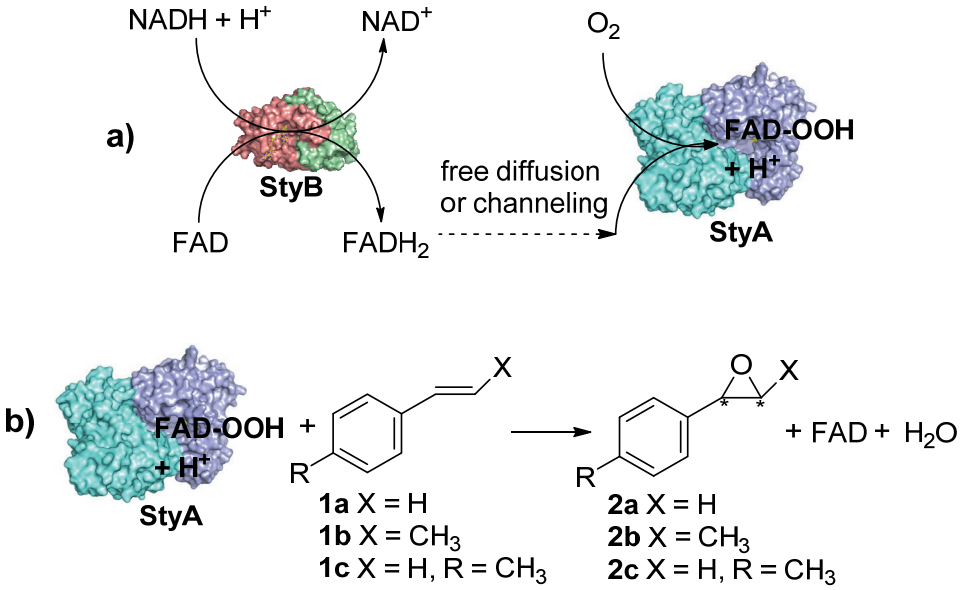

Figure 2.2. Simplified catalytic cycle of the flavin-dependent styrene monooxygenase (SMO). **a)** Step 1: Reduction of FAD to $FADH_2$ catalyzed by StyB and further transfer to StyA, whereby oxidation to FAD-OOH occurs. **b)** Step 2: Asymmetric epoxidation of styrene (or derivatives) by StyA with regeneration of oxidized FAD.

Whilst naturally occurring fused SMOs (StyA2B) have been isolated, the catalytic activity was from one to two orders of magnitude lower than the bi-enzymatic SMO system from *Pseudomonas* sp.[68] Interestingly, the epoxidation activity of StyA2B increased when an additional epoxidase enzyme (StyA1) was included.[67] All these findings reveal that the molecular interaction between the different enzymatic units has important synergistic effects on the overall catalytic cycle, besides a mere improved transfer of $FADH_2$ from one unit to the other one. However, StyA is capable of catalyzing the epoxidation also in absence of StyB as long as reduced FAD is supplied. This property was exploited for the generation of hybrid chemo-enzymatic and electro-enzymatic systems.[69-71] So far, the catalytic efficiency of these "StyA-hybrid" systems was significantly lower than that of the natural bi-enzymatic StyA-StyB. This reduced efficiency may be, in part, attributed to the lack of catalytic activation on StyA effected by StyB. Additionally, it has been shown that: *i)* the highest epoxidation activity is obtained when StyA and StyB are combined at ca. 1:1 ratio and at low FAD concentration (ca. 15 µM)[64,65,67] and *ii)* the reduction of oxidized FAD by StyB is the rate-limiting step.[66,72] Obtaining a nearly 1:1 ratio mixture of recombinant StyA and StyB in *E. coli* and in active form is still a challenging task. One issue is the difficult balancing and regulation of the expression

of both genes. The second, more severe, issue is that recombinant StyB in *E. coli* is mainly obtained as insoluble inclusion bodies (i.e. denatured form). In fact, in vitro experiments always required refolding of the inactive StyB, a lengthy and low-yielding procedure.[64-66]

Herein, we present a chimeric SMO in which reductive (StyB) and epoxidation (StyA) enzymatic units are fused with a flexible linker of 30 amino acids[73] in order to: *i)* solve the insolubility issue of StyB, *ii)* maximize the epoxidation activity (StyA–StyB 1:1 ratio), *iii)* improve $FADH_2$ transfer and find an optimum balance with coupling efficiency (NADH consumption *vs.* styrene epoxidation). A recent study reported on the catalytic mechanism of other artificially fused SMOs.[72] Nevertheless, these chimeric enzymes were either produced in insoluble (i.e. non active) form or possessed lower catalytic rate for the epoxidation of styrene (ca. 5-fold or less) compared to the natural system. The reason for this discrepancy compared to the present work will also be discussed.

2.2 Results and Discussion

2.2.1 Design of the fused SMO and initial tests for activity

The StyA and StyB genes belonging to the bi-enzymatic system of the styrene monooxygenase (SMO) from *Pseudomonas sp.* were genetically fused using a flexible linker[73] which was constituted by 30 amino acids (**section 2.4.3**). The gene construct (Fus-SMO) was designed in the following order: (N-His_6-tag)-(StyA)-(linker)-(StyB). Positioning the His_6-tag DNA sequence downstream from the T7 promotor and upstream from the StyA gene confers normally enhanced level of enzyme expression. The gene of the StyB was positioned at the end of the construct as this enzyme alone has been always expressed mainly as inclusion bodies (>95% of inactive enzyme).[65] *E. coli* BL21 D3 cells were transformed with the DNA encoding for the chimeric Fus-SMO enzyme and cells were grown on agar plate. Due to the different morphologies of the *E. coli* colonies obtained (i.e. various colors: pink, blue, white), four of them were selected for further testing of expression, solubility and activity (**Figure 2.3**). The generation of pigmented cells stems from the production of indigo (i.e. blue color) or indirubin (i.e. red) during cultivation, which is enabled by the overexpressed Fus-SMO.[74-76]

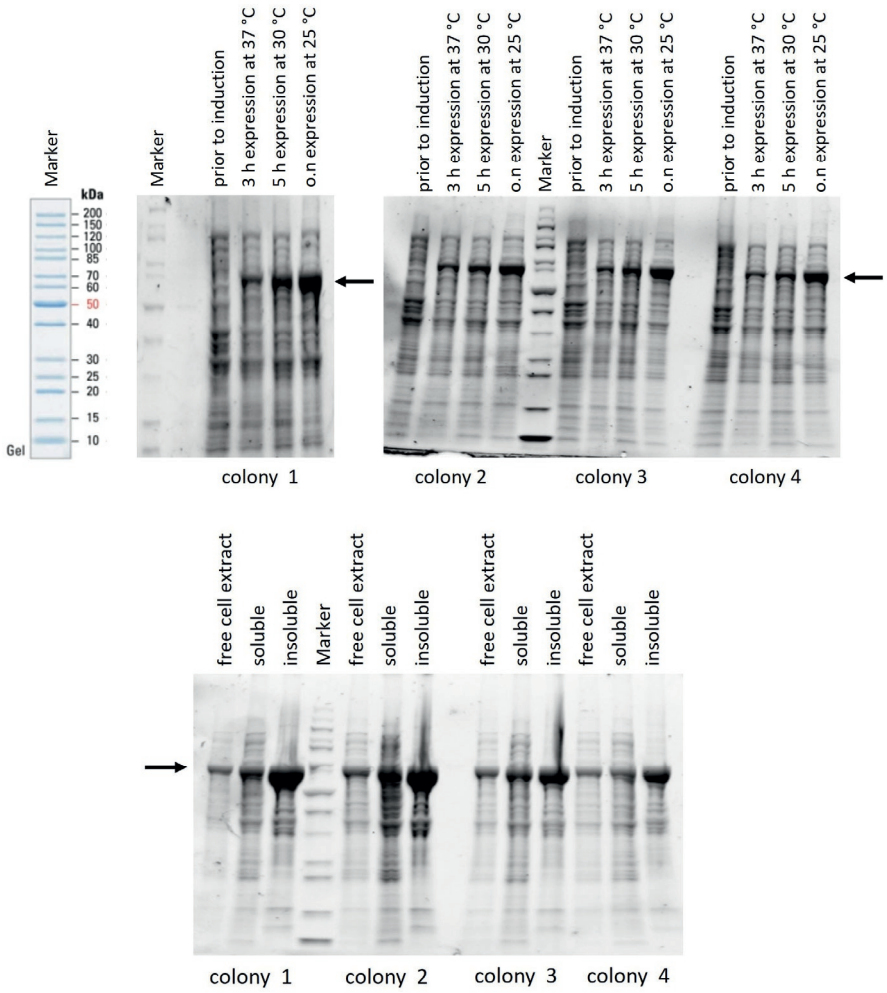

Figure 2.3. SDS-PAGE for the expression of Fus-SMO in *E. coli* BL21 DE3 as host (top); SDS-PAGE for verifying the soluble part of the expressed Fus-SMO when expression was performed at 25 °C overnight (bottom). Marker: PageRuler™ Unstained Protein Ladder (ThermoFisher Scientific)

In preliminary experiments, the conversion for the epoxidation of styrene (**1a**) was determined after a specific reaction time, using lyophilized *E. coli* whole cells overexpressing Fus-SMO in a biphasic system (aqueous buffer/*n*-decane, (**Table 2.1**). As reported in literature,[54, 60] the organic phase acts as a reservoir of styrene and reduces the molecular toxicity of the product styrene oxide. Furthermore, it prevents the spontaneous opening of the epoxide ring. Interestingly, the quantity and solubility of the expressed Fus-SMO into the cells seems to not correlate with a particular pigmentation of the host organism (**Figure 2.3**), whereas a difference

in the conversion was observed only in one case for colony 2 (**Table 2.1**). However, further optimization of the expression conditions (i.e. IPTG concentration) revealed that all the *E. coli* colonies perform the epoxidation equally well, independently from their pigmentation.

Table 2.1. Conversions [%] of **1a** (20 mM) to (*S*)-**2a** for the activity test of lyophilized whole cells containing Fus-SMO with and without the addition of FAD (50 µM).

Entry	colony	conversion of 1a after expression of Fus-SMO at 37 °C for 3 h [%]	
		- FAD	+ FAD
1	1	24	24
2	2	7	24
3	3	20	56
4	4	21	50
Entry	**colony**	**conversion of 1a after expression of Fus-SMO at 30 °C for 5 h [%]**	
		- FAD	**+ FAD**
5	1	40	22
6	2	39	26
7	3	40	26
8	4	38	23
Entry	**colony**	**conversion of 1a after expression of Fus-SMO at 25 °C o.n. [%]**	
		- FAD	**+ FAD**
9	1	55	52
10	2	74	99
11	3	53	52
12	4	52	48

The influence of the addition of exogenous FAD was also assayed (50 µM) during the reaction. Biocatalytic reactions in presence or absence of FAD afforded statistically analogous results. Hence, *E. coli* is capable of producing sufficient amount of cofactor in combination of Fus-SMO to sustain the reaction (**Table 2.1**). Nevertheless, for the sake of reproducibility of the results, this whole study was carried out by adding a minimal amount of FAD to each biocatalytic reaction because long time storage of *E. coli*/Fus-SMO (frozen pellets or lyophilized cells) was possible, but data on the stability of FAD in such conditions were not available. A glycerol stock solution prepared from the culture obtained from colony 1 was

used for the continuation of this study. Optimization of the expression conditions (25 °C, 16 h, IPTG 0.1 mM) and further testing of activity led to the production of soluble and active Fus-SMO in elevated amount (**Figure 2.4**).

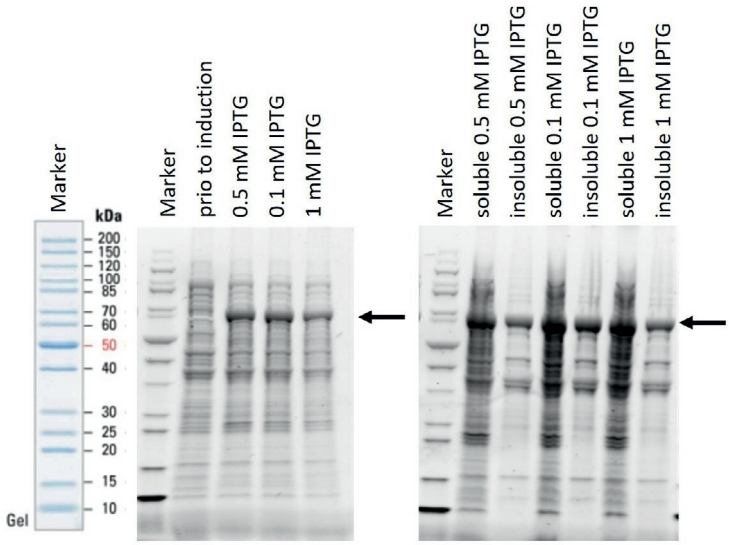

Figure 2.4. SDS-PAGE for the expression (left) of Fus-SMO using various concentrations of IPTG and solubility test (right). Marker: PageRuler™ Unstained Protein Ladder (ThermoFisher Scientific).

As shown in **Table 2.2**, whole lyophilized *E. coli* cells carrying the overexpressed Fus-SMO, under different conditions, revealed good conversions in all tested cases. All the further studies were carried out by inducing enzyme expression with the minimum amount of IPTG (0.1 mM) since no significant discrepancy was observed.

Table 2.2. Bio-conversion [%] of **1a** (20 mM) to (*S*)-**2a** in 4 mL glass vials using lyophilized whole cells containing Fus-SMO expressed with different IPTG concentrations.

Entry	lyophilized cells [mg mL^{-1}]	0.1 mM IPTG 2a [%][a)]	0.5 mM IPTG 2a [%][a)]	1 mM IPTG 2a [%][a)]
1	5	81±7	69±19	55±9
2	10	>99	85±2	>99
3	20	>99	95±6	>99

Reactions were performed in duplicates; the reported conversion is the average of two measurements

Moreover, as the biocatalytic epoxidation may also be influenced by the availability of dioxygen in the headspace, different reaction vessels were already considered (**Table 2.3**). Quantitative epoxidation of **1a** (10 mM) in 1 mL of biphasic reaction mixture (aqueous buffer/*n*-decane, 1:1, v v^{-1}) was obtained using 4 mL glass vials as

reaction vessel. Employing vials with smaller volume (2 mL) led to a maximum of 41% conversion, likely due to insufficient availability of dioxygen. The use of vials with larger volume (e.g. 20 mL) is possible, although agitation must be carefully set in order to assure an efficient mixing of the biphasic mixture.

Table 2.3. Bio-conversion [%] of **1a** (10 mM) to (*S*)-**2a** by the soluble fraction of Fus-SMO expressed with different IPTG concentrations using a variation of reaction vessels.

Entry	IPTG [mM]	2 mL Eppendorf tubes 2a [%]	4 mL glass vials 2a [%]	20 mL glass vials 2a [%]
1	0.1	40	>99	50
2	0.5	34	>99	55
3	1	41	>99	54

The bi-enzymatic StyA-StyB system has been often applied in a biphasic system, in which the organic phase was a high boiling solvent such as hexadecane, bis-(2-ethylhexyl)phthalate, etc. In preliminary experiments for the reaction in preparative scale, the difficult final evaporation of the high boiling decane led to a troublesome and high energy-consuming work-up procedure. More experiments also showed that it is possible to use low boiling organic solvents, such as *n*-heptane or even neat styrene, without affecting the productivity if lyophilised cells are employed (**Table 2.4**). Hence, a mixture of aqueous buffer (KPi, pH 8.0, 50 mM) and *n*-heptane (1:1 v v^{-1}) was selected for further experiments.

Table 2.4. Bio-epoxidation of **1a** (20 mM) by Fus-SMO (20 mg mL^{-1}) in different solvent systems.

Entry	KPi buffer [µL]	Cells [mg]	Subs. [µmol]	Organic solvent [µL] (v/v)	Conv. (*S*)-2a [%][a]	(*S*)-2a formed [µmol]	Productivity [µmol (*S*)-2a/ mg cells]
1	500	10	10	hexane [500](50%)	>99	>9.9	>0.99
2	1000	20	20	-	67±5	13.3	>0.67
3	950	20	435	styrene [50](5%)	5±0	19.6	0.98
4	980	20	20	decane [20](2%)	68±2	13.6	0.68
5	960	20	20	decane [40](4%)	69±3	13.8	0.69
6	940	20	20	decane [60](6%)	69±1	13.6	0.68
7	920	20	20	decane [80](8%)	70±2	14.0	0.70
8	900	20	20	decane [100](10%)	72±3	14.4	0.72
9	500	10	10	decane [500](50%)	>99	>9.9	>0.99
10	500	10	10	heptane [500](50%)	>99	>9.9	> 0.99

[a]Reactions were performed in duplicates and the reported conversion is the average of two measurements. The optical purity was measured for selected samples (one per each condition) by chiral HPLC. In all cases, the enantiomeric excess was >99% (*S*).

2.2.2 Determination of the coupling efficiency of Fus-SMO

The coupling efficiency of the StyA-StyB system (bi-enzymatic or fused) is defined as the ratio between the quantity of substrate epoxidated and the reducing equivalents consumed. Detailed biochemical studies have revealed that the coupling efficiency is a function of: *i)* the relative concentration of StyA and StyB, *ii)* the substrate concentration and *iii)* the FAD concentration.[65] A coupling efficiency verging towards one was measured at low FAD concentration (1 µM or less) and a StyA/StyB ratio of ca. 500. In this condition, StyB produces $FADH_2$ in extremely low concentration (nM range) and it can be quantitatively transferred to StyA. Hence, StyA produces FAD-OOH that can be almost quantitatively consumed for the epoxidation of styrene. Therefore, virtually no $FADH_2$ is wasted in the generation of H_2O_2 as by-product. The logic drawback of this specific reaction condition is that the epoxidation activity is dramatically reduced, making it inapplicable for synthetic

purposes. Therefore, the challenge is to maximize the coupling efficiency without affecting the overall epoxidation activity. We hypothesized that our Fus-SMO may have improved coupling efficiency at reaction conditions that are suitable for a high epoxidation rate. In the synthetic set-up reported in this work, NAD^+ was applied in catalytic amount (1 mM) and recycled by a formate dehydrogenase from *Candida boidinii* (Cb-FDH) and HCOONa. A set of experiments were performed in which the equivalents of HCOONa (*i.e*. the ultimate source of reducing equivalents) were gradually increased from 0 to 5. As depicted in **Figure 2.5**, only four equivalents of formate were required in order to reach full conversion of **1a** (20 mM). However, 20% conversion of **1a** was observed even without any addition of HCOONa. The hypothesis is that some endogenous enzymes from the *E. coli* lyophilized cells (10 mg mL^{-1}) can somehow regenerate, in part, the NADH cofactor. Taking into account this background activity, the remaining 80% conversion of **1a** was driven by only 4 equivalents of HCOONa corresponding to a remarkable estimated coupling efficiency of ca. 20%. The product (*S*)-**2a** was obtained in enantiopure form (*ee* >99% *S*).

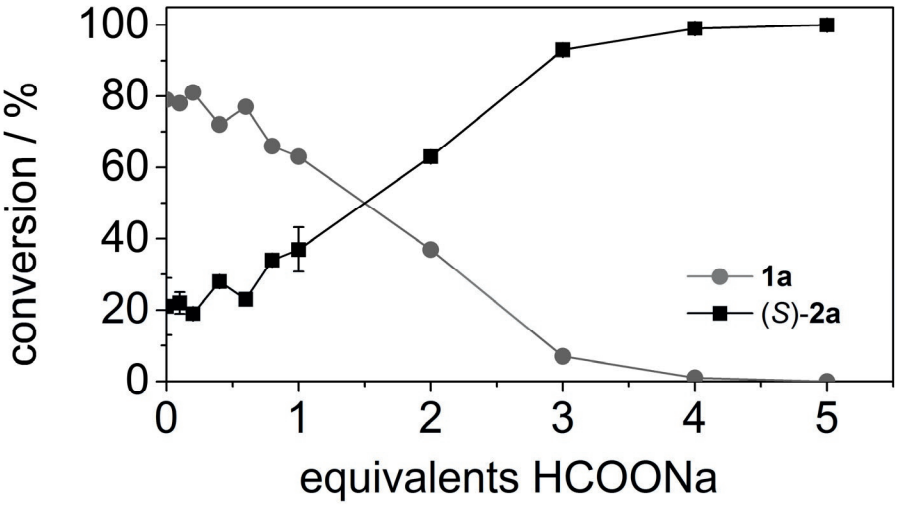

Figure 2.5. Conversion of **1a** (20 mM) to (*S*)-**2a** at varied concentration of HCOONa as final hydride donor. The bio-transformations were performed in a biphasic system KPi (pH 8.0, 50 mM)/n-heptane (1:1 v v^{-1}, 1 mL total reaction volume) containing *E. coli*/Fus-SMO lyophilized cells (10 mg mL^{-1}), NAD^+ (1mM), FAD (50 µM), HCOONa (0-100 mM) and Cb-FDH (10 µM). The mixtures were incubated at 30 °C, 180 rpm for 24 h. Conversions are the average of two independent sets of experiments, both in duplicate (for all dataset including standard deviations see **section 2.4.6**). The enantiomeric excess was determined by chiral HPLC to be >99% (*S*).

2.2.3 Influence of the dioxygen pressure

Preliminary investigation has shown that the availability of dissolved molecular oxygen might become the limiting factor for the biocatalytic epoxidation by Fus-SMO under particular reaction conditions (data not shown). It has been reported that the activity of some oxygenases can be strongly enhanced by using pure O_2 in the headspace at atmospheric pressure or even under pressure.[77,78] In order to assess properly the biocatalytic performance of our Fus-SMO, we carried out a comparative study with the original bi-enzymatic StyA-StyB construct (pSPZ10) by Panke and coworkers.[53] The pSPZ10 plasmid containing the styA and styB genes encoding for the SMO bi-enzymatic system of *Pseudomonas* sp. strain VLB120 was kindly donated by Prof. Sven Panke.[53,63,79]

Expression of StyA-StyB with pSPZ10 plasmid was initially performed in *E. coli* JM101 according to literature. The expression in *E. coli* Arctic Express cells was also tested, as this strain is capable of improving expression of insoluble proteins such as StyB and this strain was not commercially available at the time of Panke's study. Although expression of soluble StyA was significantly superior in *E. coli* JM101 (**Figure 2.6**), the tests of conversion *vs* time with lyophilized cells of *E. coli* JM101 and *E. coli* Arctic Express provided similar results (**Table 2.5**). This observation corroborates the assumption that the inefficient expression of soluble StyB in the bi-enzymatic system is the limiting factor.

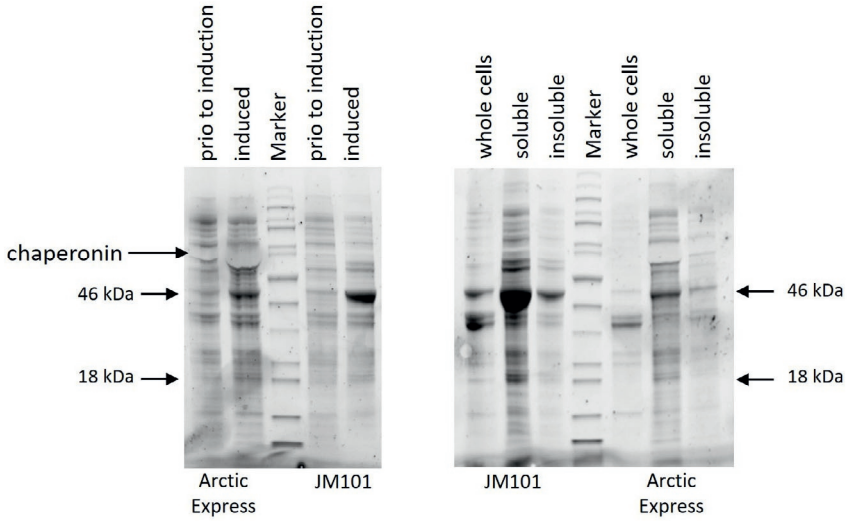

Figure 2.6. SDS-PAGE for the expression of pSPZ10-StyAStyB in *E. coli* JM101 and Arctic Express cells. The SDS-PAGE was visualized using a gel imaging system from Biorad which does not visualize proteins lacking of tryptophan residues (chaperonin from Arctic Express cells). Marker: PageRuler™ Unstained Protein Ladder (ThermoFisher Scientific); MW_{StyA} = 46 kDa and MW_{StyB} = 18 kDa

Table 2.5. Results for the bio-catalytic conversion of **1a** (10 mM) to (*S*)-**2a** for the comparison of *E. coli* JM101 and Arctic Express cells as host organism for the expression of pSPZ10-StyAStyB.

entry	cells	JM101 2a [%] [a]	Arctic Express 2a [%] [a]
1	wet fresh cells (180 mg mL^{-1})	37±1	72±13
2	frozen pellet (130 mg mL^{-1})	78±<1	95±<1
3	lyophilized whole cells (20 mg mL^{-1})	90±2	95±<1

[a]Reactions were performed in duplicates and the reported conversion is the average of two measurements.

Finally, the rates of the epoxidation reaction using *E. coli* BL21 DE3/Fus-SMO (5 mg mL^{-1}) and *E. coli* JM101/pSPZ10(StyA-StyB) (5 mg mL^{-1}) were compared by measuring the conversion after 20 min (linearity range for conversion *vs.* time), under the optimized reaction conditions (**section 2.4.7**), using styrene (50 mM) as substrate. As the coupling efficiency of both SMOs system is not perfect, formation of H_2O_2 during the reaction is expected. Hence, catalase (2 µM) was added. A set of experiments was conducted under air and O_2 at atmospheric pressure (p_{rel} 0 bar) as well as under pressurized O_2 (p_{rel} 1 to 4 bar). A pressurized closed system (**Figure 2.7**) might increase the concentration of O_2 in the liquid phase and kinetically enhance the O_2 transfer from the gas phase to the liquid phases.

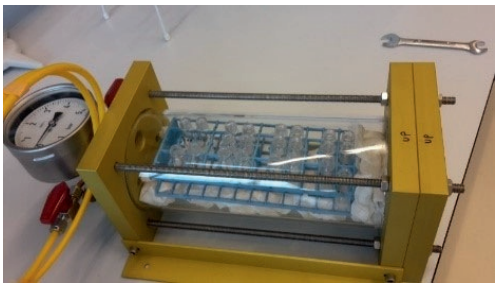

Figure 2.7. The oxygen chamber used in this study**.**

Figure 2.8 shows that the addition of catalase had a significant influence on the rate of the epoxidation. Independently from the composition and pressure of the gas phase as well as the type of SMO construct, reactions in presence of catalase were accelerated. The chimeric Fus-SMO system performed always better than the bi-enzymatic StyA-StyB system in presence of catalase at any composition and pressure of the gas phase. The maximum rate was obtained with Fus-SMO with pure O_2 at atmospheric pressure (25±2% conversion) with a productivity of 37.5 $mM_{product}$ h^{-1}. Under the same conditions the bi-enzymatic StyA-StyB gave a productivity of 25.5 $mM_{product}$ h^{-1}. Supplying O_2 under pressure was in general

detrimental for the reaction. The influence of pressure in enzyme catalysis is still a not fully understood phenomenon.[80-83] According to Le Châtelier's principle and the Eyring equation, an increase of pressure enhances the rate (*k*) of chemical reactions that have a negative activation volume ($\Delta V^{\neq}$).[84] Considering that typical $\Delta V^{\neq}$ values for enzymatic reactions are in the range of ±50 cm^{-3} mol^{-1}, the variation of the reaction rate constant (Δk) would be less than 1% within the pressure range of our study (p_{abs} from 1 to 5 bar).[80, 85-87] On the other hand, variation of pressure can have a profound effect in the enzyme structure and, therefore, activity. However, various studies evidenced that significant structural changes in enzyme structure occur at very high pressure, typically above 1 kbar.[80,85,88,89] Hence, both mentioned effects can be neglected in this study as O_2 was supplied at low pressure (max p_{abs} 5 bar). Thus, we can speculate that the increased O_2 pressure in the system may result in an increased formation of FAD-OOH, which cannot be entirely utilised for the epoxidation of styrene. Enhanced rate formation of FAD-OOH generates more H_2O_2 that is deleterious for enzyme activity. The addition of catalase can only in part counteract this process as shown in **Figure 2.8**.

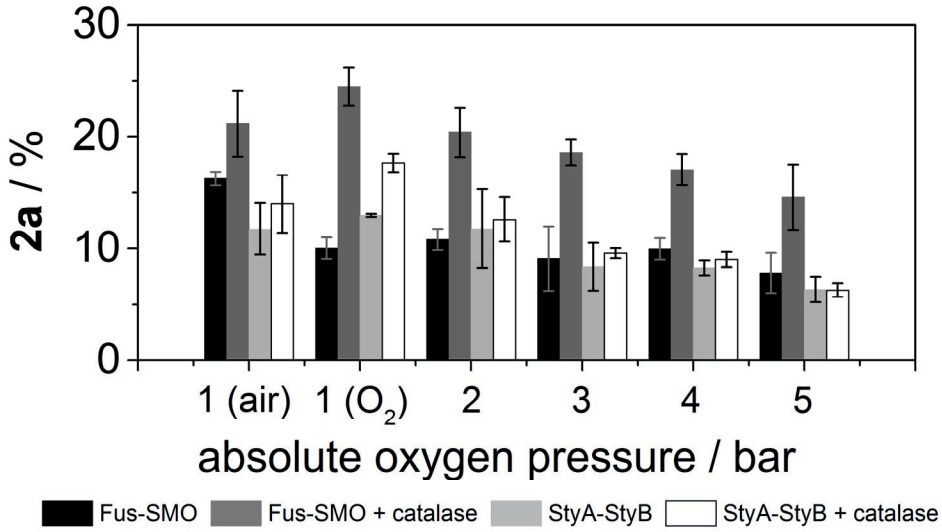

Figure 2.8. Conversion [%] of **1a** (50 mM) by lyophilized whole cells of *E. coli* BL21 DE3 expressing Fus-SMO (5 mg mL^{-1}) and *E. coli* JM101 expressing pSPZ10 (StyA-StyB) (5 mg mL^{-1}). Reactions were carried out in glass vials introduced in a sealed pressurized chamber (Figure 2.7). The bio-transformations were performed in a biphasic system KPi (pH 8.0, 50 mM)/n-heptane (1:1 v v^{-1}, 1 mL total reaction volume) containing NAD^+ (1mM), FAD (50 µM), HCOONa (250 mM, 5 eq.) and Cb-FDH (10 µM). Catalase was added in selected experiments (2 µM). The mixtures were incubated at 30 °C, 200 rpm for 20 min. Two independent experiments were carried out, both in duplicate. Error bars represent the standard deviation.

Finally, the higher catalytic activity of the *E. coli*/Fus-SMO cells compared to the *E. coli* cells expressing the bi-enzymatic StyA-StyB was further confirmed in a study in which the conversion of styrene was monitored over time (10, 20 and 30 min; section 2.4.8). *E. coli*/Fus-SMO cells showed a ca. 50% increased catalytic activity compared to *E. coli* cells expressing the bi-enzymatic StyA-StyB (**Figure 2.9**).

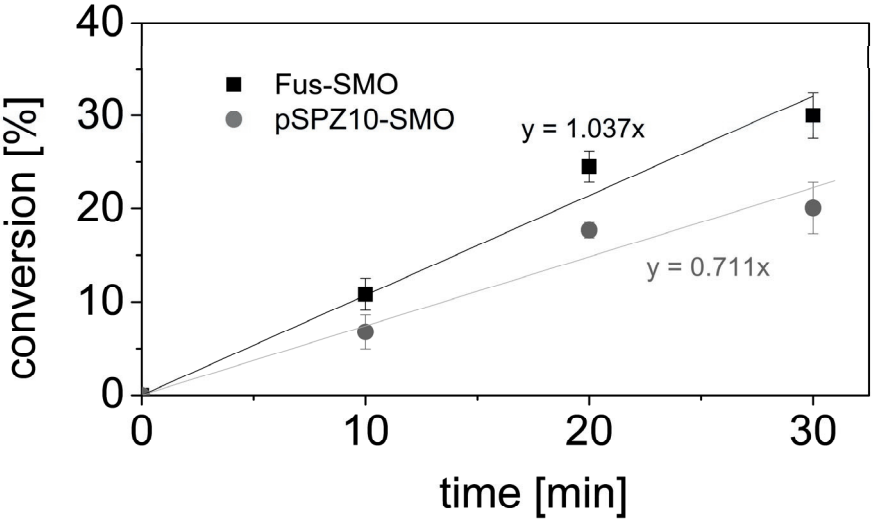

$$\frac{initial\ activity\ Fus_{SMO} - initial\ activity\ StyAStyB}{initial\ activity\ StyAStyB} \times 100 = 46\%$$

Entry	Time [min]	*E. coli* BL21 DE3/ Fus-SMO	*E. coli* JM101/pSPZ10-StyAStyB
1	10	10.8±1.7	6.8±1.8
2	20	24.5±1.7	17.7±0.8
3	30	30.0±2.5	20.1±2.8

Figure 2.9. Time study for the conversion of **1a** (50 mM) by *E. coli* BL21 DE3/Fus-SMO (5 mg mL^{-1}) and *E. coli* JM101/pSPZ10-StyA-StyB (5 mg mL^{-1}). Time range was 0, 10, 20 and 30 minutes. Reactions were carried out in 40 mL glass vials (in a sealed chamber flashed with pure molecular oxygen). The bio-transformations were performed in a biphasic system KPi (pH 8.0, 50 mM)/n-heptane (1:1 v v^{-1}, 1 mL total reaction volume) containing NAD^+ (1 mM), FAD (50 µM), HCOONa (250 mM, 5 eq.) and Cb-FDH (10 µM). The mixtures were incubated at 30 °C, 200 rpm up to 30 min. Two independent experiments were carried out and both as duplicate; hence, the reported conversions are the average of 4 measurements. Error bars represent the standard deviations.

2.2.4 Self-sufficient whole cells system for the epoxidation of styrene and derivatives

Aiming at enhancing the practical applicability, a whole cell system was created by expressing simultaneously Fus-SMO and Cb-FDH in *E. coli* BL21 DE3 as host organism. Under the optimized conditions for the co-expression (i.e. 0.1 mM IPTG at 25 °C for 16 h), the expression for both enzymes in soluble form was observed (**Figure 2.10**).

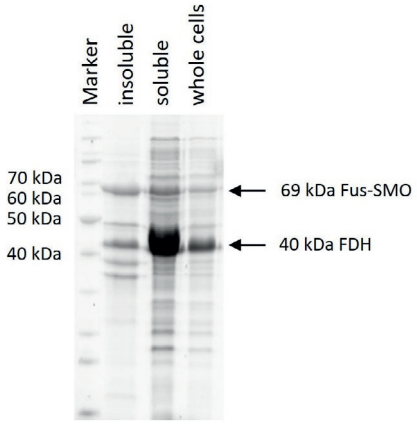

Figure 2.10. SDS-PAGE for the co-expression of Fus-SMO and FDH. Marker: PageRuler™ Unstained Protein Ladder (ThermoFisher Scientific).

Preliminary tests demonstrated that lyophilized whole cells containing co-expressed Fus-SMO and Cb-FDH were highly active for the epoxidation of **1a** and **1b** (**Table 2.6**). It is known from literature that the typical activity of Cb-FDH for the recycling of NADH at the expense of formate is ca. 180 U μmol_{enzyme}^{-1}.[90] Hence, cofactor regeneration is not the rate limiting step. Moreover, the perfect stereoselectivity of Fus-SMO was retained (*S*)-**2a** *ee* >99%; (1*S*,2*S*)-**2b** *ee* >99% and *de* >98%).

Table 2.6. Results for the biotransformation of **1a** (20 mM) and **1b** using lyophilized whole cells containing co-expressed Fus-SMO and Cb-FDH.

Entry	Product	Conversion [%]	*ee* [%]	*de* [%]
1	(*S*)-**2a**	>99	>99	n.a.
2	(1*S*,2*S*)-**2b**	75	>99	>98

n.a. = not applicable

Then, we monitored the progress of the conversion of **1a** and **1b** (50 mM) over time under the optimized reaction conditions (**Figure 2.11 and section 2.4.9**).

Lyophilized whole cells containing Fus-SMO and Cb-FDH (5 mg mL^{-1}) converted 27.1±1.2% of **1a** at 50 mM scale within the first 30 min under air. The epoxidation ran smoothly reaching 93.8±1.3% conversion after 6 h. By prolonging the reaction time, the bio-catalytic system achieved 99% conversion. The epoxidation of **1b** showed a similar trend, albeit it proceeded at a lower rate. The reason must be attributed to the lower intrinsic reactivity of SMO towards **1b**, as previously shown in **Table 2.6**. However, a maximum of 90.4±1.4% conversion into (1*S*,2*S*)-**2b** was obtained when starting with substrate **1b** (**Figure 2.11**).

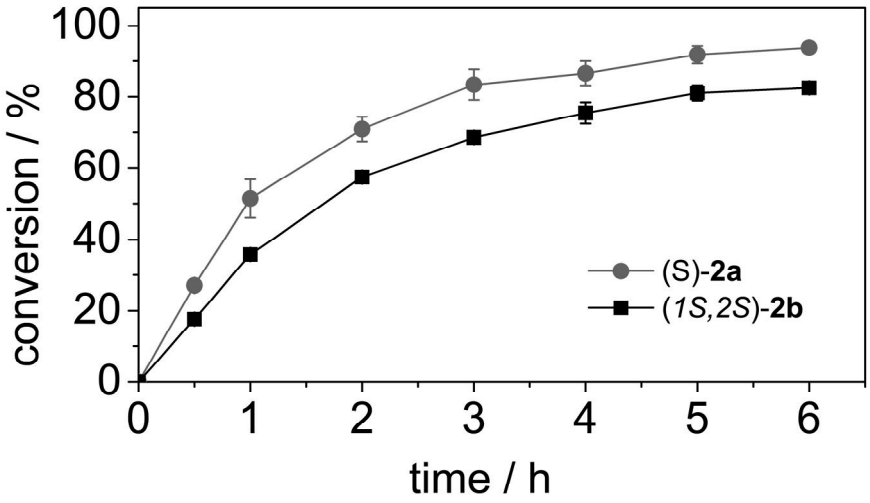

Figure 2.11. Progress of the conversion over the time for the epoxidation of **1a** and **1b** (50 mM) using lyophilized whole cells wherein Fus-SMO and Cb-FDH where co-expressed in *E. coli* BL21 DE3 (5 mg mL^{-1}). Reactions were carried out in sealed 20 mL glass vials under air at atmospheric pressure. The bio-transformations were performed in a biphasic system KPi (pH 8.0, 50 mM)/n-heptane (1:1 v v^{-1}, 1 mL total reaction volume) containing NAD^+ (1 mM), FAD (50 µM), HCOONa (250 mM, 5 eq.) and catalase (2 µM). Two independent experiments were carried out, both in duplicates. Error bars represent the standard deviation (**section 2.4.9**).

We also investigated the possibility to increase the substrate concentration from 50 mM up to 1 M for the epoxidation of **1a** and **1b** in analytical scale (total volume 1 mL) using the *E. coli* BL21 DE3/Fus-SMO/Cb-FDH (5 mg mL^{-1}) co-expressed system in 20 mL reaction vessels. The results from this study confirmed that nearly quantitative conversion can be achieved at 50 mM substrate concentration applying the current reaction conditions and technical set-up. In fact, the repetition of the epoxidation of **1a** and **1b** (50 mM) afforded the related products with 98±1 and 96±3 conversions, respectively. Increasing the substrate concentration resulted in a progressive decrease of the conversion (**Table 2.7**).

Table 2.7. Conversion [%] of **1a** (50 mM up to 1M) and **1b** (50 mM up to 1 M) to enantiopure **2a** and **2b** by lyophilized cells of co-expressed Fus-SMO and Cb-FDH in 20 mL glass vials

Entry	Substrate [mM]	2a [%]	2a [mM]	2b [%]	2b [mM]
1	50	98±1	49±1	96±3	48±1
2	75	74±2	56±2	75±1	56±1
3	100	59±	59±1	64±<1	64±<1
4	150	43±1	65±2	52±2	79±2
5	170	34±2	58±3	51±<1	87±1
6	200	29±<1	58±1	47±2	93±3
7	250	24±<1	59±<1	39±<1	98±1
8	500	11±<1	54±2	13±1	65±3
9	1000	5±<1	48±1	5±<1	50±3

Reactions were performed as duplicates; hence, the reported conversion is the average of 2 values. Error is expressed as the absolute difference between the two measurements.

The productivity of the system (*i.e*. mmol of epoxide product obtained) was partially influenced by the substrate concentration and it depended on the substrate tested. The highest productivity for the epoxidation of **1a** was observed at 150 mM substrate concentration, leading to the formation of 65±2 mM of (*S*)-**2a** (**Table 2.7, entry 4**). Instead, the highest productivity for the epoxidation of **1b** was observed at 250 mM substrate, leading to the formation of 98±1 mM of (1*S*,2*S*)-**2b** (**Table 2.7, entry 7**). In addition, we demonstrated that the productivity of the system—applying the current reaction set-up—was not limited by the volume of the gas headspace. In fact, increasing the volume of the reaction vessels up to 100 mL did not improve conversions and productivities (**Table 2.8**).

Table 2.8. Conversion [%] of **1a** (50 mM up to 1M) and **1b** (50 mM up to 1M) to enantiopure **2a** and **2b** by lyophilized cells of co-expressed Fus-SMO and Cb-FDH in 100 mL Erlenmeyer flask

Entry	Substrate [mM]	2a [%]	2a [mM]	2b [%]	2b [mM]
1	50	96±3	48±1	68±4	34±2
2	75	52±<1	39±<1	54±8	40±6
3	100	41±1	41±1	54±7	54±7
4	150	31±<1	47±<1	40±1	61±1
5	170	29±1	50±2	39±<1	66±<1
6	200	24±<1	49±1	32±2	65±3
7	250	20±1	50±3	21±<1	53±<1
8	500	12±1	58±5	13±2	67±11
9	1000	5±<1	47±2	7±<1	66±2

Reactions were performed as duplicates; hence, the reported conversion is the average of 2 values. Error is expressed as the absolute difference between the two measurements.

Finally, we investigated the influence of different modes of dioxygen supply on the rate of the biocatalytic epoxidation. Hence, experiments were conducted applying either a sealed system with a large volume of air in the headspace or a system with continuous flow of pure dioxygen (bubbling at ca. 1 mL min^{-1}). In both cases, the other reaction parameters were the same: *E. coli* cells co-expressing Fus-SMO and Cb-FDH (5 mg mL^{-1}), styrene (50 mM), catalase (2 µM), NAD^+ (1 mM), FAD (50 µM) and HCOONa (5 eq.) in a stirred mixture of aqueous buffer (25 mL, KPi, pH 8.0) and *n*-heptane (25 mL) in round-bottom flasks (**section 2.4.9**). The difference in the rate of formation of styrene oxide for the two systems was indeed minimal (ca. 10%), with the system consisting of air in the headspace performing better (**Figure 2.12**). In general, we conclude that sufficient dioxygen supply (independently from the mode) as well as efficient mixing of the biphasic reaction mixture are crucial parameters for sustaining elevated epoxidation rate for longer times.

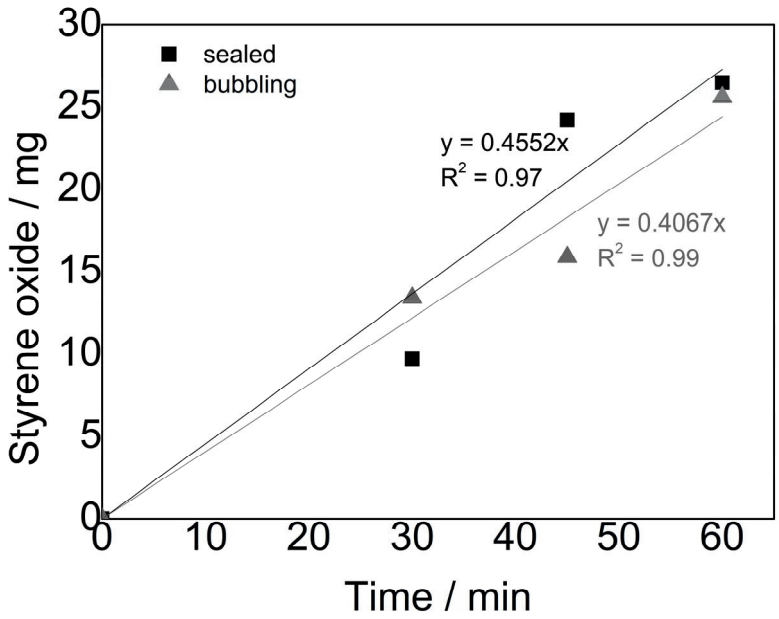

$$Relative\ difference\ in\ styrene\ oxide\ productivity = \frac{0.4552 - 0.4067}{0.4552} \times 100 = 10\%$$

Figure 2.12. Comparing different modes of dioxygen supply: seal system with air headspace (black line) and continuous flow (grey line)

2.2.5 Epoxidation on preparative scale

The bio-catalytic epoxidation using lyophilized whole cells containing co-expressed Fus-SMO and Cb-FDH was performed on preparative scale for both substrates **1a**

(50 mM, 521 mg) and **1b** (50 mM, 591 mg). The reactions were run in a biphasic system KPi (pH 8.0, 50 mM)/*n*-heptane (1:1 v v^{-1}, 200 mL total reaction volume), under the optimized reaction conditions (**section 2.4.10**). A large reaction vessel was used in order to assure a sufficient supply of molecular oxygen for the reaction as well as an efficient mixing of the biphasic reaction mixture.

The epoxidation of **1a** afforded quantitative conversion (**Table 2.9, entry 1**). The organic phase was separated from the aqueous buffer and the *n*-heptane was evaporated, affording 509 mg of (*S*)-**2a** (equal to 85% isolated yield) in very high chemical purity (99% measured by GC-FID) as well as optical purity (*ee* >99 % *S*). Hence, further purification of (*S*)-**2a** obtained from the evaporation of the organic phase was not required. The remaining aliquot of product (*S*)-**2a** (ca. 12%) was recovered upon extraction from the aqueous reaction phase. In this case, the purity was determined to be 94%. The by-product was 2-phenyl-ethanol as reported in literature for the natural StyA-StyB enzymatic system.[53, 55, 57, 58, 63] The epoxidation of **1b** afforded the product (*1S,2S*)-**2b** (**Table 2.9, entry 2**) in >99% conversion. In this case, the purities of the isolated product from the *n*-heptane reaction phase and from the extraction of the aqueous phase were similar (ca. 95%). 603 mg of (*1S,2S*)-**2b** (90% isolated yield) were obtained with elevated diastereomeric (*de* >98%) and enantiomeric excess (*ee* >99%).

Table 2.9 Upscaling for the bio-catalytic synthesis of (*S*)-**2a**-and (1*S*,2*S*)-**2b** using lyophilized whole cells containing co-expressed Fus-SMO and Cb-FDH (5 mg mL^{-1}); 200 mL total reaction volume (n-heptane/KPi buffer, 1:1 v v^{-1}).

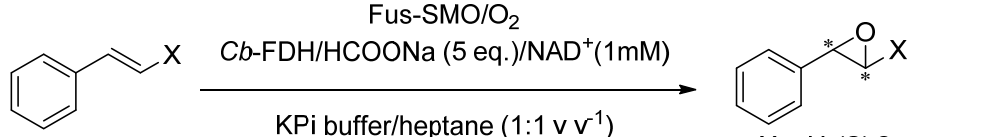

Entry	Substrate [mM]	Conversion [%]	Yield [%]	*ee* [%]	*de* [%]
1	**1a** (50)	>99	85[a]+12	>99	-
2	**1b** (50)	>99	90[b]	>99	>98

[a] This isolated yield represents the amount of pure product that was isolated from the simple evaporation of the *n*-heptane as reaction phase. No further work-up was required. The remaining amount of product (ca. 12%) was recovered after extraction from the aqueous reaction phase. However, purity was lower (ca. 94%) due to the generation of 2-phenyl-ethanol as the by-product. [b] In this case, the purities of the isolated product obtained from the *n*-heptane reaction phase and from the extraction of the aqueous phase were similar. Thus, the aliquots were combined and the total yield was reported.

2.2.6 Determination of the activity of purified Fus-SMO and comparison with literature data of bi-enzymatic StyA-StyB

As chimeric Fus-SMO was created with an N-terminal His_6-tag, the purification was easily performed by Ni^{2+} affinity chromatography (**section 2.4.11**). We carried out initial determinations of the enzymatic activity of Fus-SMO for the epoxidation of **1a** at different pH values. Data of activity showed negligible differences in the range between 6.5 and 9 (data not shown). Therefore, we selected Tris-HCl buffer (50 mM, pH 8.5) for further determination. The determination of the epoxidation activity of Fus-SMO was performed according to the general procedure reported by Otto *et al.*[64] and Tischler *et al.*[68] for the same experiment with bi-enzymatic StyA-StyB. In this way, the new data of epoxidation activity of Fus-SMO can be compared with the data reported in literature for the two-component StyA-StyB system. **Figure 2.13** shows that the specific activities of Fus-SMO and StyA-StyB system are essentially identical for the epoxidation of styrene (**1a**). However, Fus-SMO showed more than 3-fold increased activity compared to the StyA-StyB system for the epoxidation of *para*-methylstyrene (**1c**). We chose substrates **1a** and **1c** because data of epoxidation activity for two-component StyA-StyB were available in literature. Besides the retained or improved epoxidation activity of Fus-SMO, we point out another important aspect: the conditions for the maximum epoxidation activity of the two-component StyA-StyB is very complicated to reproduce *in vitro* and nearly impossible in a cell as a 1:1 mixture of StyA and StyB is required (also considering the insolubility of StyB). In contrast, Fus-SMO permits to set effortlessly the highest rate both *in vitro* as well as in a cell. Finally, comparing the epoxidation activity of our artificial Fus-SMO to natural occurring fused SMOs (StyA2B),[68] the activity of Fus-SMO was ca. 70-fold and 110-fold higher for **1a** and **1c**, respectively.

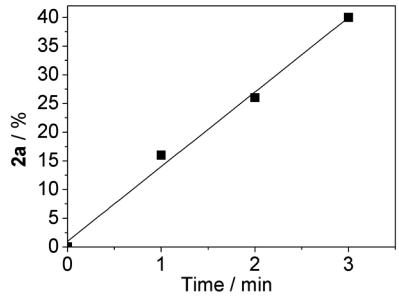

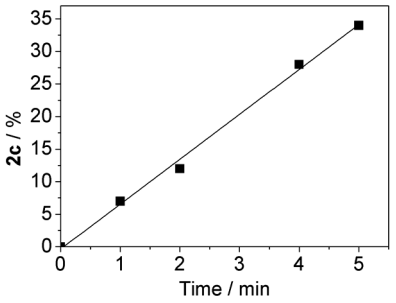

Entry	Substrate	Specific epoxidation activity		
		Two-component StyA-StyB [min^{-1}]	Natural fused StyA2B [min^{-1}]	Fus-SMO (this study) [min^{-1}][c]
1	**1a**	97[a]	1.3[b]	95±5
2	**1c**	14[b]	0.4[b]	44±4

[a]Recalculated based on the best activity data (StyA:StyB, 1:1 mol mol^{-1}) by Otto *et al.*;[64] [b] Recalculated based on best activity data (StyA:StyB, 1:1 mol mol^{-1}) by Tischler *et al.*; [68] [c] Error is expressed as the standard deviation.

- Calculation of the activity of Fus-SMO:

$$Activity\ FusSMO = \left[\frac{U}{\mu mol\ FusSMO}\right] = \frac{\frac{Slope}{100} \times 2\left[\frac{mmol\ product\ formed}{min \times l}\right] \times 10^3\left[\frac{\mu mol}{mmol}\right]}{3\left[\frac{\mu mol\ FusSMO}{l}\right]}$$

- Activity of Fus-SMO for epoxidation of **1a**

$$Activity = \left[\frac{U}{\mu mol\ FusSMO}\right] = \frac{\frac{14.2}{100} \times 2 \times 10^3}{3} = 95\ (std\ \pm 5)$$

- Activity of Fus-SMO for epoxidation of **1c**

$$Activity = \left[\frac{U}{\mu mol\ FusSMO}\right] = \frac{\frac{6.6}{100} \times 2 \times 10^3}{3} = 44\ (std\ \pm 2)$$

Figure 2.13. Initial activity purified Fus-SMO for the quantitative formation of enantiopure **2a** and **2c.** Slope conversion **2a**: 14.2±0.8; Slope conversion **2c**: 6.6±0.2 Specific activity for the epoxidation of **1a** and **1c** with Fus-SMO (this study) in Tris-HCl buffer (pH 8.5, 50 mM), two-component StyA-StyB (literature data) and natural fused StyA2B (literature data). For experimental details, see **section 2.4.12**

Influence of FAD loading and NADH recycling system on the initial activity of purified Fus-SMO

Based on the amount of FAD that is naturally bound to the purified Fus-SMO (ca. 25%), further tests with the purified Fus-SMO system were performed in order to

investigate the influence of FAD loading as well as the possibility to replace stoichiometric amount of NADH with catalytic NAD^+ in combination with the FDH recycling system. Again, the initial activity of the catalytic system was examined and styrene **1a** was used as model substrate. Four different conditions were tested: in condition A stoichiometric amount of NAD^+ and FDH recycling system were used; condition B, same as condition A but without addition of external FAD; condition C, same as condition A but with addition of 0.74 eq. of external FAD; condition D, same as condition A, but with addition of 1.74 eq. of external FAD (for experimental details see **section 2.4.12**). As shown in **Table 2.10**, the addition of FAD is of fundamental importance for a better performance of the catalytic system and it is not necessary to be in excess (though it was not detrimental, condition A) in relation to the amount of enzyme, but it is important to be at least in equimolar ratio with the enzyme (1:1 FAD:enzyme) as shown in the results with conditions C. Furthermore, it is possible to avoid using stoichiometric amount of NADH and use instead NAD^+ (in this case in stoichiometric amount compared to the substrate, however, it may be possible to go lower) in combination with the NAD^+ recycling system (Cb-FDH and HCOONa). Indeed, under these conditions (both A and C) the system performed even better than the standard assay reported above in **Figure 2.13.**

Table 2.10. Initial activity of purified Fus-SMO under various conditions

	Conditions A (NAD^+ recycling system and 5 eq. FAD)	**Conditions B** (NAD^+ recycling system and no external FAD)	**Conditions C** (NAD^+ recycling system and 0.74 eq. FAD)	**Conditions D** (NAD^+ recycling system and 1.74 eq. FAD)
Time [min]	**2a [%]**	**Styrene oxide [%]**	**2a [%]**	**2a [%]**
0	0	0	0	0
1	17	10	16	16
2	29	18	34	25
3	50	32	46	48
Slope	16.152	10.149	15.926	15.005
R^2	0.9876	0.9803	0.9948	0.9667
Activity [min^{-1}]	108	68	106	100

Equivalents NAD^+ based on substrate; equivalents FAD based on enzyme

2.2.7 Thermostability of Fus-SMO

The melting temperature of the Fus-SMO was measured in two buffers (Tris-HCl and KPi) at different pH values. Moreover, various additives, such as glycerol, NaCl and FAD were included in the assay in selected experiments. Consistent results and spectra were observed in Tris-HCl buffer from pH 7.0 up to 8.0, while at pH 9.0 two or more peaks were observed; this may indicate protein unfolding. On the other hand, no reliable results were obtained in KPi buffer. The melting temperature in Tris-HCl buffer was 35 °C at pH 7.0 and (39 °C at basic pH (from 7.5 to 8.5). Regarding the influence of the additives in selected experimental conditions, it is not very clear what the real trend is. Apparently, it seems that the pH is of critical importance depending on the additives present. In general, at pH 7 FAD addition stabilizes the enzyme (i.e., melting temperature shifts from 35 °C without any additives to 39 °C), while the sole addition of NaCl as stabilizer has a lower effect than FAD (*i.e.*, shift from 35 °C without additives to 37 °C). On the other hand, at pH 7.5 the additives have no effect on stabilization of the enzyme (*i.e.*, lower Tm observed in all cases) and the highest T_m is detected in absence of additives (39 °C). At pH 8.0, the addition of NaCl increase further the Tm from 39 °C to 41 °C, but FAD does not have any effect and a similar trend is observed at pH 8.5. The best conditions so far turned out to be at pH 8.5 with the addition of NaCl (41 °C). Further experiments disclosed that both glycerol and FAD are beneficial at pH 7.0, while at higher pH values the main influence is given by glycerol albeit the addition of NaCl is also beneficial at higher pH. In summary, the highest Tm was observed in 50 mM Tris-HCl buffer at pH 8.5 when 100 mM NaCl was added (2 °C higher compared with no addition of additives) without the need for other additives.

2.3 Conclusions

In this work, we have created a chimeric styrene monooxygenase (SMO) in which the two enzymatic units (StyA and StyB) are fused via a flexible linker. The fused SMO allowed for solving a few long-standing problems related to its application in chemical synthesis. First, the Fus-SMO was expressed mainly in soluble form whereas recombinant, singular StyB is almost completely insoluble. Second, the activity of StyA and StyB is now properly balanced as they are produced at an exact ratio of 1:1. Third, the flexible linker forces StyB and StyA to be close each other in solution, hence facilitating their contact. Therefore, the channeling transfer of FAD from StyB to StyA might be favored over the diffusive transfer. These properties permit to minimize the waste of reducing equivalents during the overall process.

Moreover, the rates of the biocatalytic epoxidation catalyzed by Fus-SMO was comparable or superior to the value reported in literature for the two-component StyA-StyB. Further comparison with naturally occurring fused SMO systems revealed that our artificial Fus-SMO is about two orders of magnitude more active. Finally, a recent study showed that another artificially fused SMO had more than 5-fold lower epoxidation rate compared to our Fus-SMO.[72] The different behavior must be attributed to the different type of linkers used for the fusion. In our work we have used a longer (i.e. 30 amino acids) and flexible (*i.e*. containing 70% of glycine) linker, whereas in ref. 72 the linkers were shorter (i.e. from 3 to 6 amino acids) and more rigid (*i.e*. no glycine residues).

When considering the application of the whole cell system, we can conclude that *E. coli* cells expressing Fus-SMO possess higher epoxidation activity than *E. coli* cells expressing separated StyA and StyB as a combination of: *i)* balanced and improved expression levels of reductase and epoxidase units; *ii)* intrinsic higher specific epoxidation activity of Fus-SMO.

Another important aspect for future applications in chemical synthesis and biotechnology is that the His_6-tagged Fus-SMO can be now easily purified. Single expression of StyA and StyB and, moreover, tedious and low-yielding refolding of StyB are no longer required. Hence, Fus-SMO can now also be applied as isolated enzyme in solution.

Finally, the genes of the Fus-SMO and the formate dehydrogenase (Cb-FDH) were co-expressed in *E. coli* and applied as a self-sufficient system for the epoxidation in more than 500 milligrams scale of two model substrates: styrene and β-methyl styrene. The epoxide products were isolated in elevated yields and in perfect diasteromerically and enantiomerically pure form. Hence, Fus-SMO retained the exquisite stereoselectivity of the parent bi-enzymatic system.

In summary, this work will open new opportunities in organic synthesis for the exploitation of the asymmetric biocatalytic epoxidation of styrene derivatives. Furthermore, the same concept might be extended to other multi-enzymatic flavin-dependent systems in order to extend the substrate scope of the reaction beyond styrene derivatives.

2.4 Experimental section

General information. Styrene (**1a**, 99.5%), (*S*)-styrene oxide ((*S*)-**2a,** >98%), racemic styrene oxide (*rac*-**2a**) and 4-methylstyrene (**1c,** >99%) were purchased from Fluka Chemicals. *trans*-β-Methyl styrene (**1b**, >97) was purchased from TCI Chemicals. (1*S*,2*S*)-1-phenylpropylene oxide (1*S,*2*S*-**2b**) and (1*R*,2*R*)-1-phenylpropylene oxide (1*R,*2*R*-**2b,** 97% purity 99% *ee*) were purchased from Sigma Aldrich. All chemicals and solvents were used without further purification. Nicotinamide cofactor (NAD^+) was purchased from Melford Biolaboratories (Chelsworth, Ipswich, UK). Flavin adenine dinucleotide (FAD) was purchased from TCI Chemicals. Catalase from bovine liver was purchased by Sigma-Aldrich (lyophilized powder, >10000 U mg-1 of protein). Catalase was added to the reactions from a stock solution. The concentration of the catalase in the reaction mixture (ca. 2 µM) was calculated considering the MW of the monomer (60 kDa) since each monomer contains a catalytic iron site. Cb-FDH was expressed and purified as described previously.[91]

2.4.1 Expression of *E. coli* JM101 and *E. coli* Arctic express cells carrying pSPZ10-StyAStyB

JM101: 800 mL of LB medium supplemented with kanamycin (50 µg mL^{-1}) were inoculated with 15 mL of an overnight culture and grown at 37 °C until an OD_{600} of 0.6-0.8 was reached. Enzyme expression was induced with DCPK (0.05% v v^{-1}), cells were grown for 16 h at 25 °C and then harvested by centrifugation.

Arctic express DE3: 800 mL of LB medium supplemented with kanamycin (50 µg mL^{-1}) and gentamycin (20 µg mL^{-1}), were inoculated with 15 mL of an overnight culture and grown at 37 °C until an OD_{600} of 0.6-0.8 was reached. Expression of the proteins was induced by the addition of DCPK (0.05% v v^{-1}). Cells were grown for 16 h at 15 °C and then harvested by centrifugation. Results are summarized in **Figure 2.6**.

2.4.2 Activity test: comparison between *E. coli* Arctic Express/pSPZ10-StyAStyB and *E. coli* JM101/pSPZ10-StyAStyB

Reaction conditions: Fresh, frozen and lyophilized *E. coli* cells of JM101 and Arctic Express DE3 containing expressed StyA and StyB (25 °C, 16 h) were subjected to activity tests for the conversion of **1a** (10 mM) to **2a** as described below:

(a) JM101

(1) 3.2 g of wet fresh cells obtained from the expression trials (directly used for bio-catalytic reaction after harvesting of the *E. coli* culture) were resuspended in 18 mL of KPi buffer (50 mM, pH 7.0, final concentration of wet fresh cells ca. 180 mg mL^{-1}). An aliquot of 0.5 mL was used for each bio-catalytic reaction. (2) Frozen cell pellets were defrosted and the wet cells were resuspended in KPi buffer to obtain a final cell concentration of ca. 130 mg mL^{-1} (50 mM, pH 7.0). An aliquot of 0.5 mL was used for each biocatalytic reaction (3) Lyophilized

cells (10 mg) were rehydrated in KPi buffer (0.5 mL, 50 mM, pH 7.0) and used for performing the activity check.

(b) Arctic Express DE3

(1) Fresh cells obtained from the expression test (2.3 g) were resuspended in KPi buffer (50 mM, pH 7; 18 mL, final concentration of wet fresh cells ca. 180 mg mL^{-1}). An aliquot of 0.5 mL was used for each test. (2) Frozen cells (2.24 g) were resuspended in KPi buffer (50 mM, pH 7; 18 mL, final concentration of wet cells ca. 130 mL^{-1}). An aliquot of 0.5 mL was used for each bio-catalytic reaction. (3) Lyophilized cells (10 mg) were rehydrated in 0.5 mL KPi buffer (50 mM, pH 7.0) and used for performing the activity check.

Bio-catalytic reactions were performed in a biphasic system (1:1, v v^{-1} buffer/decane) in 4 mL glass vials (final reaction volume 1 mL) in the presence of NAD^+ (1 mM, 0.1 eq.), HCOONa (100 mM, 10 eq.) and Cb-FDH (10 µM) for recycling of the NAD cofactor. The concentrations of coenzyme, co-substrate and recycling enzyme are calculated on the volume of the aqueous phase. The reactions were initiated by the addition of **1a** (10 mM, calculated on the volume of the organic phase) and incubated at 30 °C and 170 rpm on an orbital shaker for 16 h. The organic phase reaction mixture (decane) was separated from the aqueous phase. The aqueous phase was further extracted with EtOAc (2x 500 µL). The combined organic phases (decane + EtOAc) were dried with $MgSO_4$ and the conversions were measured by GC-FID. The results are reported in T**able 2.5**.

2.4.3 Expression and activity test for the chimeric fused SMO (Fus-SMO) in *E. coli* BL21 DE3

First expression trial of Fus-SMO

The DNA sequence encoding for styA and styB (GenBank: AF031161.1) was optimized for the expression in *E. coli* and subcloned in pET28b between NdeI and XhoI to obtain the His_6-StyA-linker-StyB (MW = 69 kDa) construct (flexible linker AA sequence: ASGGGGSGGGGSGGGGSGGGGSGGGGSGAS.[73]

When transforming BL21 DE3 cells with the plasmid, colonies of various colors (pink/white/blue colors) grew and four of them were picked and subjected to expression and solubility trials (Figure 2.3). For each colony, 400 mL of LB medium were supplemented with Kanamycin (50 µg/mL) and inoculated with 8 mL of an overnight culture. The cells were grown at 37 °C until the cell density reached a value between 0.6 and 0.8 and split into 100 mL aliquots. To each aliquot IPTG was added (1 mM final concentration) and protein expression was carried out at 37 °C for 3h, 30 °C for 5 h or 25 °C overnight (o.n.). The cells were harvested by centrifugation, washed with KPi buffer (50 mM, pH 8.0) and lyophilized.

Preliminary tests with Fus-SMO as lyophilized whole cells for the conversion of **1a** to **2a**

Lyophilized cells (20 mg) obtained from the expression test were rehydrated in KPi buffer (50 mM, pH 7.5, 1 mL) in 20 mL glass vials. After that the cofactor NAD^+ (1 mM, 0.05 eq.) was added followed by addition of HCOONa (100 mM, 5 eq.) and purified Cb-FDH (10 µM). Furthermore, FAD (50 µM) was added to selected experiments. The concentrations of coenzymes, cosubstrate and recycling enzyme are calculated in relation to the volume of the aqueous phase. Decane (1 mL) was used as biphasic solvent and the biotransformations were initiated by the addition of **1a** (20 mM, calculated on the volume of the organic phase). The mixtures were shaken at 30 °C and 180 rpm on an orbital shaker for 17 h. The organic phase (decane) was separated from the aqueous phase. The aqueous phase was further extracted with EtOAc (2x 500 µL). The combined organic phases (decane + EtOAc) were dried with $MgSO_4$ and the conversions were measured by GC-FID and results are reported in **Table 2.1**.

Optimization of the expression using various concentrations of IPTG and testing the activity of Fus-SMO in BL21 DE3

800 mL of Luria-Bertani Broth were supplemented with kanamycin (50 µg mL^{-1}) and inoculated with 15 mL of an overnight culture of *E. coli*/pET28b-Fus-SMO (colony 1). The main culture was grown at 37 °C until the cell density reached an OD_{600} of 0.6-0.8. Then, the expression of the protein was induced by the addition of IPTG (0.1, 0.5 and 1 mM, respectively) and the cells grown for additional 16 h at 25 °C and harvested by centrifugation (**Figure 2.4**).

Activity tests were first performed with the soluble fraction. The activities from all the expression conditions were assayed in order to understand the best condition for expression. Furthermore, the influence of different reaction vessels on the outcome of the biocatalytic reaction was also investigated.

Reaction conditions for the conversion of **1a** to **2a** by the soluble part of expressed Fus-SMO:

450-500 mg of cells (wet weight) obtained from the expression trials were resuspended in KPi buffer (pH 7.5, 50 mM, 3 mL) and lysed by sonication (5 sec. on, 10 sec. off, 5 min on time, 45 % amplitude). The cell debris was removed by centrifugation and only the supernatant was used for further activity tests as described below. Results are reported in **Table 2.3**.

Note: the concentrations of coenzymes, cosubstrate and recycling enzyme are always calculated on the volume of the aqueous phase, whereas the concentration of the substrate is referred to the organic phase.

Reactions performed in Eppendorf tubes (2 mL): To a 350 µL aliquot of the soluble fraction, NAD^+ (1 mM, 0.1 eq.), HCOONa (100 mM, 10 eq.), Cb-FDH (10 µM) and FAD (30 µM) were added (0.5 mL final volume of aqueous phase). Decane (0.5 mL) was used as biphasic solvent and the biotransformation was initiated by the addition of **1a** (10 mM). The reaction was shaken at 30 °C and 180 rpm on an orbital shaker for 20 h. The organic phase from the reaction mixture (decane) was separated from the aqueous phase. The aqueous phase was further extracted with EtOAc (2x 250 µL). The combined organic phases (decane + EtOAc) were dried with $MgSO_4$ and the conversions were measured by GC-FID.

Reactions performed in 4 mL glass vials: To a 350 µL aliquot of the soluble fraction, NAD^+ (1 mM, 0.1 eq.), HCOONa (100 mM, 10 eq.), Cb-FDH (10 µM) and FAD (30 µM) were added (0.5 mL final volume of aqueous phase). Decane (0.5 mL) was used as biphasic solvent and the biotransformation was initiated by the addition of **1a** (10 mM). The mixture was shaken at 30 °C and 180 rpm on an orbital shaker for 20 h. The organic phase from the reaction mixture (decane) was separated from the aqueous phase. The aqueous phase was further extracted with EtOAc (2x 250 µL). The combined organic phases (decane + EtOAc) were dried with $MgSO_4$ and the conversions were measured by GC-FID.

Reactions performed in 20 mL glass vials: To a 700 µL aliquot of the soluble fraction, NAD^+ (1 mM, 0.1 eq.), HCOONa (100 mM, 10 eq.), Cb-FDH (10 µM) and FAD (30 µM) were added (1 mL final volume of aqueous phase). Decane (1 mL) was used as biphasic solvent and the biotransformation was initiated by the addition of **1a** (10 mM). The mixture was shaken at 30 °C and 180 rpm on an orbital shaker for 20 h. The organic phase from the reaction mixture (decane) was separated from the aqueous phase. The aqueous phase was further extracted with EtOAc (2x 500 µL). The combined organic phases (decane + EtOAc) were dried with $MgSO_4$ and the conversions were measured by GC-FID.

2.4.4 Reaction conditions for the conversion of 1a to (*S*)-2a by lyophilized whole cells containing Fus-SMO

The reactions were performed in 4 mL glass vials, as this type of vessel showed highest conversion in the preliminary test (see above). Lyophilized cells obtained from the expression trial using various concentration of IPTG for induction were tested for the activity towards the conversion of **1a**. Also, the amount of lyophilized cells that is needed for the conversion of 20 mM substrate was investigated. Results are reported in **Table 2.2**.

Lyophilized cells (2.5, 5 and 10 mg) were rehydrated in KPi buffer (0.5 mL, 50 mM, pH 7.5) in 4 mL glass vials. After that the cofactor NAD^+ (1 mM, 0.05 eq.) was added followed by addition of HCOONa (100mM, 5 eq.), Cb-FDH (10 µM) and FAD (50 µM). The concentrations of coenzymes, cosubstrate and recycling enzyme are calculated on the volume of the

aqueous phase. Decane (0.5 mL) was used as biphasic solvent and the biotransformation was initiated by the addition of **1a** (20 mM, referred to the organic phase). The mixture was shaken at 30 °C and 180 rpm on an orbital shaker for 17 h. The organic phase from the reaction mixture (decane) was separated from the aqueous phase. The aqueous phase was further extracted with EtOAc (2x 250 µL). The combined organic phases (decane + EtOAc) were dried with $MgSO_4$ and the conversions were measured by GC-FID.

2.4.5 Solvent screening: bioconversion of 1a to (*S*)-2a by lyophilized cells containing Fus-SMO

For all experiments, cells were used after expression with 0.1 mM IPTG at 25 °C for 16 h.

Note: The concentrations of coenzymes, co-substrate and recycling enzyme are always calculated on the volume of the aqueous phase, the concentration of the substrate is referred to the organic phase and results are reported in **Table 2.4**.

1:1 ratio *n*-hexane or *n*-heptane/KPi buffer: Lyophilized whole cells (10 mg) were rehydrated in KPi buffer (0.5 mL, 50 mM, pH 8) in 4 mL glass vials. After that, the cofactor NAD^+ (1 mM, 0.05 eq.) HCOONa (100 mM, 5 eq.), Cb-FDH (10 µM) and FAD (50 µM) were added. Two organic solvents (*n*-hexane or *n*-heptane; 1:1, v v^{-1} with the buffer) were tested as biphasic solvents. Finally, the biotransformations were initiated by the addition of **1a** (20 mM). The reactions were shaken at 30 °C and 180 rpm on an orbital shaker for 24 h. The organic phase from the reaction mixture was separated from the aqueous phase. The aqueous phase was further extracted with MTBE (2x 250 µL). The combined organic phases were dried with $MgSO_4$ and the conversions were measured by GC-FID.

KPi buffer: Lyophilized whole cells (20 mg) were rehydrated in KPi buffer (1 mL, 50 mM, pH 8) in 4 mL glass vials. After that the cofactor NAD^+ (1 mM, 0.05 eq.), HCOONa (100 mM, 5 eq.), Cb-FDH (10 µM) and FAD (50 µM) were added. The biotransformations were initiated by the addition of **1a** (20 mM). The reactions were shaken at 30 °C and 180 rpm on an orbital shaker for 24 h. The organic compounds were extracted with MTBE (2 x 250 µL), the combined organic layers were dried over $MgSO_4$ and the conversions were measured by GC-FID.

5% styrene or 2-10% decane: Lyophilized whole cells were rehydrated in KPi buffer (50 mM, pH 8.0) in 4 mL glass vials. Then, the cofactor NAD^+ (0.1 eq), HCOONa (5 eq.), Cb-FDH (10 µM) and FAD (50 µM) were added. In selected experiments, decane was used (2-10% v v^{-1}; 1 mL total reaction volume) as second phase or styrene (5% v v^{-1}; 1 mL total reaction volume) as neat substrate. The bio-transformations were initiated by the addition of **1a** (10 – 20 µmol) in the case of decane (2 to 10 % v v^{-1}) as organic solvent or **1a** (435 mM) in the case of styrene used as neat substrate. The reactions were shaken at 30 °C and 180 rpm on

an orbital shaker for 24 h. The organic phase from the reaction mixture was separated from the aqueous phase. The aqueous phase was further extracted with MTBE (2 x 400-500 µL). The combined organic layers were dried over $MgSO_4$ and the conversions were measured by GC-FID.

2.4.6 Determination of the required reducing equivalents (i.e. equivalents of HCOONa) for the bio-conversion of 1a (20 mM) to (*S*)-2a using lyophilized whole cells containing Fus-SMO

Lyophilized whole cells of overexpressed Fus-SMO (5 mg, 10 mg mL^{-1}) were rehydrated in KPi buffer (0.5 mL, 50 mM, pH 8) in 4 mL glass vials. NAD^+ (1 mM, 0.05 eq.), HCOONa (0-100 mM, 0-5 eq.), Cb-FDH (10 µM), FAD (50 µM), *n*-heptane (0.5 mL) and **1a** (20 mM, referred to organic phase) were added and the reactions were incubated at 30 °C and 180 rpm on an orbital shaker for 24 h. The concentrations of coenzymes, cosubstrate and recycling enzyme are calculated on the volume of the aqueous phase. The organic phase from the reaction mixture (*n*-heptane) was separated from the aqueous phase. The aqueous phase was further extracted with MTBE (2x 250 µL). The combined organic phases (*n*-heptane + MTBE) were dried with $MgSO_4$ and the conversions were measured by GC-FID (**Table 2.11**).

Table 2.11. Conversions [%] of **1a** (20 mM) to (*S*)-**2a** by Fus-SMO (10 mg mL^{-1}) and various concentrations of hydride donor

Entry	HCOONa [mM]	eq. HCOONa	*(S)*-2a [%][a]
1	0	0	21±8
2	2	0.1	22±3
3	4	0.2	19±1
4	8	0.4	28±1
5	12	0.6	23±0
6	16	0.8	34±1
7	20	1	37±6
8	40	2	63±1
9	60	3	93±<1
10	80	4	99±1
11[b]	100	5	99±<1

[a] Reactions were performed in duplicates and the reported conversion is the average of two measurements. [b] The optical purity of the final product was measured by HPLC on a chiral column for sample entry 11. The enantiomeric excess was > 99% (*S*).

2.4.7 Influence of dioxygen in the headspace on the performance of Fus-SMO (expressed in *E. coli* BL21 DE3) and natural StyA-StyB (expressed in *E. coli* JM101, plasmid pSPZ10)

Effect of oxygen pressure on the bio-catalytic conversion of **1a** (50 mM) in a pressurizable chamber

Lyophilized *E. coli* cells containing Fus-SMO or natural StyA-StyB (pSPZ10 plasmid) (2.5 mg; 5 mg mL^{-1}) were rehydrated in KPi buffer (pH 8, 50 mM, 0.5 mL) in 20 mL glass vials. The buffer already contained the required amount of NAD^+ (1 mM, 0.02 eq.), HCOONa (250 mM, 5 eq.), FAD (50 µM) and Cb-FDH (10 µM). In certain experiments catalase (2 µM) was also added. The biotransformations were started by addition of *n*-heptane (0.5 mL) as the second solvent phase followed by the addition of **1a** (50 mM; calculated on the volume of the organic phase). The mixtures were shaken in a closed chamber (Figure 2.7) on an orbital shaker (200 rpm) at 30 °C for 20 minutes. The reactions were quenched by freezing in liquid nitrogen. The organic phase from the reaction mixture (*n*-heptane) was separated from the aqueous phase. The aqueous phase was further extracted with MTBE (500 µL). The combined organic phases (*n*-heptane + MTBE) were dried with $MgSO_4$ and the conversions were measured by GC-FID (**Table 2.12 and 2.13**).

Table 2.12. Conversion [%] of **1a** (50 mM) to (*S*)-**2a** using lyophilized cells containing Fus-SMO (5 mg mL^{-1}) in a closed chamber. Reaction time: 20 minutes.

Entry	O_2 pressure [bar][a]	*E. coli* BL21 DE3/Fus-SMO 2a [%][c]	*E. coli* BL21 DE3/Fus-SMO/catalase[b] 2a [%][c]
1	Atmospheric pressure	16.3±0.6	21.2±2.9
2	Saturation with pure O_2	10.0±1.0	24.5±1.7
3	1	10.8±1.0	20.4±2.2
4	2	9.1±2.9	18.6±1.1
5	3	10.0±1.0	17.1±1.4
6	4	7.8±1.8	14.6±2.9

[a] Experiments were performed in a sealed pressurized chamber; for entry 2 the chamber was saturated with pure O_2 before reactions were started; [b] final catalase concentration 2 µM; [c]Reactions were performed in duplicates and two independent experiments were performed; thus, the reported conversion is then the average of the 4 values. Errors are expressed as standard deviation.

Table 2.13. Conversion [%] of 1a (50 mM) to (S)-2a using lyophilized cells containing natural StyA and StyB (5 mg mL^{-1}) in a closed chamber. Reaction time: 20 minutes.

Entry	O_2 pressure [bar][a]	*E. coli* JM101/pSPZ10-StyAStyB 2a [%][c]	*E. coli* JM101/pSPZ10-StyAStyB /catalase[b] 2a [%][c]
1	Atmospheric pressure	11.8±2.3	14.0±2.6
2	Saturation with pure O_2	13.0±0.1	17.7±0.8
3	1	11.8±3.5	12.6±2.0
4	2	8.4±2.1	9.6±0.4
5	3	8.3±0.7	9.0±0.7
6	4	6.4±1.2	6.3±0.6

[a] Experiments were performed in a sealed pressurized chamber; for entry 2 the chamber was saturated with pure O_2 before reactions were started; [b] final catalase concentration 2 µM; [c]Reactions were performed in duplicates and two independent experiments were performed; thus, the reported conversion is then the average of the 4 values. Errors are expressed as standard deviation.

2.4.8 Final comparison of the catalytic efficiency between the chimeric Fus-SMO and the natural StyA-StyB system (from plasmid pSPZ10)

Lyophilized *E. coli* cells carrying Fus-SMO or natural StyA-StyB (plasmid pSPZ10) (2.5 mg; 5 mg mL^{-1}) were rehydrated in KPi buffer (pH 8.0, 50 mM, 0.5 mL) in 20 mL glass vials. The buffer already contained the required amount of NAD^+ (1mM, 0.02eq.), HCOONa (250 mM, 5 eq.), FAD (50 µM), Cb-FDH (10 µM) and catalase (2 µM). The biotransformations were started by the addition of *n*-heptane (0.5 mL) as the second solvent phase followed by the addition of **1a** (50 mM; calculated on the volume of the organic phase). The mixtures were shaken in a closed chamber on an orbital shaker (200 rpm) at 30 °C for 10, 20 and 30 minutes. The reactions were quenched by freezing in liquid nitrogen. The organic phase from the reaction mixture (*n*-heptane) was separated from the aqueous phase. The aqueous phase was further extracted with MTBE (500 µL). The combined organic phases (*n*-heptane + MTBE) were dried with $MgSO_4$ and the conversions were measured by GC-FID.

2.4.9 Co-expression of Fus-SMO and Cb-FDH in *E. coli* BL21 DE3

LB medium (800 mL), supplemented with kanamycin (50 µg mL^{-1}) and ampicillin (100 µg mL^{-1}), was inoculated with 15 mL of a pre-culture and grown at 37 °C until the cell density reached an OD_{600} value of 0.6-0.8. The expression was induced by the addition of IPTG (0.1 mM final concentration) and the cells were grown for further 16 h at 25 °C prior to harvesting by centrifugation at 4500 rpm. The whole cells were then washed with KPi buffer (pH 8, 50 mM), lyophilized (ca. 2g dry weight) and stored at -20 °C (**Figure 2.10**).

Activity test for the co-expressed cells

Lyophilized whole cells containing Fus-SMO and Cb-FDH (5 mg) were rehydrated in KPi buffer (pH 8, 50 mM, 0.5 mL) in 4 mL glass vials. NAD^+ (1 mM, 0.05 eq.), FAD (50 µM), HCOONa (100 mM, 5 eq.) and heptane (0.5 mL) were added. The biotransformations were started by the addition of substrate (**1a** or **1b,** 20 mM) and shaken at 30 °C, 180 rpm on an orbital shaker for 24 h. The concentrations of coenzymes, co-substrate and recycling enzyme are always calculated on the volume of the aqueous phase, the concentration of the substrate is referred to the organic phase. The organic phase from the reaction mixture (*n*-heptane) was separated from the aqueous phase. The aqueous phase was further extracted with MTBE (2 x 250 µL). The combined organic phases (*n*-heptane + MTBE) were dried with $MgSO_4$ and analyzed by GC-FID and chiral HPLC (**Table 2.6**).

Time study for the bio-catalytic epoxidation of 1a and 1b (50 mM) to enantiopure (*S*)-2a and (1*S*,2*S*)-2b using lyophilized whole cells of co-expressed Fus-SMO and Cb-FDH.

Lyophilized whole cells containing co-expressed Fus-SMO and Cb-FDH (2.5 mg, 5 mg mL^{-1}) were rehydrated in KPi buffer (pH 8, 50 mM, 0.5 mL) in a 20 mL glass vial. NAD^+ (1 mM), FAD (50 µM), HCOONa (5 eq.), catalase (2 µM), *n*-heptane (0.5 mL) and the substrates **1a** (50 mM) or **1b** (50 mM) were added. The concentration of cells, coenzyme and recycling enzyme are calculated on the volume of the aqueous phase, while the concentration of the substrate on the organic phase. The reactions were incubated at 30 °C and 200 rpm on an orbital shaker and monitored over time (0.5, 1, 2, 3, 4, 5, 6 and 24 h). The reactions were quenched by freezing in liquid nitrogen**.** The organic phase from the reaction mixture (*n*-heptane) was separated from the aqueous phase. The aqueous phase was further extracted with MTBE (500 µL). The combined organic phases (*n*-heptane + MTBE) were dried with $MgSO_4$. The conversions were analyzed by GC-FID (**Table 2.14**).

Table 2.14. Time study for the conversion of **1a** and **1b** (50 mM) by lyophilized cells of co-expressed Fus-SMO and Cb-FDH

Entry	Time [h]	*(S)*-2a [%]	(1*S*,2*S*)-2b [%]
1	0.5	27.1±1.2	17.6±0.5
2	1	51.4±5.3	35.8±1.6
3	2	70.9±3.4	57.4±0.5
4	3	83.4±4.3	68.6±1.8
5	4	86.6±3.4	75.4±3.0
6	5	91.8±2.5	81.1±2.2
7	6	93.8±1.3	82.5±1.6
8	24	98.8±1.2	90.4±1.4

Reactions were performed as duplicates in two independent experiments; hence, the reported conversion is the average of 4 values. Error is expressed as the standard deviation.

Experiments with increased substrate concentration for the bio-epoxidation of 1a and 1b (50 mM - 1 M) using lyophilized *E. coli* cells co-expressing Fus-SMO/Cb-FDH

General procedure. Lyophilized whole cells containing co-expressed Fus-SMO and Cb-FDH (2.5 mg, 5 mg mL^{-1}) were rehydrated in KPi buffer (pH 8, 50 mM, 0.5 mL) in a 20 mL glass vial. NAD^+ (1 mM), FAD (50 µM), HCOONa (5 eq.), catalase (2 µM), *n*-heptane (0.5 mL) and the substrates **1a** (from 50 to 1 M) or **1b** (from 50 mM to 1 M) were added. The concentration of cells, coenzyme and recycling enzyme are calculated on the volume of the aqueous phase, while the concentration of the substrate is calculated on the volume of on the organic phase. The reactions were incubated at 30 °C and 200 rpm on an orbital shaker for 24 h. The organic phase from the reaction mixture (*n*-heptane) was separated from the aqueous phase. The aqueous phase was further extracted with MTBE (500 µL). The combined organic phases (*n*-heptane + MTBE) were dried with $MgSO_4$. The conversions were analyzed by GC-FID (**Table 2.7**).

General procedure. Lyophilized whole cells containing co-expressed Fus-SMO and Cb-FDH (5 mg, 5 mg mL^{-1}) were rehydrated in KPi buffer (pH 8, 50 mM, 1 mL) in a 100 mL Erlenmeyer flask. NAD^+ (1 mM), FAD (50 µM), HCOONa (5 eq.), catalase (2 µM), *n*-heptane (1 mL) and the substrates **1a** (from 50 mM to 1 M) or **1b** (50 mM to 1 M) were added. The concentration of cells, coenzyme and recycling enzyme are calculated on the volume of the aqueous phase, while the concentration of the substrate is calculated on the volume of the organic phase. The reactions were incubated at 30 °C and 200 rpm on an orbital shaker for 24 h. The organic phase from the reaction mixture (*n*-heptane) was separated from the aqueous phase. The aqueous phase was further extracted with MTBE (2 x 500 µL). The combined organic phases (*n*-heptane + MTBE) were dried with $MgSO_4$. The conversions were analyzed by GC-FID (**Table 2.8**).

Study on the influence of the mode of dioxygen transfer in the biphasic biocatalytic epoxidation: sealed system with air headspace versus system with continuous flow (i.e. bubbling) of dioxygen

General procedure for the epoxidation applying a sealed system with air headspace: Lyophilized whole cells containing co-expressed Fus-SMO and Cb-FDH (125 mg, 5 mg mL^{-1}) were rehydrated in KPi buffer (pH 8, 50 mM, 25 mL) in a 500 mL three necks round-bottom flask. NAD^+ (1 mM), FAD (50 µM), HCOONa (5 eq.), catalase (2 µM), *n*-heptane (25 mL) and the substrate **1a** (50 mM) were added. The concentration of cells, coenzyme and recycling enzyme are calculated on the volume of the aqueous phase, while the concentration of the substrate is calculated on the volume of the organic phase. A set of reactions was conducted at room temperature under magnetic agitation for 30 min, 45 min, 60 min and 24 h. A vigorous agitation (ca. 700-800 rpm) was set during the reaction in order to obtain an emulsion without a visible separation between the aqueous phase and the organic phase. In this way, we can minimize the mass transfer resistance of styrene from the organic phase to the aqueous phase as well as of styrene oxide in the contrary direction. Thus, any possible kinetic limitation in the mass transfer of dioxygen from the gas phase to the liquid phases can be studied under these conditions.

The rate of the epoxidation reaction expressed as mass of styrene oxide produced per minute is reported in **Figure 2.12** (black line).

General procedure for the epoxidation applying continuous flow of dioxygen (bubbling): Lyophilized whole cells containing co-expressed Fus-SMO and Cb-FDH (125 mg, 5 mg mL^{-1}) were rehydrated in KPi buffer (pH 8, 50 mM, 25 mL) in a 100 mL three necks round-bottom flask. NAD^+ (1 mM), FAD (50 µM), HCOONa (5 eq.), catalase (2 µM), *n*-heptane (25 mL) and the substrate **1a** (50 mM) were added. The concentration of cells, coenzyme and recycling enzyme are calculated on the volume of the aqueous phase, while the concentration of the substrate is calculated on the volume of the organic phase. The flow of molecular oxygen was supplied to the reaction *via* a needle placed through a septum in one neck of the round-bottom flask. That permitted the bubbling of pure dioxygen (ca. 1 mL min^{-1}) directly into the reaction mixture. Another small needle was placed through another septum in the flask in order to prevent any overpressure. A set of reactions was conducted at room temperature under magnetic agitation for 30 min, 45 min, 60 min and 24 h. A vigorous agitation (ca. 700-800 rpm) was set during the reaction in order to obtain an emulsion without a visible separation between the aqueous phase and the organic phase. In this way, we can minimize the mass transfer resistance of styrene from the organic phase to the aqueous phase as well as of styrene oxide in the contrary direction. Thus, any possible kinetic limitation in the mass transfer of dioxygen from the gas phase to the liquid phases can be studied under these conditions.

The rate of the epoxidation reaction expressed as mass of styrene oxide produced per minute is reported in **Figure 2.12** (grey line).

General optimized procedure for the bio-catalytic synthesis of (*S*)-2a and (1*S*,2*S*)-2b by lyophilized whole cells co-expressing Fus-SMO and Cb-FDH (analytical scale). Lyophilized whole cells (5 mg) were rehydrated in KPi buffer (0.5 mL, 50 mM, pH 8) in 4 mL or 20 mL glass vials, containing NAD^+ (1 mM), HCOONa (5 eq.), FAD (50 µM) and catalase (2 µM). *n*-Heptane (0.5 mL) and the substrate **1a-b** (50 mM) were added. The concentration of the substrate is calculated on the volume of the organic phase. The concentrations of NAD^+, HCOONa are calculated on the volume of the aqueous phase. The mixture was incubated at 30 °C and 180 rpm on an orbital shaker. At the end of the reaction, the organic phase was separated from the aqueous phase. The aqueous phase was extracted with MTBE (2 x 250 µL). The combined organic phases were dried with $MgSO_4$. The conversions were measured by GC-FID, whereas the *ee* and *de* were measured by HPLC.

2.4.10 Preparative scale bio-catalytic epoxidation

General optimised procedure for the bio-catalytic synthesis of (*S*)-2a by whole cells co-expressing Fus-SMO and Cb-FDH (scale up). Lyophilized whole cells containing co-expressed Fus-SMO and Cb-FDH (500 mg, 5 mg mL^{-1}) were rehydrated in KPi buffer (pH 8, 50 mM, 100 mL) in a 1 L tri-baffled flask. NAD^+ (1 mM), FAD (50 µM), HCOONa (5 eq.) and catalase (2 µM) were added. *n*-Heptane (100 mL) and the substrate **1a** (50 mM, 521 mg, 5.00 mmol) were added. The concentration of cells, NAD^+ and HCOONa are calculated on the volume of the aqueous phase. The concentration of the substrate is calculated on the volume of the organic phase. The reaction was incubated at 30 °C and 200 rpm on an orbital shaker for 16 h. After completion of the reaction confirmed by GC-FID, the *n*-heptane phase was recovered, dried with $MgSO_4$ and evaporated under reduced pressure yielding 509 mg (85%) of (*S)*-**2a** (99% purity by GC-FID; *ee* >99% by chiral HPLC. Separately, the aqueous phase was extracted with MTBE (2 x 50 mL); the organic layer was dried with $MgSO_4$ and the solvent was evaporated under reduced pressure, affording the remaining 12% of product in 94% chemical purity.

General optimized procedure for the bio-catalytic synthesis of (1*S*, 2*S*)-2b by lyophilized whole cells co-expressing Fus-SMO and Cb-FDH (scale-up). A similar procedure was performed as reported above. Lyophilized whole cells containing co-expressed Fus-SMO and Cb-FDH (500 mg, 5 mg mL^{-1}) were rehydrated in KPi buffer (pH 8, 50 mM, 100 mL) in a 1 L tri-baffled flask. NAD^+ (1 mM), FAD (50 µM), HCOONa (5 eq.) and catalase (2 µM) were added. n-Heptane (100 mL) and substrate **1b** (50 mM, 591 mg, 5.00 mmol) was added. The concentration of cells, NAD^+ and HCOONa are calculated on the volume of the aqueous phase. The concentration of the substrate is calculated on the volume of the organic phase. The reactions were incubated at 30 °C and 200 rpm on an orbital shaker for 16 h. After completion of the reaction confirmed by GC-FID, the *n*-heptane phase was recovered and evaporated under reduced pressure. The aqueous phase was then extracted with MTBE (2 x 50 mL). In this case, the purity of the product (*1S,2S*)-**2b** was similar in the *n*-heptane phase

and in the extracted MTBE phase. Thus, the organic phases were combined, dried with $MgSO_4$ and the solvent was evaporated. The final yield was 603 mg of (*1S,2S*)-**2b** (90% isolated yield, 95% purity by GC-FID; *ee* >99% and *de* >98% by chiral HPLC.

2.4.11 Purification His_6 Fus-SMO

Expression was conducted as previously described in **section 2.4.3** (0.1 mM IPTG, 25 °C overnight).

Wet cells containing Fus-SMO (ca. 12 g) were resuspended in lysis buffer (ca. 65 mL; 50 mM KH_2PO_4, 300 mM NaCl, 10 mM imidazole, pH 8) and disrupted by sonication (10 min, amplitude 45%, pulse on 10 s, pulse off 10 s). The suspension was centrifuged (18000 rpm, 1 h, 4 °C). The supernatant was filtered through a 0.45 µm filter and loaded onto a Ni^{2+} column (5 mL, GE Healthcare) that was previously conditioned with lysis buffer. The column was washed with washing buffer (50 mM KH_2PO_4, 300 mM NaCl, 25 mM imidazole, pH 8) and the protein eluted with elution buffer (50 mM KH_2PO_4, 300 mM NaCl, 300 mM imidazole, pH 8). Purity was analyzed by SDS-Page and fractions showing >95% purity were combined and dialyzed overnight against potassium phosphate buffer (6 L, pH 8, 20 mM). The enzyme solution was concentrated and the concentration was measured spectrophotometrically by the method of Bradford (Bovine Serum Albumine standard). 128 mg of protein were obtained from ca. 12 g of wet cells, equal to 3.2 L of culture, without further optimization. The purified protein shows a yellow color which corresponds to a natural loading of FAD of ca. 25%. The loading of FAD was analyzed by UV-Vis-spectroscopy at 450 nm by using the characteristic extinction coefficient of free FAD (ε=11300 M^{-1} cm^{-1}).

2.4.12 Typical assay for the determination of the initial activity of purified His_6 Fus-SMO

The epoxidation activity of Fus-SMO with **1a** and **1c** was measured according to the procedure reported by Otto *et al*.[64] as well as Tischler *et al*.[68] The quantification of the product formation *vs* time was performed by quenching samples at different time points and determining the conversion by GC-FID. A typical sample assay contained (2 mL Eppendorf tube): Fus-SMO (3 µM), FAD (15 µM), HCOONa (150 mM), catalase (650 U), Cb-FDH (20 µM), styrene (**1a**) or 4-methylstyrene (**3a**) (2 mM, from a 50 mM stock solution in heptane) in a 1 mL total volume of Tris-HCl buffer (pH 8.5, 50 mM). The mixture was incubated at 37 °C for 1 min and the reaction was started by the addition of NADH (50 mM). The samples were shaken at 37 °C, 1400 rpm for 1, 2, 3, 4 and 5 min, respectively. Reactions were stopped by freezing in liquid nitrogen followed by extraction with MTBE (2 x 500 µL). The organic phase was separated from the aqueous layer, dried over $MgSO_4$ and injected into GC-FID.

Influence of FAD loading and NADH recycling system on the initial activity of purified Fus-SMO: The same assay as described above was used for these tests with some variations as follow:

CONDITION A: Fus-SMO (3 µM), FAD (15 µM, 5 eq. based on Fus-SMO), NAD^+ (2 mM, 1 eq. based on **1a**), HCOONa (150 mM), catalase (650 U), Cb-FDH (60 µM), styrene (**1a**) (2 mM, from a 50 mM stock solution in heptane) in a 1 mL total volume of Tris-HCl buffer (pH 8.5, 50 mM).

CONDITION B: Fus-SMO (3 µM), NAD^+ (2 mM, 1 eq. based on **1a**), HCOONa (150 mM), catalase (650 U), Cb-FDH (60 µM), styrene (**1a**) (2 mM, from a 50 mM stock solution in heptane) in a 1 mL total volume of Tris-HCl buffer (pH 8.5, 50 mM).

CONDITION C: Fus-SMO (3 µM), FAD (2.22 µM, 0.74 eq. based on Fus-SMO), NAD^+ (2 mM, 1 eq. based on **1a**), HCOONa (150 mM), catalase (650 U), Cb-FDH (60 µM), styrene (**1a**) (2 mM, from a 50 mM stock solution in heptane) in a 1 mL total volume of Tris-HCl buffer (pH 8.5, 50 mM).

CONDITION D: Fus-SMO (3 µM), FAD (5.22 µM, 1.74 eq. based on Fus-SMO), NAD^+ (2 mM, 1 eq. based on **1a**), HCOONa (150 mM), catalase (650 U), Cb-FDH (60 µM), styrene (**1a**) (2 mM, from a 50 mM stock solution in heptane) in a 1 mL total volume of Tris-HCl buffer (pH 8.5, 50 mM).

2.4.13 Thermostability measurement

The thermostability (melting temperature T_m, defined as the temperature at which 50% of the enzyme unfolds) of Fus-sMO was measured in 50 mM Tris-HCl buffer (pH 7.0, 7.5, 8.0, 8.5 and 9.0) as well as in 50 mM KPi buffer (pH 6.0, 6.5, 7.0, 7.5 and 8.0) by differential scanning fluorometry using a Biorad-7500 QPCR machine. Fluorescence data were collected as a continuous standard melt curve from 20-90 °C (1% increment, hold 1 min at 20 °C and 1 min at 90 °C), using ROX for reporter and none for quencher. Also, none was selected as passive reference. A standard sample (20 µL total final volume per well) contained the following components: Fus-SMO (1 µg), buffer (50 mM), NaCl (100 mM), Sypro Orange (5 times), Glycerol (5% vol/vol), FAD (10.7 µM) and MilliQ.

Note: Buffer, Sypro Orange and Milli-Q were always present in the mixture while all the other components (additives) were varied as shown in Table 2.15.

Table 2.15. Conditions tested for the thermostability of Fus-SMO in 50 mM Tris-HCl buffer (pH 7.0, 7.5, 8.0, 8.5, 9.0) and in 50 mM KPi buffer (pH 6.0, 6.5, 7.0, 7.5, 8.0)

Sample / Additive	1	2	3	4	5	6	7	8	9 (control)	10 (control)
NaCl	+	+	-	-	-	+	-	+	+	-
FAD	+	-	+	-	-	+	+	-	+	-
Fus-SMO	+	+	+	+	+	+	+	+	-	-
Glycerol	-	-	-	-	+	+	+	+	+	-

Table 2.16. Results for the thermostability of Fus-SMO in 50 mM Tris-HCl buffer at different pH values

Entry	FAD	NaCl	Glycerol	pH 7.0	pH 7.5	pH 8.0	pH 8.5
1	+	+	-	39 °C	38 °C	41 °C	39 °C
2	-	+	-	37 °C	37 °C	41 °C	40 °C
3	+	-	-	39 °C	37 °C	39 °C	39 °C
4	-	-	-	35 °C	39 °C	39 °C	39 °C
5	-	-	+	36 °C	35 °C (1^{st} peak) 40 °C (2^{nd} peak)	40 °C	41 °C
6	+	+	+	40 °C	39 °C	33 °C (1^{st} peak) 39 °C (2^{nd} peak)	41 °C
7	+	-	+	39 °C	29 °C	40 °C	41 °C
8	-	+	+	37 °C	40 °C	41 °C	41 °C

2.4.14 Analytical methods

GC-FID method A: determination of the conversion Column: Agilent J&W DB1701 (30 m, 250 µm, 0.25 µm). Carrier gas: H_2; Parameter: T injector 250 °C; constant pressure 14.50 psi; temperature program: 80 °C, hold 6.5 min; gradient 10 °C min^{-1} up to 160 °C, hold 5 min; gradient 20 °C min^{-1} up to 200 °C, hold 2 min; gradient 20 °C min^{-1} up to 280 °C, hold 1 min

NP-HPLC method B: determination of the enantiomeric excess (*ee*) and diastereomeric excess (*de*) Column: Daicel Chiralcel OD (0.46 cm x 25 cm); HPLC program: constant oven

temperature 25 °C; eluent composition: isocratic Hexane/Isopropanol 99:1; flow rate: 0.5 mL min^{-1}

Table 2.17. Retention time [min] of substrates and products used in this study

Compound	Retention time [min] GC-FID	Retention time [min] HPLC
1a	4.9	n.a.
(*S*)-**2a**	10.9	15.9
1b	8.9	n.a.
(*1S,2S*)-**2b**	11.9	16.1

n.a = not applicable; The absolute configuration of the products (*S*)-**2a** and (1*S*,2*S*)-**2b** were identified by comparison with authentic optically active reference compounds.

2.5 References

1. V. Farina, J. T. Reeves, C. H. Senanayake and J. J. Song, *Chem. Rev.*, 2006, 106, 2734-2793.
2. P. Kumar and P. Gupta, *Synlett*, 2009, 2009, 1367-1382.
3. S. Hwang, C. Y. Choi and E. Y. Lee, *J. Ind. Eng. Chem.*, 2010, 16, 1-6.
4. D. L. Hughes, *Org. Process Res. Dev.*, 2016, 20, 2028-2042.
5. M. Luo, X. H. Zhang and D. J. Darensbourg, *Acc. Chem. Res.*, 2016, 49, 2209-2219.
6. R. Dalpozzo, A. Lattanzi and H. Pellissier, *Curr. Org. Chem.*, 2017, 21, 1143-1191.
7. W. J. Chung and C. D. Vanderwal, *Angew. Chem. Int. Ed.*, 2016, 55, 4396-4434.
8. R. Tak, M. Kumar, T. Menapara, N. Gupta, R. I. Kureshy, N.-u. H. Khan and E. Suresh, *Adv. Synth. Catal.*, 2017, 359, 3990-4001.
9. M. El Assal, P. A. Peixoto, R. Coffinier, T. Garnier, D. Deffieux, K. Miqueu, J. M. Sotiropoulos, L. Pouysegu and S. Quideau, *J. Org. Chem.*, 2017, 82, 11816-11828.
10. A. Sharma, J. Agarwal and R. K. Peddinti, *Org. Biomol. Chem.*, 2017, 15, 1913-1920.
11. P. Radha Krishna, G. Manikanta and T. Nagaraju, *Synthesis*, 2016, 48, 4213-4220.
12. Y. Zhou, P. Yang, S. Li, L. Wang, J. Yin, J. Zhong, Y. Dong, S. Liu, M. Wang and Q. Bian, *Tetrahedron: Asymmetry*, 2017, 28, 338-343.
13. P. Lienard, P. Gradoz, H. Greciet, S. Jegham and D. Legroux, *Org. Process Res. Dev.*, 2017, 21, 18-22.
14. R. D. Gaikwad, S. S. Kabiraj and S. V. Bhat, *Flavour Fragr. J.*, 2016, 31, 350-355.
15. W. Lee, S. Kang, B. Jung, H. S. Lee and S. H. Kang, *Chem. Commun.*, 2016, 52, 3536-3539.
16. N. Veerasamy, A. Ghosh, J. Li, K. Watanabe, J. D. Serrill, J. E. Ishmael, K. L. McPhail and R. G. Carter, *J. Am. Chem. Soc.*, 2016, 138, 770-773.
17. C. Garcia-Ruiz, I. Cheng-Sanchez and F. Sarabia, *Org. Lett.*, 2015, 17, 5558-5561.
18. J. R. McCarthy, *Tetrahedron Lett.*, 2015, 56, 6846-6847.
19. K. G. Lalwani and A. Sudalai, *Eur. J. Org. Chem.*, 2015, 2015, 7344-7351.
20. A. R. Rodriguez and B. W. Spur, *Tetrahedron Lett.*, 2015, 56, 5811-5815.
21. S. Das and C. V. Ramana, *Tetrahedron*, 2015, 71, 8577-8584.
22. T. Ogata, M. Tanaka, M. Ishigaki, M. Shimizu, A. Nishiuchi, K. Inamoto and T. Kimachi, *Tetrahedron*, 2015, 71, 6672-6680.
23. S. Goodin, M. P. Kane and E. H. Rubin, *J. Clin. Oncol.*, 2004, 22, 2015-2025.
24. T. Katsuki and K. B. Sharpless, *JACS*, 1980, 102, 5974-5976.
25. W. Zhang, J. L. Loebach, S. R. Wilson and E. N. Jacobsen, *JACS*, 1990, 112, 2801-2803.
26. M. Tokunaga, J. F. Larrow, F. Kakiuchi and E. N. Jacobsen, *Science*, 1997, 277, 936-938.
27. J. H. Lutje Spelberg and E. J. de Vries, in *Enzyme Catalysis in Organic Synthesis*, eds. K. Drauz, H. Groeger and O. May, Wiley-VCH, 3rd edn., 2012, ch. 9, pp. 363-416.

28. H. Lin, J.-Y. Liu, H.-B. Wang, A. A. Q. Ahmed and Z.-L. Wu, *J. Mol. Catal. B: Enzym.*, 2011, 72, 77-89.
29. D. Yildirim, S. S. Tukel, D. Alagoz and O. Alptekin, *Enzyme Microb. Technol.*, 2011, 49, 555-559.
30. W. J. Choi, *Appl. Microbiol. Biotechnol.*, 2009, 84, 239-247.
31. M. P. Kamble and G. D. Yadav, *Catal. Today*, 2017.
32. A. Fingerhut, O. V. Serdyuk and S. B. Tsogoeva, *Green Chem.*, 2015, 17, 2042-2058.
33. F. G. Gelalcha, B. Bitterlich, G. Anilkumar, M. K. Tse and M. Beller, *Angew. Chem. Int. Ed.*, 2007, 46, 7293-7296.
34. J. P. Collman, Z. Wang, A. Straumanis, M. Quelquejeu and E. Rose, *JACS*, 1999, 121, 460-461.
35. R. L. Davis, J. Stiller, T. Naicker, H. Jiang and K. A. Jorgensen, *Angew. Chem. Int. Ed.*, 2014, 53, 7406-7426.
36. Y. Zhu, Q. Wang, R. G. Cornwall and Y. Shi, *Chem. Rev.*, 2014, 114, 8199-8256.
37. O. A. Wong, T. A. Ramirez and Y. Shi, in *Comprehensive Chirality*, eds. E. M. Carreira and H. Yamamoto, Elsevier B.V., 2012, vol. 6, 6.23, pp. 528-553.
38. Q. H. Xia, H. Q. Ge, C. P. Ye, Z. M. Liu and K. X. Su, *Chem. Rev.*, 2005, 105, 1603-1662.
39. Y. Shi, *Acc. Chem. Res.*, 2004, 37, 488-496.
40. Z.-X. Wang, Y. Tu, M. Frohn, J.-R. Zhang and Y. Shi, *JACS*, 1997, 119, 11224-11235.
41. R. V. Ottenbacher, E. P. Talsi and K. P. Bryliakov, *Catal. Today*, 2016, 278, 30-39.
42. D. P. Day and P. B. Sellars, *Eur. J. Org. Chem.*, 2017, 2017, 1034-1044.
43. R. Irie, T. Uchida and K. Matsumoto, *Chem. Lett.*, 2015, 44, 1268-1283.
44. A. J. Burke and E. P. Carreiro, in *Comprehensive Inorganic Chemistry II*, eds. J. Reedijk and K. Poeppelmeier, Elsevier B.V., 2013, vol. 6.12, pp. 309-382.
45. F. G. Gelalcha, *Adv. Synth. Catal.*, 2014, 356, 261-299.
46. Q.-P. Shi, Z.-H. Shi, N.-G. Li, Y.-P. Tang, W. Li, H. Tang, Z. Wei, M.-Z. Shen and J.-A. Duan, *Curr. Org. Chem.*, 2013, 17, 2936-2970.
47. K. Matsumoto, Y. Sawada and T. Katsuki, *Pure Appl. Chem.*, 2008, 80, 1071-1077.
48. D. Chatterjee, *Coord. Chem. Rev.*, 2008, 252, 176-198.
49. Z. Li and H. Yamamoto, *Acc. Chem. Res.*, 2013, 46, 506-518.
50. B. D. Brandes and E. N. Jacobsen, *Tetrahedron: Asymmetry*, 1997, 8, 3927-3933.
51. M. Palucki, G. J. McCormick and E. N. Jacobsen, *Tetrahedron Lett.*, 1995, 36, 5457-5460.
52. A. T. Li and Z. Li, in *Science of Synthesis, Biocatalysis in Organic Synthesis 2*, eds. K. Faber, W.-D. Fessner and N. J. Turner, Georg Thieme Verlag KG, Stuttgart (Germany), 2015, ch. 2.6, pp. 479-505.
53. S. Panke, M. G. Wubbolts, A. Schmid and B. Witholt, *Biotechnol. Bioeng.*, 2000, 69, 91-100.
54. S. Panke, M. Held, M. G. Wubbolts, B. Witholt and A. Schmid, *Biotechnol. Bioeng.*, 2002, 80, 33-41.
55. J. B. Park, B. Buhler, T. Habicher, B. Hauer, S. Panke, B. Witholt and A. Schmid, *Biotechnol. Bioeng.*, 2006, 95, 501-512.
56. A. Schmid, K. Hofstetter, H.-J. Feiten, F. Hollmann and B. Witholt, *Adv. Synth. Catal.*, 2001, 343, 732-737.
57. K. Hofstetter, J. Lutz, I. Lang, B. Witholt and A. Schmid, *Angew. Chem. Int. Ed.*, 2004, 43, 2163-2166.
58. D. Kuhn, M. A. Kholiq, E. Heinzle, B. Bühler and A. Schmid, *Green Chem.*, 2010, 12, 815.
59. Y. Xu, X. Jia, S. Panke and Z. Li, *Chem. Commun.*, 2009, 1481-1483.
60. S. Wu, Y. Chen, Y. Xu, A. Li, Q. Xu, A. Glieder and Z. Li, *ACS Catal.*, 2014, 4, 409-420.
61. S. Wu, Y. Zhou, T. Wang, H. P. Too, D. I. Wang and Z. Li, *Nat. Commun.*, 2016, 7, 11917.
62. Y. Zhou, S. Wu and Z. Li, *Angew. Chem. Int. Ed.*, 2016, 55, 11647-11650.
63. S. Panke, B. Witholt, A. Schmid and M. G. Wubbolts, *Appl. Environ. Microbiol.*, 1998, 64, 2032-2043.

64. K. Otto, K. Hofstetter, M. Rothlisberger, B. Witholt and A. Schmid, *J. Bacteriol.*, 2004, 186, 5292-5302.
65. A. Kantz, F. Chin, N. Nallamothu, T. Nguyen and G. T. Gassner, *Arch. Biochem. Biophys.*, 2005, 442, 102-116.
66. E. Morrison, A. Kantz, G. T. Gassner and M. H. Sazinsky, *Biochemistry*, 2013, 52, 6063-6075.
67. D. Tischler, R. Kermer, J. A. Groning, S. R. Kaschabek, W. J. van Berkel and M. Schlomann, *J. Bacteriol.*, 2010, 192, 5220-5227.
68. D. Tischler, D. Eulberg, S. Lakner, S. R. Kaschabek, W. J. van Berkel and M. Schlomann, *J. Bacteriol.*, 2009, 191, 4996-5009.
69. F. Hollmann, P. C. Lin, B. Witholt and A. Schmid, *J. Am. Chem. Soc.*, 2003, 125, 8209-8217.
70. F. Hollmann, K. Hofstetter, T. Habicher, B. Hauer and A. Schmid, *J. Am. Chem. Soc.*, 2005, 127, 6540-6541.
71. R. Ruinatscha, C. Dusny, K. Buehler and A. Schmid, *Adv. Synth. Catal.*, 2009, 351, 2505-2515.
72. T. Heine, K. Tucker, N. Okonkwo, B. Assefa, C. Conrad, A. Scholtissek, M. Schlomann, G. Gassner and D. Tischler, *Appl. Biochem. Biotechnol.*, 2016.
73. X. Chen, J. L. Zaro and W. C. Shen, *Adv. Drug Deliv. Rev.*, 2013, 65, 1357-1369.
74. J. W. Bae, M. Park, Y. J. Jeong, S. Park and S.-G. Lee, *J. Ind. Eng. Chem.*, 2009, 15, 520-523.
75. K. E. O'Connor, A. D. W. Dobson and S. Hartmans, *Appl. Environ. Microbiol.*, 1997, 4287-4291.
76. A. Berry, T. C. Dodge, M. Pepsin and W. Weyler, *J. Ind. Microbiol. Biotechnol.*, 2002, 28, 127-133.
77. M. Lara, F. G. Mutti, S. M. Glueck and W. Kroutil, *Eur. J. Org. Chem.*, 2008, 2008, 3668-3672.
78. A. Rajagopalan, M. Schober, A. Emmerstorfer, L. Hammerer, A. Migglautsch, B. Seisser, S. M. Glueck, F. Niehaus, J. Eck, H. Pichler, K. Gruber and W. Kroutil, *ChemBioChem*, 2013, 14, 2427-2430.
79. S. Panke, V. de Lorenzo, A. Kaiser, B. Witholt and M. G. Wubbolts, *Appl. Environ. Microbiol.*, 1999, 65, 5619-5623.
80. M. J. Eisenmenger and J. I. Reyes-De-Corcuera, *Enzyme Microb. Technol.*, 2009, 45, 331-347.
81. S. Chakraborty, N. Kaushik, P. S. Rao and H. N. Mishra, *Compr. Rev. Food Sci. Food Saf.*, 2014, 13, 578-596.
82. S. Hay, M. J. Sutcliffe and N. S. Scrutton, *Proc. Natl. Acad. Sci. U.S.A.*, 2007, 104, 507-512.
83. S. Hay and N. S. Scrutton, *Nat. Chem.*, 2012, 4, 161-168.
84. A. E. e. L. C. principle, *Add Eyring equation; Le Chatelier: "At equilibrium a system tends to minimize the effect of any external factor by which it is perturbed. Consequently, elevated pressures favor changes that reduce a systems' overall volume".*
85. V. V. Mozhaev, K. Heremans, J. Frank, P. Masson and C. Balny, *Proteins*, 1996, 24, 81-91.
86. D. B. Northrop, *Biochim. Biophys. Acta*, 2002, 1595, 71-79.
87. M. Groβ, G. Auerbach and R. Jaenicke, *FEBS Lett.*, 1993, 321, 256-260.
88. C. Dirix, T. Duvetter, A. V. Loey, M. Hendrickx and K. Heremans, *Biochem. J.*, 2005, 392, 565-571.
89. Z. Knez, C. G. Laudani, M. Habulin and E. Reverchon, *Biotechnol. Bioeng.*, 2007, 97, 1366-1375.
90. H. Schutte, J. Flossdorf, H. Sahm and M.-R. Kula, *Eur. J. Biochem.*, 1976, 62, 151-160.
91. T. Knaus, W. Böhmer and F. G. Mutti, *Green Chem.*, 2017, 19, 453-463.

Chapter 3

Regio- and Stereoselective Multi-enzymatic Aminohydroxylation of β-methylstyrene using Dioxygen, Ammonia and Formate

This chapter is based on the following publication:

Maria L. Corrado, Tanja Knaus and Francesco G. Mutti, Regio- and stereoselective multi-enzymatic aminohydroxylation of β-methylstyrene using dioxygen, ammonia and formate, *Green Chemistry,* **2019,** 21(23), 6246-6251

Supporting information is available under doi: 10.1039/C9GC03161H

Abstract. *In this work, we present an enzymatic route for the formal regio- and stereoselective aminohydroxylation of β-methylstyrene. In the first step, β-methylstyrene was converted in all four 1-phenylpropane-1,2-diol stereoisomers in high isolated yields (78-85%) and excellent optical purities (er 95->99.5% and dr >99.5%) by combining a fused-styrene monooxygenase (Fus-SMO) with stereocomplementary epoxide hydrolases (EHs). In the second step, each 1-phenylpropane-1,2-diol stereoisomer was converted into either (1R,2R)- or (1S,2R)-phenylpropanolamine through a regio- and stereoselective enzymatic hydrogen-borrowing (HB) amination that combined an alcohol dehydrogenase with an amine dehydrogenase. The HB-amination proceeded with >99% analytical yield, 74% isolated yield, and high selectivity (er and dr >99.5). The enzymatic route only consumes dioxygen and one equivalent of ammonia and formate, producing one equivalent of carbonate as by-product. The biocascade entails highly selective epoxidation, hydrolysis and hydrogen-borrowing alcohol amination. Thus, β-methylstyrene was converted into (1R,2R)- and (1S,2R)-phenylpropanolamine in 59–63% isolated yields, and up to >99.5 dr and er.*

3.1 Introduction

Chiral 1,2-amino alcohol moieties are found in a plethora of natural products and active pharmaceutical ingredients (APIs), including antibiotics, anti-asthma drugs, hormones, alkaloids, enzyme inhibitors, and β-adrenergic blockers.[1-4] They also find application as ligands or auxiliaries in asymmetric organic synthesis.[5-7] In this context, phenylpropanolamines (PPAs, **5**) are particularly interesting as intermediates or final products due to their pharmaceutical properties. PPAs can be isolated as a mixture of diastereomers (1*S*,2*S*)-**5** and (1*R*,2*S*)-**5** from the leaves of *Celastraceae* and *Ephedraceae* plant families.[8,9]

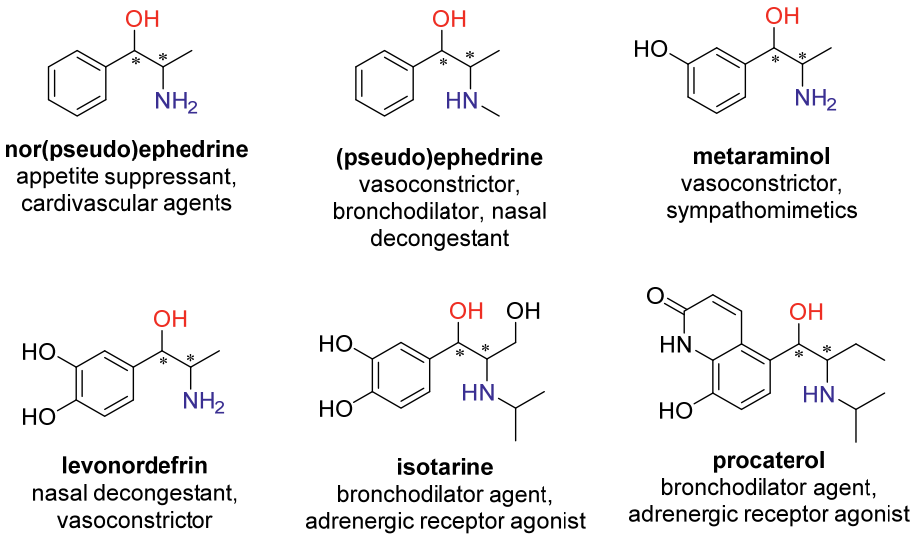

Figure 3.1. Examples of phenylpropanolamine.[3]

Chemical synthesis of PPAs commonly consumes various reagents in suprastoichiometric amounts and leads to high yields yet modest optical purities or vice versa.[2,3,10-14] Moreover, most of these methods require several isolation and purification steps of intermediates along the synthetic route, thus increasing significantly E-factors, solvent demands, and energy consumption (e.g., for evaporation).[15,16] In some cases, catalytic steps involving the use of toxic transition metals are needed, thereby contributing to an unfavorable environmental footprint of the process. For instance, trans-β-methylstyrene (*trans*-**1**) was converted into (1*R*,2*R*)-**5** through oxazoline intermediate in 75% overall yield, 99% *de*, but 86% *ee*.[17] The synthesis of the four PPA isomers **5** was accomplished *via* a multi-step route, which comprised an asymmetric reduction of α-functionalized ketones using chiral

reducing agents. Although yields ranged from 40% to 98%, a mixture of stereoisomers was always isolated.[18] The PPA isomers **5** were also obtained in six steps in ca. 40% yield, 96% *ee* and *dr* starting from *rac*-2-phenyl-2-trimethylsilyloxyacetonitrile.[10] In a recent study, the direct 1,2-aminohydroxylation of *cis*- and *trans*-**1** using $PivONH_3OTf$ as aminating reagent was catalyzed by Fe(II)-phthalocyanine. Although the reaction proceeded with perfect regioselectivity, only moderate yields (up to 26%) of a mixture of diastereomers were obtained.[19]

With the aim of finding viable alternatives to the use of toxic reagents and waste reduction to fulfill the criteria of green chemistry,[15,16,20] a number of biocatalytic routes towards PPAs synthesis have been reported. For instance, chemo-enzymatic approaches for the preparation of PPAs have combined either hydroxynitrile lyases (HNL) or Baker's yeasts with a chemical reduction step.[3] In the former case, (1*S*,2*R*)-**5** and (1*R*,2*S*)-**5** (35–47% yield) were obtained in high optical purities (99% *ee*, 90-92% *de*) through a five-step route.[21, 22] In the latter case, (1*R*,2*R*)-**5** and (1*R*,2*S*)-**5** were obtained as a mixture of diastereomers in moderate yields.[23,24]

Although fully enzymatic methods for the synthesis of 1,2-amino alcohols possessing one stereogenic center were recently developed,[25-27] only three routes are currently available for the stereoselective preparation of PPAs thereby creating two stereogenic centers.[3, 4] The first route converts 1-phenyl-1,2-propanedione into (1*R*,2*S*)-**5** or (1*S*,2*S*)-**5** through a one-pot and sequential combination of an ω-transaminase (ωTA) with an alcohol dehydrogenase (ADH).[28] The second route comprises an enzymatic carboligation between benzaldehyde and pyruvate followed by a stereoselective transamination to yield (1*R*,2*S*)-**5** and (1*R*,2*R*)-**5** (up to >95% conversion; 98% *de* and >99% *ee*).[11] A similar route was lately reported for the enzymatic synthesis of (1*R*,2*S*)-**5** (60% yield; *ee* and *de* >99.5%).[29] Conversely, the synthesis of (1*S*,2*R*)-**5** using the two above-mentioned enzymatic approaches was reported with ca. 20% conversion and moderate levels of diastereomeric purities (60-80% *de*).[28] The third enzymatic method entails the enantioselective aminohydroxylation of styrene derivatives catalyzed by an engineered hemoprotein. Starting from trans-anethole, the 1,2-amino alcohol product was obtained with 95% *ee* and 87:13 *dr*.[30]

In this work, we report a strategy for the synthesis of (1*S*,2*R*)-**5** and (1*R*,2*R*)-**5** in high optical purity by implementing a biocatalytic dual-enzyme hydrogen-borrowing (HB) amination.[31] Notably, HB-amination by pairing an alcohol dehydrogenase (ADH) with either an amine dehydrogenase (AmDH) or a reductive aminase (RedAm) was previously applied for the amination of molecules possessing only one

hydroxyl moiety.[31-35] Herein, we investigated the potential of the biocatalytic HB-amination for a concomitant regio- and stereoselective amination of the synthetically relevant 1-phenylpropane-1,2-diol (**3**). Furthermore, the selective bioamination was integrated in a multi-enzymatic route that starts from the inexpensive and easily available substrate **1** (**Figure 3.2**).

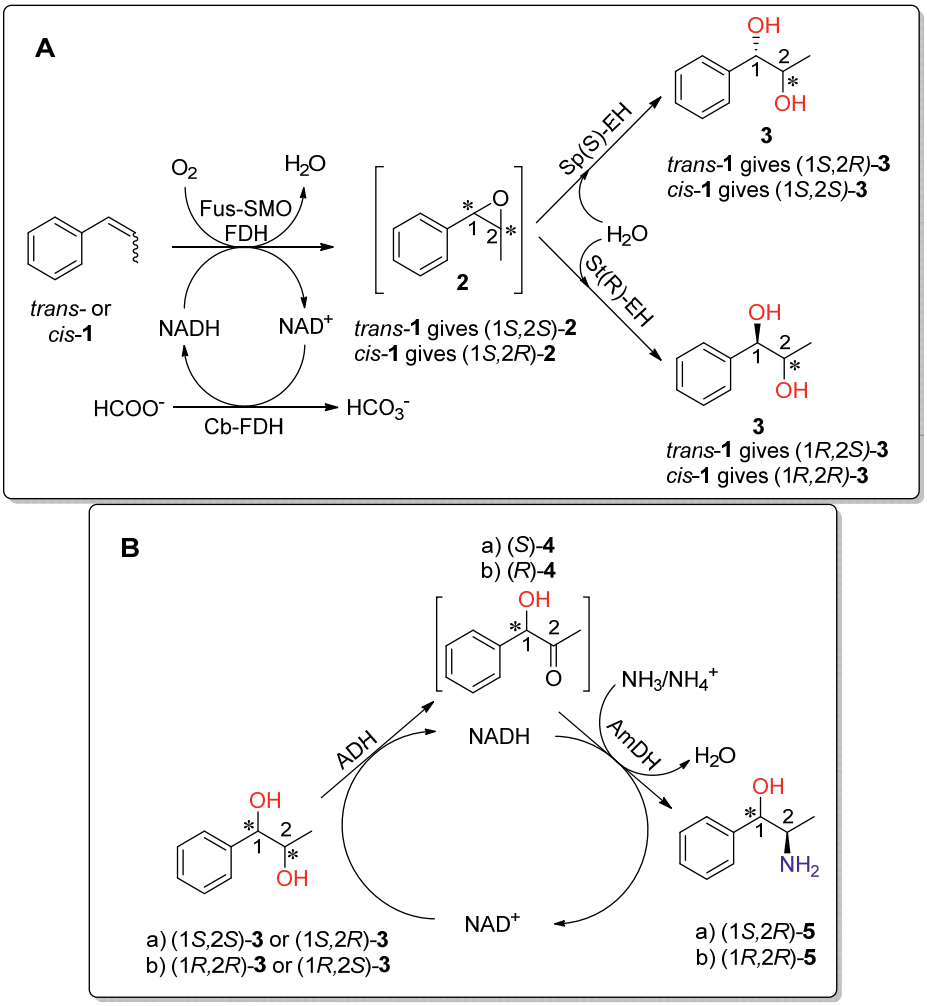

Figure 3.2. **A)** One-pot cascade for the stereoselective dihydroxylation of **1** (20-50 mM) in KPi buffer (pH 8.0, 50 mM)/heptane (1:1 v v^{-1}) using *E. coli*/Fus-SMO/Cb-FDH (5 mg mL^{-1}), *E. coli*/Sp(*S*)-EH or St(*R*)-EH (20 mg mL^{-1}), HCOONa (5 eq.), NAD^+ (1 mM), FAD (50 µM). **B)** One-pot regio- and stereospecific HB-amination (ADH/AmDH) of **3** (5-20 mM) in $HCOONH_4$ buffer (pH 8.5, 1 M), NAD^+ (1 mM). Note: the names of all wild-type strains from which the enzymes used in this study were recombinantly expressed (and, in case, engineered) are reported in **section 3.4.1**.

3.2 Results and discussion

3.2.1 Enzymatic synthesis chiral diols

All of the four diol isomers (**3**) were enzymatically synthesized from *cis*- or *trans*-β-methylstyrene **1** through a one-pot cascade that combined our fused styrene monooxygenase (Fus-SMO)[36] with either Sp(*S*)-EH or St(*R*)-EH as stereocomplementary epoxide hydrolases (**Figure 3.2A**).[37] The enzymes were expressed and used as *E. coli* lyophilized cells. The stereoselectivity of combined epoxidation and hydrolysis was initially studied in a one-pot concurrent cascade on analytical scale, in which *trans*-**1** or *cis*-**1** (20 mM) were incubated in a biphasic mixture of KPi buffer (50 mM, pH 8.0, 0.5 mL) and heptane (0.5 mL), containing *E. coli*/Fus-SMO (10 mg), either *E. coli*/Sp(*S*)-EH or *E. coli*/St(*R*)-EH (10 mg), FAD (50 μM), NAD^+ (1 mM), and Cb-FDH (10 μM)/HCOONa (100 mM) for NADH recycling. The use of an aqueous/organic biphasic system limited the molecular toxicity of the epoxide intermediates to the enzymes, as well as prevent the possible spontaneous opening of the epoxide formed, reduced the loss of volatile **1**, and enabled a practical isolation of the final diol products by simple phase separation followed by extraction. The four stereoisomers of diol **3** were obtained with elevated diastereomeric ratios (**Table 3.1**).

Table 3.1. One-pot cascade for the conversion [%] of *trans* or *cis*-**1** (20 mM) to optically active **3** catalyzed by lyophilized whole cells expressing Fus-SMO in combination with either Sp(*S*)-EH or St(*R*)-EH. The stereochemistry of the diols (**3**) was determined accurately by HPLC analysis.

Substrate	Enzymatic system	Conversion [%][a]	Product distribution[b] (1*R*,2*R*)-**3** (1*S*,2*S*)-**3** (1*R*,2*S*)-**3** (1*S*,2*R*)-**3**			
			A	**B**	**C**	**D**
trans-**1**	Fus-SMO/Sp(*S*)-EH	99±<1	n.d.	n.d.	0.1	99.9
trans-**1**	Fus-SMO/St(*R*)-EH	86±9	0.5	0.2	99.0	0.3
cis-**1**	Fus-SMO/Sp(*S*)-EH	53±2	5.5	92.5	0.1	2.0
cis-**1**	Fus-SMO/St(*R*)-EH	71±<1	98.8	0.2	n.d.	1

[a] GC-FID. [b] HPLC; average of two samples

Thus, we performed the one-pot cascade slightly above three hundred milligrams scale, which yielded diols **3** in quantitative conversion, high isolated yields (78–85%), and high optical purity (**Table 3.2**). Fus-SMO and Cb-FDH were co-expressed in the same host in this latter set of experiments.[36]

Table 3.2. Conversion [%] of *trans* or *cis*-**1** to optically active **3** in a biocatalytic cascade that combines Fus-SMO/Cb-FDH and two stereo-complementary EHs.

Substrate	EH	Conversion [%][a]	Isolated yield [%]	*er* [%][b]	*dr* [%][b]
trans-**1**	Sp(*S*)-EH	>99	85 (323 mg)	99:1 (1*S*,2*R*)-**3**	>99.5:<0.5
trans-**1**	St(*R*)-EH	>99	78 (297 mg)	>99.5:<0.5 (1*R*,2*S*)-**3**	>99.5:<0.5
cis-**1**	Sp(*S*)-EH	>99	83 (316 mg)	95.5:4.5 (1*S*,2*S*)-**3**	>99.5:<0.5
cis-**1**	St(*R*)-EH	>99	79 (301 mg)	>99.5:<0.5 (1*R*,2*R*)-**3**	>99.5:<0.5

[a]determined by GC-FID; [b] analyzed by HPLC

3.2.2 Screening secondary NAD(P)$^+$-dependent alcohol dehydrogenases (ADHs)

3.2.2.1 Bio-catalytic oxidation of 1-phenyl-1,2-propanediol (3)

Next, we focused on the second part of the multi-enzymatic process, which is the conversion of a diol enantiomer **3** into optically active PPA (**5**, **Figure 3.2B**). Initially, we investigated the single oxidation of diol **3** (as a mixture of the four stereoisomers) by screening a panel of eleven stereocomplementary ADHs (six NAD^+ and five $NADP^+$ dependent) which ideally would lead to the formation of intermediate **4**. The ADHs were tested either as purified enzymes (*i.e.*, 50 µM Aa-ADH,[38] Lbv-ADH,[39] or Lb-ADH[40]) or lyophilized whole cells (*i.e.*, 20 mg mL^{-1} of *E.coli* cells expressing Sy-ADH,[41] Pp-ADH,[42] Bs-BDHA,[43] Ls-ADH,[44] Te-ADH variant 1, 2, or 3,[45] or Rs-ADH.[46] The reactions were run for 24 h in Tris-HCl buffer (pH 7.5, 50 mM) at 30 °C, with the only exception being the oxidation catalyzed by Ls-ADH which was conducted in KPi buffer (pH 6.5, 100 mM) at 40 °C. The reactions were supplemented with NAD^+ or $NADP^+$ (1 mM), which were recycled by a specific NAD(P)H oxidase—i.e., NOX[47] (0.5 µM) for NADH or YcnD[48] (5 µM) for NADPH. For an overview of the reaction pathway see **Scheme 3.1.** The reaction does not proceed with perfect selectivity and a mixture of products were formed considering also that the substrate was used a mixture of all the four possible isomers in the same pot (**Table 3.3**).

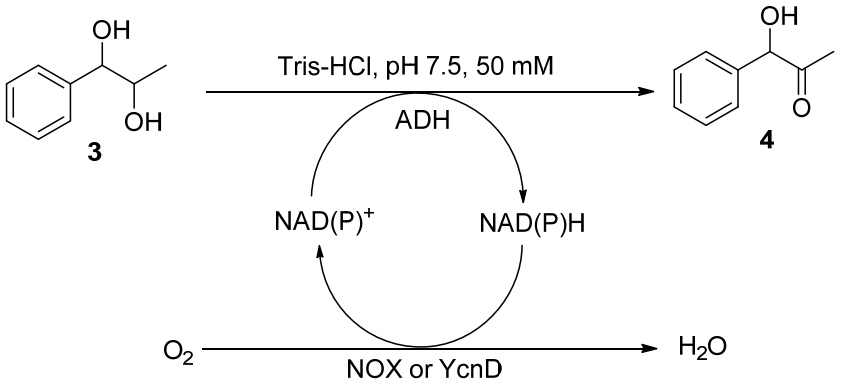

Scheme 3.1. Bio-catalytic oxidation of diol **3**

As shown in **Table 3.3**, only three NAD^+-dependent ADHs, namely Aa-ADH, Bs-BDHA, and Ls-ADH, proved to be sufficiently active towards diol **3** isomers (entry 1, 5 and 6). In these three cases, the desired 1-hydroxy-1-phenylpropan-2-one intermediate (**4**) was obtained as the main product (31%, 36%, and 15% conversions, respectively). However, 2-hydroxy-1-phenylpropan-1-one (**4'**) (9-22%) and fully oxidized di-ketone product (**7**) (2–5%) were also detected. Notably, the three ADHs exhibited varying stereoselectivity. Whereas Bs-ADH oxidized (1*S*,2*R*)-**3** and (1*R*,2*S*)-**3**, Ls-ADH oxidized (1*S*,2*R*)-***3*** and (1*R*,2*R*)-**3** and Aa-ADH oxidized (1*R*,2*R*)-**3**, (1*S*,2*S*)-**3** and (1*R*,2*S*)-**3**. It is important to note that the composition of the reaction mixture might be partly determined by a possible spontaneous chemical isomerization between **4** and **4'** (and their enantiomers) due to a tautomeric equilibrium. Hence, three ADHs, namely Aa-ADH, Bs-BDHA and Ls-ADH, turned out to be suitable candidates for the regioselective oxidation of the four isomers of diol **3**. **Figure 3.3** depicts a graphical summary of the preferred selectivity of the ADHs within our synthetic strategy along with a general view on the conceived synthetic routes to obtain intermediate **4** in enantiomerically pure form.

Table 3.3. Oxidation [%] of diol **3** by NAD(P)$^+$-dependent ADHs.

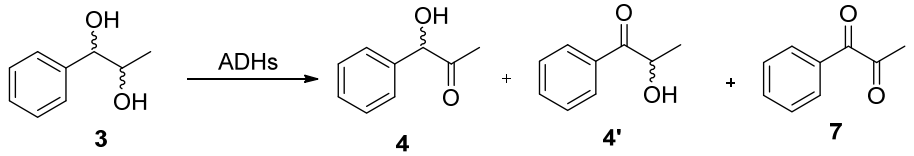

3 mixture of all four isomers — **4** — **4'** — **7**

Entry	ADH	Coenzyme	4 [%][b]	4' [%][b]	7 [%][b]	Catalyst form[c]	Accepted diol isomers[a]
1	Aa-ADH	NAD^+	31	20	5	Purified (N-His_6 tag)	1*R*,2*R*/1*S*,2*S* /1*R*,2*S*
2	Lbv-ADH	NAD^+	4	4	2	Purified (no tag)	-
3	Sy-ADH	NAD^+	<1	<1	<1	Lyophilized whole cells	-
4	Pp-ADH	NAD^+	<1	<1	<1	Lyophilized whole cells	-
5	Bs-BDHA	NAD^+	36±3	22±2	4±1	Lyophilized whole cells	1*S*,2*R*/1*R*,2*S*
6	Ls-ADH	NAD^+	15±1	9±<1	2±<1	Lyophilized whole cells	1*S*,2*R*/1*R*,2*R*
7	Lb-ADH	$NADP^+$	8	7	2	Purified (no tag)	-
8	Te-ADH_{v1}	$NADP^+$	<1	<1	<1	Lyophilized whole cells	-
9	Te-ADH_{v2}	$NADP^+$	3±2	1±1	<1	Lyophilized whole cells	-
10	Te-ADH_{v3}	$NADP^+$	<1	<1	<1	Lyophilized whole cells	-
11	Rs-ADH	$NADP^+$	<1	<1	<1	Lyophilized whole cells	-

[a] This refers to the preference of the enzyme for the conversion of *diol* **3** which is a mixture of the four possible stereoisomers as described in this column; [b] average of two samples; [c] see section 3.4.1 for more details.

Figure 3.3. Overview on the preferred regio- and stereo-selectivity of various ADHs deduced from the conversion of diol **3** (used as a mixture of all four possible isomers).

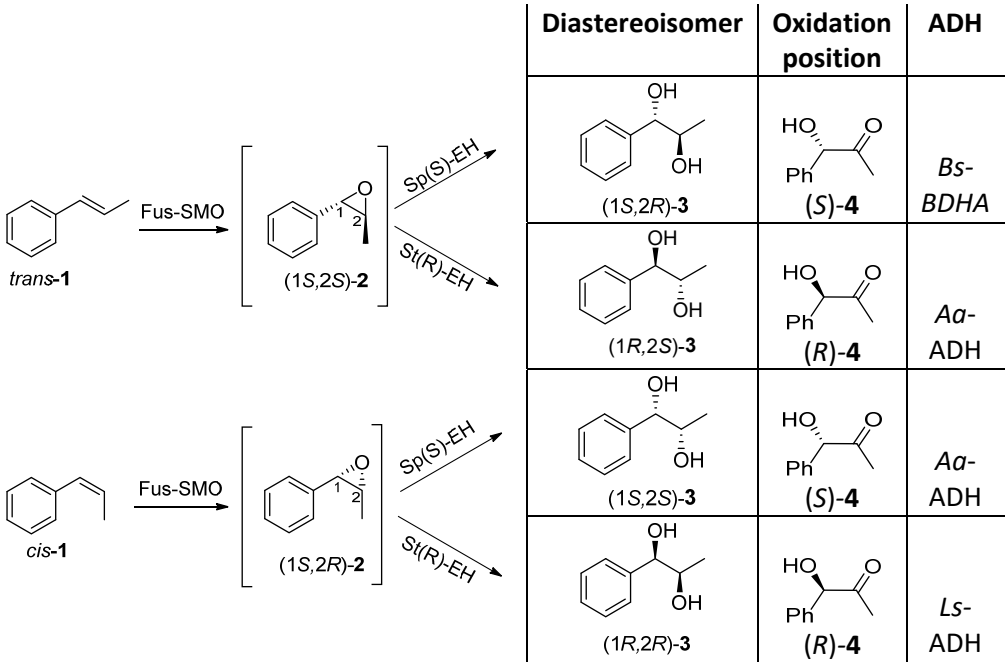

3.2.2.2 Bio-catalytic reduction of 1-phenyl-1,2-propanedione (7)

For the sake of clarity, the panel of NAD(P)$^+$-dependent ADHs, described above, was also tested for the bio-reduction of substrate **7** (20 mM). The reactions were carried out in Tris-HCl buffer (pH 7.5, 50 mM) supplemented with NAD^+ (1 mM), HCOONa (100 mM) and Cb-FDH (10 µM), the latter for internally recycling the NADH coenzyme. The general reaction pathway is depicted in **Scheme 3.2**. Also in this reverse pathway, the biotransformation led to the formation of multiple products as reported in **Table 3.4**; nevertheless, the bio-reduction proceeded with higher selectivity than the oxidation as well as more ADHs showed to be active on this reverse reaction.

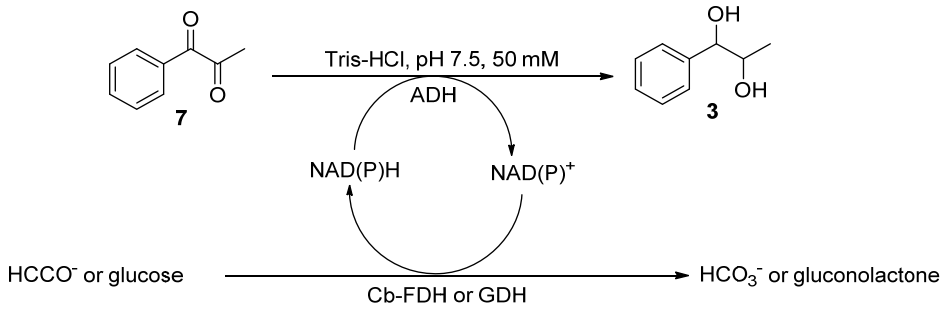

Scheme 3.2. Bio-catalytic reduction of diketone **7**

As shown in **Table 3.4**, only Aa-ADH leads to the formation of **3** as single product (entry 1) which may indicate no selectivity within the two carbonyl moieties (α and β position). On the other hand, the other four NAD^+-dependent ADHs led to the formation of all the three possible expected products in different ratios: except for Sy-ADH which forms **4** (entry 4) as the main product, the remaining two ADHs (Lbv and Pp; entry 2-3) form mainly **3**, thought LBv-ADH shows to form **3** and **4** in a 1:1 ratio. Furthermore, formation of isomer **4'** was also observed in all cases except for Aa-ADH, though it is always lower than the correspondent isomer **4**. This may be due to thermodynamic equilibria, hence, isomer **4** may be preferred over **4'**. In general, only Sy-ADH showed the greatest preference for the formation of **4** (63 %), which seems to be able to discriminate between the two ketone moieties. Regarding the $NADP^+$-dependent ADHs, in the case of the three variants of Te-ADH, no conversion into **3** was observed (entry 6-8). On the other hand, all the three variants showed a similar trend for the formation of either **4** or **4'**. Nevertheless, only Te-ADH-v2 (entry 7) showed the highest preference for the formation of **4'**. Lb-ADH leads to the formation of **3** (entry 9) as the major component of the mixture. As last, Rs-ADH shows the formation of **4** as the main component of the products mixture (entry 10), while its isomer **4'** is formed in 17% yield. In both cases, product **3** was observed in 3% yield only.

Table 3.4. Conversion [%] for the enzymatic reduction of compound **7** (20 mM) by a panel of NAD(P)$^+$-dependent ADHs

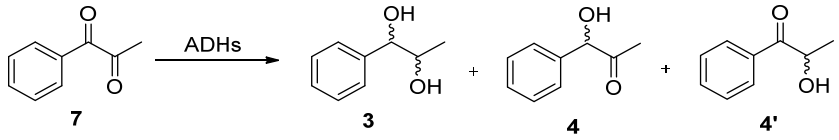

Entry	ADH	7 [%]	3 [%]	4 [%]	4' [%]	Cofactor	Catalyst form
1	Aa-ADH	2	98	n.d.	n.d.	NAD^+	Purified (N-His_6 tag)
2	Lbv-ADH	3	45	45	7	NAD^+	Purified (no tag)
3	Pp-ADH	2	73[a]	14	11	NAD^+	Lyophilized *E. coli* cells
4	Sy-ADH	2	8	63	26	NAD^+	Lyophilized *E. coli* cells
5	Bs-BDHA	3	54[a]	39	5	NAD^+	Lyophilized *E. coli* cells
6	Te-ADH_{v1}	7	n.d.	53	40	$NADP^+$	Lyophilized *E. coli* cells
7	Te-ADH_{v2}	5	n.d.	19	76	$NADP^+$	Lyophilized *E. coli* cells
8	Te-ADH_{v3}	11	n.d.	36	52	$NADP^+$	Lyophilized *E. coli* cells
9	Lb-ADH	3	72	23	2	$NADP^+$	Purified (no tag)
10	Rs-ADH	3	10	70	17	$NADP^+$	Lyophilized *E. coli* cells

[a] Sum of two peaks which correspond to the two diastereomers (two couples of enantiomers)

3.2.3 Hydrogen borrowing bio-amination cascade with substrate (1*S*,2*S*)-3

In the next step, we investigated the biocatalytic reductive amination of the synthetically obtained hydroxy-ketone intermediate (*rac*-**4**, 20 mM), by screening three "(*R*)-selective" amine dehydrogenases[49-51] (Ch1-AmDH, Rs-PhAmDH and Bb-AmDH; 100 µM) in $HCOONH_4$ buffer (pH 8.5, 1 M; 1 mL reaction volume) in the presence of NAD^+ (1 mM) and Cb-FDH (14.1 µM) at 30 °C for 24 h. Ch1-AmDH and Rs-PhAmDH showed conversion to **5** (24% and 79%, respectively) as a mixture of diastereomers (1*S*,2*R* and 1*R*,2*R*), whereas Bb-AmDH was inactive towards *rac*-**4** (data not shown).

3.2.3.1 Influence of the temperature for the hydrogen-borrowing amination of (1*S*,2*S*)-3

Therefore, we initially tested the HB-amination on analytical scale using (1*S*,2*S*)-**3** (5 mM) as a substrate and combining Aa-ADH and AmDH (Ch1-AmDH or Rs-PhAmDH) in a 50:50 ratio (μM) in one pot. The reactions were conducted in $HCOONH_4$ buffer (pH 8.5, 1 M, 0.5 mL final volume) supplemented with NAD^+ (1 mM).

First, the influence of the temperature (20, 30, 40 and 50 °C) was investigated. Ch1-AmDH generally was the best performing AmDH for the HB-amination of (1*S*,2*S*)-**3** in combination with Aa-ADH. As reported in **Table 3.5**, high conversions into the target product **5** were observed under all the tested temperatures. Nevertheless, quantitative conversion and high product yield (89±2%) were consistently obtained at 30 °C for 48 h (entry 3 and 4). Therefore, this temperature and reaction time were chosen for further studies. Notably, the combination of ADH and AmDH in one pot prevented the formation of the byproducts **4'** and **7**, which were previously detected in the single ADH-catalyzed oxidation of **3**. However, other by-products were observed in this non-optimized HB-amination, particularly 2-amino-1-phenylpropan-1-one (**8**, ca. 8%).

Table 3.5. Conversions [%] for (1*S*,2*S*)-**3** (5 mM) at different temperatures by combining Aa-ADH (50 μM) and AmDH (50 μM)

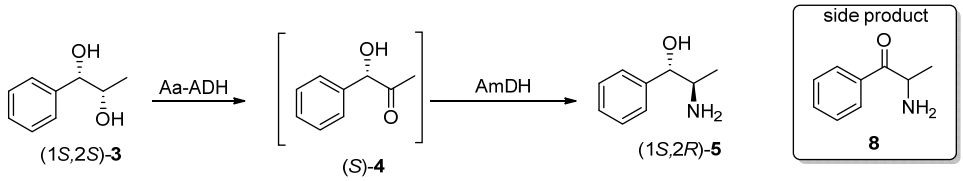

Entry	Enzymatic system	T [°C]	Conversion [%][a]	5 [*SR*] [%][a]	8 [%][a][b]	Unidentified [%][a][b]
1	Aa-ADH/Ch1-AmDH	20	96±2	87±1	4±<1	5±1
2	Aa-ADH/Rs-PhAmDH	20	49±1	45±1	3±<1	2±<1
3	Aa-ADH/Ch1-AmDH	30	>99	89±2	8±2	4±<1
4	Aa-ADH/Rs-PhAmDH	30	>99	89±<1	6±<1	6±<1
5	Aa-ADH/Ch1-AmDH	40	89±1	81±2	5±<1	2±<1
6	Aa-ADH/Rs-PhAmDH	40	86±1	79±1	4±<1	3±<1

Table 3.5 *(Continued)*

Entry	Enzymatic system	T [°C]	Conversion [%][a]	5 [*SR*] [%][a]	8 [%][a][b]	Unidentified [%][a][b]
7	Aa-ADH/Ch1-AmDH	50	>99	91±1	6±<1	3±<1
8	Aa-ADH/Rs-PhAmDH	50	92±1	85±1	5±<1	2±<1

[a] Determined by GC-FID; [b] This may come, at least in part, from decomposition of the amino alcohols product (also present in the reference compound purchased by Sigma Aldrich upon injection in GC-MS or GC-FID); *er* and *dr* were not determined at this stage.

3.2.3.2 Optimization HB-bioamination cascade for (1*S*,2*S*)-3 as substrate

3.2.3.2.1 Initial optimization of the enzymes loading for the hydrogen-borrowing amination of (1*S*,2*S*)-3

Next, we proceeded with the optimization of the HB-amination of (1*S*,2*S*)-**3** (5 mM) using varied molar ratios of Aa-ADH and either Ch1-AmDH or Rs-PhAmDH. The reactions were carried out in $HCOONH_4$ bufer (pH 8.5, 1 M) supplemented with NAD^+ (1 mM). The stereochemistry of the final products **5** was assigned by RP-HPLC after derivatization with the chiral reagent GITC (**section 3.4.6**, see also **Figure 3.4**) and comparison with authentic optically active reference compounds that were either purchased or chemically synthesized (**section 3.4.5**). Examples for the calculation of enantiomeric and diastereomeric ratio are given in chapter 4, section 4.4.3.

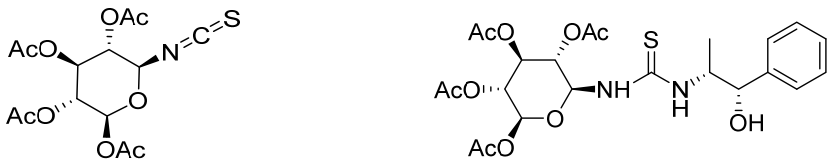

GITC **GITC**-(1*S*,2*R*)-**5**

Figure 3.4. Structures of GITC (left) and GITC-derivatized amino alcohols obtained in this study (right).

As reported in **Table 3.6**, under these conditions, Aa-ADH (20 µM) and Ch1-AmDH (50 µM) were the best combination in terms of analytical yield into (1*S*,2*R*)-**5** (87±1%), chemoselectivity (ca. 2% of by-products), and optical purity (*er* >99.5:<0.5 and *dr* 95:5) (entry 3-4). Nevertheless, both 10:50 and 24:60 enzyme ratios (entry 1-2 and 5-6) led also to the formation of the desired product in moderate to high conversions. Notably, the intrinsic stereoselectivity of the HB-amination was

perfect, as the *dr* of 95:5 reflects the level of optical purity of substrate (1*S*,2*S*)-**3** obtained in the previous cascade for the synthesis of the substrate (**Table 3.2**).

Table 3.6. Conversions [%] for (1*S*,2*S*)-**3** (5 mM) by combining different ratios of Aa-ADH and AmDH at 30 °C

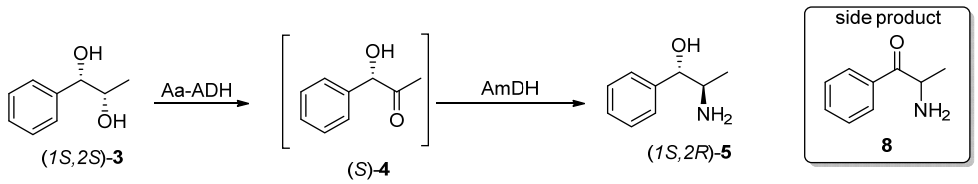

Entry	Enzymatic system	ADH: AmDH [µM]	Conversion [%][a]	5 [*SR*] [%][a]	*er* [%][b]	*dr* [%][b] [*SS*:*RR*:*RS*:*SR*]	8 [%][a,c]	Unidentified [%][a,c]
1	Aa-ADH/Ch1-AmDH	10:50	80±5	74±4	n.m.	n.m.	4±<1	2±<1
2	Aa-ADH/Rs-PhAmDH	10:50	61±6	55±6	n.m.	n.m.	4±<1	2±<1
3	Aa-ADH/Ch1-AmDH	20:50	89±1	87±1	>99.5:<0.5	0:5:0:95	n.d.	2±<1
4	Aa-ADH/Rs-PhAmDH	20:50	68±3	66±3	>99.5:<0.5	0:5:0:95	n.d.	2±<1
5	Aa-ADH/Ch1-AmDH	24:60	>99	86±6	>99.5:<0.5	0:4:0:96	6±3	8±1
6	Aa-ADH/Rs-PhAmDH	24:60	>99	87±5	>99.5:<0.5	0:5:0:95	6±2	8±1

[a] Determined by GC-FID analysis; [b] Determined by RP-HPLC after derivatization with a chiral reagent; [c] This may come, at least in part, from decomposition of the amino alcohols product (also present in the reference compound purchased by Sigma Aldrich upon injection in GC-MS or GC-FID). ***Note:*** *the fact that the diastereomeric ratio of the product (1S,2R)-**5** is not absolutely perfect must not be attributed to the hydrogen-borrowing amination step. In fact, the enantiomeric ratio of the diol substrate (1S,2S)-**3**—obtained in the previous enzymatic step—was not perfect (95.5:4.5) and that reflected on the subsequent amination step.*

3.2.3.2.2 Further optimization of the hydrogen-borrowing amination of (1*S*,2*S*)-3

The screening at higher substrate concentration (10 to 30 mM, (1*S*,2*S*)-**3**) was performed with the following conditions disclosed so far: Aa-ADH (24 µM), Ch1-AmDH (60 µM) in $HCOONH_4$ buffer (pH 8.5, 1 M, 0.5 mL) at 30 °C for 48 h as described in section 3.4.6. Though the best conditions in the screening reported in

table 3.6 showed a better performance when enzymes ratio 20:50 was used, no consistent results were observed once the reaction was performed again under such conditions. On the other hand, the 24:60 ratio showed more persistent results and for this reason the substrate loading was tested by using 24:60 enzymes ratio. Interestingly, the application of a higher substrate concentration further improved the chemoselectivity of the HB-amination, as reported in **Table 3.7**. For instance, at 10 mM concentration of (1*S*,2*S*)-**3** substrate, the desired product (1*S*,2*R*)-**5** was obtained in 69±1% analytical yield with ≤1% of by-products, while *er* and *dr* remained unaltered (entry 1). However, a further increase of substrate concentration while maintaining the same concentrations of Aa-ADH and Ch1-AmDH (24:60 µM) resulted in reduced yields (33-51%)(entry 2-5).

Table 3.7. Conversion [%] for (1*S*,2*S*)-**3** (varied concentration: 10 to 30 mM) at 30 °C combining Aa-ADH (24 µM) and Ch1-AmDH (60 µM)

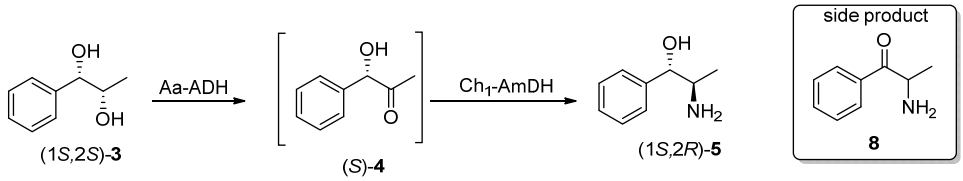

Entry	3 [*SS*] [mM]	Conversion [%][a]	5 [*SR*] [%][a]	*er* [%][b]	*dr* [%][b] [*SS*:*RR*:*RS*:*SR*]	8 [%][a][c]	Unidentified [%][a][c]
1	10	70±<1	69±<1	>99.5:<0.5	0.8:3.5:0:95.7	<1	1±<1
2	15	52±2	51±2	>99.5:<0.5	0:2.5:0:97.5	<1	1±<1
3	20	42±1	41±1	>99.5:<0.5	0:2.3:0:97.7	<1	1±<1
4	25	36±<1	36±<1	>99.5:<0.5	0:2.4:0:97.6	<1	1±<1
5	30	34±1	33±1	>99.5:<0.5	0:1.8:0:98.2	<1	1±<1

[a] Determined by GC-FID analysis; [b] Determined by RP-HPLC after derivatization with a chiral reagent; [c] This may come, at least in part, from decomposition of the amino alcohols product (also present in the reference compound purchased by Sigma Aldrich upon injection in GC-MS or GC-FID). ***Note:*** *the fact that the diastereomeric ratio of the product (1S,2R)-**5** is not absolutely perfect must not be attributed to the hydrogen-borrowing amination step. In fact, the enantiomeric ratio of the diol substrate (1S,2S)-**3**—obtained in the previous enzymatic step—was not perfect (95.5:4.5) and that reflected on the subsequent amination step.*

Based on the results observed at higher substrate loading (**Table 3.7**), a fine tuning of the reaction conditions by varying the relative amount of dehydrogenases and substrate concentration was performed. The results reported in **Table 3.8** summarize the tests that were carried out. Initially, 10 mM of (1*S*,2*S*)-**3** was kept constant while both Aa-ADH and Ch1-AmDH were first doubled (48:120 µM, respectively) as well as used three times more concentrated (72:180 µM,

respectively) than the initial conditions; this would allow to investigate the possibility to reach higher conversion and analytical yields. However, as shown in entry 1 and 2, even though higher conversions were observed, these are comparable to the results obtained at 24:60 µM enzymes loading (78-85% *vs*. 70%, respectively), which may indicate that some inhibition is occurring. By increasing the substrate loading to 15 mM and keeping the enzymes concentrations at 72:180 µM (ADH:AmDH), there was not a huge improvement Surprisingly, when the loading of the Aa-ADH and the Ch1-AmDH was reversed (60:24 µM ADH:AmDH) full conversion as well as high analytical yields were observed from 5 up to 20 mM substrate loading (entry 4-6). Finally, the optimal conditions for the conversion of (1*S*,2*S*)-**3** into (1*S*,2*R*)-**5** were disclosed as follow: (1*S*,2*S*)-**3** (20 mM), Aa-ADH (70 µM), Ch1- AmDH (35 µM), under which (1*S*,2*R*)-**5** was obtained in 98±1% analytical yield and high optical purity (entry 9).

Table 3.8. Conversion [%] for (1*S*,2*S*)-**3** (varied concentration: 5 to 20 mM) at 30 °C using varied enzyme concentrations (Aa-ADH/Ch1-AmDH)

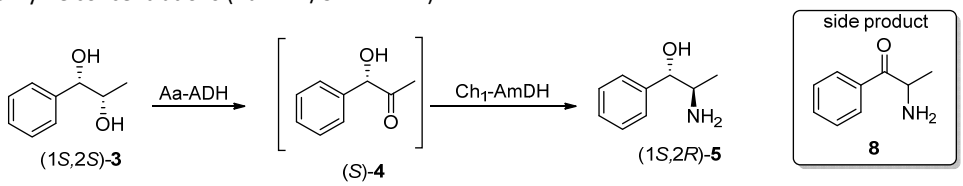

Entry	3 [*SS*] [mM]	ADH: AmDH [µM]	Conversion [%][a]	5 [*SR*] [%][a]	*er* [%][b]	*dr* [%][b] [*SS*:*RR*:*RS*:*SR*]	8 [%][a,c]	Unidentified [%][a,c]
1	10	48:120	78±1	75±1	>99.5:<0.5	0:6:0:94	1±<1	3±<1
2	10	72:180	85	82	>99.5:<0.5	0:6:0:94	1	2
3	15	72:180	69±1	67±1	>99.5:<0.5	0:6:0:94	1±<1	2±<1
4	5	60:24	>99±<1	94±6	>99.5:<0.5	2:6:0:92	n.d.	6±1
5	10	60:24	>99±<1	96±2	>99.5:<0.5	2:5:0:93	1±<1	3±<1
6	20	60:24	>99±<1	97±1	>99.5:<0.5	1:4:0:95	<1	2±<1
7	5	70:35	>99±<1	96±<1	>99.5:<0.5	2:7:0:91	<1	4±<1
8	10	70:35	>99±<1	97±1	>99.5:<0.5	2:6:0:92	<1	3±<1
9	20	70:35	>99±<1	98±<1	>99.5:<0.5	1:4:0:95	1±<1	2±<1

[a] Determined by GC-FID analysis; [b] Determined by RP-HPLC after derivatization with a chiral reagent; [c] This may come, at least in part, from decomposition of the amino alcohols product (also present in the reference compound purchased by Sigma Aldrich upon injection in GC-MS or GC-FID). ***Note:*** *the fact that the diastereomeric ratio of the product (1S,2R)-**5** is not absolutely perfect must not be attributed to the hydrogen-borrowing amination step. In fact, the enantiomeric ratio of the diol substrate (1S,2S)-**3**—obtained in the previous enzymatic step—was not perfect (95.5:4.5) and that reflected on the subsequent amination step.*

Finally, we monitored the progress of the HB-amination of (1*S*,2*S*)-**3** (20 mM) over time under the optimized conditions reported in **Table 3.8**, entry 9. As depicted in **Figure 3.5**, and in **section 3.4.7** for more detailed data, 42 hours are required for the reaction to reach completion leading to the exclusive formation of product **5** (1*S*,2*R*-**5**).

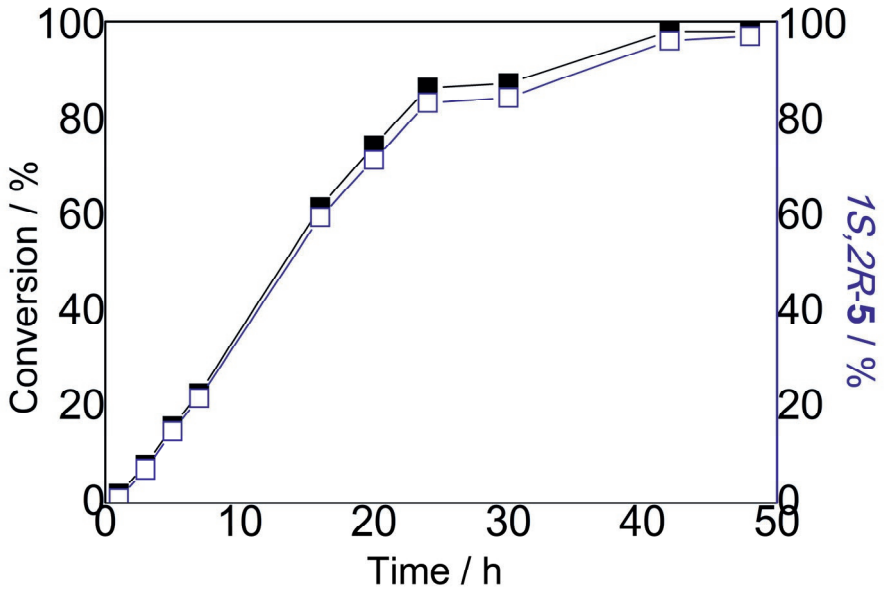

Figure 3.5. Progress of the regio- and stereospecific HB amination of (1*S*,2*S*)-**3** (20 mM) to yield (1*S*,2*R*)-**5** catalyzed by Aa-ADH (70 µM) and Ch1-AmDH (35 µM) in $HCOONH_4$ buffer (pH 8.5, 1 M, 0.5 mL) containing NAD^+ (1 mM).

3.2.4 Hydrogen borrowing bio-amination cascade with substrate (1*R*,2*R*)-3

Next, the biocatalytic HB-amination was investigated on the diol isomer (1*R*,2*R*)-**3**. As reported previously in **Table 3.3**, Ls-ADH was the best performing alcohol dehydrogenase for the oxidation of this isomer. As for its enantiomer (1*S*,2*S*)-**3**, a temperature study was also performed in the case of (1*R*,2*R*)-**3** by combining Ls-ADH with either Ch1-AmD or Rs-PhAmDH.

3.2.4.1 Temperature study

The influence of the temperature (30, 40 and 50 °C) for the HB-amination of (1*R,*2*R*)-**3** (5 mM) was investigated combining Ls-ADH (50 µM) with AmDH (50 µM, Ch1-AmDH or Rs-PhAmDH). The reactions were run for 48 h in $HCOONH_4$ buffer (pH 8.5, 1 M, 0.5 mL) in the presence of NAD^+ (1 mM) as described in **section 3.4.6**. As

shown in **Table 3.9**, Ls-ADH with Ch1-AmDH was found to be the best combination for the amination of (1*R*,2*R*)-**3** at 30 °C, although Rs-AmDH also performed efficiently, yielding (1*R*,2*R*)-**5** with perfect regio- and stereoselectivity (*er* >99.5:<0.5, *dr* >99.5:<0.5). Under all other tested temperatures, the conversion of substrate (1*R*,2*R*)-**3** dropped significantly as well as the analytical yield of (1*R*,2*R*)-**5**. Moreover, in this case, the diastereomeric ratio of the product was assessed for all conditions: the higher the temperature, the lower the diastereoselctivity; the latter was determined by GC-FID analysis.

Table 3.9. Conversions [%] for (1*R*,2*R*)-**3** (5 mM) at different temperatures by combining Ls-ADH and AmDH

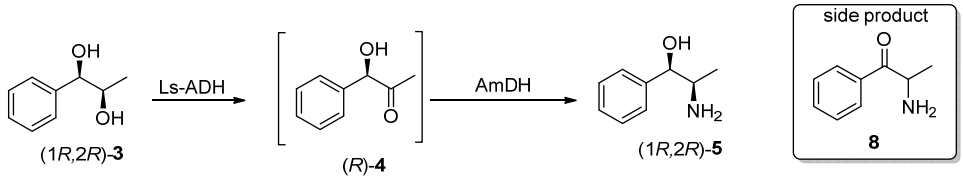

Entry	Enzymatic system	T [°C]	Conversion [%][a]	5 [*RR*] [%][a]	*er* [%][b]	*dr* [%] [*SS*:*RR*/ *RS*:*SR*]	8 [%][a,c]	Unidentified [%][a,c]
1	Ls-ADH/Ch1-AmDH	30	>99±<1	93±1	>99.5:<0.5	0:>99.5/0:0[b]	2±<1	5±<1
2	Ls-ADH/Rs-PhAmDH	30	90±6	84±5	>99.5:<0.5	0:>99.5/0:0[b]	1±<1	5±1
3	Ls-ADH/Ch1-AmDH	40	89±1	82±2	n.m.	77/23[a]	4±<1	3±<1
4	Ls-ADH/Rs-PhAmDH	40	66±1	63±2	n.m.	73/27[a]	2±<1	2±<1
5	Ls-ADH/Ch1-AmDH	50	19±3	18±3	n.m.	48.5/51.5[a]	1±<1	1±<1
6	Ls-ADH/Rs-PhAmDH	50	17±1	16±1	n.m.	61/39[a]	<1	1±<1

[a] Determined by GC-FID analysis; [b] Determined by RP-HPLC after derivatization with a chiral reagent; "0" means that the other diastereomers and enantiomer were never observed. [c] This may come, at least in part, from decomposition of the amino alcohols product (also present in the reference compound purchased by Sigma Aldrich upon injection in GC-MS or GC-FID).

3.2.4.2 Optimization cascade with (1*R*,2*R*)-3 as substrate

3.2.4.2.1 Increase in the substrate concentration for the hydrogen-borrowing amination of (1*R*,2*R*)-3

The next step was to investigate the biocatalytic system at higher substrate concentration by keeping unaltered the enzymes loading. The biocatalytic reactions

were carried out with substrate (1*R,*2*R*)-**3** (10 to 30 mM) in $HCOONH_4$ buffer (pH 8.5, 1 M, 0.5 mL) in the presence of NAD^+ (1 mM) and by combining Ls-ADH (50 µM) and Ch1-AmDH (50 µM) at 30 °C for 48 h as described in **section 3.4.6**. As reported in **Table 3.10**, the Ls-ADH/Ch1-AmDH combination also tolerated higher substrate concentrations (87±1% yield at 30 mM of (1*R,*2*R*)-**3**) with the best results obtained at 15-20 mM substrate loading (entry 2-3).

Table 3.10. Conversion [%] for (1*R,*2*R*)-**3** (varied concentrations: 10-30 mM) at 30 °C combining Ls-ADH (50 µM) and Ch1-AmDH (50 µM)

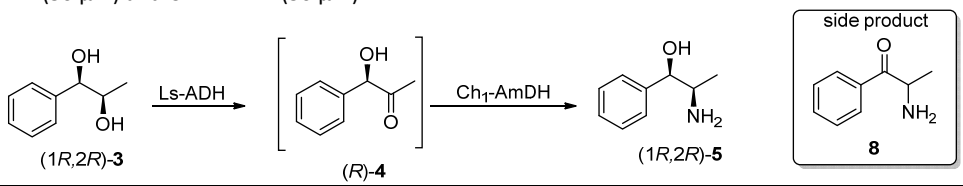

Entry	3 [*RR*] [mM]	Conversion [%][a]	5 [*RR*] [%][a]	*er* [%][b]	*dr* [%][b] [*SS*:*RR*:*RS*:*SR*]	8 [%][a,c]	Unidentified [%][a,c]
1	10	93±2	92±4	>99.5:<0.5	0:>99.5:0:0	1±<1	1±<1
2	15	96±1	93±1	>99.5:<0.5	0:>99.5:0:0	<1	2±<1
3	20	95±<1	93±<1	>99.5:<0.55	0:>99.5:0:0	1±<1	2±<1
4	25	91±1	89±<1	>99.5:<0.5	0:>99.5:0:0	<1	2±<1
5	30	89±1	87±1	>99.5:<0.5	0:>99.5:0:0	1±<1	1±<1

[a] Determined by GC-FID analysis; [b] Determined by RP-HPLC after derivatization with a chiral reagent; "0" means that the other diastereomers and enantiomer were never observed; [c] This may come, at least in part, from decomposition of the amino alcohols product (also present in the reference compound purchased by Sigma Aldrich upon injection in GC-MS or GC-FID).

Also for this substrate, the optical purity of the product was determined by RP-HPLC after derivatization with the chiral reagent GITC as reported in **section 3.4.6** and shown in **Figure 3.6**.

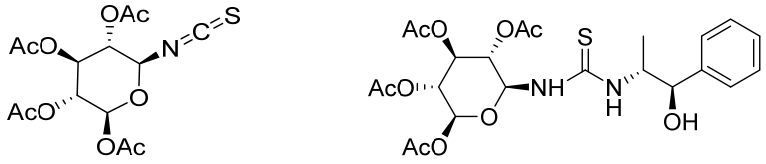

GITC *GITC*-(1*R,*2*R*)-**5**

Figure 3.6. Structures of GITC (left) and GITC-derivatized amino alcohols obtained in this study (right).

3.2.4.2.2 Further optimization of the hydrogen-borrowing amination of (1*R,*2*R*)-3

The ratio between Ls-ADH and Ch1-AmDH was optimized at various substrate concentrations as shown in **Table 3.11**. Biocatalytic reactions were performed as

described in **section 3.4.6**. Under the optimal conditions (Ls-ADH 35 µM, Ch1-AmDH 70 µM, 20 mM (1*R,*2*R*)-**3**), (1*R,*2*R*)-**5** was obtained in 99±1% analytical yield and perfect stereoselectivity (entry 5).

Table 3.11. Conversion [%] for (1*R*,2*R*)-**3** (varied concentrations: 5 to 20 mM) at 30 °C combining Ls-ADH and Ch1-AmDH at various concentrations.

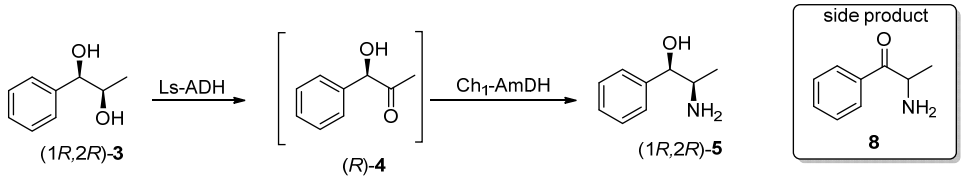

Entry	3 [*RR*] [mM]	ADH: AmDH [µM]	Conversion [%][a]	5 [*RR*] [%][a]	*er* [%][b]	*dr* [%][b] [*SS*:*RR*: *RS*:*SR*]	8 [%][a,c]	Unidentified [%][a,c]
1	20	24:60	>99	98±<1	>99.5:<0.5	0:>99.5:0:0	<1	1±<1
2	20	50:60	>99	98±<1	>99.5:<0.5	0:>99.5:0:0	1±<1	1±<1
3	20	35:70	>99	99±<1	>99.5:<0.5	0:>99.5:0:0	<1	1±<1
4	20	60:24	99±2	96±2	>99.5:<0.5	0:>99.5:0:0	1±<1	2±<1
5	20	70:35	>99	98±1	>99.5:<0.5	0:>99.5:0:0	1±<1	2±<1

[a] Determined by GC-FID analysis; [b] Determined by RP-HPLC after derivatization with a chiral reagent; "0" means that the other diastereomers and enantiomer were never observed; [c] This may come, at least in part, from decomposition of the amino alcohols product (also present in the reference compound purchased by Sigma Aldrich upon injection in GC-MS or GC-FID).

3.2.5 Hydrogen borrowing bio-amination cascade with substrate (1*S*,2*R*)-3

Two different ADHs (Ls-ADH and Bs-BDHA; 50 µM) were combined with two AmDHs (Ch1-AmDH and Rs-PhAmDH; 50 µM) in $HCOONH_4$ buffer (pH 8.5, 1 M, 0.5 mL) at 30 °C for 48 hours. The reactions were performed as described in section 3.4.6. Bs-BDHA and Ls-ADH (50 µM each) operated similarly well in combination with Ch1-AmDH for the amination of (1*S*,2*R*)-**3** (5 mM) to give (1*S*,2*R*)-**5** at 30 °C (**Table 3.12**). Bs-BDHA was used for further studies as it provided a slightly higher yield than Ls-ADH (91±3% vs. 89±1%).

Table 3.12. Conversion [%] for (1*S*,2*R*)-**3** (5 mM) at 30 °C with 50:50 µM ADH:AmDH

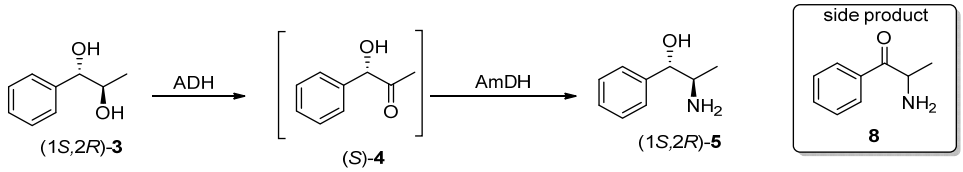

(1*S*,2*R*)-**3** (*S*)-**4** (1*S*,2*R*)-**5**

Entry	Enzymatic system	Conversion [%][a]	5 [*SR*] [%][a]	*er* [%][b]	*dr* [%][b] [*SS*:*RR*: *RS*:*SR*]	8 [%][a,c]	Unidentified [%][a,c]
1	Ls-ADH/Ch1-AmDH	96±1	89±1	>99.5:<0.5	0:4:0:96.0	3±<1	4±<1
2	Ls-ADH/Rs-PhAmDH	65±1	59±1	>99.5:<0.5	0:5.5:0:94.5	2±<1	3±<1
3	Bs-BDHA/Ch1-AmDH	98±2	91±3	>99.5:<0.5	0:4.5:0:95.5	2±<1	4±<1
4	Bs-BDHA/Rs-PhAmDH	95±1	90±1	>99.5:<0.5	0:3.9:0:96.1	2±<1	4±<1

[a] Determined by GC-FID analysis; [b] Determined by RP-HPLC after derivatization with a chiral reagent; [c] This may come, at least in part, from decomposition of the amino alcohols product (also present in the reference compound purchased by Sigma Aldrich upon injection in GC-MS or GC-FID). ***Note:*** *the fact that the diastereomeric ratio of the product (1S,2R)-**5** is not absolutely perfect must not be attributed to the hydrogen-borrowing amination step. In fact, the enantiomeric ratio of the diol substrate (1S,2R)-**3**—obtained in the previous enzymatic step—was not perfect (99:1) and that reflected on the subsequent amination step.*

3.2.5.1 Optimization cascade with (1*S*,2*R*)-3 as substrate

3.2.5.1.1 Increase in substrate concentration for the hydrogen-borrowing amination of (1*S*,2*R*)-3

The biocatalytic reactions were carried out with substrate (1*S,*2*R*)-**3** (varied concentration: 10 to 30 mM) in $HCOONH_4$ buffer (pH 8.5, 1 M, 0.5 mL) in the presence of NAD^+ (1 mM) and by combining Bs-BDHA (50 µM) and Ch1-AmDH (50 µM) at 30 °C for 48 hours as described in **section 3.4.6**. Increasing the substrate concentration at constant enzymes loading afforded 95±1%, 91±1%, 87±1%, and 80±1% analytical yields at 15, 20, 25, and 30 mM concentrations of (1*S,*2*R*)-**3**, respectively (**Table 3.13**). Stereoselectivity was also high under all substrate loading with >99.5:<0.5 *er* and 98:2 *dr*. Also in this case, the *dr* reflects the enantiopurity of the diol substrate, whereas the HB-amination is stereospecific.

Table 3.13. Conversion [%] for (1*S*,2*R*)-**3** (varied concentration: 10 to 30 mM) at 30 °C combining Bs-BDHA (50 μM) and Ch1-AmDH (50 μM).

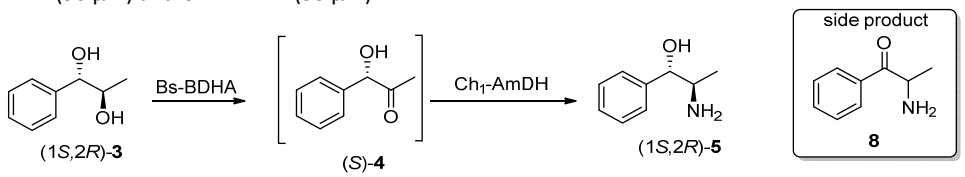

Entry	3 [*SR*] [mM]	Conversion [%][a]	5 [*SR*] [%][a]	*er* [%][b]	*dr* [%][b] [*SS*:*RR*: *RS*:*SR*]	8 [%][a][c]	Unidentified [%][a][c]
1	10	>99	92±2	>99.5:<0.5	0:2.9:0:97.1	2±<1	6±<1
2	15	99±1	95±1	>99.5:<0.5	0:2.4:0:97.6	1±<1	3±<1
3	20	95±2	91±1	>99.5:<0.5	0:2.2:0:97.8	2±1	2±<1
4	25	89±1	87±1	>99.5:<0.5	0:2.2:0:97.8	1±<1	2±<1
5	30	82±1	80±1	>99.5:<0.5	0:2.2:0:97.8	1±<1	1±<1

[a] Determined by GC-FID analysis; [b] Determined by RP-HPLC after derivatization with a chiral reagent; [c] This may come, at least in part, from decomposition of the amino alcohols product (also present in the reference compound purchased by Sigma Aldrich upon injection in GC-MS or GC-FID). ***Note:*** *the fact that the diastereomeric ratio of the product (1S,2R)-**5** is not absolutely perfect must not be attributed to the hydrogen-borrowing amination step. In fact, the enantiomeric ratio of the diol substrate (1S,2R)-**3**—obtained in the previous enzymatic step—was not perfect (99:1) and that reflected on the subsequent amination step.*

3.2.5.1.2 Further optimization of the hydrogen-borrowing amination of (1*S*,2*R*)-3

Further experiments were performed by varying the substrate as well as the enzymes concentration according to the general procedure reported in **section 3.4.6**. As shown in **Table 3.14**, further tuning of the enzyme ratio did not provide any significant improvement compared to the results obtained in table 3.13; hence, 15 mM substrate loading and 50:50 μM enzyme ratio (Bs-BDHA:Ch1-AmDH) revealed to be the optimal conditions (Table 3.13, entry 2).

Table 3.14. Conversion [%] for (1*S*,2*R*)-**3** at 30 °C after further optimization of enzyme and substrate concentrations using Bs-BDHA in combination with Ch1-AmDH

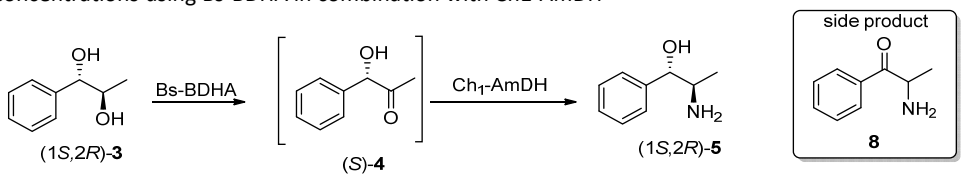

(1*S*,2*R*)-**3** (*S*)-**4** (1*S*,2*R*)-**5**

Entry	3 [*SR*] [mM]	Enzymes ratio [µM]	Conversion [%][a]	5 [*SR*] [%][a]	*er* [%][b]	*dr* [%][b] [*SS*:*RR*: *RS*:*SR*]	8 [%][a,c]	Unidentified [%][a,c]
1	10	24:60	94±<1	89±<1	>99.5:<0.5	0:2.5:0:97.5	1±<1	4±<1
2	15	24:60	90±1	87±1	>99.5:<0.5	0:2.1:0:97.9	1±<1	2±<1
3	20	24:60	79±<1	77±<1	>99.5:<0.5	0:2:0:98	1±<1	2±<1
4	25	24:60	72±<1	71±<1	>99.5:<0.5	0:2:0:98	1±<1	1±<1
5	30	24:60	65±2	63±2	>99.5:<0.5	0:2.1:0:97.9	1±<1	1±<1
6	10	60:24	97±1	93±1	>99.5:<0.5	0:3:0:97	1±<1	3±<1
7	10	70:35	97±<1	93±<1	>99.5:<0.5	0:3:0:97	1±<1	3±<1

[a] Determined by GC-FID analysis; [b] Determined by RP-HPLC after derivatization with a chiral reagent; [c] This may come, at least in part, from decomposition of the amino alcohols product (also present in the reference compound purchased by Sigma Aldrich upon injection in GC-MS or GC-FID). ***Note:*** *the fact that the diastereomeric ratio of the product (1S,2R)-**5** is not absolutely perfect must not be attributed to the hydrogen-borrowing amination step. In fact, the enantiomeric ratio of the diol substrate (1S,2R)-**3**—obtained in the previous enzymatic step—was not perfect (99:1) and that reflected on the subsequent amination step.*

3.2.6 Hydrogen borrowing bio-amination cascade with substrate (1*R*,2*S*)-3

The last case was the amination of (1*R,*2*S*)-**3** to yield (1*R,*2*R*)-**5** (also obtained previously starting from (1*R,*2*R)*-**3**). Two different ADHs (Aa-ADH and Bs-BDHA; 50 µM) were combined with two AmDHs (Ch1-AmDH and Rs-PhAmDH; 50 µM) in $HCOONH_4$ buffer (pH 8.5, 1 M, 0.5 mL) at 30 °C for 48 hours according to the general procedure reported in **section 3.4.6**. Aa-ADH was again the optimal ADH, whereas Ch1-AmDH performed slightly better than Rs-PhAmDH (**Table 3.15**; 75±5% vs. 63±3% analytical yield, entry 1-2) with 50 µM of each enzyme and at 5 mM of *1R,2S*-**3**. Further optimization did not lead to any significant improvement, which is likely due to the insufficient activity of Aa-ADH on (1*R,*2*S*)-**3**. Indeed, in the case of (1*R*,2*R*)-**3** as substrate clearly demonstrates that the (1*R*)-**4** intermediate is efficiently aminated by Ch1-AmDH (**Table 3.11**). No further tests were then carried out by using (1*R*,2*S*)-**3** as substrate.

Table 3.15. Conversion [%] for (1*R*,2*S*)-**3** (5 mM) at 30 °C with 50:50 µM ADH:AmDH.

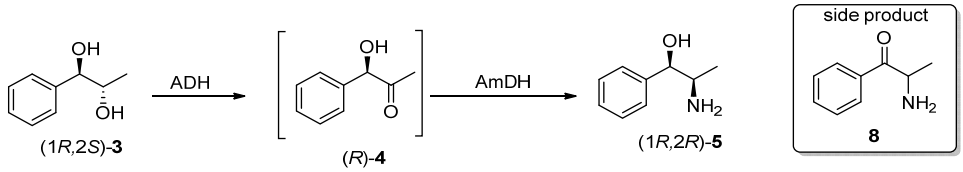

Entry	Enzymatic system	Conversion [%][a]	5 [*RR*] [%][a]	*er* [%][b]	*dr* [%][b] [*SS*:*RR*:*RS*:*SR*]	8 [%][a,c]	Unidentified [%][a,c]
1	Aa-ADH/ Ch1-AmDH	80±5	75±5	>99.5:<0.5	0:>99.5:0:0	2±<1	4±1
2	Aa-ADH/ Rs-PhAmDH	69±5	63±3	>99.5:<0.5	0:>99.5:0:0	2±1	4±1
3	Bs-BDHA/ Ch1-AmDH	18±<1	16±1	>99.5:<0.5	0:>99.5:0:0	1±<1	1±<1
4	Bs-BDHA/ Rs-PhAmDH	16±<1	14±1	>99.5:<0.5	0:>99.5:0:0	1±<1	1±<1
5[d]	Aa-ADH/ Ch1-AmDH	58±1	57±1	>99.5:<0.5	0:>99.5:0:0	1±<1	<1

[a] Determined by GC-FID analysis; [b] Determined by RP-HPLC after derivatization with a chiral reagent; "0" means that the other diastereomers and enantiomer were never observed; [c] This may come, at least in part, from decomposition of the amino alcohols product (also present in the reference compound purchased by Sigma Aldrich upon injection in GC-MS or GC-FID); [d]Performed at 10 mM substrate loading.

3.2.7 Overview optimal experimental conditions for accessing (1*S*,2*R*)-5 and (1*R*,2*R*)-5

After varying various parameters (temperature, reaction time, substrate and enzymes loading) in the HB-bioamination of all the four diol isomers **3**, the optimal conditions for accessing the desired PPAs **5** were disclosed. However, as reported in **Table 3.16**, only two out of the four possible isomers of **5** could be obtained. This is due to the lack of (*S*)-selective AmDHs, requiring further research in this direction. All the four diol isomers **3** tested led to the formation of either (1*R*,2*R*)-**5** or (1*S*,2*R*)-**5**. Nevertheless, (1*R*,2*R*)-**3** (20 mM, entry 2-3) is the best substrate for the enzymatic synthesis of (1*R*,2*R*)-**5** in terms of substrate loading, conversion, analytical yield as well as stereoselectivity compared to the results obtained with substrate (1*R*,2*S*)-**3** (5 mM, entry 5). On the other hand, a similar trend was observed for the synthesis of (1*S*,2*R*)-**5** starting by either (1*S*,2*S*)-**3** (20 mM, entry 1) or (1*S*,2*R*)-**3** (15 mM, entry 4). Though both substrates lead to high conversion and analytical yields, (1*S*,2*R*)-**3** gave a slightly higher diastereoselectivity ratio than (1*S*,2*S*)-**3** (2.4:97.6 vs 5:95, respectively). Anyway, as mentioned also earlier, the *dr*

reflects the imperfect stereoselectivity of one of the EH (Sp(*S*)-EH) used in the enzymatic cascade for the synthesis of these chiral diol substrates (**Table 3.2**).

Table 3.16. Regio- and stereospecific HB-amination of optically active **3** in $HCOONH_4$ buffer (pH 8.5, 1 M, 0.5 mL) containing NAD^+ (1 mM) at 30 ºC and different enzyme concentrations (ADH/Ch1-AmDH) for 48 h.

Entry	Sub.	ADH	ADH: AmDH [µM]	Conv. [%][a]	Product [%][a]	*er* [%][b]	*dr* [%] [*SS*:*RR*/ *RS*:*SR*][b]
1	(1*S*,2*S*)-**3**[d]	Aa-ADH	70:35	>99	98±1	>99.5 (1*S*,2*R*-**5**)	1:4/0:95[c]
2	(1*R*,2*R*)-**3**[d]	Ls-ADH	24:60	>99	98±1	>99.5 (1*R*,2*R*-**5**)	0:>99.5/0:0
3	(1*R*,2*R*)-**3**[d]	Ls-ADH	35:70	>99	99±1	>99.5 (1*R*,2*R*-**5**)	0:>99.5/0:0
4	(1*S*,2*R*)-**3**[e]	Bs-BDHA	50:50	>99	95±1	>99.5 (1*S*,2*R*-**5**)	0:2.4/0:97.6[c]
5	(1*R*,2*S*)-**3**[f]	Aa-ADH	50:50	80±5	75±5	>99.5 (1*R*,2*R*-**5**)	0:>99.5/0:0

[a] Measured by GC-FID; [b] measured by RP-HPLC after derivatization with a chiral reagent; [c] *dr* due to initial optical purity of substrate; [d] 20 mM; [e] 15 mM; [f] 5 mM. "0" means that the other diastereomers and/or enantiomer were never observed

3.2.8 Preparative scale HB-bioamination cascade

In order to evaluate its applicability, the regio- and stereoselective dual enzyme HB-amination of 1,2-diols was performed on a slightly above one hundred milligrams scale for (1*R,*2*R*)-**3** (20 mM, 105 mg, 0.690 mmol) and (1*S,*2*R*)-**3** (15 mM, 102 mg, 0.670 mmol) to yield (1*R,*2*R*)-**5** and (1*S,*2*R*)-**5**, respectively. The reactions were performed in $HCOONH_4$ buffer (pH 8.5, 1 M) supplemented with NAD^+ (1 mM) at 30 °C for 48 h. Both amino alcohol products **5** were quantitatively obtained with high chemoselectivity (<2% by-products) as well as regio- and stereoselectivity. Upon extraction with MTBE, (1*R,*2*R*)-**5** and (1*S,*2*R*)-**5** could be isolated in elevated yield (74%), *er* (>99.5:<0.5) and *dr* (>99.5:<0.5 or 98:2, respectively), as summarized in **Table 3.17**.

Table 3.17. Overview for the one pot hydrogen-borrowing amination of enantiomerically pure or enantiomerically enriched diols **3** in semi-preparative scale in $HCOONH_4$ buffer (pH 8.5, 1 M) at 30 °C for 48 h. Ch1-AmDH was used as aminating enzyme in all cases.

Sub.	ADH	ADH: AmDH [μM]	Conv. [%][b]	Isolated yield [%]	*er* [%][a]	*dr* [%][b] [*SS*:*RR*: *RS*:*SR*]
(1*R,*2*R*)-**3**[c]	Ls-ADH	24:60	>94	74 (77 mg)	<0.5:>99.5 (1*R,*2*R*-**5**)	0:>99.5:0:0
(1*S,*2*R*)-**3**[d]	Bs-BDHA	50:50	>99	74 (75 mg)	<0.5:>99.5 (1*S,*2*R*-**5**)	0:2.3:0:97.7

[a] determined by RP-HPLC after derivatization with a chiral compound; [b] determined by GC-FID analysis and further confirmed by NP-HPLC analysis and ^{1}H-NMR; "0" means that the other diastereomers and enantiomer were never observed; [c] 20 mM, 105 mg, 0.690 mmol; [d] 15 mM, 102 mg, 0.670 mmol

Therefore, considering the asymmetric dihydroxylation step (**Table 3.2**) along with the hydrogen-borrowing amination step (**Table 3.17**), the overall yields for the conversion of substrate **1** into optically active **5** were found to be 59% and 63%, respectively (**Table 3.18**).

Table 3.18. Overall yields for the multi-enzymatic conversion [%] of **1** (*trans or cis*) into (1*R*,2*R*)-**5** or (1*S*,2*R*)-**5**.

Entry	Sub.	Step 1 Yield [%]	Step 2 Yield [%]	Combined Yield [%]	*er* [%]	*dr* [%] [*SS*/*RR*: *RS*/*SR*]
1	*trans*-**1**	85[b]	74	63	<0.5:>99.5 (1*S*,2*R*-**5**)	2:98[a]
2	*cis*-**1**	79[c]	74	59	<0.5:>99.5 (1*R*,2*R*-**5**)	>99.5:>0.5

[a]dependent on stereoselectivity of Step 1; [b] (1*S*,2*S*)-**3**; [c] (1*R*,2*R*)-**3**

3.2.9 Estimation and comparison of simple E-factor (sEF) and solvent demand

Table 3.19 shows a comparison of estimated values of simple E-factor and solvent demand among the enzymatic approach describe in this work, another enzymatic approach and two chemical methods involving catalytic steps. The advantage of using biocatalytic cascades rather than other chemical methods for the synthesis of phenylpropanolamines (PPAs, **5**) is evident according the data reported in Table 3.19. Though the approach by Sehl *et al.* towards the preparation of (1*R*,2*R*)-**5** turned out to have a lower E factor (4 vs. 10-11), it cannot be directly compared to our study because: *i*) A different starting material (benzaldehyde vs. β-

methylstyrenes) was used. Consequently, the method by Sehl *et al*. consists of a one-pot two-enzyme route. Conversely, our study comprises a total of five enzymes within two separated cascade reactions; *ii*) The data for the method by Sehl *et al.* are calculated for a reaction on analytical scale for which a conversion was measured but the product was not isolated; *iii*) The biocatalysts were used in different forms (e.g., purified enzymes, lyophilized free cells extract or lyophilized whole cells) and therefore the mass of biocatalysts used is not entirely comparable (*i.e*., in the first step of our process we have used lyophilized whole cells that contribute significantly to the waste mass). By considering these factors, we deem the actual sEF values of the two biocatalytic processes to be essentially equivalent. Regarding the two chemical methods, the E-factor were in the range between 50 and 120 which is 5 to 12-fold higher than our approach. Moreover, the waste generated for the preparation of the required catalysts for these reactions has not been considered in this calculation as these data could not be accessed in a reliable manner. Furthermore, in terms of selectivity, we obtained compound **5** as individual isomers (either 1*R*,2*R*-**5** or 1*S*,2*R*-**5**) therefore with very high *er* and *dr*. On the other hand, as shown in **Table 3.19**, the two chemical methods could lead only to a mixture of isomers and low yield (as in the case of Legnani *et al.*) or high yield but low enantioselectivity (Minakata *et al.*).

Table 3.19. Simplified E-factor (sEF) and solvent demand calculations for various methods for the synthesis of chiral **5**

Entry	System	sEF[a][b]	Solvent demand [mL mg^{-1} $_{product}$]	Stereoselectivity
1	This work	10-11	1.8-2.3	(1*R*,2*R*)-**5** (>99.5:<0.5 *er* and *dr*) (1*S*,2*R*)-**5** (>99.5:<0.5 *er*; 2.3:97.7 *dr*)
2	Sehl *et al.*[11]	4	0.8	(1*R*,2*R*)-**5** (*ee* >99%; *de* >98%)
3	Legnani *et al*.[19]	52-80	4.2-6.9	*ee* n.a. *dr* = 1.2:1.0 [*RR*/*SS*:*SR*/*RS*] *dr* = 1.0:3.0 [*RR*/*SS*:*SR*/*RS*]
4	Minakata *et al*.[17]	116	5.0	(1*R*,2*R*)-**5** (*ee* 86%; *de* n.a.)

[a] Generated waste for the preparation of catalyst was not included; [b] Reaction buffers and other solvents were not included here, but calculated apart (see solvent demand); n.a. means not available.

3.3 Conclusions

In conclusion, we developed a sequential multi-enzymatic process for the conversion of β-methylstyrene into phenylpropanolamines with high chemo-, regio-, and stereoselectivity. The use of multiple enzymes in one pot has several economic and environmental advantages as this eliminates the need for intermediate isolation steps, which generally lead to time-, solvent- and energy-consuming workups.[52-55] The present approach consists of four enzymatic reactions but required the sole and easy isolation of the diol intermediates **3**. The enzymatic route consumes only dioxygen and one equivalent of ammonia and formate and produces only one equivalent of carbonate as by-product. With the aim of critically evaluating the greenness of our methodology to obtain optically active PPAs, we have estimated and compared the simple E-factors (*i.e.*, sEF, without solvents contribution) and the solvent demand for: *i*) our process; *ii*) a representative multi-step chemical route involving metalorganic complexes;[17] *iii*) a recently reported direct and catalytic 1,2-aminohydroxylation of *cis*- and *trans*-**1**;[19] *iv*) and another highly atom-efficient one-pot two-step biocatalytic route starting from benzaldehyde.[11] The representative multi-step chemical route by Minakata *et al.*[17] results in a sEF above 110, mainly due to the intermediate purification step and the required excess of starting material. The direct and catalytic 1,2-aminohydroxylation by Legnani *et al.*[19] results in a sEF between ca. 50 and 80, depending on the reaction conditions. The main reason for this sEF value is the moderate conversion and the suprastoichiometric amount of a complex aminating agent. Notably, in these two chemical methods, the sEF associated to the preparation of the catalysts was not included as these data could not be accessed in a reliable manner. Therefore, the actual sEF must be higher than estimated herein. Furthermore, as the final products are never obtained in optically pure form, an additional recrystallization step to upgrade *er* and *dr* would further increase the sEF of the process. In comparison, the biocatalytic route by Sehl *et al.*[11] results in the lowest sEF of ca. 4 due to the internal recycling of pyruvate between the two steps. However, the data used for the calculation of this sEF relate to a reaction on analytical scale, for which a conversion was measured but the product was not isolated. The new biocatalytic route described in this work results in a sEF of ca. 10. However, in our case, the reactions were conducted slightly above 300 mg (step 1) and 100 mg (step 2) scale, and the products were isolated. Moreover, comparing our methodology with the other biocatalytic route by Sehl *et al.*, the starting material is different (β-methylstyrene vs. benzaldehyde) and different biocatalyst's

forms were used (e.g., lyophilized cells, lyophilized crude cell extract, purified enzyme). By considering these factors, we deem the actual sEF values of the two biocatalytic processes to be essentially equivalent. Additionally, the solvent demand of the two biocatalytic processes was also from two to six-fold lower compared with the values calculated for the chemical processes.

Finally, this work reports the first case in which the regioselectivity of the dual-enzyme HB-amination was investigated and exploited in preparative scale, thus further demonstrating the potential of this reaction in asymmetric synthesis. The currently attainable number and diversity of enantiomeric products are limited by the availability of complementary regio- and stereoselective ADHs and AmDHs. However, protein engineering and the discovery of novel AmDHs and ADHs are expected to enhance the applicability of this synthetic methodology towards the synthesis of a wide variety of enantiopure PPAs as well as other structurally diverse 1,2-amino alcohols.

3.4 Experimental Section

General information. *trans*-1-Phenyl-1-propene *(trans*-β-methylstyrene, *trans*-**1**), *cis*-1-phenyl-1-propene *(cis*-β-methylstyrene, *cis*-**1**), 1-phenylpropane-1,2-dione (**7**), GITC and FAD were purchased from TCI chemicals. (2*R,*3*R*)-(+)-2-methyl-3-phenyloxirane *(*2*R,*3*R*-**2**), (2*S,*3*S*)-(−)-2-methyl-3-phenyloxirane (2*S,*3*S*-**2**), (1*S,*2*R*)-(+)- 2-amino-1-phenyl-1-propanol (1*S,*2*R*-**5**), (1*R,*2*S*)-(-)- 2-amino-1-phenyl-1-propanol *(*1*R,*2*S*-**5**) and catalase from bovine liver (lyophilized powder, >10000 U mg^{-1} of protein) were purchased from Sigma Aldrich. Nicotinamide cofactor (NAD^+) was purchased from Melford Biolaboratories (Chelsworth, Ipswich, UK). All chemicals and solvents were used without further purification. The amino alcohol references (1*S,*2*S/*1*R*-2*R)*-2-amino-1-phenyl-1-propanol (1*S,*2*S/*1*R,*2*R*-**5**), (1*R,*2*S*)-1-amino-1-phenylpropan-2-ol (1*R,*2*S*-**9**), (1*S,*2*R*)-1-amino-1-phenylpropan-2-ol (1*S,*2*R*-**9**), (1*S,*2*S/*1*R,*2*R)*-1-amino-1-phenylpropan-2-ol (1*S,*2*S/*1*R,*2*R*-**9**), 1-phenylpropane-1,2-diol (diol **3** as a mixture of all the four possible isomers), and *rac*-1-hydroxy-1-phenylpropan-2-one (*rac*-**4)** were chemically synthesized as reported in section 3.4.5. ^{1}H NMR spectra were recorded on a Brucker (400 MHz) spectrometer in $CDCl_3$.

3.4.1 Enzymes used in this study

Table 3.20. Source and expression conditions for enzymes used in this study. For the definition of enzyme classes, see abbreviations list

Name	Source/Comment	Plasmid	Tag	Expression/ Purification	Used form	Ref
Fus-SMO	Fused SMO from *Pseudomonas* sp. VLB120	pET28b	N-His_6	Ref. 36	lyophilized whole cells	36
Fus-SMO (1) + Cb-FDH (2)	Fused SMO coexpressed with Cb-FDH	pET28b/ pET21a	N-His_6 (1)/No-Tag (2)	Ref. 36	lyophilized whole cells	36
Sp(S)-EH	*Sphingomonas* sp. HXN200	pET28b	N-His_6	1 mM IPTG, 25 °C 16 h	lyophilized whole cells	37
St(R)-EH	*Solanum tuberosum*	pET28b	N-His_6	1 mM IPTG, 25 °C 16 h	lyophilized whole cells	37
Rs-ADH	*Ralstonia* sp.	pET28b	N-Strep	0.5 mM IPTG, 25 °C 16 h	lyophilized whole cells	46
Aa-ADH	*Aromatoleum aromaticum*	pET28b	N-His_6	Ref. 33	purified	38
Pp-ADH	*Paracoccus pantotrophus* DSM 11072	pMS47/ pEamTA	C-His_6	2 mM IPTG, 25 °C, 16 h	lyophilized whole cells	42
Sy-ADH	*Shingobium yanoikuyae* DSM 6900	pET26b	C-Strep	0.5 mM IPTG, 25 °C 16 h	lyophilized whole cells	41
Te-ADH-v1	I86A variant from *Thermoanaerobacter ethanolicus*	pET21a	C-Strep	0.5 mM IPTG, 25 °C 16 h	lyophilized whole cells	45

Table 3.20. *(Continued)*

Name	Source/Comment	Plasmid	Tag	Expression/ Purification	Used form	Ref
Te-ADH-v2	W110A variant from *Thermoanaerobacter ethanolicus*	pET42a	GST	0.5 mM IPTG, 25 °C 16 h	lyophilized whole cells	45
Te-ADH-v3	I86A W110A variant from *Thermoanaerobacter ethanolicus*	pET42a	GST	0.5 mM IPTG, 25 °C 16 h	lyophilized whole cells	45
Lb-ADH	*Lactobacillus brevis*	pET21a	no Tag	0.5 mM IPTG, 25 °C 16 h	purified	40
Lbv-ADH	variant from *Lactobacillus brevis*	pET21a	no Tag	Ref. 31	purified	39
Ls-ADH	*Leifsonia* sp.	pET21a	no Tag	0.5 mM IPTG, 25 °C 16 h	lyophilized whole cells and purified	44
Bs-BDHA	*Bacillus subtilis* BGSC1A1	pET28b	N-His_6	0.5 mM IPTG, 25 °C 16 h	purified	43
Ch1-AmDH	Chimeric AmDH	pET28b	N-His_6	Ref. 31	purified	49
Rs-PhAmDH	variant from *Rhodoccoccus* sp.	pET28b	N-His_6	Ref. 56	purified	50
Cb-FDH	*Candida boidinii*	pET28b	N-His_6	Ref. 56	purified	56
YcnD	NAD(P)H-dependent oxidase from *Bacillus subtilis*	pET21a	no Tag	Ref. 45	purified	48
NOx	NADH-dependent oxidase from *Streptococcus mutans*	pET21a	C-His_6	Ref. 57	purified	47

Expression of the enzymes: For recombinant expression, 800 mL of LB medium supplemented with the appropriate antibiotic (100 µg mL^{-1} ampicillin or 50 µg mL^{-1} kanamycin) were inoculated with 15 mL of an overnight culture harboring the desired vector with genes for the expression of the enzymes. *E. coli* BL21 DE3 cells was used as host organism. Cells were grown at 37 °C until an OD_{600} of 0.6 to 1 was reached and expression of protein was induced by the addition of IPTG. Protein expression was carried out overnight and after harvesting of the cells (4 °C, 4500 rpm, 10 min), the remaining cell pellets were washed with buffer (for lyophilized cells: 50 mM Tris-HCl buffer, pH 8.0 for ADHs and 50

mM KPi, pH 8.0 for EHs; or lysis buffer for enzymes that were subsequently purified by affinity chromatography).

Purification by Nickel affinity chromatography: His_6-tagged proteins were resuspended in lysis buffer (50 mM KH_2PO_4, 300 mM NaCl, 10 mM imidazole, pH 8.0) prior to cell disruption and protein purification was performed by Ni-NTA affinity chromatography using pre-packed Ni-NTA HisTrap HP columns (GE Healthcare), previously equilibrated with lysis buffer. After loading of the filtered lysate, the column was washed with sufficient amounts of wash buffer (50 mM KH_2PO_4, 300 mM NaCl, 25 mM imidazole, pH 8.0), and bound protein was recovered with elution buffer (50 mM KH_2PO_4, 300 mM NaCl, 200 mM imidazole, pH 8.0). Purity was analysed by SDS-PAGE and fractions showing >95% purity were combined and dialyzed overnight against Tris-HCl buffer (6 L, pH 8.0, 20 mM). The enzyme solutions were concentrated and their concentration was determined spectrophotometrically based on their extinction coefficient at 280 nm.

Purification by anion exchange chromatography: Proteins devoid of a tag were purified by anion exchange chromatography using a HiPrepQ HP 16/10 column (GE Healthcare). The lysate was dissolved in start buffer (20 mM Tris-HCl, pH 8.0) and after cell disruption and centrifugation loaded onto the column. The elution of the proteins was performed with a gradient between start buffer and elution buffer (20 mM Tris-HCl, 1 M NaCl, pH 8.0). After SDS-PAGE, fractions containing the desired proteins in a sufficient purity were pooled, dialyzed against 50 mM K_2HPO_4/KH_2PO_4 buffer (pH 7.0) overnight, and concentrated. The final concentration was determined at 280 nm by UV-vis spectroscopy.

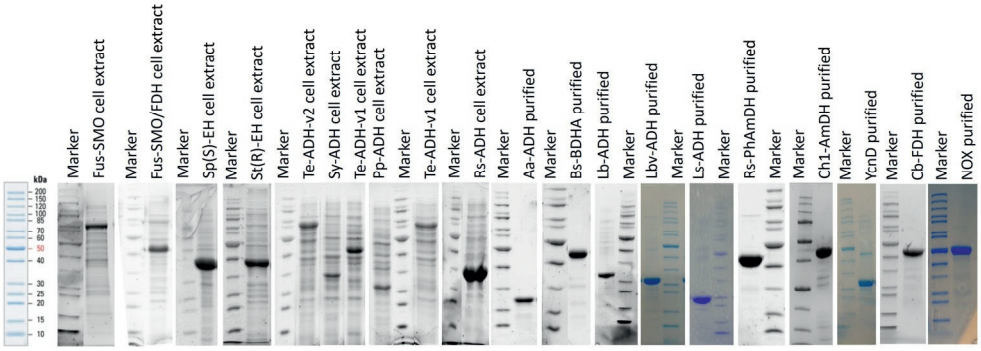

Figure 3.7. SDS-PAGEs of lyophilized whole cells (crude cell extract before lyophilization of the cells) or purified enzymes. Marker: PageRuler™ Unstained Protein Ladder (ThermoFisher Scientific).

3.4.2 One-pot cascade for the dihydroxylation of *trans* or *cis*-1 to optically active 3

Analytical scale: preliminary investigation on the stereo-complementarity of two EHs[37]

General remark: The concentrations of coenzymes, co-substrate and recycling enzyme are always calculated on the volume of the aqueous phase, whereas the concentration of the substrate is referred to the organic phase.

Reaction conditions**:** Lyophilized *E. coli* cells co-expressing Fus-SMO (10 mg) and either Sp(*S*)-EH or St(*R*)-EH (10 mg) were rehydrated in KPi buffer (0.5 mL, 50 mM, pH 8.0) in 4 mL glass vials. After that, the cofactor NAD^+ (1 mM, 0.05 eq.), HCOONa (100 mM, 5 eq.), purified Cb-FDH (10 µM) and FAD (50 µM) were added. Heptane (0.5 mL; 1:1 volumetric ratio with the buffer) was used as biphasic solvent. Finally, the biocatalytic reactions were initiated by the addition of *trans-or cis*-**1** (20 mM). The reactions were incubated at 30 °C and 180 rpm on an orbital shaker for 24 h. After saturation of the aqueous phase with solid NaCl, the organic compounds were extracted with MTBE (2 x 250 µL). The combined organic phases were dried over $MgSO_4$. Conversions were measured by GC-FID, while *er* [%] and *dr* [%] were determined by HPLC. The results are summarized in Table 3.1.

Preparative scale: enzymatic synthesis of enantiomerically pure 3

General remark: The concentrations of coenzymes and co-substrate are always calculated on the volume of the aqueous phase, whereas the concentration of the substrate is referred to the organic phase.

Reaction conditions: Lyophilized *E. coli* cells co-expressing Fus-SMO/Cb-FDH (250 mg, 5 mg mL^{-1}) were rehydrated in KPi buffer (50 mL, 50 mM, pH 8.0) in a baffled Erlenmeyer flask (500 mL). After that, NAD^+ (1 mM), HCOONa (5 eq.), FAD (50 µM) and catalase (0.1 mg mL^{-1}) were added. Heptane (50 mL; 1:1 volumetric ratio with the buffer) was used as biphasic solvent. Finally, the biocatalytic reactions were initiated by the addition of substrate *trans* or *cis*-**1** (50 mM, 2.5 mmol). The reactions were incubated at 30 °C and 200 rpm on an orbital shaker. After 6 hours, lyophilized *E.coli* cells expressing either Sp(S)-EH or St(R)-EH (1 g, 20 mg mL^{-1}) were added and the reactions were further incubated at 30 °C and 170 rpm on an orbital shaker for 30 h. Heptane was removed, the aqueous phase was saturated with solid NaCl and the organic compounds extracted with MTBE (3 x 25 mL). After drying over $MgSO_4$, the organic phase was removed under reduced pressure. The conversions and purity of the isolated products were determined by GC-FID, while *er* [%] and *dr* [%] were analyzed by HPLC (**Table 3.2**).

3.4.3 Screening of NAD(P)$^+$-dependent ADHs for the bio-catalytic oxidation of 1-phenylpropane-1,2-diol (3)

The aim of this experiment was to determine the regio-and stereoselectivity of a panel of ADHs (6 NAD$^+$-dependent and 5-NADP$^+$-dependent ADHs) for the oxidation of diol **3** as test substrate (mixture of all four possible stereoisomers). The results for the screening are summarized in **Table 3.3**.

Reaction conditions for the biocatalytic oxidation of diol 3 using lyophilized *E. coli* cells expressing one of the following NAD(P)$^+$-dependent ADHs: Sy-ADH, Pp-ADH, Bs-BDHA, Te-ADH-v1, Te-ADH-v2, Te-ADH-v3 and *Rs*-ADH.

Lyophilized *E. coli* cells (20 mg mL^{-1}) were rehydrated in an Eppendorf tube (1.5 mL) in Tris-HCl buffer (0.5 mL, pH 7.5, 50 mM) containing NAD(P)$^+$ (1 mM, 0.1 eq.) and diol **3** (10 mM). NOx (0.5 µM) for NAD$^+$-dependent ADHs or YcnD (5 µM) for NADP$^+$-dependent ADHs, respectively, was also added for cofactor regeneration. The mixtures were incubated at 30 °C, 170 rpm for 24 h on an orbital shaker and, after saturation of the aqueous layer with solid NaCl, the organic compounds were extracted with MTBE (2 x 250 µL). The organic layers were dried over $MgSO_4$ and analyzed by GC-FID and HPLC.

Reaction conditions for the biocatalytic oxidation of diol 3 using lyophilized *E. coli* cells expressing the NAD$^+$-dependent Ls-ADH.

Lyophilized *E. coli* cells (10 mg mL^{-1}) were rehydrated in an Eppendorf tube (2 mL) in KPi buffer (1 mL, pH 6.5, 100 mM) containing NAD$^+$ (1 mM, 0.1 eq.) and diol **3** (10 mM). NOx (0.5 µM) was also added for cofactor regeneration. The mixture was incubated at 40 °C, 170 rpm for 24 h on an orbital shaker. After saturation of the aqueous layer with solid NaCl, extraction was performed with MTBE (2 x 500 µL). The organic layer was dried over $MgSO_4$ and analyzed by GC-FID and HPLC.

General reaction conditions for the bio-oxidation of diol 3 by NAD(P)$^+$-dependent ADHs using one of the following purified ADHs: Lbv-ADH, Aa-ADH and Lb-ADH.

Tris-HCl buffer (0.5 mL, pH 7.5, 50 mM) was added to an Eppendorf tube (1.5 mL) containing NAD$^+$ or NADP$^+$ (1 mM, 0.1 eq.) and diol **3** (10 mM). NOx (0.5 µM) for NAD$^+$-dependent ADHs or YncD (5 µM) for NADP$^+$-dependent ADHs, respectively, was also added. As last, the tested ADH (50 µM) was added. The mixture was incubated at 30 °C, 170 rpm for 24 h on an orbital shaker. After saturation of the aqueous layer with solid NaCl, extraction was performed with MTBE (2 x 250 µL). The organic layer was dried over $MgSO_4$ and analyzed by GC-FID and HPLC.

3.4.4 Screening secondary NAD(P)$^+$-dependent ADHs for the bio-catalytic reduction of 1-phenyl-1,2-propanedione (7)

Reaction conditions lyophilized *E. coli* cells carrying overexpressed NAD$^+$-dependent ADHs (*Pp*-ADH, *Sy*-ADH, *Bs*-BDHA)

Lyophilized *E.coli* cells carrying the required ADH (20 mg mL^{-1}) were rehydrated in an Eppendorf tube (2 mL) in Tris-HCl buffer (pH 7.5, 50 mM, 1 mL final volume) followed by addition of NAD$^+$ (1 mM), HCOONa (100 mM) and purified Cb-FDH (10 µM). Substrate **7** (20 mM) was added as last. The mixture was incubated at 30 °C, 170 rpm for 24 h on an orbital shaker. After saturation of the aqueous phase with solid NaCl, extraction was performed with EtOAc (2 x 500 µL). The organic layer was dried over $MgSO_4$ and conversion was analyzed by GC-FID (method A).

Reaction conditions purified NAD$^+$-dependent ADHs (*Aa*-ADH, *Lbv*-ADH)

Tris-HCl buffer (pH 7.5, 50 mM, 1 mL final volume) was added to an Eppendorf tube (2 mL) followed by NAD$^+$ (1 mM), HCOONa (100 mM) and purified Cb-FDH (10 µM). Then, ADH (50 µM) and substrate **7** (20 mM) were added as last. The mixture was incubated at 30 °C, 170 rpm for 24 h on an orbital shaker. After saturation of the aqueous phase with solid NaCl, extraction was performed with EtOAc (2 x 500 µL). The organic layer was dried over $MgSO_4$ and conversion was analyzed by GC-FID (method A).

Reaction conditions lyophilized *E. coli* cells carrying overexpressed NADP$^+$-dependent ADHs (*Te*-ADH$_{V1,V2,V3}$, *Rs*-ADH)

Lyophilized *E. coli* cells carrying the ADH (20 mg mL^{-1}) were rehydrated in an Eppendorf tube (2 mL) in Tris-HCl buffer (pH 7.5, 50 mM, 1 mL final volume) followed by addition of NADP$^+$ (1 mM), glucose (100 mM) and GDH (1 mg; lyophilized crude extract, Codexis, GDH-105, ca. 50 U mg^{-1}). Substrate **7** (20 mM) was added as last. The mixture was incubated at 30 °C, 170 rpm for 24 h on an orbital shaker. After saturation of the aqueous phase with solid NaCl, extraction was performed with EtOAc (2 x 500 µL). The organic layer was dried over $MgSO_4$ and conversion was analyzed by GC-FID (method A).

Reaction conditions purified NADP$^+$-dependent ADHs (*Lb*-ADH)

Tris-HCl buffer (pH 7.5, 50 mM, 1 mL final volume) was added to an Eppendorf tube (2 mL) followed by NADP$^+$ (1 mM), glucose (100 mM) and GDH (1 mg; lyophilized crude extract, Codexis, GDH-105, ca. 50 U mg^{-1}). Then, ADH (50 µM) and substrate **7** (20 mM) were added as last. The mixture was incubated at 30 °C, 170 rpm for 24 h on an orbital shaker. After saturation of the aqueous phase with solid NaCl, extraction was performed with EtOAc (2 x 500 µL). The organic layer was dried over $MgSO_4$ and conversion was analyzed by GC-FID (method A).

3.4.5 Chemical synthesis of substrates and reference compounds

Chemical synthesis of rac-1-hydroxy-1-phenylpropan-2-one (*rac*-4)[58-60]

(i) To a 100 mL round bottom flask, benzaldehyde (9.4 mmol, 1 g) and K_2CO_3 (6.5 mmol, 900 mg) were added. After that, TMSCN (12.25 mmol, 1.2 g, 1.3 eq.) was added and the reaction mixture was stirred at room temperature. The progress of the reaction was followed by GC-MS. After completion, the excess of K_2CO_3 was removed by filtration, followed by washing with DCM. The solvent was removed under reduced pressure and a brown oil was obtained (1.68 g, 87% yield, >95% purity based on ^{1}H-NMR analysis), which was then directly used in the next step. The crude product was analyzed by ^{1}H-NMR (400 MHz in $CDCl_3$, δ ppm): 7.54-7.46 (m, 2H, aromatics); 7.46-7.39 (m, 3H, aromatics); 5.51 (s, 1H, CH); 0.25 (s, 3H, CH_3).

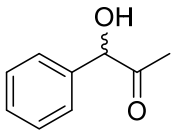

(ii) A solution of MeMgI (15.6 mmol, 3 M solution in ethyl ether) in dry Et_2O (26 mL) was placed in a 100 mL dry round-bottom flask that was equipped with a condenser and a dropping funnel. The apparatus was kept under nitrogen atmosphere. The crude protected mandelonitrile (1.6 g, 7.8 mmol), obtained in the previous step, was dissolved in dry Et_2O (10 mL) and added dropwise using a dropping funnel. The reaction mixture was stirred and refluxed for 24 h; then, it was cooled to room temperature, poured into ice containing concentrated H_2SO_4 (98%, 1.65 mL in 42 g ice) and stirred further at room temperature for 6.5 h. Afterwards, the layers were separated and the water phase was extracted with Et_2O (2 x 50 mL). The organic layers were combined, dried over $MgSO_4$ and concentrated under reduced pressure. The desired product was identified by GC-MS and purified by flash column chromatography on silica gel (hexane:EtOAc 8:2; $Rf_{product}$=0.4), affording 30% yield. The isolated product was analyzed by GC-MS (m/z 150), GC-FID and ^{1}H-NMR. The combination of these analytical data correlates with a mixture of ca. 90% *rac*-**4** and ca. 10% of 1-phenylpropane-1,2-dione (**7**).

^{1}H-NMR (400 MHz in $CDCl_3$; δ ppm): 7.42-7.27 (m, 5H aromatics); 4.32 (s, broad, 1H, OH); 5.08 (s, 1H, CH); 2.07 (s, 3H, CH_3).

Chemical synthesis of 1-phenylpropane-1,2-diol (diol 3) as a mixture of all four possible stereoisomers

In a round-bottom flask cooled on ice, $NaBH_4$ (13.5 mmol, 511 mg) was dissolved in MeOH (10 mL). Then, **7** (3.37 mmol, 500 mg) was added. The mixture was stirred at room temperature for 4 h. After completion of the reaction monitored by TLC analysis (PE/EtOAc 1:1; $Rf_{product}$ = 0.4), the solvent was removed under reduced pressure. The crude oil was washed with KPi buffer (50 mM, pH 4-5). The resulting aqueous layer was saturated with solid NaCl and extracted with MTBE (3 x 20 mL). The combined organic layers were dried over $MgSO_4$ and concentrated under reduced pressure. The product was isolated as a white solid (470 mg, 92%) and analyzed by GC-FID (>99% pure; HPLC (*dr*: 5:5:45:45 [RR:SS:RS:SR]),

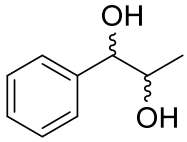

GC-MS (m/z 152) and ^{1}H-NMR (400 MHz in $CDCl_3$; only ppm (δ) of the main diastereomer reported): 7.38-7.34 (t, *J* = 4.2 Hz, 5H; CH aromatics); 4.7 (d, *J* = 4.3 Hz, 1H, CH); 4.07-3.99 (m, 1H, CH); 1.10 (d, *J* = 6.4 Hz, 3H, CH_3).

Chemical synthesis of 1R,2S-1-amino-1-phenylpropan-2-ol (1R,2S-9)

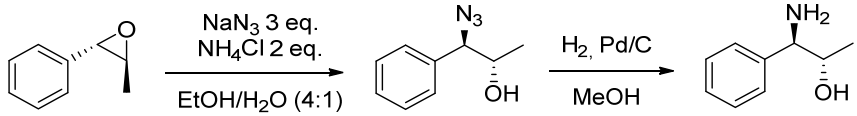

(2*S*,3*S*)-**2** (1*R*,2*S*)-**11** (1*R*,2*S*)-**9**

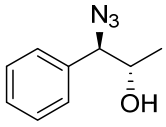

(i) Nucleophilic ring opening of (2*S*,3*S*)-2-methyl-3-phenyloxirane (2*S*,3*S*-**2**) by NaN_3 [61]: In a 50 mL two-neck round-bottom flask, the epoxide (2*S*,3*S*)-**2** (200 mg, 1.5 mmol) was dissolved in a mixture of EtOH/H_2O (4:1, 10 mL total volume) followed by addition of NaN_3 (290 mg, 4.5 mmol, 3 eq.) and NH_4Cl (160 mg, 3 mmol, 2 eq.). The reaction was heated up to 60 °C and stirred for 22 h. Upon completion, the organic compounds were extracted with MTBE (3 x 10 mL). The organic layers were combined, washed with H_2O (1 x 20 mL) and then with brine (1 x 20 mL), dried over $MgSO_4$ and concentrated under reduced pressure. The isolated product was obtained in 83% yield (ca. 220 mg) as a brown liquid and analyzed by GC-MS. The crude product was used in the next step without further purification (>99 purity by GC-MS analysis; m/z 177). $Rf_{(2S,3S\text{-}2)}$ = 0.8 (PE/EtOAc 1:1); $Rf_{(1R,2S\text{-}11)}$ = 0.7 (PE/EtOAc 1:1)

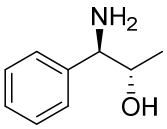

(ii) Chemical hydrogenation of (1*R*,2*S*)-1-azido-1-phenylpropan-2-ol (1*R*,2*S*-**11**)**:** In a 25 mL one-neck round bottom flask, Pd/C (10% wt., 15 mg) was added followed by MeOH (5 mL). Then (1*R,*2*S*)-**11** (110 mg, 0.564 mmol) was added as a solution in MeOH (3 mL). The flask was sealed with a septum and hydrogen atmosphere was supplied with a balloon. The reaction mixture was stirred at room temperature. No full conversion was achieved after 21 h and more catalyst was added (20% wt.). The reaction did not go to completion even after 48 h according to TLC analysis. After the workup, the product was isolated in pure form. The reaction mixture was filtered over a celite pad and concentrated under reduced pressure to yield a sticky clear yellow gel (52 mg, 61%, *de* >99%). The isolated product was analyzed by GC-MS (m/z 151) and ^{1}H-NMR (>95% purity). $Rf_{(1R,2S\text{-}11)}$ = 0.88 (DCM/MeOH 3:1); $Rf_{(1R,2S\text{-}9)}$ = 0.3 (DCM/MeOH 3:1). ^{1}H-NMR ($CDCl_3$, δ ppm, 400 MHz): 7.36-7.34 (m, 5H), 4.04-3.97 (m, 2H), 1.05 (d, *J* = 6.0 Hz, 3H).

Chemical synthesis of *1S,2R*-9

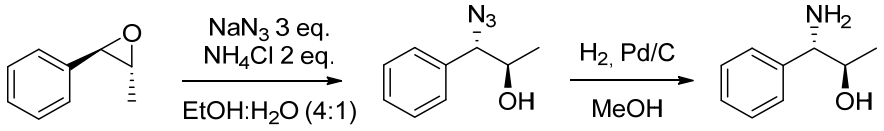

(2*R*,3*R*)-**2** (1*S*,2*R*)-**11** (1*S*,2*R*)-**9**

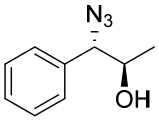

(i) Nucleophilic ring opening of (2*R*,3*R*)-**2** by NaN_3[61]: In a 50 mL two-neck round-bottom flask, the epoxide (2*R,*3*R*)-**2** (200 mg, 1.5 mmol) was dissolved in a mixture of EtOH/H_2O (4:1, 10 mL total volume) followed by addition of NaN_3 (290 mg, 4.5 mmol, 3 eq.) and NH_4Cl (160 mg, 3 mmol, 2 eq.). The reaction was heated up to 60 °C and stirred for 22 h. Upon completion, the organic compounds were extracted with MTBE (3 x 10 mL). The organic layers were combined, washed with H_2O (1 x 20 mL) and then with brine (1 x 20 mL), dried over $MgSO_4$ and concentrated under reduced pressure. The isolated product was obtained as a brown liquid (85%) and analyzed by GC-MS. The crude product was used in the next step without further purification (>97% purity). $Rf_{(2R,3R\text{-}\mathbf{2})}$ = 0.8 (PE/EtOAc 1:1); $Rf_{(1S,2R\text{-}\mathbf{11})}$ = 0.7 (PE/EtOAc 1:1)

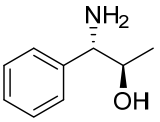

(ii) Chemical hydrogenation of (1*S*,2*R*)-**11:** In a 25 mL one-neck round bottom flask, Pd/C (35% wt., 50 mg) was added followed by MeOH (5 mL). Then, substrate (1*S,*2*R*)-**11** (140 mg, 0.790 mmol) was added as a solution in MeOH (3 mL). The flask was sealed with a septum and hydrogen atmosphere was supplied with a balloon. The reaction mixture was stirred at room temperature for 24 h, filtered over a celite pad and concentrated under reduced pressure to yield a sticky clear yellow gel (63 mg, 53%, *de* >99%). The isolated product was analyzed by GC-MS and ^{1}H-NMR. No further purification was required (>95% purity). $Rf_{(1S,2R\text{-}\mathbf{11})}$ = 0.9 (DCM/MeOH 3:1); $Rf_{(1S,2R\text{-}\mathbf{9})}$ = 0.22 (DCM/MeOH 3:1). ^{1}H-NMR ($CDCl_3$, δ ppm, 400 MHz): 7.37-7.27 (m, 5H), 3.99-3.94 (m, 2H), 1.05 (d, *J* = 6.1 Hz, 3H).

Chemical synthesis of *1S,2S*/*1R,2R*-9 as racemic mixture

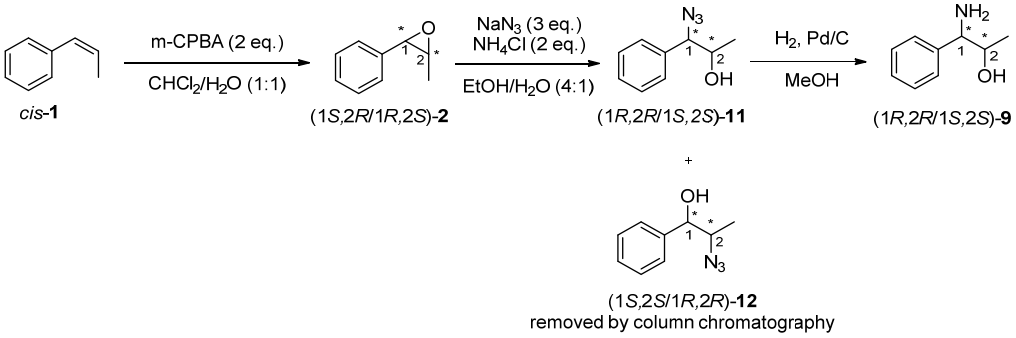

cis-**1** (1*S*,2*R*/1*R*,2*S*)-**2** (1*R*,2*R*/1*S*,2*S*)-**11** (1*R*,2*R*/1*S*,2*S*)-**9**

(1*S*,2*S*/1*R*,2*R*)-**12**
removed by column chromatography

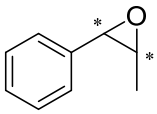

(i) Chemical epoxidation of *cis*-β-methylstyrene (*cis*-**1**)[13]: In a 25 mL round bottom flask, DCM (4 mL) and H_2O (4 mL) were added followed by substrate *cis*-**1** (150 mg, 1.27 mmol) and cooled down to 0 °C. Then *m*-CPBA (438 mg, 2.54 mmol, 2 eq.) was added in portions over 20 min and the reaction mixture was stirred for 18 h at room temperature. Upon completion, the mixture was quenched with a saturated solution of K_2CO_3 (5 mL) and the organic compounds extracted with MTBE (3 x 15 mL). The combined organic layers were washed with brine, dried over $MgSO_4$ and concentrated under reduced pressure to yield the desired epoxide product as a colorless liquid (97% yield, 168 mg). The isolated product was analyzed by GC-MS (m/z 134). No further purification was required (>98% purity). $Rf_{\textit{cis}\text{-}\mathbf{1}}$ = 0.75 (PE/EtOAc 1:1); $Rf_{(1S,2R/1R,2S\text{-}\mathbf{2})}$ = 0.45 (PE/EtOAc 1:1)

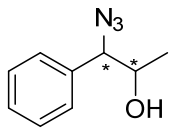

(ii) Nucleophilic ring opening of (1*S,*2*R*/1*R,*2*S*)-**2** by NaN_3 [61]: In a 25 mL two-neck round-bottom flask, the epoxide *1S,2R/1R,2S*-**2** (160 mg, 1.17 mmol) was dissolved in a mixture of EtOH/H_2O (4:1, 8 mL total volume) followed by addition of NaN_3 (229 mg, 3.5 mmol, 3 eq.) and NH_4Cl (126 mg, 2.34 mmol, 2 eq.). The reaction was heated up to 60 °C and stirred for 22 h. No full conversion was obtained even after further addition of NaN_3 and stirring for longer time. Therefore, the organic compounds were extracted with MTBE (3 x 15 mL). The organic layers were combined, washed with H_2O (1 x 20 mL) and then with brine (1 x 50 mL), dried over $MgSO_4$ and concentrated under reduced pressure. The crude product (169 mg) was isolated as a mixture of three compounds as confirmed by TLC and GC-MS analysis. The mixture was then purified by flash column chromatography (PE/EtOAc 5:1) to yield (1*S,*2*S/*1*R,*2*R)*-**11** as a brown liquid (53.6 mg) and (1*S,*2*S/*1*R,*2*R*)-2-azido-1-phenylpropan-1-ol (1*S,*2*S/*1*R,*2*R*-**12**) as a dark yellow liquid (49.8 mg). The two azido alcohol isomers were analyzed by GC-MS and confirmed by ^{1}H-NMR. $Rf_{\mathbf{2}}$ = 0.55 (PE/EtOAc 5:1); $Rf_{(1S,2S/1R,2R\text{-}\mathbf{11})}$ = 0.2 (PE/EtOAc 5:1); $Rf_{(1S,2S/1R,2R\text{-}\mathbf{12})}$ = 0.4 (PE/EtOAc 5:1). ^{1}H-NMR (1*S,*2*S/*1*R,*2*R*)-**11** ($CDCl_3$, δ ppm, 400 MHz): 7.43-7.35 (m, 3H, CH aromatics), 7.32-7.30 (m, 2H, CH aromatics), 4.31 (d, *J* = 8.0 Hz, 1H, CH), 3.89 (p, *J* = 6.4 Hz, 1H, CH), 2.39 (broad, 1H, OH), 1.04 (d, *J* = 6.3 Hz, 3H, CH_3).

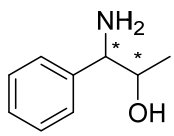

(iii) Chemical hydrogenation of (1*S,*2*S*/1*R,*2*R*)-**11:** In a 25 mL one-neck round bottom flask, Pd/C (30% wt., 16 mg) was added followed by MeOH (2.5 mL). Then (1*S,*2*S/*1*R,*2*R*)-**11** (54 mg, 0.305 mmol) was added as a solution in MeOH (1 mL). The flask was sealed with a septum and hydrogen atmosphere was supplied with a balloon. The reaction mixture was stirred at room temperature for 24 h, then filtered over a celite pad and concentrated under reduced pressure to yield an off-white solid (45.6 mg, 99.6%, de >98%). The isolated product was analyzed by GC-MS (m/z 151) and ^{1}H-NMR. No further purification was required (>95% purity). $Rf_{(1S,2S/1R,2R\text{-}\mathbf{11})}$ = 0.89 (DCM/MeOH 3:1); $Rf_{(1S,2S/1R,2R\text{-}\mathbf{9})}$ = 0.22 (DCM/MeOH 3:1). ^{1}H-

NMR 1S,2S/1R,2R-**9** ($CDCl_3$, δ ppm, 400 MHz): 7.36-7.28 (m, 5H, CH aromatics), 3.94-3.87 (m, 1H, CH), 3.78 (d, *J* = 8.8 Hz, 1H, CH), 1.02 (d, *J* = 6.1 Hz, 3H, CH_3).

Chemical synthesis of 2-amino-1-phenyl-1-propanol (1*S*,2*S*-5 and 1*R*,2*R*-5) as a racemic mixture

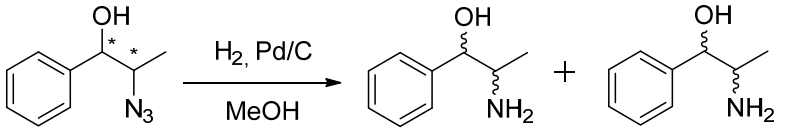

(1*S*,2*S*/1*R*,2*R*)-**12** (1*S*,2*S*/1*R*,2*R*)-**5** (1*S*,2*R*/1*R*,2*S*)-**5**

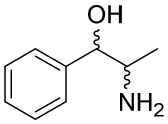

(i) Chemical hydrogenation of (1*S*,2*S*/1*R*,2*R*)-**12**: In a 25 mL one-neck round bottom flask, Pd/C (30% wt., 15 mg) was added followed by MeOH (2 mL). Then (1*S,*2*S*/1*R,*2*R*)-**12** (50 mg, 0.282 mmol) was added as a solution in MeOH (1 mL). The flask was sealed with a septum and hydrogen atmosphere was supplied with a balloon. The reaction mixture was stirred at room temperature for 24 h, then filtered over a celite pad and concentrated under vacuum to yield an off-white solid (24.7 mg, 58%, de >51%). The isolated product was analyzed by GC-MS (m/z 151). No further purification was required (>95% purity). $Rf_{(1S,2S/1R,2R\text{-}\mathbf{12})}$ = 0.64 (DCM/MeOH 3:1); $Rf_{\mathbf{5}}$ = 0.18 (DCM/MeOH 3:1).

^{1}H-NMR (1*S,*2*S*/1*R,*2*R*)-**12** ($CDCl_3$, δ ppm, 400 MHz): 7.40-7.31 (m, 5H, CH aromatics), 4.48 (d, *J* = 7.4 Hz, 1H, CH), 3.68 (p, *J* = 6.7 Hz, 1H, CH), 2.47 (broad, 1H, OH), 1.13 (d, *J* = 6.7 Hz, 3H).

^{1}H-NMR (1*S,*2*S*/1*R,*2*R*)-**5** ($CDCl_3$, δ ppm, 400 MHz): 7.33-7.32 (m, 5H, aromatics), 4.97 (broad, 1H, OH), 4.31 (d, *J* = 6.6 Hz, 1H, CH), 3.12-3.07 (m, 1H, CH), 2.06 (broad, 2H, NH_2), 1.04 (d, *J* = 6.2 Hz, 3H, CH_3).

3.4.6 One pot hydrogen-borrowing amination of enantiopure or enantioenriched diols 3

This section describes the screened conditions for the optimization of the hydrogen-borrowing-cascade for the amination of enantiomerically pure or enantiomerically enriched substrates **3**.

General experimental procedure for the biocatalytic hydrogen-borrowing amination

In an Eppendorf tube (1.5 mL), $HCOONH_4$ buffer (0.5 mL, pH 8.5, 1 M) and NAD^+ (1 mM) were added followed by purified ADH (varied concentrations) and AmDH (varied concentrations). Enantiomerically pure or enantioenriched diol **3** (5 to 30 mM) was added as last. The mixture was incubated at 30 °C (otherwise stated), 170 rpm for 48 h on an orbital shaker and, after that, quenched with 10 M KOH (100 µL). The aqueous layer was saturated with solid NaCl and the organic compounds extracted with MTBE (1 x 500 µL). The organic

layer was dried over $MgSO_4$ and analyzed by GC-FID and/or GC-MS to determine the conversion, while diastereomeric and enantiomeric excesses were analyzed by HPLC after derivatization with a chiral reagent (GITC) as reported below. All experiments were performed in duplicate and the results reported are the average of two samples.

Derivatization of the amino alcohols with GITC to determine the *er and dr* by RP-HPLC[62]

The aqueous reaction mixture (20 µL) was dissolved in acetonitrile (180 µL) to yield a final concentration of 0.5 mM. Then, GITC (2,3,4,6-Tetra-O-acetyl-β-D-glucopyranosyl isothiocyanate) (1.5 mM) and Et_3N (1.5 mM) were added as a solution in acetonitrile (200 µL). The mixture was incubated at room temperature at 1000 rpm for 35 min. Before injection into the RP-HPLC, the samples were centrifuged and filtered if required.

3.4.7 Time study for the one pot hydrogen-borrowing amination of (1*S*,2*S*)-3 under optimized conditions

A time study for the amination of (1*S*,2*S*)-**3** (20 mM) with the optimized conditions determined before was performed: Aa-ADH (70 µM) in combination with Ch1-AmDH (35 µM) in $HCOONH_4$ buffer (pH 8.5, 1 M, 0.5 mL) and in the presence of NAD^+ (1 mM). The reactions were stopped at different time points (1, 3, 5, 7, 16, 20, 24, 30, 42 and 48 h).

Table 3.21. Time study for the one pot hydrogen-borrowing amination of (1*S*,2*S*)-**3** (20 mM) by combining Aa-ADH (70 µM) and Ch1-AmDH (35 µM) in $HCOONH_4$ buffer (pH 8.5, 1 M, 0.5 mL)

Time [h]	Conversion [%][a]	(1*S*,2*R*)-5 [%][a]	8 [%][a][b]	Unidentified [%][a][b]
1	2	1	<1	<1
3	7	7	<1	<1
5	16	15	<1	<1
7	23	22	1	<1
16	62	60	2	<1
20	75	72	2	<1
24	87	84	2	1
30	88	85	2	<1
42	>99	97	2	<1
48	>99	98	2	<1

[a] Determined by GC-FID analysis; [b] This may come, at least in part, from decomposition of the amino alcohols product (also present in the reference compound purchased by Sigma Aldrich upon injection in GC-MS or GC-FID).

3.4.8 One pot biocatalytic hydrogen-borrowing amination of enantiomerically pure or enantiomerically enriched diols 3 in semi-preparative scale (100 mg)

Reaction conditions for the preparative scale biocatalytic hydrogen-borrowing amination of (1*R*,2*R*)-3 to yield (1*R*,2*R*)-5: To a 100 mL Erlenmeyer flask, $HCOONH_4$ buffer (33 mL final volume, pH 8.5, 1 M), (1*R,*2*R*)-**3** (20 mM, 105 mg, 0.690 mmol), Ls-ADH (24 µM), Ch1-AmDH (60 µM) and NAD^+ (1 mM) were added. The mixture was incubated at 30 °C and 170 rpm on an orbital shaker for 48 h. The reaction was quenched with KOH (4 mL, 10 M). The aqueous layers were saturated with solid NaCl and the extraction was performed with MTBE (3 x 20 mL). The organic layers were then dried over $MgSO_4$ and concentrated under reduced pressure.

Reaction conditions for the preparative scale biocatalytic hydrogen-borrowing amination of (1*S*,2*R*)-3 to yield (1*S*,2*R*)-5: To a 100 mL Erlenmeyer flask, $HCOONH_4$ buffer (44 mL final volume, pH 8.5, 1 M), 1*S,*2*R*-**3** (15 mM, 102 mg, 0.670 mmol), Bs-BDHA (50 µM), Ch1-AmDH (50 µM) and NAD^+ (1 mM) were added. The mixture was incubated at 30 °C and 170 rpm on an orbital shaker for 48 h. The reaction was quenched with KOH (5 mL, 10 M), the aqueous layers were saturated with solid NaCl and the extraction was performed with MTBE (4 x 20 mL). The organic layers were then dried over $MgSO_4$ and concentrated under reduced pressure.

3.4.9 Analytical methods

Determination of the conversion by GC-FID

Note: *For the analysis of the outcome of the biocatalytic hydrogen-borrowing cascade, various analytical techniques were used. The formation of the targeted optically active amino alcohols* ***5*** *was initially investigated by using GC-FID. However, under certain conditions, both diol substrate and amino alcohol products tend to partly decompose at elevated temperature during GC injection, thus resulting in possible formation of benzaldehyde. Nevertheless, we could exclude any chemical formation of benzaldehyde during the reaction as benzaldehyde was never observed when the samples were analyzed by normal-phase HPLC analysis. Finally, reverse-phase HPLC (C18 column) was used for the determination of the enantiomeric as well as diastereomeric ratio. In order to do so, the amino alcohol products were derivatized with a chiral reagent (GITC) and compared with the chemically synthesized references.*

Method A: Column: Agilent J&W DB1701 (30 m, 250 µm, 0.25 µm). Carrier gas: H_2; Parameter: T injector 250 °C; constant pressure 6.9 psi; temperature program: 80 °C, hold 6.5 min; gradient 10 °C min^{-1} up to 160 °C, hold 5 min; gradient 20 °C min^{-1} up to 200 °C, hold 2 min; gradient 20 °C min^{-1} up to 280 °C, hold 1 min.

Method B: Column: Agilent J&W DB1701 (30 m, 250 µm, 0.25 µm). Carrier gas: H_2; Parameter: T injector 250 °C; constant pressure 6.9 psi; temperature program: 80 °C, hold 6.5 min; gradient 5 °C min^{-1} up to 160 °C, hold 5 min; gradient 20 °C min^{-1} up to 200 °C, hold 2 min; gradient 20 °C min^{-1} up to 280 °C, hold 4 min.

Table 3.22. Retention times [min] for the compound analyzed by GC-FID

Compound	[min]	Method	Compound	[min]	Method	Compound	[min]	Method
 *cis*-**1**	6.8	A	 *trans*-**1**	8.1	A	 (1*S*,2*R*)-**2**	10.8	A
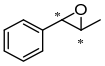 (1*S*,2*S*)-**2**	11.4	A	 (1*S*,2*R*)-**3**	18.9 23.8	A B	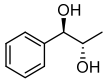 (1*R*,2*S*)-**3**	18.9 23.8	A B
 (1*S*,2*S*)-**3**	18.7 23.6	A B	 (1*R*,2*R*)-**3**	18.7 23.6	A B	**3** Mixture of all possible four isomers	Two pairs of enantiomers [SS/RR:SR/RS] 18.7:18.9	A
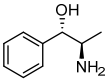 (1*S*,2*R*)-**5**	17.4 21.1	A B	 (1*R*,2*S*)-**5**	17.4 21.1	A B	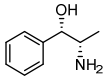 (1*S*,2*S*)-**5**	17.3 20.9	A B
 (1*R*,2*R*)-**5**	17.3 20.9	A B	 **4**	15.6 19.2	A B	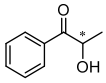 **4'**	15.8 19.4	A B
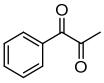 **7**	13.6 16.6	A B	 **8**	16.8 19.9	A B	 **10**	8.3 8.5	A B

General GC-MS method

Method C: Column Agilent DB-1701 (30 m, 250 µm, 0.25 µm); injector temperature 250 °C; constant pressure 71.8 kPa; temperature program: 80 °C/hold 6.5 min; 160 °C/rate 10 °C min^{-1}/hold 5 min; 200 °C/rate 20 °C min^{-1}/hold 2 min; 280 °C/rate 20 °C min^{-1}/hold 1 min.

Method for the determination of the enantiomeric excess and diastereomeric excess by HPLC

Method D: Column Chiralcel-OD (0.46 cm x 25 cm); HPLC program: constant oven temperature 10 °C; constant pressure 14 bar; eluent composition: Hexane:Isopropanol 97:3, 1 mL/min, detection at 210 nm.

Method E: Column: Nucleosil C_{18} HD (0.46 cm x 25 cm); HPLC program: constant oven temperature 30 °C; eluent composition: isocratic MeOH + 0.1% TFA/MilliQ + 0.1% TFA 50:50; flow rate: 1 mL min^{-1}, detection at 248 nm.

Table 3.23. Retention times for compounds analyzed by HPLC

Compound	[min]	Method	Compound	[min]	Method
3 Mixture of all possible four isomers	**4 peaks** 33.4/33.7 35.3/35.6 39.1/43.1 41.1/45.4	D	 (1*S*,2*R*)-**3**	39.1/43.1	D
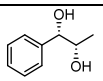 (1*S*,2*S*)-**3**	35.3/35.6	D	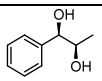 (1*R*,2*R*)-**3**	33.4/33.7	D
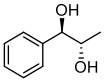 (1*R*,2*S*)-**3**	41.1/45.4	D	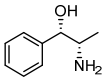 (1*S*,2*S*)-**5**	18.6[a]	E
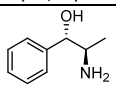 (1*S*,2*R*)-**5**	38.1[a]	E	 (1*R*,2*S*)-**5**	26.7[a]	E
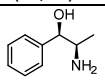 (1*R*,2*R*)-**5**	20.7[a]	E			

[a] after derivatization with GITC.

3.5 References

1. M. Breuer, K. Ditrich, T. Habicher, B. Hauer, M. Kesseler, R. Sturmer and T. Zelinski, *Angew. Chem. Int. Ed.*, 2004, 43, 788-824.
2. S. C. Bergmeier, *Tetrahedron*, 2000, 56, 2561-2576.
3. T. Sehl, Z. Maugeri and D. Rother, *J. Mol. Catal. B: Enzym.*, 2015, 114, 65-71.
4. P. Gupta and N. Mahajan, *New J. Chem.*, 2018, 42, 12296-12327.
5. J. Vicario, D. Badia, L. Carrillo, E. Reyes and J. Etxebarria, *Curr. Org. Chem.*, 2005, 9, 219-235.
6. K. Everaere, A. Mortreux and J.-F. Carpentier, *Adv. Synth. Catal.*, 2003, 345, 67-77.
7. D. J. Ager, I. Prakash and D. R. Schaad, *Chem. Rev.*, 1996, 96, 835-876.
8. R. Krizevski, N. Dudai, E. Bar and E. Lewinsohn, *J. Ethnopharmacol.*, 2007, 114, 432-438.
9. G. Grue-Soerensen and I. D. Spenser, *JACS*, 1994, 116, 6195-6200.
10. H. K. Lee, S. Kang and E. B. Choi, *J. Org. Chem.*, 2012, 77, 5454-5460.
11. T. Sehl, H. C. Hailes, J. M. Ward, R. Wardenga, E. von Lieres, H. Offermann, R. Westphal, M. Pohl and D. Rother, *Angew. Chem. Int. Ed.*, 2013, 52, 6772-6775.
12. J. A. Groeper, S. R. Hitchcock and G. M. Ferrence, *Tetrahedron: Asymmetry*, 2006, 17, 2884-2889.
13. G. Sello, F. Orsini, S. Bernasconi and P. D. Gennaro, *Tetrahedron: Asymmetry*, 2006, 17, 372-376.
14. J. H. Schrittwieser, F. Coccia, S. Kara, B. Grischek, W. Kroutil, N. d'Alessandro and F. Hollmann, *Green Chem.*, 2013, 15, 3318-3331.
15. R. A. Sheldon, *Green Chem.*, 2017, 19, 18-43.
16. R. A. Sheldon, *ACS Sustain. Chem. Eng.*, 2017, 6, 32-48.

17. S. Minakata, M. Nishimura, T. Takahashi, Y. Oderaotoshi and M. Komatsu, *Tetrahedron Lett.*, 2001, 42, 9019-9022.
18. D. J. Kim and B. T. Cho, *Bull. Korean Chem. Soc.*, 2003, 24, 1641-1648.
19. L. Legnani and B. Morandi, *Angew. Chem. Int. Ed.*, 2016, 55, 2248-2251.
20. H. C. Erythropel, J. B. Zimmerman, T. M. de Winter, L. Petitjean, F. Melnikov, C. H. Lam, A. W. Lounsbury, K. E. Mellor, N. Z. Janković, Q. Tu, L. N. Pincus, M. M. Falinski, W. Shi, P. Coish, D. L. Plata and P. T. Anastas, *Green Chem.*, 2018, 20, 1929-1961.
21. F. Effenberger, B. Hörsch, S. Förster and T. Ziegler, *Tetrahedron Lett.*, 1990, 31, 1249-1252.
22. F. Effenberger, B. Gutterer and T. Ziegler, *Liebigs Ann. Chem.*, 1991, 1991, 269-273.
23. O. C. Kreutz, P. J. S. Moran and J. A. R. Rodrigues, *Tetrahedron: Asymmetry*, 1997, 8, 2649-2653.
24. P. J. S. Moran, J. A. R. Rodrigues, I. Joekes, E. C. S. Brenelli and R. A. Leite, *Biocatalysis*, 2009, 9, 321-328.
25. S. Wu, Y. Zhou and Z. Li, *Chem. Commun.*, 2019, 55, 883-896.
26. S. Wu, Y. Zhou, T. Wang, H. P. Too, D. I. Wang and Z. Li, *Nat. Commun.*, 2016, 7, 11917.
27. Z. B. Sun, Z. J. Zhang, F. L. Li, Y. Nie, H. L. Yu and J. H. Xu, *ChemCatChem*, 2019, 11, 3802-3807.
28. T. Sehl, H. C. Hailes, J. M. Ward, U. Menyes, M. Pohl and D. Rother, *Green Chem.*, 2014, 16, 3341-3348.
29. X. Wu, M. Fei, Y. Chen, Z. Wang and Y. Chen, *Appl. Microbiol. Biotechnol.*, 2014, 98, 7399-7408.
30. I. Cho, C. K. Prier, Z. J. Jia, R. K. Zhang, T. Gorbe and F. H. Arnold, *Angew. Chem. Int. Ed.*, 2019, 58, 3138-3142.
31. F. G. Mutti, T. Knaus, N. S. Scrutton, M. Breuer and N. J. Turner, *Science*, 2015, 349, 1525-1529.
32. F.-F. Chen, Y.-Y. Liu, G.-W. Zheng and J.-H. Xu, *ChemCatChem*, 2015, 7, 3838-3841.
33. W. Böhmer, T. Knaus and F. G. Mutti, *ChemCatChem*, 2018, 10, 731-735.
34. M. P. Thompson and N. J. Turner, *ChemCatChem*, 2017, 9, 3833-3836.
35. S. L. Montgomery, J. Mangas-Sanchez, M. P. Thompson, G. A. Aleku, B. Dominguez and N. J. Turner, *Angew. Chem. Int. Ed.*, 2017, 56, 10491-10494.
36. M. L. Corrado, T. Knaus and F. G. Mutti, *ChemBioChem*, 2018, 19, 679-686.
37. S. Wu, Y. Chen, Y. Xu, A. Li, Q. Xu, A. Glieder and Z. Li, *ACS Catal.*, 2014, 4, 409-420.
38. H. W. Hoffken, M. Duong, T. Friedrich, M. Breuer, B. Hauer, R. Reinhardt, R. Rabus and J. Heider, *Biochemistry*, 2006, 45, 82-93.
39. N. H. Schlieben, K. Niefind, J. Muller, B. Riebel, W. Hummel and D. Schomburg, *J. Mol. Biol.*, 2005, 349, 801-813.
40. K. Niefind, J. Muller, B. Riebel, W. Hummel and D. Schomburg, *J. Mol. Biol.*, 2003, 327, 317-328.
41. I. Lavandera, A. Kern, V. Resch, B. Ferreira-Silva, A. Glieder, W. M. Fabian, S. de Wildeman and W. Kroutil, *Org. Lett.*, 2008, 10, 2155-2158.
42. I. Lavandera, A. Kern, M. Schaffenberger, J. Gross, A. Glieder, S. de Wildeman and W. Kroutil, *ChemSusChem*, 2008, 1, 431-436.
43. J. Zhang, T. Xu and Z. Li, *Adv. Synth. Catal.*, 2013, 355, 3147-3153.
44. K. Inoue, Y. Makino and N. Itoh, *Appl. Environ. Microbiol.*, 2005, 71, 3633-3641.
45. T. Knaus, L. Cariati, M. F. Masman and F. G. Mutti, *Org. Biomol. Chem.*, 2017, 15, 8313-8325.
46. I. Lavandera, A. Kern, B. Ferreira-Silva, A. Glieder, S. de Wildeman and W. Kroutil, *J. Org. Chem.*, 2008, 73, 6003-6005.
47. J. Matsumoto, M. Higuchi, M. Shimada, Y. Yamamoto and Y. Kamio, *Biosci. Biotechnol. Biochem.*, 1996, 60, 39-43.
48. A. Morokutti, A. Lyskowski, S. Sollner, E. Pointner, T. B. Fitzpatrick, C. Kratky, K. Gruber and P. Macheroux, *Biochemistry*, 2005, 44, 13724-13733.

49. B. R. Bommarius, M. Schurmann and A. S. Bommarius, *Chem. Commun.*, 2014, 50, 14953-14955.
50. L. J. Ye, H. H. Toh, Y. Yang, J. P. Adams, R. Snajdrova and Z. Li, *ACS Catal.*, 2015, 5, 1119-1122.
51. M. J. Abrahamson, J. W. Wong and A. S. Bommarius, *Adv. Synth. Catal.*, 2013, 355, 1780-1786.
52. J. H. Schrittwieser, S. Velikogne, M. Hall and W. Kroutil, *Chem. Rev.*, 2018, 118, 270-348.
53. R. A. Sheldon and J. M. Woodley, *Chem. Rev.*, 2018, 118, 801-838.
54. R. A. Sheldon and D. Brady, *ChemSusChem*, 2019, 12, 2859-2881.
55. T. Knaus and F. G. Mutti, *Chim. Oggi-Chem. Today*, 2017, 35, 34-37.
56. T. Knaus, W. Böhmer and F. G. Mutti, *Green Chem.*, 2017, 19, 453-463.
57. T. Knaus, V. Tseliou, L. D. Humphreys, N. S. Scrutton and F. G. Mutti, *Green Chem.*, 2018, 20, 3931-3943.
58. B. He, Y. Li, X. M. Feng and G. L. Zhang, *Synlett*, 2004, 1776-1778.
59. E. C. R. J. Brussee, and A. van der Gen *Tetrahedron Lett.*, 1988, 4485-4488.
60. E. Toukoniitty, P. Mäki-Arvela, M. Kuzma, A. Villela, A. K. Neyestanaki, T. Salmi, R. Sjöholm, R. Leino, E. Laine and D. Y. Murzin, *J. Catal.*, 2001, 204, 281-291.
61. Y. Kim, H. K. Pak, Y. H. Rhee and J. Park, *Chem. Commun.*, 2016, 52, 6549-6552.
62. M. S. Malik, E.-S. Park and J.-S. Shin, *Green Chem.*, 2012, 14, 2137.

Chapter 4

One-pot cascade for the synthesis of chiral phenylpropanolamines by pairing alcohol dehydrogenases with stereocomplementary ω-transaminases

This chapter is partially based on the following publications:

Maria L. Corrado, Tanja Knaus and Francesco G. Mutti, Regio- and stereoselective multi-enzymatic aminohydroxylation of β-methylstyrene using dioxygen, ammonia and formate, *Green Chemistry,* **2019,** 21(23), 6246-6251
Supporting information is available under doi: 10.1039/C9GC03161H

Maria L. Corrado, Tanja Knaus, Wesley Böhmer and Francesco G. Mutti, One-pot cascade for the synthesis of chiral phenylpropanolamines by pairing alcohol dehydrogenases with stereocomplementary ω-transaminases, *manuscript in preparation*.

Abstract. *In this chapter, we present an enzymatic one-pot cascade for the biocatalytic conversion of chiral 1-phenylpropane-1,2-diol to chiral phenylpropanolamine and its isomers by combining selected alcohol dehydrogenases with six stereocomplementary ω-transaminases. The aim of this work is to exploit the potential of these classes of enzymes for accessing* (1*S,2S*) *and* (1*R,2S*)*-2-amino-1-phenylpropan-1-ol in a one-pot fashion, hence complementing the work described in the previous chapter regarding the formal regio- and stereoselective aminohydroxylation of β-methylstyrene to yield either* (1*R,2R*)- *or* (1*S,2R*)- *2-amino-1-phenylpropan-1-ol. Thus, both* (1*S,2S*) *and* (1*R,2S*)*-2-amino-1-phenylpropan-1-ol were obtained with moderate to high analytical yields (76-88%) as well as high optical purity (er and dr >99.5:<0.5). Furthermore, depending on the choice of diol substrate, alcohol dehydrogenase and ω-transaminase, the* (1*S,2R*)*-1-amino-1-phenylpropan-2-ol isomer could also be obtained via this route in moderate analytical yield (58-61%) and high optical purity (er and dr >99.5:<0.5). Nevertheless, in this last case the regioisomer* (1*R,2R*)*-2-amino-1-phenylpropan-1-ol was also formed. However, the* (1*S,2R*)*-1-amino-1-phenylpropan-2-ol was the preferred product (rr 91:9).*

4.1 Introduction

As was discussed in the previous chapter and reported in literature, phenylpropanolamine (PPA) moieties are found in a plethora of pharmaceutical active ingredients.[1-7] Also they are applied directly either as biological active compounds or as auxiliaries and ligands in asymmetric organic synthesis[8,9] We have previously demonstrated the potential of the biocatalytic HB-bioamination cascade[10] for the chemo-, regio- and stereoselective synthesis of this high-value class of compounds from chiral diols. Nevertheless, due to the current scarcity of *S*-selective AmDHs, only two out of the four isomers of nor(pseudo)ephedrine could be obtained.[2] In order to apply the HB-bioamination of diols for the synthesis of phenylpropanolamines, we designed another one-pot biocatalytic cascade, in which the secondary NAD^+-dependent ADHs are combined with stereocomplementary aminotransferases. This class of enzymes, also named as transaminases, catalyze the transfer of an amino group from an amine donor such as alanine to a keto-moiety acceptor via the action of pyridoxal phosphate cofactor (PLP). Transaminases have been studied for a long time and mainly for the asymmetric synthesis of α-chiral amines.[11-14] Compared with AmDHs as well as other aminating enzymes such as IREDs or RedAms, the use of TAs requires PLP coenzyme for the effective amination to occur, a (supra)-stoichiometric amount of amino donor (usually alanine) is needed in order to shift the reaction equilibrium towards the product. Moreover, the by-product originated from the amino donor is often a suitable substrate for the TA itself or it may inhibit the reaction as well. Much research has been carried out on transaminases, thereby creating variants capable of accepting different amino donor (e.g., isopropylamine)[15-17] as well as optimizing efficient internal recycling system, which are able to selectively react with the byproduct and, for instance, convert it back to the amino donor (e.g., alanine dehydrogenase-catalyzed recycling).[18,19] As mentioned in our previous work,[2] only few enzymatic strategies are described in the literature for the synthesis of nor(pseudo)ephedrine (NE and NPE). Notably, in all of them the amination step is performed by transaminases (**Figure 4.1**).[1,20-22] Nevertheless, both strategies start from either the cheap and readily available benzaldehyde (**Figure 4.1A**) or from carbonyl-containing compounds (**Figure 4.1B**).

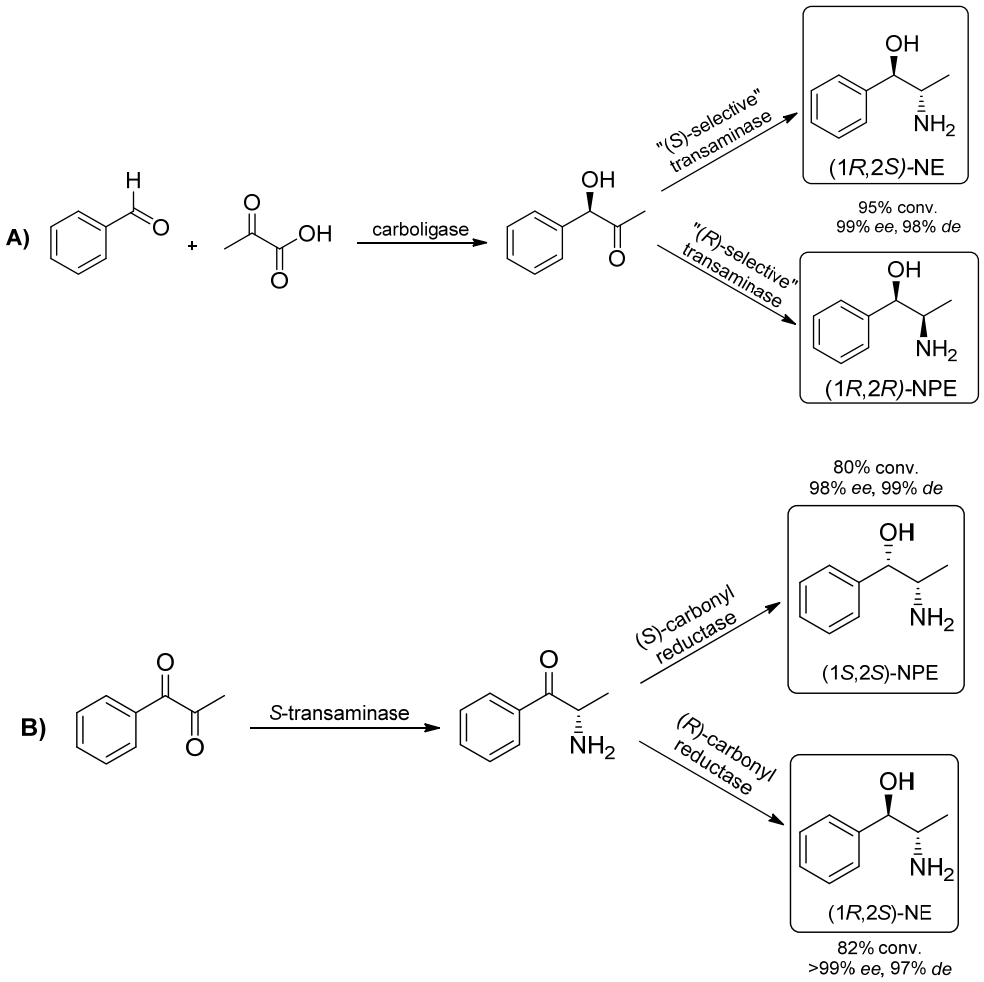

Figure 4.1. Selected literature examples for the enzymatic synthesis of phenylpropanolamine[1, 20, 21]

In this work, a selection of six stereocomplementary ω-transaminases (ωTAs), namely At(*R*)-ωTA from *Aspergillus terreus,*[23,24] As(*R*)-ωTA from *Arthrobacter* sp.,[25] Ac(*S*)-ωTA from *Arthrobacter citreus,*[12] Cv(*S*)-ωTA from *Chromobacterium violaceum* (DSM 30191),[26] Bm(*S*)-ωTA from *Bacillus megaterium* SC6394,[12, 27] Vf(*S*)-ωTA from *Vibrio fluvialis,*[11, 28] was paired with one of the following NAD^+-dependent ADHs: Aa-ADH from *Aromatoleum aromaticum,*[29] Bs-BDHA from *Bacillus subtilis* BGSC1A1,[30, 31] or Ls-ADH from *Leifsonia* sp.[32] in order to complement the previously reported HB-bioamination of chiral diols **3**.[2] Thus, we investigated the potential of this one-pot cascade (ADH/TAs) for synthesizing (1*S*,2S)-**5** and (1*R*,2*S*)-**5**, as well as the other four possible PPAs structural isomers in which the amino group is adjacent to the phenyl ring (**5'**). **Scheme 4.1** depicts the general pathway design of

the one-pot cascade. Similarly to the case of the HB-bioamination cascade, the NAD^+ coenzyme and the pyruvate by-product are internally recycled by the combined action of an alcohol dehydrogenase (ADH) and an alanine dehydrogenase from *Bacillus sphaericus* (Bs-AlaDH).[33] The latter enzyme requires ammonia/ammonium species, constituting the reaction buffer, and NADH to convert pyruvate back to alanine that is the ultimate amino donor. Furthermore, as for the HB-bioamination cascade, the chiral diol substrates were enzymatically synthesized using the one-pot biphasic cascade, whereby a fused-styrene monooxygenase (Fus-SMO) was combined with one of two available stereocomplementary epoxide hydrolases (EHs) thereby yielding all of the four diol isomers, as previously described.[2,34]

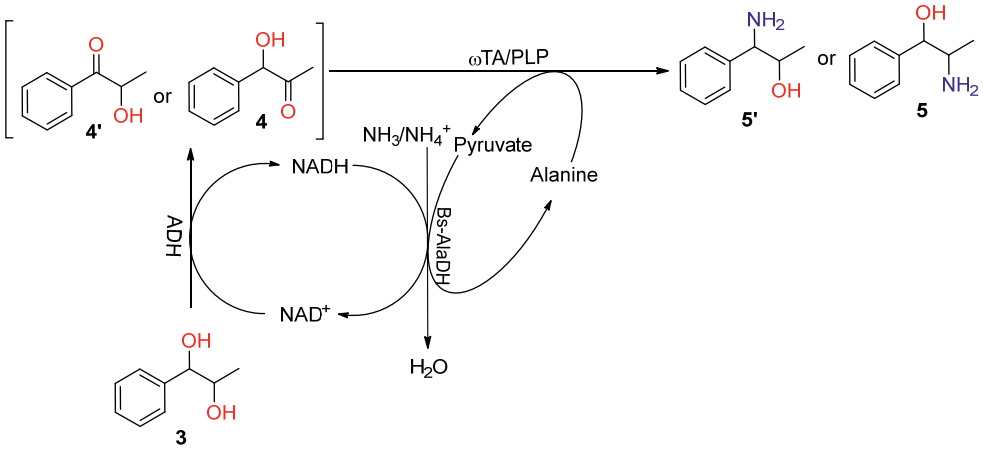

Scheme 4.1. One-pot biocatalytic network for the synthesis of chiral PPAs from diol by pairing ADHs with stereocomplementary ωTAs

Hence, we have developed a one-pot enzymatic network for the synthesis of (1*S*,2*S*)-**5** and (1*R*,2*S*)-**5** in moderately high analytical yields (76-88%) as well as optical purity (enantiomeric ratio, *er* and diastereomeric ratio, *dr* >99.5:<0.5). Furthermore, depending on the chosen diol substrate, ADH and ωTA, the other two isomers (1*R*,2*R*)-**5** and (1*S*,2*R*)-**5** can also be accessed. Moreover, the (1*S*,2*R*)-**5'** isomer could also be obtained via this route in moderate analytical yield (58-61%) and high optical purity (*er* and *dr* >99.5:<0.5) while (1*R*,2*R*)-**3** was used as substrate for the one-pot cascade catalyzed by Aa-ADH and either At(*R*)-ωTA or As(*R*)-ωTA. Despite the regioisomer (1*R*,2*R*)-**5** was formed as well, amino alcohol **5'** was the preferred product (regioisomeric ratio, *rr* 91:9 **[5':5]**). Examples of the calculations used to determine the *er*, *dr* and *rr* are reported in section 4.4.3.

4.2 Results and discussion

4.2.1 Enzymatic synthesis of optically active diols and ADHs selection

Chiral substrates **3** were enzymatically synthesized as reported previously,[2] and **Scheme 4.2** depicts the overall cascade. The one-pot cascade comprises the conversion of the prochiral substrate **1** to epoxide **2** catalyzed by our fused styrene monooxygenase co-expressed with a formate dehydrogenase (Fus-SMO/CbFDH)[34] followed by the hydrolysis catalyzed by an epoxide hydrolase (either Sp(*S*)-EH from *Sphingomonas* sp. HXN200 or stereocomplementary St(*R*)-EH from *Solanum tuberosum).*[35] Thus, all of the four optically active isomers of product **3** could be obtained in high isolated yields and optical purities.

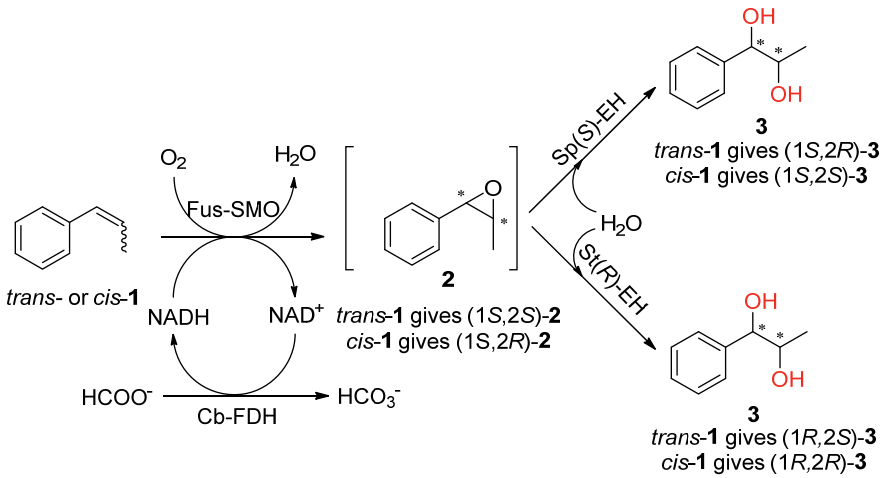

Scheme 4.2. One-pot enzymatic cascade for the synthesis of chiral substrate **3** catalyzed by Fus-SMO/Cb-FDH system paired with two stereocomplementary EHs.

The selection of the ADHs for the bio-oxidation of substrate **3** was performed as reported in chapter 3 and elsewhere.[2] Therefore, we tested the same secondary NAD^+-dependent ADHs for this study. In more details, we used Aa-ADH from *Aromatoleum aromaticum*[29] on substrate (1*S*,2*S*)-**3**, (1*R*,2*S*)-**3** and (1*R*,2*R*)-**3**; Ls-ADH from *Leifsonia* sp.[32] on substrate (1*R*,2*R*)-**3** and Bs-BDHA from *Bacillus subtilis* BGSC1A1[30, 31] on substrate (1*S*,2*R*)-**3**. In general, we have used the optimized conditions (substrate vs. enzymes loading) applied for the HB-bioamination cascade descried previously in chapter 3.[2] **Table 4.1** provides an overview of the ADHs screening.

Table 4.1. Bio-oxidation [%] of diol **3** (20 mM) by NAD^+-dependent ADHs.

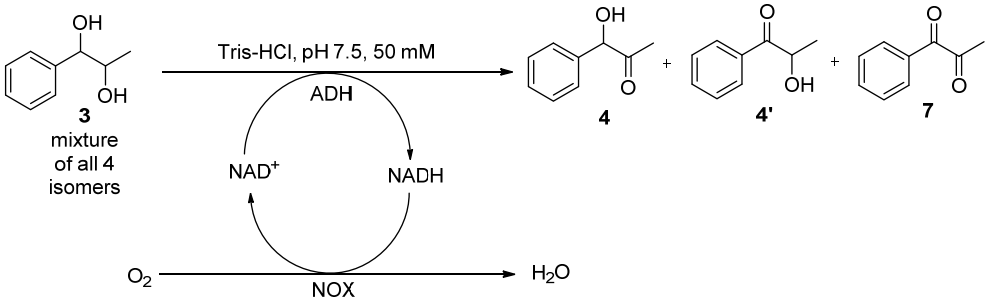

Entry	ADHs	Coenzyme	4 [%][b]	4' [%][b]	7 [%][b]	Catalyst form[c]	Accepted diol isomers[a]
1	Aa-ADH	NAD^+	31±<1	20±<1	5±<1	Purified (N-His_6 tag)	1*R*,2*R*/1*S*,2*S*/ 1*R*,2*S*
2	Bs-BDHA	NAD^+	36±3	22±2	4±1	Lyophilized whole cells	1*S*,2*R*/1*R*,2*S*
3	Ls-ADH	NAD^+	15±1	9±<1	2±<1	Lyophilized whole cells	1*S*,2*R*/1*R*,2*R*

[a] This refers to the preference of the enzyme for the conversion of diol **3**, which is a mixture of the four possible stereoisomers as described in this column; [b] average of two samples; [c] see section 4.4.1.

4.2.2 Initial tests with two stereocomplementary ωTAs

4.2.2.1 One-pot cascade for the conversion of chiral 3 by purified ADHs coupled with lyophilized *E. coli* whole cells of either Cv(S)-ωTAs or At(R)-ωTAs

The initial tests were performed to assess the possibility to couple ADHs and ωTAs in one-pot for the conversion of chiral diols **3**. Therefore, both (1*S*,2*S*)-**3** (10 mM) and (1*R*,2*R*)-**3** (10 mM) were used as model substrates; however, only Aa-ADH (50 µM) was paired with either Cv(*S*)-ωTA or At(*R*)-ωTA (20 mg mL^{-1}). The one-pot cascade was carried out in Tris-HCl buffer (pH 7.5, 50 mM), in which the screening of the NAD^+-dependent ADHs was initially performed, and supplemented with NAD^+ (1 mM), PLP (1 mM) and D-or L-Alanine (50 mM). Moreover, a lactate dehydrogenase (LDH, 1 mg mL^{-1}, lyophilized crude extract, Codexis, LDH-101, ca. 60 U mg^{-1}) was added for internal recycling of the NAD^+ coenzyme. **Scheme 4.3** depicts the general pathway.

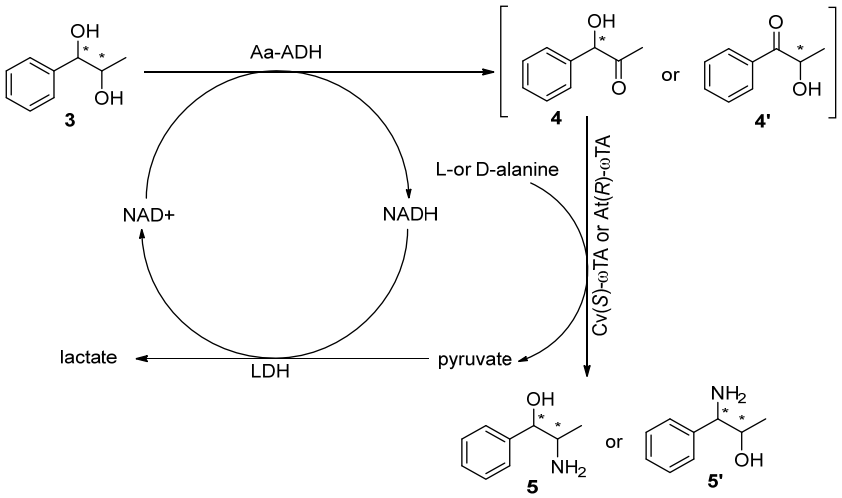

Scheme 4.3. One-pot cascade for the conversion of chiral **3** catalyzed by purified Aa-ADH coupled with stereocomplementary ωTA as lyophilized whole cells

As depicted above **Table 4.2**, two pathways can occur of which the main route, which is also the desired one, can lead to the formation of either intermediate **4** or **4'** depending on the ADH used. Consequently, the transamination of either one of the two intermediates can then form either product **5** or **5'**. Furthermore, a side reaction can take place in which the diol substrates **3** undergoes full oxidation, thus leading to the formation of compound **7** that can then be aminated to afford either product **8** or **8'** depending on the selectivity of the transaminases. The preliminary results of this one-pot cascade for the conversion of (1*S*,2*S*)-**3** and (1*R*,2*R*)-**3** are reported in **Table 4.2**. The biotransformations were analyzed by GC-MS in order to be able to identify the products formed. In all of the tested cases, low conversions were achieved (18-33%), and this may be due to the use of lyophilized cells carrying the transaminases. Moreover, trace amounts of compounds **8** and **8'** were detected by GC-MS analysis (entry 1-2). Notably, the conversion of (1*S*,2*S*)-**3** led to the formation of both intermediates **4** and **4'** (5% vs. 2%) when Cv(*S*)-ωTA was used; however, compound **5** (11%) was the only amino alcohol detected (entry 1). Similar results were observed in the case using At(*R*)-ωTA in which product **5** (19%) formed predominantly (entry 2). On the other hand, when substrate (1*R*,2*R*)-**3** was used, no amino alcohol formation was detected when Aa-ADH was coupled with Cv(*S*)-ωTA (entry 3). In fact, only intermediates **4** and **4'**, almost in equal amount, were observed. Conversely, when using At(*R*)-ωTA, (1*R*,2*R)*-**3** (entry 4) was converted

almost exclusively in product **5'** (32%). At this stage of the work, stereochemistry of the products was not taken into consideration.

Table 4.2. Conversion [%] of chiral **3** (10 mM) in the one-pot cascade catalyzed by Aa-ADH (50 µM) coupled with lyophilized *E. coli* whole cells of two stereocomplementary ωTAs (20 mg mL^{-1}) in Tris-HCl buffer (pH 7.5, 50 mM; 30 °C).

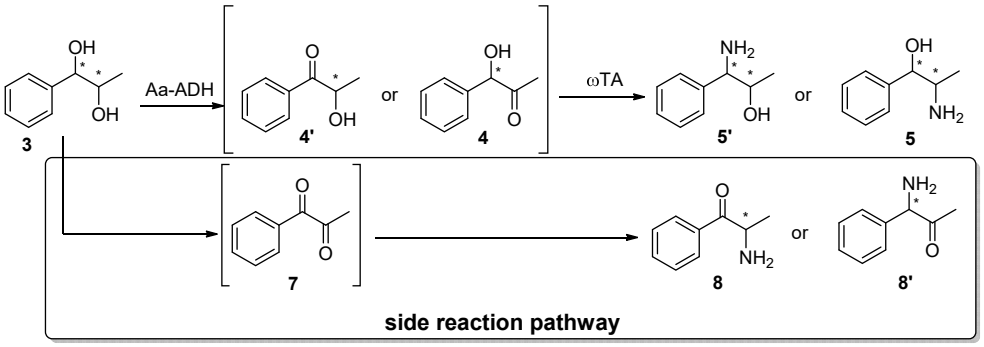

Entry	Substrate	ωTA	Conv. [%][a]	7 [%]	4' [%]	4 [%]	5' [%]	5 [%]	8 [%]	8' [%]
1	(1*S*,2*S*)-**3**	Cv*(S)*	18	n.d.	2	5	n.d.	11	<1	n.d.
2	(1*S*,2*S*)-**3**	At*(R)*	22	n.d.	n.d.	n.d.	n.d.	19	n.d.	3
3	(1*R*,2*R*)-**3**	Cv*(S)*	28	n.d.	10	18	n.d.	n.d.	n.d.	n.d.
4	(1*R*,2*R*)-**3**	At*(R)*	33	n.d.	n.d.	n.d.	32	1	n.d.	n.d.

[a]GC-MS analysis to identify peaks; reactions were performed in duplicate and the reported conversions are the average of two samples

Hence, depending on the substrate used as well as on the combination of ADHs and ωTAs, a different regioselective behavior can be observed. It is noteworthy that, when (1*R*,2*R)*-**3** was tested for the conversion to the corresponding amino alcohol through HB-bioamination cascade (as described in chapter 3) catalyzed by Aa-ADH and any of the AmDHs, no product formation was detected. Based on these preliminary results (**Table 4.2**), we investigated further the regioselectivity of this enzymatic one-pot cascade for obtaining phenylpropanolamine products of complementary absolute configurations to the cascade's products described in chapter 3.

4.2.2.2 One-pot cascade for the conversion of chiral 3 catalyzed by purified ADHs coupled with purified stereocomplementary ωTAs: Cv(*S*)-ωTA and At(*R*)-ωTA

To understand if the low conversion values reported in **Table 4.2** were caused by the use of lyophilized whole cells, a similar cascade was designed in which all of the enzymes were used in purified form. The main difference with the previous cascade was the use of a different internal recycling system. In fact, an alanine

dehydrogenase (Bs-AlaDH from *Bacillus sphaericus*)[33] was added to the same pot for the conversion of NADH to NAD^+, the latter of which is then re-utilized by the ADHs. Bs-AlaDH converts the pyruvate, produced after the transamination step, back to the alanine which re-enters the cycle as amino donor. The Bs-AlaDH requires also ammonia, sourced from the buffer, and release H_2O as the sole byproduct (**Scheme 4.4**). Thus, the biotransformations were performed in $HCOONH_4$ buffer (pH 8.5, 1 M) supplemented with NAD^+ (1 mM), PLP (1 mM), L-or D-alanine (25 mM) and Bs-AlaDH (20 µM). For these tests, both (1*S*,2*S*)-**3** (5 mM) and (1*R*,2*R*)-**3** (5 mM) were used as substrates. However, compared with the first experiments, Aa-ADH (50 µM) was tested again on both substrates, albeit Ls-ADH (50 µM) was also tested on substrate (1*R*,2*R*)-**3** because it showed good conversion of this substrate during the ADHs' screening (as also described in chapter 3). Again, two stereocomplementary ωTAs were tested: Cv(*S*)-ωTA and At(*R*)-ωTA (50 µM). Furthermore, due to the low conversions observed in the previous tests, the substrate loading was reduced from 10 mM to 5 mM. Moreover, in these latter set of experiments, all of the possible amino alcohol products were chemically synthesized to have them as reference compounds.

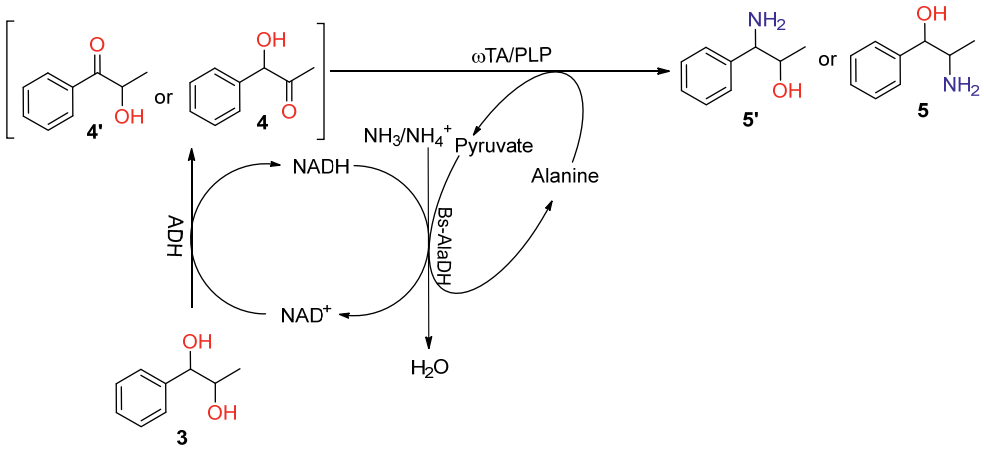

Scheme 4.4. One-pot cascade for the conversion of chiral substrates **3** catalyzed by ADHs coupled with stereocomplementary ωTAs.

As shown in **Table 4.3**, under all tested conditions, high conversions (59-93%) were observed (entry 1-6). This might be due to the lower substrate loading as well as the use of the enzymes in purified form for the cascade. Substrate (1*S*,2*S*)-**3** was converted in 91% when Aa-ADH was coupled with Cv(*S*)-ωTA (entry 1). The main product was the target vicinal amino alcohol **5** (60%), although accumulation of

intermediates **4** and **4'** (13 vs. 8%, respectively) was detected. Nevertheless, the reaction proceeded with full regioselectivity towards **5** and no traces of **5'** were detected. On the other hand, the expected possible side reaction occurred as well, thereby leading to the formation of the double oxidized compound **7** (8%) and consequently to its aminated counterpart **8** (8%). Similar results were observed in the case of At(*R*)-ωTA (entry 2); conversion of (1*S*,2*S*)-**3** raised up to 83%, however, lower trace amounts of intermediates **4** and **4'** (4% vs. 2%) were also detected as for compound **7** (3%). Notably, with this enzymatic system (Aa-ADH/At(*R*)-ωTA), no side product **8** was observed; this can be due to the intrinsic activity of this "*R*-selective" transaminase which might perform the transamination at a greater rate than the Cv(*S*)-ωTA on intermediate **4** rather than on compound **7**.

Table 4.3. Conversion [%] of optically active **3** (5 mM) in the one-pot cascade catalyzed by ADH (50 µM) paired with two stereocomplementary ωTAs (50 µM) in $HCOONH_4$ buffer (pH 8.5, 1 M; 30 °C)

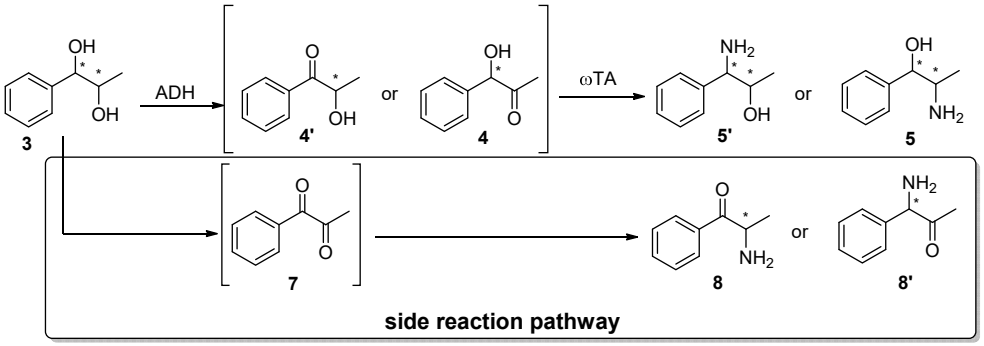

Entry	Substrate	ADH	ωTA	Conv. [%][a]	4' [%]a	4 [%]a	5' [%]a	5 [%]a	7 [%]a	8 [%]a	8' [%]a
1	(1*S*,2*S*)-**3**	Aa-ADH	Cv*(S)*	91±9	8±4	13±6	n.d.	60±19	8±3	8±3	n.d.
2	(1*S*,2*S*)-**3**	Aa-ADH	At*(R)*	83±2	2±2	4±4	n.d.	75±10	3±3	n.d.	n.d.
3	(1*R*,2*R*)-**3**	Aa-ADH	Cv*(S)*	61±16	8±3	6±1	n.d.	31±13	10±6	3±3	3±3
4	(1*R*,2*R*)-**3**	Aa-ADH	At*(R)*	59±7	2±2	1±1	30±3	38±4	1±1	n.d.	n.d.
5	(1*R*,2*R*)-**3**	Ls-ADH	Cv*(S)*	86±5	4±<1	7±1	n.d.	65±<1	4±1	2±2	n.d.
6	(1*R*,2*R*)-**3**	Ls-ADH	At*(R)*	93±4	n.d.	n.d.	n.d.	91±4	n.d.	n.d.	n.d.

[a]Reactions were performed in duplicate and the reported results are the average of two samples.

When the enzymatic system Aa-ADH/Cv(*S*)-ωTA was tested for the conversion of (1*R*,2*R*)-**3** (entry 3), the main product was again the vicinal amino alcohol **5** (31%). However, intermediates **4** and **4'** as well as compound **7** were all detected (6%, 8% and 10%, respectively). Moreover, both side products **8** and **8'** (3%) were observed under the tested conditions, although no amino alcohol **5'** formed. On the other hand, when the enzymatic system Aa-ADH/At(*R*)-ωTA was tested with (1*R*,2*R*)-**3** (entry 4), both amino alcohols **5** and **5'** were obtained (38% vs. 30%, respectively). In contrast, traces of the other compounds (1-2%) were observed and no formation of side products **8** and **8'** was detected. These results show that Aa-ADH is indeed capable of oxidizing both hydroxyl moieties (only if *R*-configured), and that At(*R*)-ωTA is accordingly able to perform the transamination of both intermediate **4** and **4'** and approximately at the same rate (i.e., a slight preference was observed for compound **4)**. These preliminary results well-indicate the possibility to obtain both regioisomers **5** and **5'** by applying the same enzymatic system. Finally, (1*R*,2*R*)-**3** was also tested in the one-pot cascade with Ls-ADH coupled with either Cv(*S*)-ωTA or At(*R*)-ωTA (entry 5-6). In the case of Cv(*S*)-ωTA, conversion raised up to 86% and only amino alcohol **5** was detected (65%). As observed previously with this "(*S*)-selective" ωTA, a mixture of intermediates (**4** and **4'**) and side products (**7** and **8**) was formed. On the other hand, we observed high chemo-and regioselectivity for the conversion of (1*R*,2*R*)-**3** catalyzed by Ls-ADH/At(*R*)-ωTA (entry 6) showing a substrate conversion of 93% while the formation of amino alcohol **5** was 91%. This is a clear evidence that Ls-ADH is highly selective for the oxidation of (1*R*,2*R*)-**3** to intermediate **4**, as previously demonstrated,[2] as well as At(*R*)-ωTA performs the transamination very efficiently. Hence, in summary, the use of lower substrate loading and purified enzymes was beneficial to the performance of the tested enzymatic systems. Furthermore, the use of Bs-AlaDH as cofactor recycling enzyme can also be advantageous compared to the LDH system**.**

4.2.2.2.1 Temperature study: (1*S*,2*S*)-3 as model substrate

Before proceeding with the screening of selected (*R*)-and (*S*)-ωTAs, we carried out a temperature study for the one-pot cascade described in **Scheme 4.4**. Substrate (1*S*,2*S*)-**3** (5 mM) was chosen as the model substrate to perform this study, and Aa-ADH was then coupled with either Cv(*S*)-ωTA (20, 30, 40 and 50 °C) or At(*R*)-ωTA (30, 40 and 50 °C). Both ADH and ωTA were used in equimolar ratio (50:50 µM). As showed in **Table 4.4**, high conversions (up to >99%) were observed with all tested enzymatic systems at all temperatures (entry 1-7). However, the best performance

in terms of amino alcohol **5** formation as well as stereoselctivity was observed at 30 °C (entry 2 and 3). In the case of Cv(*S*)-ωTA, formation of product **5** was similar at both 30 °C and 40 °C (entry 2 and 4); however, the *dr* dropped from 99:1 (30 °C) to 73:27 (40 °C). On the other hand, at 50 °C (entry 6), formation of **5** was only 29% and the *dr* dropped even more significantly (41:59). Again, At(*R*)-ωTA turned out to be a better enzyme than Cv(*S*)-ωTA; indeed, at all temperatures tested (entry 3, 5 and 7), the same *dr* was preserved (99:1) though the conversion into product **5** decreased from 92% (30 °C) to 88% (40 °C) and 53% (50 °C). In general, the optimal temperature to perform this cascade is 30 °C; therefore, the study was continued using this temperature.

Table 4.4. Conversion [%] of (1*S*,2*S*)-**3** (5 mM) in the one-pot cascade catalyzed by Aa-ADH (50 µM) coupled with two stereocomplementary ωTAs (50 µM) in $HCOONH_4$ buffer (pH 8.5, 1 M) at various temperatures

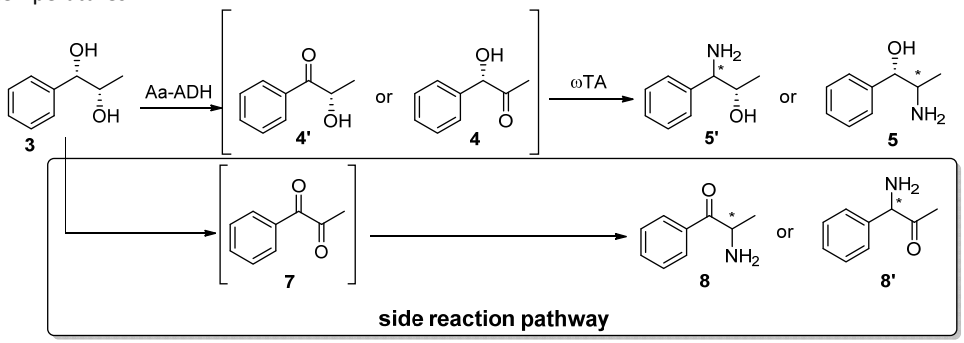

Entry	ωTA	T [°C]	Conv. [%][b]	5 [%][b]	*dr* [%][a]	4 [%][b]	4' [%][b]	7 [%][b]	8 [%][b]
1	Cv(*S*)	20	97±1	67±1	n.d.	7±<1	5±<1	7±<1	3±<1
2	Cv(*S*)	30	>99	54±8	99:1	13±5	12±3	7±<1	10±1
3	At(*R*)	30	>99	92±1	99:1	1±<1	1±<1	1±<1	3±<1
4	Cv(*S*)	40	94±2	58±3	73:27	8±1	9±1	4±1	13±1
5	At(*R*)	40	>99	88±<1	99:1	2±<1	2±<1	1±<1	4±<1
6	Cv(*S*)	50	96±1	29±1	41:59	20±<1	19±<1	9±1	16±<1
7	At(*R*)	50	95±<1	53±1	99:1	13±<1	11±<1	7±<1	8±<1

[a]Analyzed by GC-FID. [b]Reactions were performed in duplicate and the reported results are the average of two samples. Compounds **5'** and **8'** were not detected.

4.2.3 Screening selected stereocomplementary ωTAs in a one-pot cascade with secondary NAD$^+$-dependent ADHs

To further explore the potential of this cascade for accessing phenylpropanolamine isomers (i.e., optically active **5** and **5'**), a panel of stereocomplementary ωTAs was tested in combination with the selected ADHs and identified for each optically active substrate **3**. The screening was performed under the optimized conditions for each isomer of substrate **3** (10-20 mM, depending on the isomer) as described in chapter 3 and previously published.[2] All biotransformations were carried out in $HCOONH_4$ buffer (pH 8.5, 1 M; 30 °C) supplemented with NAD^+ (1 mM), PLP (1 mM), D-or L-alanine (5 eq.) and Bs-AlaDH (20 µM). The general reaction is depicted in **Scheme 4.5**. Regarding the ADHs, as shown above in **Table 4.1**, Aa-ADH was used for (1*S*,2*S*)-**3** (20 mM), (1*R*,2*R*)-**3** (10 mM) and (1*R*,2*S*)-**3** (10 mM). Ls-ADH was used for (1*R*,2*R*)-**3** (20 mM) while Bs-BDHA used for (1*S*,2*R*)-**3** (15 mM). Six stereocomplementary ωTAs were selected for the screening, namely: Cv(*S*)-ωTA from *Chromobacterium violaceum* (DSM 30191),[26] Vf(*S*)-ωTA from *Vibrio fluvialis,*[11, 28] Bm(*S*)-ωTA from *Bacillus megaterium* (SC6394),[12, 27] Ac(*S*)-ωTA from *Arthrobacter citreus,*[12] At(*R*)-ωTA from *Aspergillus terreus*[23, 24] and As(*R*)-ωTA from *Arthrobacter sp.*[25] Furthermore, at this stage, the chemo-, regio- and stereoselective outcome of the cascade was investigated by analyzing the product through RP-HPLC (C18 column) after derivatization of the amino group with a chiral reagent (GITC, **section 4.4.3**).

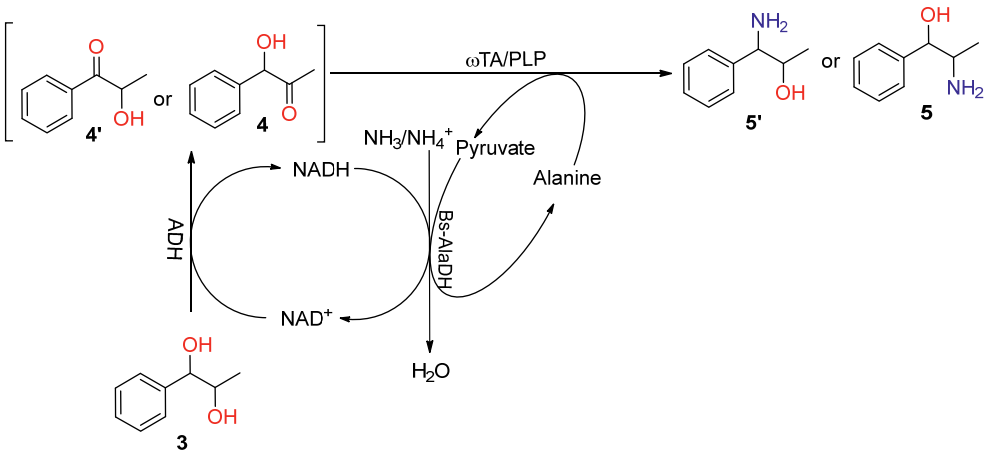

Scheme 4.5. One-pot cascade for the conversion of chiral substrates **3** catalyzed by ADHs coupled with stereocomplementary ωTAs.

4.2.3.1 Screening stereocomplementary ωTAs on chiral (1*S*,2*S*)-3

The first screening of the ωTAs was performed on substrate (1*S*,2*S*)-**3** (20 mM). As mentioned above, Aa-ADH (70 μM) was coupled with the five purified stereocomplementary ωTAs (35 μM); only Vf(*S*)-ωTA was used as lyophilized *E. coli* whole cells (20 mg mL^{-1}).

As reported in **Table 4.5**, elevated conversions (up to >99%) were observed in almost all the cases except for Vf(*S*)-ωTA (48%) and Ac(*S*)-ωTA (14%) (entry 2 and 4). Moreover, formation of product **5'** and by-product **8'** was not detected with any of the enzymatic systems tested on (1*S*,2*S*)-**3**; conversely, only traces of **7** were observed. When Cv(*S*)-ωTA was coupled with Aa-ADH (entry 1), substrate conversion was high (94%) and the main product was the vicinal amino alcohol **5** (86%). Approximately equal amounts of intermediates **4** and **4'** (4% *vs.* 2%) as well as by-product **8** (2%) were detected. Similar results were observed with the enzymatic system Aa-ADH/Bm(*S*)-ωTA (entry 3): conversion of (1*S*,2*S*)-**3** increased above 90% and the vicinal amino alcohol **5** was obtained in 86%; intermediates **4** and **4'** as well as by-product **8** were just detected in traces (3%, 2% and 1%, respectively). The best performing enzymatic systems were either Aa-ADH/At(*R*)-ωTA or Aa-ADH/As(*R*)-ωTA (entry 5 and 6). Quantitative conversion of the substrate was observed (up to >99%), and the main product formed was the vicinal amino alcohol **5** (96% and 90%, respectively). Nevertheless, intermediates and byproduct formation followed again the trend observed so far. On the other hand, Aa-ADH/Vf(*S*)-ωTA system generated the amino alcohol **5** in only 11% (entry 2), whereas the main products were intermediate **4** (15%) and byproduct **8** (13%). It may be that enzyme's product inhibition occur that results in the accumulation of intermediate **4,** which can then undergo over-oxidation to **7** and subsequent amination to form by-product **8**. Even lower conversion was instead detected in the case of Ac(*S*)-ωTA (entry 4); in fact, amino alcohol **5** was formed only in 7% conversion and accumulation of intermediate **4** was observed again. In summary, Aa-ADH coupled with either Cv(*S*), Bm(*S*), At(*R*) or As(*R*) turned out to be highly regioselective since only product **5** was detected and formation of **5'** did not occur. On the other hand, moderate to high chemoselectivity was observed in all cases. Indeed, both intermediates **4** and **4'** were formed although only in tiny amounts of constant quantity in all cases; this may indicate that a thermodynamic equilibrium has been reached. Regarding the stereoselectivity, Cv(*S*) and Bm(*S*) formed the product **5** in moderate *er* (86:14 [*SS*:*RR*]) and high although non-perfect *dr* (93:7 and 95:5 [*SS*:*RS*], respectively). On the other hand, high stereoselectivity was

achieved when the two "(*R*)-selective" ωTAs (*i.e.*, At(*R*) and As(*R*)) were applied; indeed, the enantiomeric ratio of product **5** was 99:1 [***SR***:*RS*], whereas *dr* 2:98 and 4:96 [*RR*:***SR***], respectively. The lower diastereomeric ratio compared to the *er* for these last two enzymatic systems derives from the imperfect *er* of the intermediate (1*S*,2*S)*-**3**, obtained after stereoselective hydrolysis of the epoxide intermediate.[2] Based on the selectivity of the enzymes employed in the cascade, the expected stereochemistry of product **5** was confirmed by RP-HPLC analysis and comparison with reference compounds.

Table 4.5. One pot bio-catalytic conversion of (1*S*,2*S*)-**3** (20 mM) by Aa-ADH (70 μM) coupled with stereocomplementary ωTAs (35 μM) in $HCOONH_4$ (pH 8.5, 1 M) and 30 °C.

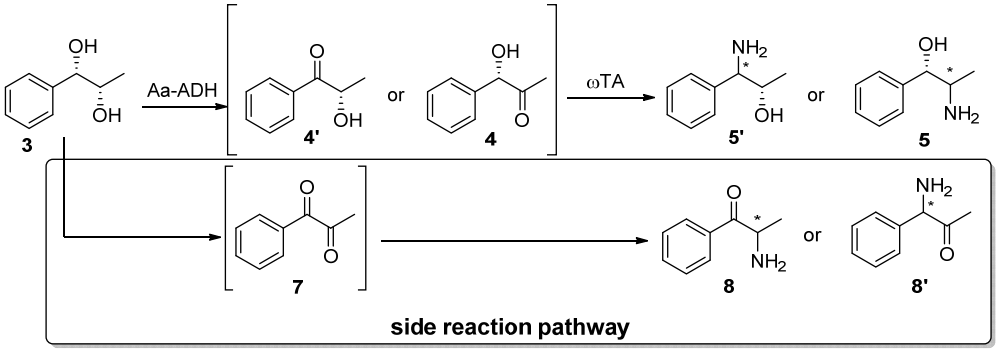

Entry	ωTA	Conv. [%][c]	4' [%][c]	4 [%][c]	5 [%][c]	*er* 5 [%][b]	*dr* 5 [%][b]	7 [%][c]	8 [%][c]
1	Cv(*S*)	94±1	2±<1	4±1	86±<1	86:14 ***SS***:*RR*	93:7 ***SS***:*RS*	<1	2±<1
2	Vf(*S*)[a]	48±10	9±1	15±2	11±4	n.m.	n.m.	<1	13±2
3	Bm(*S*)	91±<1	2±<1	3±<1	86±<1	86:14 ***SS***:*RR*	95:5 ***SS***:*RS*	<1	1±<1
4	Ac(*S*)	14±<1	1±<1	6±<1	7±<1	n.m.	n.m.	<1	n.d.
5	At(*R*)	>99	<1	1±<1	96±<1	99:1 ***SR***:*RS*	2:98 *RR*:***SR***	<1	1±<1
6	As(*R*)	98±<1	1±<1	2±<1	90±1	99:1 ***SR***:*RS*	4:96 *RR*:***SR***	<1	2±<1

[a]Used as lyophilized *E. coli* whole cells (20 mg mL^{-1}). [b] Determined by achiral RP-HPLC (C18 column) after derivatization of the amino group with a chiral reagent (GITC). [c]Reactions were performed in duplicate and the reported results are the average of two samples; compounds **5'** and **8'** were not detected.

4.2.3.2 Screening stereocomplementary ωTAs on chiral (1*R*,2*R*)-3

The same type of screening as described above was performed on substrate (1*R*,2*R*)-**3** (20 mM). As mentioned earlier, both Ls-ADH (35 μM) as well as Aa-ADH

(50 µM) were paired with the selected stereocomplementary ωTAs (70 and 50 µM, respectively).

As reported in **Table 4.6**, all the tested enzymatic systems in which Ls-ADH was used, resulted in elevated conversions (88—>99%). The only exception was in the case of Ac(*S*)-ωTA (33%) that resulted in the formation of the amino alcohol **5** in 22% (entry 4). On the other hand, the system Ls-ADH/Vf(*S*)-ωTA (entry 2) led to full conversion of the substrate; however, product **5** was not formed while the main products were intermediate **4** (54%), **4'** (13%) and by-product **8** (33%). With all the other enzymatic combinations, intermediates **4** and **4'** as well as compound **7** and **8** were only observed in traces. Furthermore, as for the conversion of (1*S*,2*S*)-**3** catalyzed by the enzymatic system Aa-ADH/ωTAs, only amino alcohol **5** formed while product **5'** and byproduct **8'** were not detected in any of the tested conditions on substrate (1*R*,2*R*)-**3**. In the case of Ls-ADH/Cv(*S*)-ωTA (entry 1), 88% conversion was obtained and amino alcohol **5** formed in 76%. Similar results were observed in the case of the "(*S*)-selective" Bm(*S*)-ωTA (90% overall conversion, 81% of **5**, entry 3). Once again, the best performance was observed with the two "(*R*)-selective" ωTAs (At(*R*) and As(*R*). Entries 5 and 6 show that in fact, >99% conversion was obtained with both enzymatic systems and amino alcohol **5** was the main product (95% and 90%, respectively). Considering all the tested enzymatic systems, product **5** was obtained with high enantiomeric ratio (>99.5:<0.5 [***RS***:*SR*] or >99.5:<0.5 [**RR**:SS]) and diastereomeric ratio (>99.5:<0.5[***RS***:*RR*/*SS*] or >99.5:<0.5 [***RR***:*SR*/*RS*]). Compared with the results obtained with (1*S*,2*S*)-**3** as substrate, these higher stereoselective outcome can only derive from the ADH used. Indeed, it seems that Ls-ADH has higher reactivity for substrate (1*R*,2*R*)-**3** than Aa-ADH has for substrate (1*S*,2*S*)-**3**. Finally, based on the selectivity of the enzymes employed in the cascade, the expected stereochemistry of product **5** was confirmed by RP-HPLC analysis.

Table 4.6. One-pot biocatalytic conversion of (1*R*,2*R*)-**3** (20 mM) catalyzed by Ls-ADH (35 µM) coupled with stereocomplementary ωTAs (70 µM) in $HCOONH_4$ (pH 8.5, 1 M) and 30 °C.

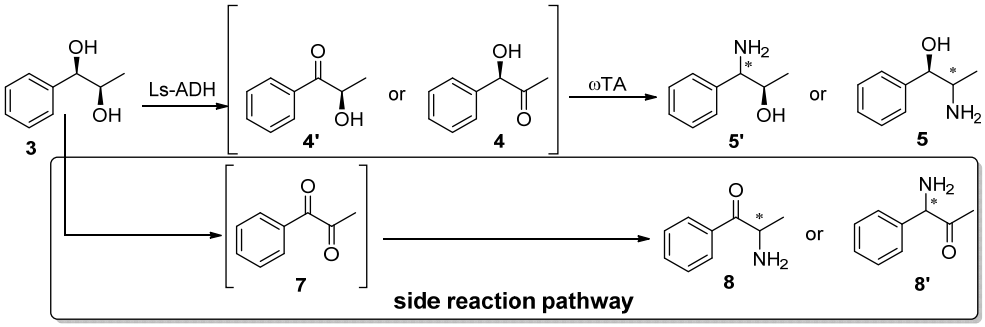

Entry	ωTA	Conv. [%][c]	4' [%][c]	4 [%][c]	5 [%][c]	*er* 5 [%][b]	*dr 5* [%][b]	7 [%][c]	8 [%][c]
1	Cv(*S*)	88±<1	1±<1	4±<1	76±<1	>99.5:<0.5 ***RS***:*SR*	>99.5:<0.5 ***RS***:*RR*/*SS*	<1	7±<1
2	Vf(*S*)[a]	>99	13±2	54±1	n.d.	n.m.	n.m	n.d.	33±3
3	Bm(*S*)	90±<1	1±<1	3±<1	81±<1	>99.5:<0.5 ***RS***:*SR*	96:2:2 ***RS***:*SS*:*RR*	<1	5±<1
4	Ac(*S*)	33±<1	3±<1	7±<1	22±<1	n.m.	n.m.	2±<1	2±<1
5	At*(R)*	>99	n.d.	2±<1	95±<1	>99.5:<0.5 ***RR***:*SS*	>99.5:<0.5 ***RR***:*SR*/*RS*	n.d.	2±<1
6	As*(R)*	>99	n.d.	4±<1	90±<1	>99.5:<0.5 ***RR***:*SS*	>99.5:<0.5 ***RR***:*SR*/*RS*	<1	6±<1

[a]Used as lyophilized *E. coli* whole cells (20 mg mL^{-1}). [b]Determined by achiral RP-HPLC (C18 column) after derivatization of the amino group with a chiral reagent (GITC). [c]Reactions were performed in duplicate and the reported results are the average of two samples; compounds **5'** and **8'** were not detected.

Based on the preliminary results reported in **Table 4.2** and **Table 4.3**, in which the formation of the regioisomer **5'** was observed, (1*R*,2*R*)-**3** (10 mM) was tested as substrate for the enzymatic one-pot cascade catalyzed by Aa-ADH (50 µM) coupled with the selected stereocomplementary ωTAs (50 µM).

As shown in **Table 4.7**, moderate conversions (20-76%) were observed with all tested *S*-selective ωTAs (entry 1-4) and they all led exclusively to the formation of product **5** (7-26%). Moreover, in all cases, accumulation of intermediates **4** and **4'** was also observed with the most prominent system being once again the Aa-ADH/Vf(*S*)-ωTA (61% **4**, entry 2). On the other hand, trace amounts of both compound **7** and by-product **8** were formed. In general, the cascades proceeded with elevated regio- and stereoselectivity thus yielding product **5** in high enantiomeric ratio (>99.5:<0.5 [***RS***:*SR*]) as well as diastereomeric ratio (>99.5:<0.5 [***RS***:*SS*/*RR*]) with the only exception being the case of Bm(*S*)-ωTA (*dr* 14:86 [*RR*:*RS*]). Nevertheless, Aa-ADH/At(*R*)-ωTA and Aa-ADH/As(*R*)-ωTA (entry 5 and 6) were the

most interesting enzymatic systems. In both cases, high conversions were observed (94-97%) despite both regioisomers **5** and **5'** were formed. With At(*R*)-ωTA (entry 5), **5'** (58%) was the main product formed followed by product **5** (21%) and by-product **8'** (13%); traces of both intermediate **4** (2%) as well as by-product **8** were detected. Comparable results were obtained with As(*R*)-ωTA (entry 6). Furthermore, both enzymatic systems displayed high enantiomeric and diastereomeric ratios for both regioisomer products (**5'**, *er* >99.5:<0.5 [***SR***:*RS*]; **5'**, *dr* up to >99.5:<0.5 [***SR***:*RR*/*SS*]; **5**, *er* >99.5:<0.5 [***RR***:*SS*]; **5**, *dr* >99.5:<0.5 [***RR***:*SR*/*RS*]). Therefore, in terms of regioselectivity, both enzymatic systems showed a higher preference for the formation of isomer **5'**, hence giving very similar regioisomeric ratio (*rr*) of 91:9 [**5':5**] for Aa-ADH/At(*R*)-ωTA and 92:8 [**5':5**] for Aa-aDH/As(*R*)-ωTA, respectively (analysis performed by RP-HPLC after derivatization with GITC; all detected isomers are considered). It might be that by further tuning the enzymes loading the regiopreference could be increased. Based on the selectivity of the enzymes employed in the cascades, the expected stereochemistry of products **5** and **5'** were confirmed. In fact, (1*R*,2*S*)-**5**, (1*R*,2*R*)-**5** and (1*S*,2*R*)-**5'** were formed, thus retaining the expected stereoselectivity of the ω-transaminases. In the case of product (1*S*,2*R*)-**5'**, one must consider the occurrence of the switch of the Cahn-Ingold-Prelog (CIP) priority.

Table 4.7. One-pot biocatalytic conversion of (1*R*,2*R*)-**3** (10 mM) by Aa-ADH (50 µM) coupled with stereocomplementary ωTAs (50 µM) in $HCOONH_4$ (pH 8.5, 1 M) and 30 °C.

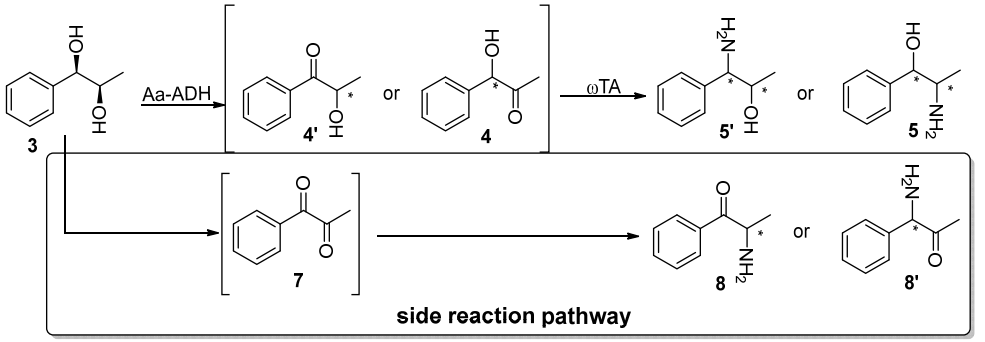

Entry	ωTA	Conv. [%][d]	4' [%][d]	4 [%][d]	5' [%][d]	*er* 5' [%][b]	*dr* 5' [%][b]	5 [%][d]	*er* 5 [%][b]	*dr* 5 [%][b]	7 [%][d]	8 [%][d]	8' [%][d]
1	Cv(*S*)	47±1	3±1	15±1	n.d.	n.m.	n.m.	24±1	>99.5:<0.5 [***RS***:*SR*]	>99.5:<0.5 [***RS***:*SS/RR]*	<1	5±<1	n.d.
2	Vf(*S*)[a]	76±7	10±1	61±6	n.d.	n.m.	n.m.	24±7	n.m.	n.m.	<1	3±<1	1±<1
3	Bm(*S*)	47±<1	2±<1	14±1	n.d.	n.m.	n.m.	26±<1	>99.5:<0.5 [***RS***:*SR*]	14:86 [*RR*:***RS***]	<1	5±<1	n.d.
4	Ac(*S*)	20±1	3±<1	9±1	n.d.	n.m.	n.m.	7±<11	n.m.	n.m.	2±<1	1±<1	n.d.
5	At(*R*)	97±1	n.d.	2±<1	58±1	>99.5:<0.5 [***SR***:*RS*][c]	95:5 [***SR***:*RR*][c]	21±<1	>99.5:<0.5 [***RR***:*SS*]	>99.5:<0.5 [***RR***:*SR/RS*]	n.d.	1±<1	13±<1
6	As(*R*)	94±1	n.d.	3±2	61±<1	>99.5:<0.5 [***SR***:*RS*][c]	>99.5:<0.5 [***SR***:*RR/SS*][c]	16±<1	>99.5:<0.5 [***RR***:*SS*]	>99.5:<0.5 [***RR***:*SR/RS*]	<1	2±<1	10±<1

[a] Used as lyophilized *E. coli* whole cells (20 mg mL^{-1}). [b] Determined by achiral RP-HPLC (C18 column) after derivatization of the amino group with a chiral reagent (GITC). [c] Switch of the CIP priority. [d]Reactions were performed in duplicate and the reported results are the average of two samples.

4.2.3.3 Screening stereocomplementary ωTAs on chiral (1*S*,2*R*)-3

The same screening was then carried out on substrate (1*S*,2*R*)-**3** (15 mM) by pairing in one-pot Bs-BDHA (50 µM) with the selected stereocomplementary ωTAs (50 µM). As reported in **Table 4.8**, high conversions (92-98%) were observed with all tested enzymatic systems except for Vf(*S*)-ωTA (29%, entry 2) and Ac(*S*)-ωTA (16%, entry 4). Moreover, only product **5** (therefore no formation of **5'**) was observed for all systems. By-product **8'** was not detected in any of the tested conditions, while compound **7** was detected only in traces (<1%). Using Cv(*S*)-ωTA (entry 1), the cascade proceeded with 92% conversion and product **5** formed in 86%, while only traces of intermediates **4** and **4'**, and byproduct **8** were detected. Similar results were observed with Bm(*S*)-ωTA (entry 3) that resulted in a conversion up to 94% and formation of product **5** in 88%. On the other hand, both Vf(*S*)-ωTA and Ac(*S*)-ωTA (entry 2 and 4) led to low conversion and the formation of amino alcohol **5** was mediocre (3% vs. 6%, respectively). In the case of Vf(*S*), both intermediate **4** and **4'** (11% and 6%) and by-product **8** (8%) were detected. For the Ac(*S*) system, only intermediate **4** was detected in 4% along with traces of **4'** and **8** (<1%). Nevertheless, Bs-BDHA/At(*R*)-ωTA (entry 5) and Bs-BDHA/As(*R*)-ωTA (entry 6) were the best performing cascade systems, thereby leading to nearly quantitative conversions (98% and 97%, respectively). Furthermore, in both cases, the main product observed was the amino alcohol **5** (95% and 92%) along with traces of intermediates **4** and **4'** and by-product **8** (1-3%). Therefore, all of the cascades with Cv(*S*), Bm(*S*), At(*R*) and As(*R*) proceeded with high regio- and chemoselectivity. Moreover, amino alcohol **5** was always obtained with high enantiomeric ratio (>99.5:<0.5 [***SS***:*RR*] or >99.5:<0.5 [***SR***:*RS*]) and moderate diastereomeric ratio (96:4 [***SS***:*RS*] or 98:2 [***SR***:*RR*]); the latter stems from the imperfect enantiomeric ratio of substrate (1*S*,2*R*)-**3**. Based on the selectivity of the enzymes employed in the cascades, the expected stereochemistry of product **5** was confirmed by RP-HPLC analysis.

Table 4.8. One-pot bio-catalytic conversion of (1*S*,2*R*)-**3** (15 mM) catalyzed by Bs-BDHA (50 µM) coupled with stereocomplementary ωTAs (50 µM) in $HCOONH_4$ (pH 8.5, 1 M) and 30 °C.

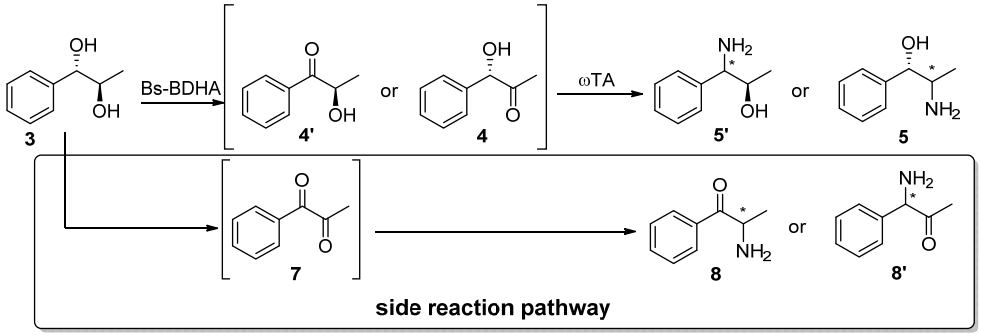

Entry	ωTA	Conv. [%][c]	4' [%][c]	4 [%][c]	5 [%][c]	*er* 5 [%][b]	*dr* [%][b]	7 [%][c]	8 [%][c]
1	Cv(*S*)	92±3	1±<1	3±<1	86±3	>99.5:<0.5 ***SS***:*RR*	96:4 ***SS***:*RS*	<1	3±1
2	Vf(*S*)[a]	29±<1	6±<1	11±<1	3±<1	n.m.	n.m.	<1	8±1
3	Bm(*S*)	94±1	1±<1	2±<1	88±1	>99.5:<0.5 ***SS***:*RR*	96:4 ***SS***:*RS*	<1	3±<1
4	Ac(*S*)	16±<1	<1	4±<1	6±<1	n.m.	n.m.	n.d.	<1
5	At(*R*)	98±2	1±<1	1±<1	95±2	>99.5:<0.5 ***SR***:*RS*	98:2 ***SR***:*RR*	<1	2±<1
6	As(*R*)	97±1	1±<1	1±<1	92±<1	>99.5:<0.5 ***SR***:*RS*	97:3 ***SR***:*RR*	<1	3±<1

[a]Used as lyophilized *E. coli* whole cells (20 mg mL^{-1}). [b]Determined by achiral RP-HPLC (C18 column) after derivatization of the amino group with a chiral reagent (GITC). [c]Reactions were performed in duplicate and the reported results are the average of two samples; compounds **5'** and **8'** were not detected.

4.2.3.4 Screening stereocomplementary ωTAs on chiral (1*R*,2*S*)-3

Finally, the screening was performed on substrate (1*R*,2*S*)-**3** (10 mM) by pairing in one-pot Aa-ADH (70 µM) with the selected stereocomplementary ωTAs (35 µM). As shown in **Table 4.9**, high conversions (87% up to >99%) were achieved for all of the tested enzymatic cascades, the exception being for Aa-ADH/Ac(S)-ωTA (entry 4) that yielded 23% conversion (along with 10% of **5**). In the case of Cv(*S*)-ωTA (entry 1), amino alcohol **5** (77%) was the main product and formation of its regioisomer **5'** did not occur; moreover, only traces of intermediates **4** (1%), **4'** (3%) and compound **7** (2%) were detected although 10% of by-product **8** was observed. According to the previously observed trend, similar results were observed for the enzymatic system Aa-ADH/Bm(*S*)-ωTA (entry 3). On the other hand, although Aa-ADH/Vf(*S*)-ωTA system (entry 2) displayed very high conversion (99%), only 4% of amino alcohol product **5** was formed because the major products were intermediate **4** (33%), its

aminated counterpart **8** (45%) and intermediate **4'** (13%). Furthermore, traces of **5'** (1%) and **7** (1%) were also observed. Regarding the *R*-selective ωTAs, both At(*R*)-ωTA (entry 5) and As(*R*)-ωTA (entry 6) led to full substrate conversion and high analytical yield of amino alcohol **5** (87% and 84%, respectively). In the case of reaction catalyzed by At(*R*), intermediates **4** and **4'** and compound **7** were not detected as the only by-products **8** (4%) and **8'** (4%) were obtained. As(*R*) showed an equal product distribution among **4**, **4'** and **7** (1%) and by-product **8** was formed in 13% conversion. It is noteworthy that, only trace amounts of amino alcohol **5'** were instead observed (up to 5%) when Aa-ADH was coupled with either At(*R*)-ωTA or As(*R*)-ωTA, even though substrate (1*R*,2*S*)-**3** possess (*R*) absolute configuration at the α-position; this has previously showed to be beneficial in the conversion of substrate (1*R*,2*R*)-**3** to amino alcohol **5'** (**Table 4.7**, entry 5 and 6). Anyway, high regioselectivity was revealed for the synthesis of amino alcohol **5**: namely 14:86 [**5':5**] by applying Aa-ADH/At(*R*)-ωTA and 25:75 [**5':5**] by applying Aa-ADH/As(*R*)-ωTA (determined by RP-HPLC analysis after derivatization with GITC, hence, considering all isomers). In general, under all tested conditions, product **5** was always obtained with high enantiomeric ratio (>99.5:<0.5 [***RS***:*SR*] or >99.5:<0.5 [***RR***:*SS*]) albeit with low to moderate diastereomeric ratio (**Table 4.9**, *dr* **5**). Based on the selectivity of the enzymes employed in the cascades, the expected stereochemistry of product **5** was confirmed. On the other hand, the stereochemistry for product **5'** was not determined in this case due to the too low conversion that prevented accurate analytical measurements.

Table 4.9. One-pot biocatalytic conversion of (1*R*,2*S*)-**3** (10 mM) catalyzed by Aa-ADH (70 µM) coupled with stereocomplementary ωTAs (35 µM) in $HCOONH_4$ (pH 8.5, 1 M) and 30 °C.

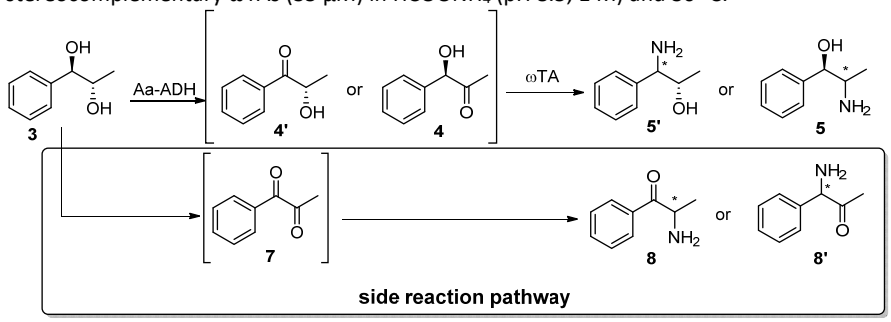

Entry	ωTA	Conv. [%][c]	4' [%][c]	4 [%][c]	5' [%][c]	5 [%][c]	*er* 5 [%][b]	*dr 5* [%][b]	7 [%][c]	8 [%][c]	8' [%][c]
1	Cv(*S*)	92±1	3±<1	1±<1	n.d.	77±<1	>99.5:<0.5 ***RS***:*SR*	17:83 *RR*:***RS***	2±<1	10±1	n.d.
2	Vf(*S*)[a]	99±1	13±6	33±10	1±1	4±4	n.m.	n.m.	1±<1	45±11	n.d.
3	Bm(*S*)	87±1	2±<1	1±<1	n.d.	76±<1	>99.5:<0.5 ***RS***:*SR*	31:69 *RR*:***RS***	3±1	7±1	n.d.
4	Ac(*S*)	23±1	5±<1	5±<1	n.d.	10±<1	n.m.	n.m.	2±<1	1±<1	n.d.
5	At(*R*)	>99	n.d.	n.d.	5±<1	87±<1	>99.5:<0.5 ***RR***:*SS*	70:30 ***RR***:*RS*	n.d.	4±<1	4±<1
6	As(*R*)	>99	1±<1	<1	1±<1	84±<1	>99.5:<0.5 ***RR***:*SS*	83:17 ***RR***:*RS*	1±<1	13±<1	n.d.

[a]Used as lyophilized *E. coli* whole cells (20 mg mL^{-1}). [b]Determined by achiral RP-HPLC (C18 column) after derivatization of the amino group with a chiral reagent (GITC). [c]Reactions were performed in duplicate and the reported results are the average of two samples.

4.2.4 Overview of amino alcohol products obtained in this study and associated enzymatic systems

Table 4.10 shows a full overview of the possible combination of ADHs and ω-TAs in a one-pot cascade fashion for the conversion of chiral diols **3** to optically active phenylpropanolamine isomers **5** and/or regioisomer **5'**.

Table 4.10. Overview of all the best ADH/ωTA combination in the one-pot cascade reaction for the conversion of chiral diols **3** to either optically active **5** or **5'** amino alcohols.

Entry	Sub.	ADH	TA	5 [%]	*er* 5 [%][a]	*dr* 5 [%][a]	5' [%]	*er* 5' [%][a]	*dr* 5' [%][a]	*rr* [5':5] [%][a]
1	(1*S*,2*R*)-**3**[b]	Bs-BDHA	Cv(*S*)	86±3	>99.5:<0.5 [***SS***:*RR*]	96:4 [***SS***:*RS*]	n.d.	n.a.	n.a.	n.a.
2	(1*S*,2*R*)-**3**[b]	Bs-BDHA	Bm(*S*)	88±1	>99.5:<0.5 [***SS***:*RR*]	96:4 [***SS***:*RS*]	n.d.	n.a.	n.a.	n.a.
3	(1*R*,2*R*)-**3**[c]	Ls-ADH	Cv(*S*)	76±<1	>99.5:<0.5 [***RS***:*SR*]	>99.5:<0.5 [***RS***:*RR*/*SS*]	n.d.	n.a.	n.a.	n.a.
4	(1*R*,2*R*)-**3**[c]	Ls-ADH	Bm(*S*)	81±<1	>99.5:<0.5 [***RS***:*SR*]	96:2/2 [***RS***:*SS*/*RR*]	n.d.	n.a.	n.a.	n.a.
5	(1*S*,2*R*)-**3**[b]	Bs-BDHA	At(*R*)	95±2	>99.5:<0.5 [***SR***:*RS*]	98:2 [***SR***:*RR*]	n.d.	n.a.	n.a.	n.a.
6	(1*S*,2*R*)-**3**[b]	Bs-BDHA	As(*R*)	92±<1	>99.5:<0.5 [***SR***:*RS*]	97:3 [***SR***:*RR*]	n.d.	n.a.	n.a.	n.a.
7	(1*S*,2*S*)-**3**[c]	Aa-ADH	At(*R*)	96±<1	99:1 [***SR***:*RS*]	2:98 [*RR*:***SR***]	n.d.	n.a.	n.a.	n.a.
8	(1*S*,2*S*)-**3**[c]	Aa-ADH	As(*R*)	90±1	99:1 [***SR***:*RS*]	4:96 [*RR*:***SR***]	n.d.	n.a.	n.a.	n.a.
9	(1*R*,2*R*)-**3**[c]	Ls-ADH	At(*R*)	95±<1	>99.5:<0.5 [***RR***:*SS*]	>99.5:<0.5 [*RR*:*SR*/*RS*]	n.d.	n.a.	n.a.	n.a.
10	(1*R*,2*R*)-**3**[c]	Ls-ADH	As(*R*)	90±<1	>99.5:<0.5 [***RR***:*SS*]	>99.5:<0.5 [***RR***:*SR*/*RS*]	n.d.	n.a.	n.a.	n.a.
11	(1*R*,2*R*)-**3**[d]	Aa-ADH	At(*R*)	21±<1	>99.5:<0.5 [***RR***:*SS*]	>99.5:<0.5 [***RR***:*SR*/*RS*]	58±1	>99.5:<0.5 [***SR***:*RS*]	95:5 [***SR***:*RR*]	91:9
12	(1*R*,2*R*)-**3**[d]	Aa-ADH	As(*R*)	16±<1	>99.5:<0.5 [***RR***:*SS*]	>99.5:<0.5 [***RR***:*SR*/*RS*]	61±<1	>99.5:<0.5 [***SR***:*RS*]	>99.5:<0.5 [***SR***:*RR*/*SS*]	92:8

n.d. = not detected; n.a. = not applicable. [a] Determined by RP-HPLC analysis after GITC derivatization; only observed isomers reported. [b] 15 mM; [c] 20 mM; [d] 10 mM.

4.3 Conclusions

In conclusion, we have developed a one-pot enzymatic cascade in which secondary NAD^+-dependent ADHs were combined with a selection of stereocomplementary ω-TAs for the synthesis of chiral phenylpropanolamine isomers (1*S*,2*S*)-**5** and (1*R*,2*S*)-**5** starting from chiral diol substrates. The latter were also enzymatically synthesized by a one-pot cascade consisting of a Fus-SMO in combination with two stereocomplementary EHs to be able to access all of the four diol isomers. The amino alcohols (1*S*,2*S*)-**5** and (1*R*,2*S*)-**5** were obtained in high analytical yields (81-86%) and high stereoselectivity (*er* up to >99.5) in the biocatalytic conversion of (1*S*,2*R*)-**3** catalyzed by Bs-BDHA with either Cv(*S*)-ωTA (86%) or Bm(*S*)-ωTA (88%). Similar results were observed for the conversion of (1*R*,2*R*)-**3** catalyzed by Ls-ADH with either Cv(*S*)-ωTA (76%) or Bm(*S*)-ωTA (81%), respectively. Moreover, the (1*R*,2*R*)-**5** and (1*S*,2*R*)-**5** isomers—which were previously obtained via the enzymatic hydrogen-borrowing (HB) amination cascade incorporated into the formal regio- and stereoselective aminohydroxylation of β-methylstyrene **1**[2]—can also be accessed by this alternative ADH/ωTAs cascade. The best results were obtained in the bioconversion of (1*R*,2*R*)-**3** into (1*R*,2*R*-**5** catalyzed by Ls-ADH combined with either At(*R*)-ωTA (95%) or As(*R*)-ωTA (90%). In the case of (1*S*,2*R*)-**5** synthesis, (1*S*,2*R*)-**3** was converted through the combination of Bs-BDHA with either At(*R*)-ωTA (95%) or As(*R*)-ωTA (92%); as alternative (1*S*,2*S*)-**3** was also converted through the combination of Aa-ADH with either At(*R*)-ωTA (96%) or As(*R*)-ωTA (90%). Therefore, all these enzyme combinations operated well. Finally, depending on the substrate choice, and selected ADH and ωTA, we could also access the regioisomer (1*S*,2*R*)-**5'** (*er* and *dr* up to >99.5; *rr* 91:9 [**5':5**]); (1*R*,2*R*)-**3** was converted to the amino alcohol **5'** by combining Aa-ADH with either At(*R*)-ωTA (58%) or As(*R*)-ωTA (61%) in a one-pot fashion. The one-pot cascade reported in this work perfectly complements the HB-bioamination system, thus enabling the enzymatic synthesis of all four phenylpropanolamine isomers with comparable analytical yields and stereoselectivity. Furthermore, the production of regioisomer (1*S*,2*R*)-**5'** by applying different combinations of substrate and enzymes is a promising route to be further explored for the synthesis of the three other chiral isomers of **5'**.

4.4 Experimental section

General information: ADHs used in this study were expressed and purified as described in chapter 3;[2] chiral diol substrates **3** were synthesized according to the procedure reported in chapter 3.[2] Furthermore, chemical synthesis of amino alcohols references is also reported in chapter 3.[2]

4.4.1 Enzymes used in this study

Table 4.11. Source and expression conditions for enzymes used in this study. For the definition of enzyme classes, see abbreviations list

Name	Source/Comment	Plasmid	Tag	Expression /Purification	Used form	Ref
Fus-SMO (1) + Cb-FDH (2)	Fused SMO coexpressed with Cb-FDH	pET28b/pET 21a	N-His_6 (1)/No-Tag (2)	Ref. [34]	lyophilized whole cells	34
Sp(S)-EH	*Sphingomonas* sp. HXN200	pET28b	N-His_6	1 mM IPTG, 25 °C 16 h	lyophilized whole cells	35
St(R)-EH	*Solanum tuberosum*	pET28b	N-His_6	1 mM IPTG, 25 °C 16 h	lyophilized whole cells	35
Aa-ADH	*Aromatoleum aromaticum*	pET28b	N-His_6	Ref. [36]	purified	29
Ls-ADH	*Leifsonia* sp.	pET21a	no Tag	0.5 mM IPTG, 25 °C 16 h	purified	32
Bs-BDHA	*Bacillus subtilis* BGSC1A1	pET28b	N-His_6	0.5 mM IPTG, 25 °C 16 h	purified	31
Bs-AlaDH	*Bacillus sphaericus*	pET28b-v	N-$Strep_3$	0.5 mM IPTG, 25 °C 16 h	purified	33
Cv(S)-ωTA	*Chromobacterium violaceum* DSM 30191	pET28b-v	N-His_6	0.5 mM IPTG, 25 °C 16 h	purified	26
At(R)-ωTA	*Aspergillus terreus*	pET21a	C-His_6	0.5 mM IPTG, 25 °C 16 h	purified	23, 24
Ac(S)-ωTA	*Arthrobacter citreus*	pET28b-v	N-His_6	0.5 mM IPTG, 25 °C 16 h	purified	12
Bm(S)-ωTA	*Bacillus megaterium* SC6394	pET28b-v	N-His_6	0.5 mM IPTG, 25 °C 16 h	purified	27, 12

Table 4.11. *(Continued)*

Name	Source/Comment	Plasmid	Tag	Expression /Purification	Used form	Ref
Vf(S)-ωTA	*Vibrio fluvialis*	pET28b-v	N-His_6	0.5 mM IPTG, 25 °C 16 h	lyophilized whole cells	11, 28
As(R)-ωTA	*Arthrobacter* species	pET21a	C-His_6	0.5 mM IPTG, 25 °C 16 h	purified	25

4.4.1.1 General procedures for expression and purification of enzymes

Important note: in the case of transaminases, protein concentration was determined according to Bradford assay using Ovalbumin as standard protein.[13]

Expression of the enzymes: For recombinant expression, 800 mL of LB medium supplemented with the appropriate antibiotic (100 µg mL^{-1} ampicillin or 50 µg mL^{-1} kanamycin) were inoculated with 15 mL of an overnight culture harboring the desired vector with genes for the expression of the enzymes. *E. coli* BL21 DE3 cells were used as host organism. Cells were grown at 37 °C until an OD600 of 0.6 to 1 was reached, and expression of protein was induced by the addition of IPTG. Protein expression was carried out overnight and, after harvesting of the cells (4 °C, 4500 rpm, 10 min), the remaining cell pellets were washed with buffer (for lyophilized cells: 50 mM Tris-HCl buffer, pH 8.0 for ADHs and 50 mM KPi, pH 8.0 for EHs; or lysis buffer for enzymes that were subsequently purified by affinity chromatography).

Purification by Nickel affinity chromatography: His_6-tagged proteins were resuspended in lysis buffer (50 mM KH_2PO_4, 300 mM NaCl, 10 mM imidazole, pH 8.0) prior to cell disruption and protein purification was performed by Ni-NTA affinity chromatography using pre-packed Ni-NTA HisTrap HP columns (GE Healthcare), previously equilibrated with lysis buffer. After loading of the filtered lysate, the column was washed with sufficient amounts of wash buffer (50 mM KH_2PO_4, 300 mM NaCl, 25 mM imidazole, pH 8.0), and bound protein was recovered with elution buffer (50 mM KH_2PO_4, 300 mM NaCl, 200 mM imidazole, pH 8.0). Purity was analyzed by SDS-PAGE and fractions showing >95% purity were combined and dialyzed overnight against Tris-HCl buffer (6 L, pH 8.0, 20 mM). The enzyme solutions were concentrated and their concentration was determined spectrophotometrically based on their extinction coefficient at 280 nm.

Purification by Strep affinity chromatography: 3N-strep-tagged proteins were resuspended in binding buffer (100 mM Tris-HCl, 150 mM NaCl and 1 mM EDTA, pH 8.0) prior to cell disruption and protein purification was performed by Strep affinity chromatography using pre-packed columns (GE Healthcare), previously equilibrated with

binding buffer. The supernatant was split in 4 aliquots after filtration (typically 4 x 10 mL). Bound protein was recovered with elution buffer (100 mM Tris-HCl, 150 mM NaCl, 1 mM EDTA and 2.5 mM desthiobiotin, pH 8.0). All the aliquots were reloaded three times on the column. Purity was analyzed by SDS-PAGE and fractions showing >95% purity were combined and dialyzed overnight against Tris-HCl buffer (6 L, pH 8.0, 20 mM). The enzyme solutions were concentrated and their concentration was determined spectrophotometrically based on their extinction coefficient at 280 nm.

4.4.2 General procedure for initial tests with Aa-ADH and two stereocomplementary ωTAs

Lyophilized whole *E. coli* cells carrying overexpressed either Cv(S)-ωTA (20 mg mL^{-1}) or At(R)-ωTA (20 mg mL^{-1}) were rehydrated in an Eppendorf tube (1.5 mL) in Tris-HCl buffer (0.5 mL, pH 7.5, 50 mM) containing L-or D-alanine (50 mM, 5 eq.), PLP (1 mM), NAD^+ (1 mM) and LDH (1 mg mL^{-1}). Then purified Aa-ADH (50 µM) was also added followed by substrate **3** (either (1*S*,2*S*)-**3** or (1*R*,2*R*)-**3**) (10 mM). The mixture incubated at 30 °C, 170 rpm for 48 h on an orbital shaker. The mixture was quenched with 10 M KOH (100 µL) and extracted with MTBE (1 x 500 µL). The organic layer was dried over $MgSO_4$ and analyzed by GC-MS (method A).

4.4.3 One pot bio-catalytic conversion of optically active substrate 3 by purified ADHs coupled with purified stereocomplementary ωTAs

$HCOONH_4$ buffer (0.5 mL, pH 8.5, 1 M) supplemented with NAD^+ (1 mM), PLP (1mM) and D or L-Alanine (5 eq.) was added to an Eppendorf tube (1.5 mL) followed by Bs-AlaDH (20 µM), ADH (35-70 µM) and ωTA (35-70 µM). Chiral substrate **3** (10-20 mM) was added as last. The mixture was incubated at 30 °C (otherwise stated), 170 rpm for 48 h on an orbital shaker. The mixture was then quenched with 10 M KOH (100 µL), the aqueous layer saturated with solid NaCl and the extraction was performed with MTBE (1 x 500 µL). The organic layer was dried over $MgSO_4$ and analyzed by GC-FID (method B). Before quenching, an aliquot of the aqueous phase was derivatized with GITC (2,3,4,6-Tetra-O-acetyl-β-D-glucopyranosyl isothiocyanate) and analyzed by RP-HPLC (method C).

General procedure for the derivatization of the amino alcohol products to determine *er*, *dr* and *rr*[37]

The aqueous reaction mixture (20 µL) was dissolved in acetonitrile (180 µL) to yield a final concentration of 0.5 mM. Then, GITC (2,3,4,6-Tetra-O-acetyl-β-D-glucopyranosyl isothiocyanate) (1.5 mM) and Et_3N (1.5 mM) were added as a solution in acetonitrile (200 µL). The mixture was incubated at room temperature at 1000 rpm for 35 min. Before injection into the RP-HPLC, the samples were centrifuged and filtered if required.

Examples for the calculation of *er, dr* and *rr.*

These examples refer to the data reported for the conversion of substrate (1*R*,2*R)*-**3** by the catalytic system Aa-ADH/At(R)-ωTA **(1)** and Aa-ADH/As(R)-ωTA **(2)**. For more details see section 4.2.3.2, Table 4.7, entry 5 and 6. The same principle was applied to determine the *e.r.* and *d.r.* for all the other tested catalytic systems described in this thesis. Note that, in most of the cases not all isomers were formed during the reactions, hence they were not included in the calculations (see Tables in results and discussion). The isomers distribution was determined by RP-HPLC after derivatization with GITC (**Figure 4.2**).

Example (1): Aa-ADH/At(R)-ωTA	**Example (2):** Aa-ADH/As(R)-ωTA
er (**5'**) = (1*S*,2*R*)-**5'**:(1*R*,2*S*)-**5' =** >99.5:<0.5	*er* (**5'**) = (1*S*,2*R*)-**5'**:(1*R*,2*S*)-**5' =** >99.5:<0.5
dr (**5'**) = (1*S*,2*R*)-**5'**: (1*R*,2*R*)-**5' =** 95:5	*dr* (**5'**) = (1*S*,2*R*)-**5'**: [(1*R*,2*R*)-**5'** + (1*S*,2*S*)-**5'**] **=** >99.5:<0.5
rr (**5':5**) = [(1*S*,2*R*)-**5'** + (1*R*,2*R*)-**5'**]: (1*R*,2*R*)-**5** = 91:9	*rr* (**5':5**) = (1*S*,2*R*)-**5'** : (1*R*,2*R*)-**5** = 92:8

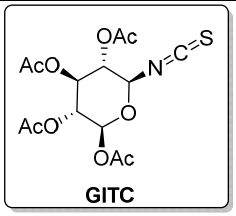

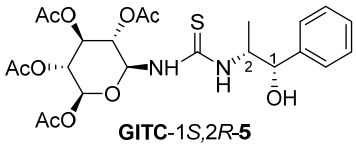

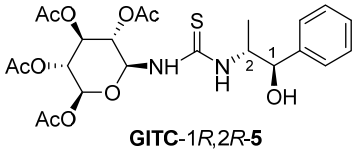

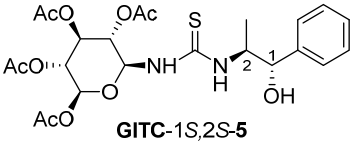

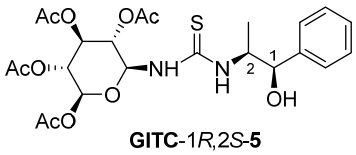

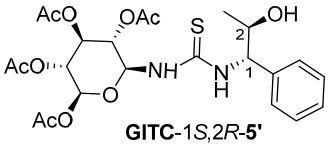

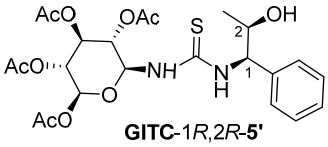

Figure 4.2. Derivatized amino alcohols for *er*, *dr* and *rr* determination

4.4.4 Analytical methods

GC-MS Method A: Column Agilent DB-1701 (30 m, 250 µm, 0.25 µm); injector temperature 250 °C; constant pressure 71.8 kPa; temperature program: 80 °C/hold 6.5 min; 160 °C/rate 10 °C min^{-1}/hold 5 min; 200 °C/rate 20 °C min^{-1}/hold 2 min; 280 °C/rate 20 °C min^{-1}/hold 1 min.

GC-FID Method B: Column: Agilent J&W DB1701 (30 m, 250 µm, 0.25 µm). Carrier gas: H_2 Parameter: T injector 250 °C; constant pressure 6.9 psi; temperature program: 80 °C, hold 6.5 min; gradient 5 °C min^{-1} up to 160 °C, hold 5 min; gradient 20 °C min^{-1} up to 200 °C, hold 2 min; gradient 20 °C min^{-1} up to 280 °C, hold 4 min.

RP-HPLC Method C: Column: Nucleosil C_{18} HD (0.46 cm x 25 cm): HPLC program: constant oven temperature 30 °C; eluent composition: isocratic MeOH + 0.1% TFA/MilliQ + 0.1% TFA 50:50; flow rate: 1 mL min^{-1}, detection at 248 nm.

Table 4.12. Retention times and associated analytical methods

Compound	Retention time [min]	Method
(1*S*,2*R*)-**5'**	22.4	B
	13.8	C
(1*R*,2*S*)-**5'**	22.3	B
	17.2	C
(1*R*,2*R*)-***5'***	21.9	B
	15.7	C
(1*S*,2*S*)-**5'**	21.8	B
	18.5	C
8'	21.1	B

For the retention times of chiral substrates **3** (all four isomers), chiral amino alcohols **5** (all four isomers), compounds **4**, **4'**, **7** and **8** and associated methods see chapter 3.

4.5 References

1. T. Sehl, Z. Maugeri and D. Rother, *J. Mol. Catal. B: Enzym.*, 2015, 114, 65-71.
2. M. L. Corrado, T. Knaus and F. G. Mutti, *Green Chem.*, 2019, 21, 6246-6251.
3. G. Grue-Soerensen and I. D. Spenser, *J. Am. Chem. Soc.*, 1994, 116, 6195-6200.
4. R. Krizevski, E. Bar, O. Shalit, Y. Sitrit, S. Ben-Shabat and E. Lewinsohn, *Phytochemistry*, 2010, 71, 895-903.
5. R. Krizevski, N. Dudai, E. Bar and E. Lewinsohn, *J. Ethnopharmacol.*, 2007, 114, 432-438.
6. M. Breuer, K. Ditrich, T. Habicher, B. Hauer, M. Kesseler, R. Sturmer and T. Zelinski, *Angew. Chem. Int. Ed.*, 2004, 43, 788-824.
7. P. Gupta and N. Mahajan, *New J. Chem.*, 2018, 42, 12296-12327.
8. D. J. Ager, I. Prakash and D. R. Schaad, *Chem. Rev.*, 1996, 96, 835-876.
9. K. Everaere, A. Mortreux and J.-F. Carpentier, *Adv. Synth. Catal.*, 2003, 345, 67-77.
10. F. G. Mutti, T. Knaus, N. S. Scrutton, M. Breuer and N. J. Turner, *Science*, 2015, 349, 1525-1529.

11. F. G. Mutti, C. S. Fuchs, D. Pressnitz, N. G. Turrini, J. H. Sattler, A. Lerchner, A. Skerra and W. Kroutil, *Eur. J. Org. Chem.*, 2012, 2012, 1003-1007.
12. N. van Oosterwijk, S. Willies, J. Hekelaar, A. C. Terwisscha van Scheltinga, N. J. Turner and B. W. Dijkstra, *Biochemistry*, 2016, 55, 4422-4431.
13. W. Bohmer, T. Knaus, A. Volkov, T. K. Slot, N. R. Shiju, K. Engelmark Cassimjee and F. G. Mutti, *J. Biotechnol.*, 2019, 291, 52-60.
14. D. Koszelewski, K. Tauber, K. Faber and W. Kroutil, *Trends Biotechnol.*, 2010, 28, 324-332.
15. P. Kelefiotis-Stratidakis, T. Tyrikos-Ergas and I. V. Pavlidis, *Org. Biomol. Chem.*, 2019, 17, 1634-1642.
16. M. D. Patil, G. Grogan, A. Bommarius and H. Yun, *Catalysts*, 2018, 8, 254.
17. A. W. H. Dawood, M. S. Weiß, C. Schulz, I. V. Pavlidis, H. Iding, R. O. M. A. de Souza and U. T. Bornscheuer, *ChemCatChem*, 2018, 10, 3943-3949.
18. N. Richter, J. E. Farnberger, D. Pressnitz, H. Lechner, F. Zepeck and W. Kroutil, *Green Chem.*, 2015, 17, 2952-2958.
19. A. Lerchner, A. Jarasch and A. Skerra, *Biotechnol. Appl. Biochem.*, 2016, 63, 616-624.
20. T. Sehl, H. C. Hailes, J. M. Ward, U. Menyes, M. Pohl and D. Rother, *Green Chem.*, 2014, 16, 3341-3348.
21. T. Sehl, H. C. Hailes, J. M. Ward, R. Wardenga, E. von Lieres, H. Offermann, R. Westphal, M. Pohl and D. Rother, *Angew. Chem. Int. Ed.*, 2013, 52, 6772-6775.
22. X. Wu, M. Fei, Y. Chen, Z. Wang and Y. Chen, *Appl. Microbiol. Biotechnol.*, 2014, 98, 7399-7408.
23. A. Lyskowski, C. Gruber, G. Steinkellner, M. Schurmann, H. Schwab, K. Gruber and K. Steiner, *PloS One*, 2014, 9, e87350.
24. F. G. Mutti, C. S. Fuchs, D. Pressnitz, J. H. Sattler and W. Kroutil, *Adv. Synth. Catal.*, 2011, 353, 3227-3233.
25. A. Iwasaki, Y. Yamada, N. Kizaki, Y. Ikenaka and J. Hasegawa, *Appl. Microbiol. Biotechnol.*, 2006, 69, 499-505.
26. U. Kaulmann, K. Smithies, M. E. B. Smith, H. C. Hailes and J. M. Ward, *Enzyme Microb. Technol.*, 2007, 41, 628-637.
27. R. L. Hanson, B. L. Davis, Y. Chen, S. L. Goldberg, W. L. Parker, T. P. Tully, M. A. Montana and R. N. Patel, *Adv. Synth. Catal.*, 2008, 350, 1367-1375.
28. J. S. Shin, H. Yun, J. W. Jang, I. Park and B. G. Kim, *Appl. Microbiol. Biotechnol.*, 2003, 61, 463-471.
29. H. W. Hoffken, M. Duong, T. Friedrich, M. Breuer, B. Hauer, R. Reinhardt, R. Rabus and J. Heider, *Biochemistry*, 2006, 45, 82-93.
30. J. Zhang, S. Wu, J. Wu and Z. Li, *ACS Catal.*, 2014, 5, 51-58.
31. J. Zhang, T. Xu and Z. Li, *Adv. Synth. Catal.*, 2013, 355, 3147-3153.
32. K. Inoue, Y. Makino and N. Itoh, *Appl. Environ. Microbiol.*, 2005, 71, 3633-3641.
33. T. Ohashima and K. Soda, *Eur. J. Biochem.*, 1979, 100, 29-30.
34. M. L. Corrado, T. Knaus and F. G. Mutti, *ChemBioChem*, 2018, 19, 679-686.
35. S. Wu, Y. Chen, Y. Xu, A. Li, Q. Xu, A. Glieder and Z. Li, *ACS Catal.*, 2014, 4, 409-420.
36. W. Bohmer, T. Knaus and F. G. Mutti, *ChemCatChem*, 2018, 10, 731-735.
37. M. S. Malik, E.-S. Park and J.-S. Shin, *Green Chem.*, 2012, 14, 2137.

Chapter 5

Multi-enzymatic cascades for the synthesis of optically active phenylethanolamine isomers

Part of this chapter is based on the following publication:

Maria L. Corrado, Tanja Knaus, Jan Vilím and Francesco G. Mutti, multi-enzymatic cascades for the synthesis of optically active phenylethanolamine isomers, *manuscript in preparation.*

Abstract. *In this work, multi-enzymatic cascades were investigated for the one-pot synthesis of optically active 2-amino-2-phenylethan-1-ol and 2-amino-1-phenylethan-1-ol. Each couple of enantiomers was obtained in high conversions (analytical yields 70-97%) as well as perfect enantioselectivity (ee >99%) through stereocomplementary multi-enzymatic cascades. Optically pure* (*S*)*-2-amino-2-phenylethan-1-ol and* (*R*)*-2-amino-2-phenylethan-1-ol could be obtained starting from substrate* (*R*)*-1-phenylethane-1,2-diol by pairing an Aa-ADH from* Aromatoleum aromaticum *with one of the two stereocomplementary ωTAs, namely At(R)-ωTA from* Aspergillus terreus *and Bm(S)-ωTA from* Bacillus megaterium *SC6394, respectively. On the other hand, an orthogonal bioamination cascade was designed for the enzymatic synthesis of optically pure* (*S*)*-2-amino-1-phenylethan-1-ol and* (*R*)*-2-amino-1-phenylethan-1-ol. In these cases, an alcohol oxidase variant of choline oxidase from* Arthrobacter chlorophenolicus *(AcCO6) was combined with Ch1-AmDH. Thus, either* (*S*)*-1-phenylethane-1,2-diol or* (*R*)*-1-phenylethane-1,2-diol were converted to the optically active vicinal amino alcohol 2-amino-1-phenylethan-1-ol (analytical yield 98%) with full retention of the substrates stereochemistry (ee up to >99%).*

5.1 Introduction

Chiral β-amino alcohols motifs are widely spread in biologically active compounds and bioactive natural products such as antibiotics, neurotransmitters, β-adrenergic blockers as well as anti-HIV drugs.[1-3] Furthermore, these highly valuable moieties find large application in asymmetric organic synthesis, for instance as ligand, chiral auxiliaries and even catalysts.[4-6] Among the vast class of 1,2-amino alcohols, phenylethanolamines play a central role in this context. **Figure 5.1** provides a selection of bioactive compounds containing this pattern.

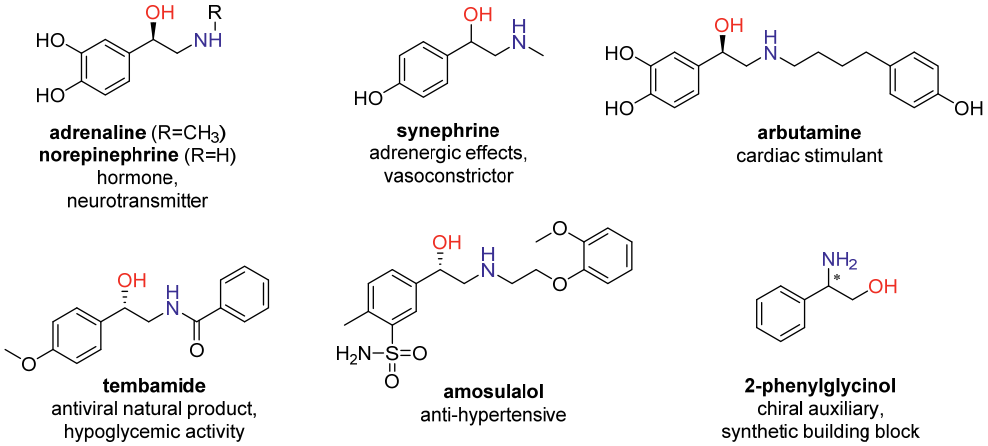

Figure 5.1. Examples of biologically active compounds carrying the phenylethanolamine moiety.

The availability of highly selective asymmetric synthesis methods is necessary for obtaining these valuable compounds in high optical purity. Many chemical methods were reported throughout the years such as the Sharpless asymmetric aminohydroxylation of terminal olefins,[7,8] asymmetric hydrogenation of prochiral amino ketones[9] as well as epoxide ring-opening with amines.[10-13] Nevertheless, these methods have some limitations regarding their selectivity due to the often failure in affording enantiomerically pure compounds and/or the requirement for toxic metals and reagents in suprastochiometric amount.[14-16] Consequently, resolution techniques are still widely used for the preparation of optically pure amino alcohols.[9] Various biocatalytic strategies for the synthesis of chiral 1,2-amino alcohols have also been developed.[17-26] However, only few methods are currently available for the target synthesis of phenylethanolamines.[18,23,27,28] Sello *et al.* envisioned the ring-opening of styrene oxide—previously formed in the bio-epoxidation of styrene with a styrene monooxygenase—by ammonia under microwave irradiation.[29] On the other hand, Sun *et al.* reported a multi-enzymatic

cascade for the asymmetric synthesis of (*R)*-phenylglycinol ((*R*)-**5a**) starting from racemic styrene oxide.[30] An interesting chemo-enzymatic method was reported by Schrittwieser *et al.*, in which a one-pot three-step enzymatic process converted a series of halo ketones to the correspondent amino alcohols including the natural antiviral (*S*)-tembamide product.[3] Few years later, Wu *et al.* reported the conversion of styrene to (*S*)-2-amino-2-phenylethan-1-ol ((*S*)-**5a**) by modular cascade biocatalysis.[31] More recently, Cho *et al.* described the direct enantioselective aminohydroxylation of olefins to unprotected amino alcohols catalyzed by an engineered haemoprotein.[2]

In this work, we present two distinct one-pot multi-enzymatic cascades for the synthesis of optically pure 2-amino-2-phenylethan-1-ol (**5a**) and 2-amino-1-phenylethan-1-ol (**5a'**). In the first case, (*R*)-**3a** was converted to either (*S*)-**5a** or (*R*)-**5a** by pairing a "secondary NAD^+-dependent" ADH (Aa-ADH from *Aromatoleum aromaticum*[32] that oxidizes substrate **3a** to the hydroxyketone intermediate **4a** with one between two stereocomplementary ω-transaminases (At(*R*)-ωTA from *Aspergillus terreus*[33,34] and Bm(*S*)-ωTA from *Bacillus megaterium* (SC6394),[35, 36] respectively for (*S*)-**5a**) and (*R*)-**5a** . Both products were obtained with elevated analytical yields (70-97%) and high optical purity (*ee* >99%). Moreover, an alanine dehydrogenase (Bs-AlaDH from *Bacillus sphaericus*)[37] was added to close the catalytic cycle. This enzyme requires ammonia, sourced from the buffer, and NADH that is regenerated in situ through the reaction catalyzed by the ADH in the oxidation step of the cascade. Thus, Bs-AlaDH converts the pyruvate by-product, which is originated from the transamination reaction, back to alanine; NAD^+ is concomitantly regenerated and re-enters the cycle in the oxidation step catalyzed by the ADH (**Scheme 5.1B**).

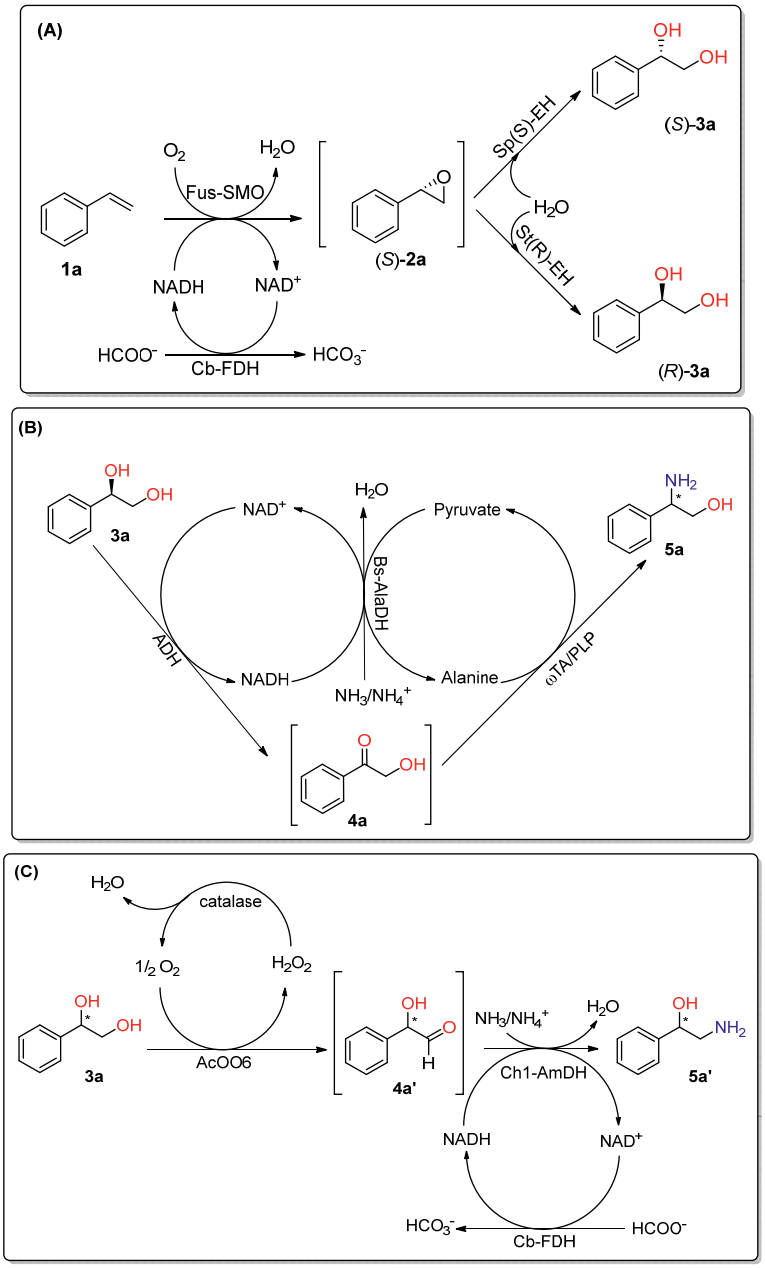

Scheme 5.1. Biocatalytic cascades for the multi-enzymatic synthesis of optically pure phenylethanolamine. **A)** one-pot cascade for the enantioselective dihydroxylation of styrene **1a** (20-50 mM) in KPi buffer (pH 8.0, 50 mM)/heptane (1:1 v v^{-1}) using *E. coli*/Fus-SMO/Cb-FDH (5 mg mL^{-1}), *E.coli*/Sp(*S*)-EH or St(*R*)-EH (20 mg mL^{-1}), HCOONa (5 eq.), NAD^+ (1 mM), FAD (50 µM) and catalase (0.1 mg mL^{-1}); **B)** One-pot multi-enzymatic cascade for the enantioselective amination (ADH/TA/AlaDH) of **3a** (10 mM) in $HCOONH_4$ buffer (pH 8.5, 1 M), NAD^+ (1 mM), PLP (1 mM), L/D-Alanine (50 mM, 5 eq.); **C)** Orthogonal bioamination cascade (AcCO6/AmDH) of **3a** (10 mM) in $HCOONH_4$ buffer (pH 8.5, 1 M), NAD^+ (1 mM), catalase (0.1 mg mL^{-1}) and Cb-FDH (10 µM).

On the other hand, the approach for the synthesis of optically active **5a'** consists in an orthogonal bioamination cascade.[38, 39] In fact, the oxidation of either (*S*)-**3a** or (*R*)-**3a** is carried out by an alcohol oxidase (AcCO6 variant of choline oxidase from *Arthrobacter chlorophenolicus*)[40] followed by reductive amination of the hydroxyaldehyde intermediate **4a'** catalyzed by an AmDH (Ch1-AmDH).[41] This results in the formation of optically active vicinal amino alcohols (*S*)-**5a'** and (*R*)-**5a'** in high analytical yield (98%) and full retention of the substrates stereochemistry (*ee* up to >99%). The cascade entails two more enzymes: a catalase is needed in the oxidation step for the disproportion of H_2O_2 and a formate dehydrogenase (Cb-FDH from *Candida boidinii*)[42] is required for NADH recycling at the expenses of formate present in the reaction buffer (**Scheme 5.1C**). Furthermore, these cascades integrate into the biocatalytic retrosynthesis strategy in which optically active diol substrates (e.g., **3a**) are obtained through a one-pot bio-epoxidation of styrene **1a** (catalyzed by a fused-styrene monooxygenase, Fus-SMO)[43] followed by epoxide hydrolysis. The use of stereocomplementary epoxide hydrolases (EHs)[44] gives access to both enantiomers of **3a** (**Scheme 5.1A**).

5.2 Results and discussion

5.2.1 Synthesis of chiral diols

5.2.1.1 Screening of organic solvents for the biphasic system

The chiral diol substrates **3a** were enzymatically synthesized by a one-pot cascade conversion of styrene; the engineered styrene monooxygenase (Fus-SMO)[43] was combined with two stereocomplementary epoxide hydrolases (EHs)[44] in the form of lyophilized *E. coli* whole cells (**Scheme 5.2**).

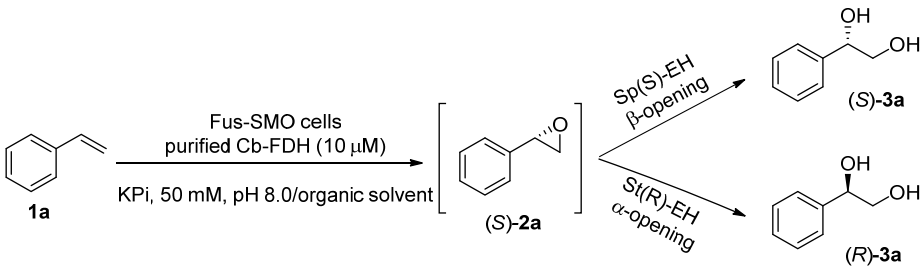

Scheme 5.2. One-pot cascade for the enantioselective dihydroxylation of styrene (**1a**).

It is reported in literature that it is advantageous to perform the epoxidation step in a biphasic system in order to limit substrate volatility as well as "confine" the epoxide, which can exert molecular toxicity, in the organic phase. In fact, the epoxidations catalyzed by styrene monooxygenases are mainly reported in

hexadecane/aqueous buffer.[44, 45] However, hexadecane has a very high boiling point that implies the consumption of a lot of energy for solvent evaporation and lengthy product drying. As shown in **Table 5.1**, various solvents (v v^{-1}) were tested with the aim of finding an organic solvent with a lower boiling point. We mainly tested *n*-hexane, *n*-heptane and *n*-decane as possible candidates. While *n*-heptane and *n*-hexane (entry 1, 4, 5 and 8) gave comparable results, *n*-heptane turned out to be the best solvent choice due to the slightly higher boiling point compared with *n*-hexane. Notably, the system performed very well when the reaction was run in buffer only (entry 2 and 6) or when 2-10% *n*-decane was added. Furthermore, the one-pot epoxidation/hydrolysis was also performed in neat styrene, hence acting simultaneously as organic solvent and substrate (entry 3 and 7). Though the conversions did not exceed 3%, the same productivity was observed as for the optimal reaction conditions comprising a 1:1 (v v^{-1}) KPi/*n*-heptane mixture as solvent system. Nonetheless, **Table 5.1** shows that high enantioselectivity was always reached for all screened conditions.

Table 5.1. Bio-conversion of **1a** (20 mM) to chiral **3a** by Fus-SMO paired with one between two stereocomplementary EHs in different solvent systems.

Entry	EH	KPi buffer (pH 8.0, 50 mM) [µL]	Organic solvent	Conversion [%][b]	*ee* [%][a]
1	Sp(*S*)-EH	500	[0.5 mL] hexane (50%)	>99	>99 (*S*)
2	Sp(*S*)-EH	1000	-	>79	99 (*S*)
3	Sp(*S*)-EH	950	[50 µL] styrene (5%)	2.5	n.m.
4	Sp(*S*)-EH	500	[0.5 mL] heptane (50%)	>90	98 (*S*)
5	St(*R*)-EH	500	[0.5 mL] hexane (50%)	>99	97 (*R*)
6	St(*R*)-EH	1000	-	>88	97 (*R*)
7	St(*R*)-EH	950	[50 µL] styrene (5%)	3	n.m.
8	St(*R*)-EH	500	[500 mL] heptane (50%)	>99	97 (*R*)
9	Sp(*S*)-EH	980	[20 µL] decane (2%)	>80	99 (*S*)
10	Sp(*S*)-EH	960	[40 µL] decane (4%)	>72	>98 (*S*)
11	Sp(*S*)-EH	940	[60 µL] decane (6%)	>78	99 (*S*)
12	Sp(*S*)-EH	920	[80 µL] decane (8%)	>63	99 (*S*)
13	Sp(*S*)-EH	900	[100 µL] decane (10%)	>59	99 (*S*)
14	St(*R*)-EH	980	[20 µL] decane (2%)	>66	97 (*R*)
15	St(*R*)-EH	960	[40 µL] decane (4%)	>60	97 (*R*)
16	St(*R*)-EH	940	[60 µL] decane (6%)	>55	97 (*R*)
17	St(*R*)-EH	920	[80 µL] decane (8%)	>54	98 (*R*)
18	St(*R*)-EH	900	[100 µL] decane (10%)	>70	97 (*R*)

[a]Analyzed by chiral HPLC (OD-H column); n.m. = not measured. [b]Reactions were all performed in duplicate and the results reported are the average of the two samples.

The next step was to co-express the Fus-SMO along with the NADH-recycling enzyme (Cb-FDH) in the same host organisms, as previously demonstrated by us,[43] and use it as lyophilized whole cells for the synthesis of chiral 1-phenylpropane-1,2-diols **3a.**[46] Under optimized conditions, the (*R*)- and (*S*)- enantiomers of **3a** were synthesized by using the one-pot cascade depicted in **Scheme 5.3**. After extraction, the desired chiral diols were isolated in 240 mg (67% isolated yield; *ee* >99% (*R*); *ee* >98% (*S*)).

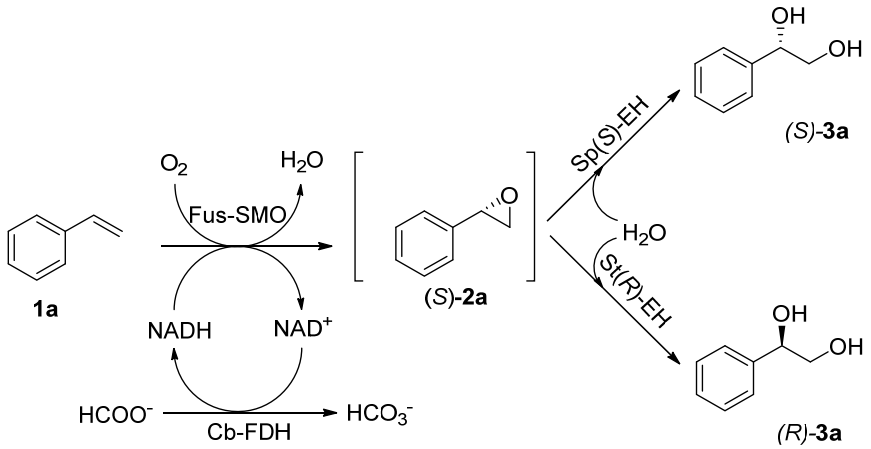

Scheme 5.3. One-pot biocatalytic epoxidation/hydrolysis of **1a** (50 mM) catalyzed by co-expressed Fus-SMO/Cb-FDH as *E. coli* whole cells (5 mg mL^{-1}) and *E. coli* whole cells carrying either Sp(*S*)-EH or St(*R*)-EH (20 mg mL^{-1}), in KPi buffer (pH 8.0, 50 mM)/heptane (1:1 v v^{-1}) supplemented with FAD (50 µM), HCOONa (5 eq.), NAD^+ (1 mM) and catalase (0.1 mg mL^{-1}).

5.2.2 Screening secondary $NAD(P)^+$-dependent ADHs

5.2.2.1 Biocatalytic reduction of substrate 4a

The bio-reduction of 2-hydroxyacetophenone **4a** (20 mM) was initially investigated by screening ten secondary $NAD(P)^+$-dependent ADHs: Aa-ADH from *Aromatoleum aromaticum,*[32] Lbv-ADH variant from *Lactobacillus brevis,*[47] Pp-ADH from *Paracoccus pantotrophus* (DSM 11072),[48] Sy-ADH from *Sphingobium yanoikuyae* (DSM 6900),[49] Bs-BDHA from *Bacillus subtilis* (BGSC1A1),[50, 51] Te-$ADH_{v1,v2,v3}$ variant from *Thermoanaerobacter ethanolicus,*[38] Lb-ADH from *Lactobacillus brevis*[52] and Rs-ADH from *Ralstonia sp.*[53] The reactions were carried out in Tris-HCl buffer (pH 7.5, 50 mM, 1 mL final volume) and an internal NAD(P)H recycling system was included (for NADH-dependent ADHs: 1 mM NAD^+, 100 mM HCOONa, 10 µM Cb-FDH; for NADPH-dependent ADHs: 1 mM $NADP^+$, 100 mM glucose, 1 mg mL^{-1} GDH as lyophilized crude extract from Codexis, GDH-105, ca. 50 U mg^{-1}). The general reaction is depicted in **Scheme 5.4**.

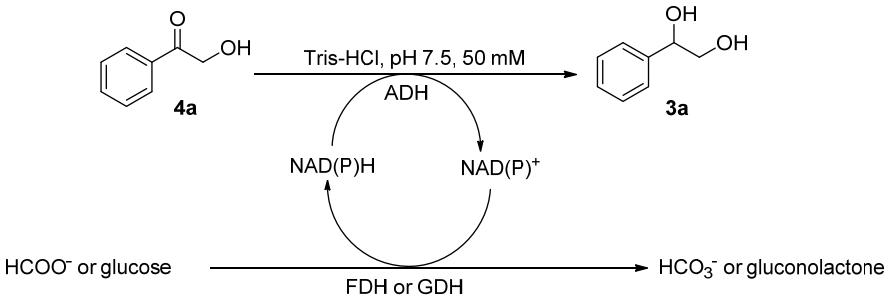

Scheme 5.4. Biocatalytic reduction of **4a** catalyzed by secondary NAD(P)H-dependent ADHs

The testing for suitable ADHs capable of performing such biotransformation is important because **4a** is also the intermediate in the cascade to the vicinal amino alcohol. We investigated the reduction of **4a** to get an initial understanding on the most active ADHs towards the aromatic substrates. As shown in **Table 5.2,** reactions catalyzed by Aa-ADH, Lbv-ADH, Bs-BDHA and Rs-ADH led to full conversion (entry 1, 2, 5 and 10), while Pp-ADH and Sy-ADH provided moderate conversions on this substrate (entry 3 and 4). Additionally, Lb-ADH showed also high conversion to diol **3a** (entry 9). On the other hand, among the three Te-ADH variants tested, only the use of Te-ADH$_{v1}$ afforded mediocre conversion into the diol compound (entry 6) while conversion was not observed at all by applying the other two variants (entry 7-8). In summary, most of the tested ADHs were active towards hydroxyketone **4a**, the exceptions being for variant 2 and 3 of Te-ADH.

Table 5.2. Biocatalytic reduction of **4a** (20 mM) catalyzed by secondary NAD(P)H-dependent ADHs in Tris-HCl buffer (pH 7.5, 50 mM)

Entry	ADH	Coenzyme	3a [%][b]	Catalyst form[a]
1	Aa-ADH	NADH	>99	Purified (N-His$_6$ tag)
2	Lbv-ADH	NADH	>99	Purified (no tag)
3	Pp-ADH	NADH	70	Lyophilized *E. coli* whole cells
4	Sy-ADH	NADH	42	Lyophilized *E. coli* whole cells
5	Bs-BDHA	NADH	>99	Lyophilized *E. coli* whole cells
6	Te-ADH$_{v1}$	NADPH	6	Lyophilized *E. coli* whole cells
7	Te-ADH$_{v2}$	NADPH	n.c.	Lyophilized *E. coli* whole cells
8	Te-ADH$_{v3}$	NADPH	n.c.	Lyophilized *E. coli* whole cells
9	Lb-ADH	NADPH	86	Purified (no tag)
10	Rs-ADH	NADPH	>99	Lyophilized *E. coli* whole cells

[a]For more details see section 5.4.1. [b]Reactions were performed in duplicate and the results reported are the average of the two samples; n.c. = no conversion.

5.2.2.2 Biocatalytic oxidation of *rac*-3a in Tris-HCl buffer

As above-mentioned, our interest is on the oxidation of **3a** (**Scheme 5.1B-C**). Hence, eleven secondary NAD(P)$^+$-dependent ADHs were also tested for the biocatalytic oxidation of *rac*-**3a** (20 mM) into the correspondent hydroxyketone **4a**. **Scheme 5.5** depicts the general reaction for the biocatalytic transformation. The first screening was performed in Tris-HCl buffer (pH 7.5, 50 mM; 1 mL final reaction volume) by using *rac*-**3a** (20 mM) as substrate. The reaction were run in the presence of either NAD$^+$ (1 mM) combined with NOX (10 µM) as internal (NAD$^+$) cofactor-recycling enzyme or NADP$^+$ (1 mM) combined with YcnD (10 µM) as internal (NADP$^+$) cofactor-recycling enzyme. The screened biocatalysts were used either as lyophilized *E. coli* whole cells (Bs-BDHA or Pp-ADH or Sy-ADH or Bs-BDHA or Ls-ADH or Te-ADH$_{v1, v2, v3}$; 20 mg mL^{-1}) or as purified enzymes (Aa-ADH or Lbv-ADH or Lb-ADH; 50 µM). Only reactions with Ls-ADH were carried out in KPi buffer (pH 6.5, 100 mM) since previous tests performed in our laboratory showed that this enzyme is more sensitive towards higher pH values.

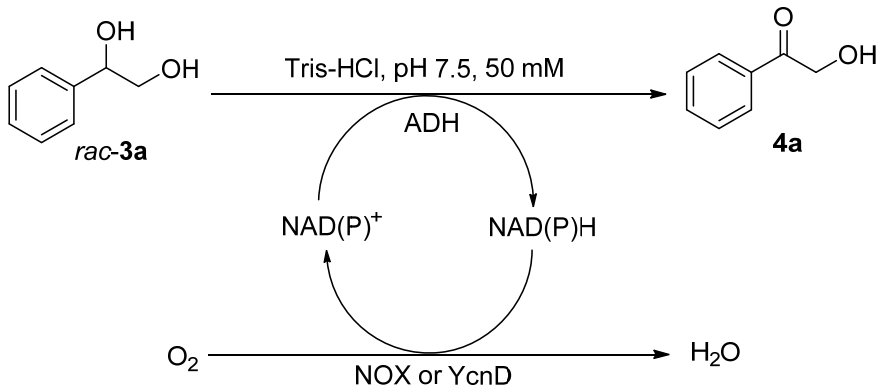

Scheme 5.5. Biocatalytic oxidation of *rac*-**3a** catalyzed by secondary NAD(P)$^+$-dependent ADHs

As reported in **Table 5.3**, conversion into the hydroxyketone **4a** was not detected at all for Pp-ADH, Sy-ADH, Te-ADH$_{v1}$, Te-ADH$_{v2}$ and Te-ADH$_{v3}$ (entry 2, 3 and 8-10); in contrast, moderate conversions were identified with both Ls-ADH and Rs-ADH (entry 6 and 12). Greater conversions were observed by applying Aa-ADH, LBv-ADH, Bs-BDHA and Lb-ADH (entry 1, 4, 5 and 11; consider that the substrate **3a** was used as racemate and that ADHs are supposed to be enantioselective). In fact, the reaction never reached completion in any of the investigated cases, which confirms the enantioselective behavior of the enzymes. We did not continue any further with Lb-ADH since this ADH is NADP$^+$-dependent and, at this stage, we decided to focus

on the subsequent reductive amination step that is catalyzed by NADH-dependent aminating enzymes. Interestingly, the 50% conversion threshold was surpassed in the case of Aa-ADH and Lbv-ADH, thus indicating that these ADHs can also convert the other, less favored, enantiomer; conversely, in the case of Bs-BDHA, the racemic substrate was only half converted to the desired product that indicates the enantioselectivity of the enzyme (entry 5). To prove that unequivocally, one should measure the *ee* of the unreacted diol after the oxidation. A further experiment was conducted with Aa-ADH and Lbv-ADH in which both were introduced together into the bio-catalytic system (25 µM each). As the two ADHs are stereocomplementary, we assumed that both enantiomers would have got oxidized. Indeed, 89% conversion was observed (entry 7). In general, four out of six NAD^+-dependent ADHs showed activity towards the oxidation of the *rac*-**3a**, albeit none of them led to full conversion. Moreover, compared with the bio-reduction of compound **4a** by the same ADHs (**Table 5.2**), only few enzymes showed also activity in the oxidation direction.

Table 5.3. Screening of secondary $NAD(P)^+$-dependent ADHs for the biocatalytic oxidation of *rac*-**3a** (20 mM) in Tris-HCl buffer (pH 7.5, 50 mM)

Entry	ADH	4a [%]	Coenzyme	Catalyst form[c]
1	Aa-ADH	71	NAD^+	Purified (N-His_6 tag)
2	Pp-ADH [b]	n.c.	NAD^+	Lyophilized *E. coli* whole cells
3	Sy-ADH [b]	n.c.	NAD^+	Lyophilized *E. coli* whole cells
4	Lbv-ADH	81	NAD^+	Purified (no tag)
5	Bs-BDHA	45	NAD^+	Lyophilized *E. coli* whole cells
6	Ls-ADH[54] [b]	14±1	NAD^+	Lyophilized *E. coli* whole cells
7	Aa-ADH[a] +Lbv-ADH[a]	89	NAD^+	Purified
8	Te-ADH_{v1}	n.c.	$NADP^+$	Lyophilized *E. coli* whole cells
9	Te-ADH_{v2}	n.c.	$NADP^+$	Lyophilized *E. coli* whole ells
10	Te-ADH_{v3}	n.c.	$NADP^+$	Lyophilized *E. coli* whole cells
11	Lb-ADH	58	$NADP^+$	Purified (no tag)
12	Rs-ADH	24	$NADP^+$	Lyophilized *E. coli* whole cells

[a]Used in 25 µM. [b] Reactions were performed in duplicate and the reported conversion is the average of the two samples; n.c. = no conversion. [c]For more details see section 5.4.1.

The next step was to disclose which ADH is active on which enantiomer of **3a**. Hence, the bio-oxidation was carried out by using the optically pure diols **3a** (10 mM) under the same reaction conditions as described above for the racemic substrate. From the results reported in **Table 5.4**, we can conclude that Lbv-ADH (no tag) is the only enzyme that accept the (*S*)-enantiomer (entry 4) while, as

expected, Aa-ADH and BDHA (entry 6 and 10) showed to be the active ones on the (*R*)-enantiomer.

Table 5.4. Screening of secondary NAD^+-dependent ADHs for the bio-oxidation of (*S*)-**3a** (10 mM) and (*R*)-**3a** (10 mM) in Tris-HCl buffer (pH 7.5, 50 mM).

Entry	Substrate	ADH	Coenzyme	4a [%]	Catalyst form[b]
1	(*S*)-**3a**	Aa-ADH[a]	NAD^+	n.c.	Purified (N-His_6 tag)
2	(*S*)-**3a**	Pp-ADH	NAD^+	n.c.	Lyophilized *E. coli* whole cells
3	(*S*)-**3a**	Sy-ADH	NAD^+	2	Lyophilized *E. coli* whole cells
4	(*S*)-**3a**	Lbv-ADH	NAD^+	>99	Purified (no tag)
5	(*S*)-**3a**	Bs-BDHA[a]	NAD^+	n.c.	Lyophilized *E. coli* whole cells
6	(*R*)-**3a**	Aa-ADH [a]	NAD^+	84±8	Purified
7	(*R*)-**3a**	Pp-ADH	NAD^+	2	Lyophilized *E. coli* whole cells
8	(*R*)-**3a**	Sy-ADH	NAD^+	1	Lyophilized *E. coli* whole cells
9	(*R*)-**3a**	Lbv-ADH [a]	NAD^+	1±<1	Purified (no tag)
10	(*R*)-**3a**	Bs-BDHA	NAD^+	69	Lyophilized *E. coli* whole cells

[a]Reactions were performed in duplicate and the reported conversion is the average of the two independent samples; n.c. = no conversion. [b]For more details see section 5.4.1.

5.2.2.3 Biocatalytic oxidation of substrate 3a by NAD^+-dependent ADHs in $HCOONH_4$ buffer

Up to this point, the selected ADHs were tested in Tris-HCl buffer. However, the subsequent reductive amination catalyzed by an amine dehydrogenase (AmDH)[39,46] was supposed to be carried out in $HCOONH_4$ buffer (pH 8.5, 1 M). For this reason, we investigated the bio-oxidation of *rac*-**3a** (10-20 mM) in this buffer. As before, an internal NAD^+-recycling system was included in the reaction cycle (NOx, 10 µM) as depicted in **Scheme 5.6**.

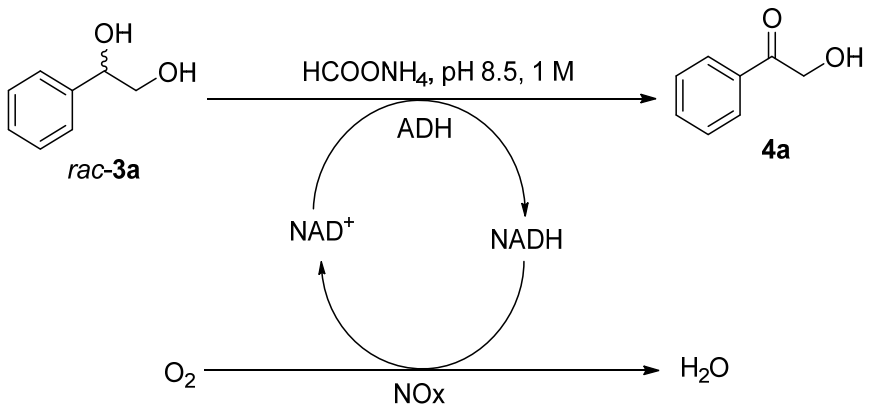

Scheme 5.6. Biocatalytic oxidation of *rac*-**3a** by secondary NAD^+-dependent ADHs in $HCOONH_4$ buffer.

As reported in **Table 5.5**, the reactions did not proceed as expected and according to the previous results observed in the bio-oxidation of *rac*-**3** in Tris-HCl buffer (pH 7.5, 50 mM). The poor activity of Lbv-ADH (conv. 7%; entry 4) is, for instance, remarkable. Nevertheless, the use of Aa-ADH, Ls-ADH and Bs-BDHA (entry 1-3) led from moderate to good conversions considering that substrate **3a** was used as racemate. Furthermore, the reactions were run at 20 mM substrate concentration in the case of Aa-ADH, Bs-BDHA and Ls-ADH. Finally, as an extra test, the biocatalytic oxidation was performed in the presence of concomitantly added Lbv-ADH and Aa-ADH (25 µM each) in the same pot. However, conversion did not increase than when Aa-ADH was used as catalyst alone (entry 1 *vs*. entry 5).

Table 5.5. Biocatalytic oxidation of *rac*-**3a** (10-20 mM) by secondary $NAD(P)^+$-dependent ADHs (50 µM) in $HCOONH_4$ buffer (pH 8.5, 1 M, 30 °C).

Entry	*rac*-3a [mM]	ADH	4a [%][b]	Catalyst form
1	20	Aa-ADH	32±<1	Purified (N-His_6 tag)
2	20	Bs-BDHA	28±<1	Purified (N-His_6 tag)
3	20	Ls-ADH	23±<1	Purified (no tag)
4	10	Lbv-ADH	7±<1	Purified (His_6)
5	10	Aa-ADH[a] + Lbv-ADH[a]	33±<1	Purified

[a]Used in 25 µM. [b]All reactions were performed in duplicate and the reported conversion is the average of the two independent samples.

Nonetheless, the low activity of the tested ADHs in $HCOONH_4$ buffer may be caused by the high ionic strength of the buffer (*i.e*., concentration of 1 M).Furthermore, the batch of Lbv-ADH used in this last study was expressed and purified as a His_6-tagged protein while the batch used in Tris-HCl for the reduction/oxidation was expressed and purified as no tagged protein. It has previously been reported that

the presence of poly-histidine tag on the enzyme may influence the outcome of the reaction due to different types of interactions.[39] Finally, one must also consider a possible variation in the catalytic performance of NOX from Tris-HCl (pH 7.5, 50 mM) to $HCOONH_4$ (pH 8.5, 1 M) buffers. **Figure 5.2** depicts a graphical comparison for the outcome of the bio-oxidation of *rac*-**3a** in Tris-HCl and $HCOONH_4$ buffer.

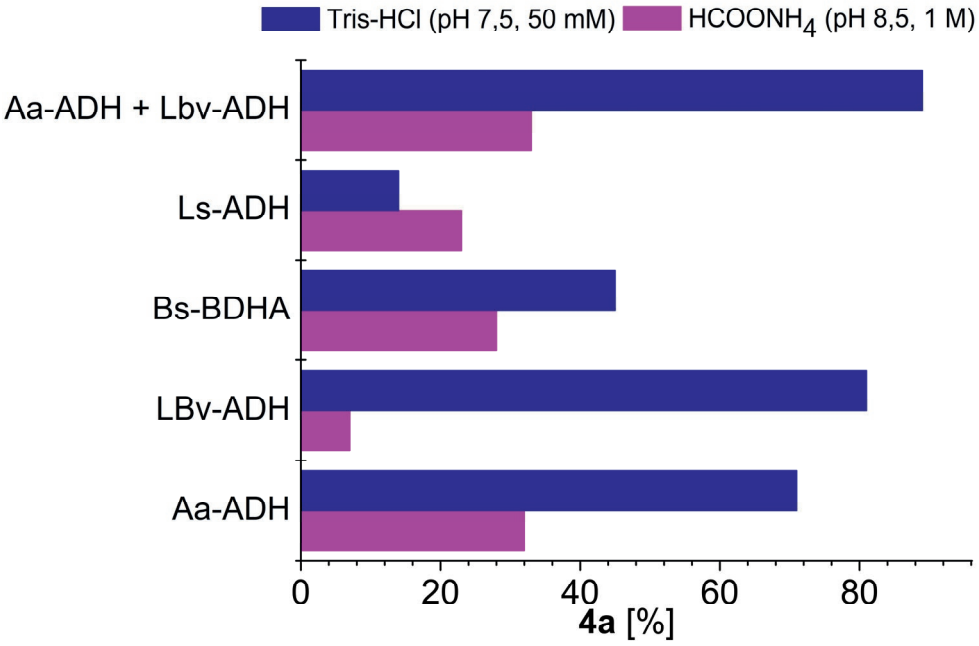

Figure 5.2. Comparison of the bio-oxidation of *rac*-**3a** performed in Tris-HCl (pH 7.5, 50 mM) and $HCOONH_4$ (pH 8.5, 1 M).

5.2.3 Enzymatic synthesis of optically pure 2-amino-2-phenylethan-1-ol (5a)

5.2.3.1 HB-bioamination cascade in $HCOONH_4$ buffer

The next step was to perform the one-pot HB-bioamination of substrate **3a**. Thus, we could exclude, for instance, a negative effect on the catalytic activity and/or stability of the NOx enzyme in $HCOONH_4$ buffer (pH 8.5, 1 M). The reactions were supplemented with catalytic amount of NAD^+ coenzyme (1 mM), which is then internally recycled by the ADH/AmDH system itself[39,46] (**Scheme 5.7**), and incubated for 48 h and 30 °C on an orbital shaker (170 rpm).

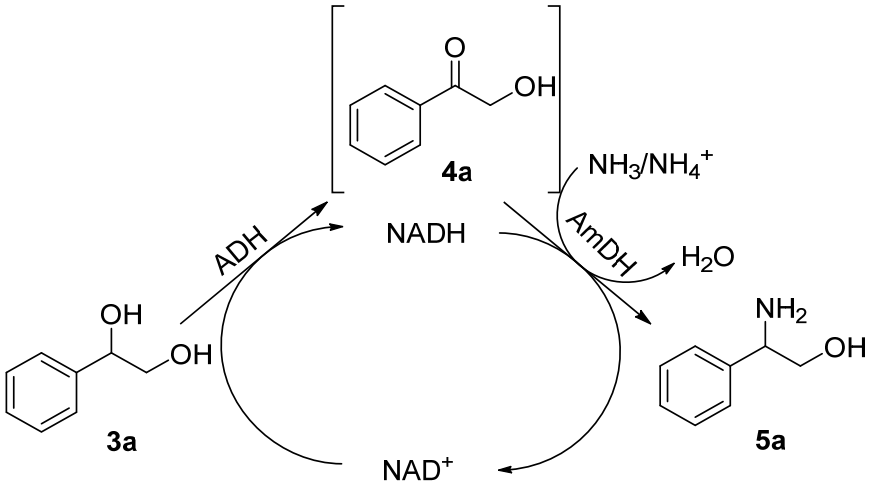

Scheme 5.7. HB-bioamination cascade for the conversion of substrate **3a** to **5a** in $HCOONH_4$ buffer

The ADHs employed for the one-pot cascade are the ones that have given a positive result in the bio-oxidation screening in $HCOONH_4$ buffer such as Aa-ADH, Bs-BDHA and Lbv-ADH (**Table 5.5**). Moreover, three (*R*)-selective AmDHs were paired with the selected ADHs such as Ch1-AmDH,[41] Rs-PhAmDH (variant from *Rhodoccoccus* sp.*)*[55] and LE-AmDH (variant from Ɛ-LysDH).[56] The first screening was performed by combining the ADHs and AmDHs in a 1:1 ratio (50 µM each) and by using **3a** as a racemic substrate. As reported in **Table 5.6**, the conversions were mediocre in all the tested cases. The best results (9-12%) were obtained when Bs-BDHA was combined with either Ch1-AmDH or LE-AmDH (entry 7 and 9). On the other hand, Rs-PhAmDH was found to be inactive in all of the tested conditions (entries 2, 5 and 8). Similar results were obtained in the case of Ch1-AmDH combined with either Aa-ADH or Lbv-ADH (entry 1 and 4), although Aa-ADH resulted in slightly better conversion (6% vs. 1%). A further test was the combination of both Aa-ADH and Lbv-ADH in equimolar ratio (25 µM each) in the same pot with AmDHs (entry 10-12); nevertheless, this attempt did not bring any advantage in terms of conversions.

Table 5.6. One-pot HB-bioamination of *rac*-**3a** (10 mM) catalyzed by selected ADHs in combination with (*R*)-selective AmDHs in 50:50 μM ratio.

Entry	ADH	AmDH [μM]	Conv. [%][c]	5a [%][c]	*ee* 5a [%]	4a [%][c]
1	Aa-ADH	Ch1-AmDH	7±<1	6±<1	n.m.	1±<1
2	Aa-ADH	Rs-PhAmDH	1±<1	n.d.	n.m.	1±<1
3	Aa-ADH	LE-AmDH[a]	6±1	5±<1	n.m.	2±<1
4	Lbv-ADH	Ch1-AmDH	1±<1	1±<1	n.m.	<1
5	Lbv-ADH	Rs-PhAmDH	<1	n.d.	n.m.	<1
6	Lbv-ADH	LE-AmDH[a]	n.c.	n.d.	n.m.	n.d.
7	Bs-BDHA	Ch1-AmDH	15±1	12±<1	n.m.	2±1
8	Bs-BDHA	Rs-PhAmDH	3±<1	n.d.	n.m.	3±<1
9	Bs-BDHA	LE-AmDH[a]	11±1	9±<1	n.m.	3±1
10	Aa-ADH[b]+Lbv-ADH[b]	Ch1-AmDH	4±<1	4±<1	n.m.	n.d.
11	Aa-ADH[b]+Lbv-ADH[b]	Rs-PhAmDH	1±<1	1±<1	n.m.	n.d.
12	Aa-ADH[b]+Lbv-ADH[b]	LE-AmDH[a]	6±<1	4±<1	n.m.	2±<1

[a]Used in 90 μM. [b]Used in 25 μM. [c]All reactions were performed in duplicate and the reported conversion is the average of the two independent samples.

The same one-pot HB-bioamination was performed by using the enantiomerically pure substrates (*R*)-**3a** or (*S*)-**3a** (10 mM). The used ADHs were selected based on the selectivity displayed in previous results (**Table 5.4**). Lbv-ADH was selective for the conversion of (*S*)-**3a** while Aa-ADH and Bs-BDHA for the conversion of substrate (*R*)-**3a**. **Table 5.7** shows the tests performed with (*S*)-**3a** (10 mM), in which Lbv-ADH (50 μM) was combined with each selected AmDHs (*i.e.*, either Ch1-AmDH, Rs-PhAmDH or LE-AmDH). In these experiments, the formation of the target amino alcohol **5a** was minimal and only observed in the case of LE-AmDH (entry 3). As previously mentioned, this lack of catalytic activity might be due to the presence of the poly-histidine tag on Lbv-ADH that can affect its activity and/or from any interaction with the poly-histidine tag of the AmDH. Furthermore, it is also known that AmDH are not very active towards the reductive amination at the benzylic position.

Table 5.7. One-pot HB-bioamination cascade for the conversion of (*S*)-**3a** (10 mM) catalyzed by Lbv-ADH coupled with three AmDHs (50:50 μM) ($HCOONH_4$, pH 8.5, 1 M, 30 °C).

Entry	AmDH	Conv.[%] [b]	5a [%][b]	*ee* 5a [%]	4a [%][b]
1	Ch1-AmDH	n.c.	n.d.	n.m.	n.d.
2	Rs-PhAmDH	n.c.	n.d.	n.m.	n.d.
3	LE-AmDH[a]	2±<1	2±<1	n.m.	n.d.

[a]Used in 90 μM. [b]Reactions were performed in duplicate and results are reported as average of the two samples; n.d. = not detected; n.m. = not measured.

The same screening was performed using the (*R*)-enantiomer as substrate (*R*-**3a**, 10 mM). In this case, two ADHs were previously found to be active towards this substrate, namely Aa-ADH and Bs-BDHA (50 µM). Moreover, the three *R*-selective AmDHs were also tested in this case. As shown in **Table 5.8**, Rs-PhAmDH gave no conversion at all into product **5a** (entry 2 and 7), while Ch1-AmDH and LE-AmDH displayed similar results when combined with either Aa-ADH or Bs-BDHA. The latter enzyme gave slightly better conversion (12-19%; entry 6 and 8). Though perfect enantioselectivity was observed, the low conversions make the system be far away from a potential applicability in preparative scale.

Table 5.8. One-pot HB-bioamination of (*R*)-**3a** (10 mM) catalyzed by a 50:50 µM combination of ADH:AmDH ($HCOONH_4$, pH 8.5, 1 M, 30 °C).

Entry	ADH	AmDH	Conv. [%][d]	5a [%][d]	*ee* 5a [%][b]	4a [%][d]
1	Aa-ADH	Ch1-AmDH	6±<1	6±<1	n.m.	n.d.
2	Aa-ADH	Rs-PhAmDH	n.c.	n.d.	n.m.	n.d.
3	Aa-ADH	LE-AmDH[a]	7±1	7±1	>99 (*S*)[c]	n.d.
6	Bs-BDHA	Ch1-AmDH	19±2	17±2	>99 (*S*)[c]	2±<1
7	Bs-BDHA	Rs-PhAmDH	n.c.	n.d.	n.m.	n.d.
8	Bs-BDHA	LE-AmDH[a]	12±<1	11±<1	>99 (*S*)[c]	1±<1

[a]Used in 90 µM. [b]Analyzed by RP-HPLC (C18 HD column) after derivatization of the amino group with GITC. [c]Switch of the CIP priority. [d]Reactions were performed in duplicate and results are reported as average of the two samples; n.d. = not detected; n.m. = not measured

Notably, when LE-AmDH was tested for the reductive amination on substrate **4a**, it resulted in quite high conversion (>60% **5a**, >99% (*S*)). In summary, considering the obtained results, the one-pot HB-bioamination was put on the side and a different route was investigated.

5.2.3.2 One-pot cascade for the conversion of 3a to 5a combining ADHs and ω-transaminases in Tris-HCl buffer

To perform the bioamination of substrate **3a**, another one-pot cascade was designed. The selected ADHs (Aa-ADH, Bs-BDHA and Lbv-ADH) were tested with two stereocomplemenatry ωTAs such as At(*R*)-ωTA from *Aspergillus terreus*[33,34] and Cv(*S*)-TA from *Chromobacterium violaceum* (DSM 30191).[57] The general reaction scheme is depicted in **Scheme 5.8**. To internally recycle the NAD^+/NADH cofactor, an additional enzyme is required, namely the alanine dehydrogenase from *Bacillus sphaericus* (Bs-AlaDH).[37] This enzyme requires NH_3 and NADH to convert pyruvate, the by-product coming from the transamination reaction, back to alanine that is the

ultimate amino donor of the process. Moreover, the required NH_3 was supplied as $HCOONH_4$ salt (3 eq.). The initial testing of this cascade was performed in Tris-HCl buffer (pH 7.5, 50 mM) because the best results for the screening of selected ADHs towards the bio-catalytic oxidation of substrate **3a** (**Figure 5.2**) were observed under these conditions. The reactions were supplemented with NAD^+ (1 mM), D-or L-Alanine (50 mM, depending on the selectivity of the chosen ωTA), ωTA (50 μM), ADH (50 μM), $HCOONH_4$ (30 mM), Bs-AlaDH (20 μM) and *rac*-**3a** (10 mM). Additionally, the single enantiomers of **3a** (10 mM) were tested as substrates.

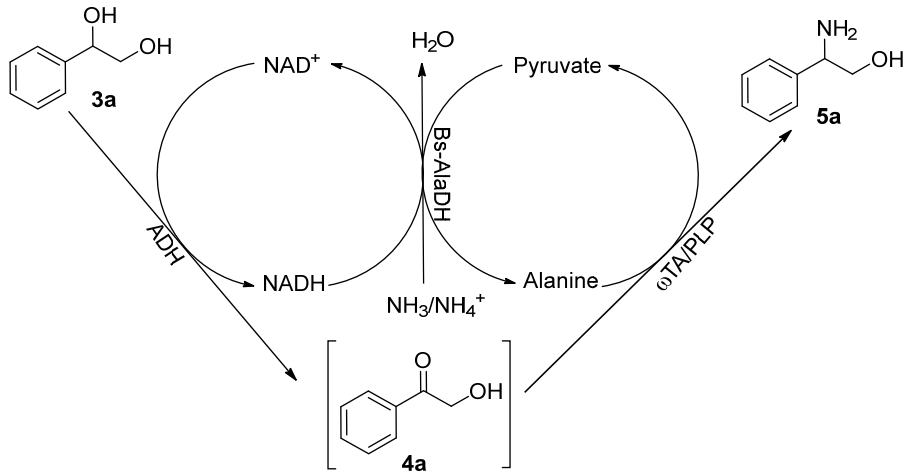

Scheme 5.8. One-pot oxidation/transamination of substrate **3a** to amino alcohol **5a** in Tris-HCl buffer.

As reported in **Table 5.9**, conversion into product **5a** was not observed when Cv(*S*)-ωTA was combined with any of the selected ADHs (entry 1, 3, 5, 7, 9 and 11). In some cases though, the activity of the ADHs was still retained (entry 1, 5 and 9) thus leading to the formation of intermediate **4a**. In this set of experiments, either Aa-ADH/Lbv-ADH (entry 9-10) or Bs-BDHA/Lbv-ADH (entry 11-12) combinations were also used in the same pot along with the selected ωTAs. Additionally, Aa-ADH, Bs-BDHA and Lbv-ADH were all combined together for the conversion of substrate *rac*-**3a**. Nevertheless, in all tested cases, the formation of product **5a** was moderate, and in general less than one would expect from the results obtained from the ADHs screening in Tris-HCl buffer (see Table 5.3). One difference with the previous tests is that in this case purified enzymes were used for both ADHs and ωTAs. However, moderate to high conversion were observed when At(*R*)-ωTA was coupled with either Aa-ADH, Bs-BDHA or Lbv-ADH (entry 2, 4, 6). On the other hand, lower conversions were obtained in the cases where two or more ADHs were combined

in the same pot with the ωTAs for the conversion of *rac*-**3a** (entry 8, 10 and 12). Hence, from these results, it can be concluded that though the ADHs were more active in Tris-HCl buffer (pH 7.5, 50 mM), this is not the best buffer system to perform the one pot oxidation/transamination cascade. Furthermore, it was not possible to find a suitable combination of stereocomplementary ADHs that were able to directly convert substrate *rac*-**3a** to the desired amino alcohols. Thus, either (*R*)-**3a** or (*S*)-**3a** have to be used as substrates for this one-pot biotransformation. However, in all tested cases so far, the only promising results were obtained when (*R*)-**3a** was used as starting material.

Table 5.9. Screening of two stereocomplementary ωTAs (50 µM) with selected ADHs (50 µM) in Tris-HCl buffer (pH 7.5, 50 mM, 30 °C) for the one-pot bioconversion of substrate **3a** (10 mM) to **5a**.

Entry	Sub.	ADH	ωTA	Conv. [%][d]	4a [%][d]	5a [%][d]	*ee* 5a [%][b]
1	(*R*)-**3a**	Aa-ADH	Cv(*S*)	19±1	19±1	n.d.	n.m.
2	(*R*)-**3a**	Aa-ADH	At(*S*)	32±10	n.d.	32±10	>99 (*S*)[c]
3	(*R*)-**3a**	Bs-BDHA	Cv(*S*)	n.c.	n.d.	n.d.	n.m.
4	(*R*)-**3a**	Bs-BDHA	At(*R*)	56±1	n.d.	56±1	>99 (*S*)[c]
5	(*S*)-**3a**	Lbv-ADH	Cv(*S*)	10±3	10±3	n.d.	n.m.
6	(*S*)-**3a**	Lbv-ADH	At(*R*)	25±7	3±3	22±4	>99 (*S*)[c]
7	*rac*-**3a**	Aa-ADH[a]+Bs-BDHA[a]+ Lbv-ADH	Cv(*S*)	n.c.	n.d	n.d.	n.m.
8	*rac*-**3a**	Aa-ADH[a]+Bs-BDHA[a]+ Lbv-ADH	At(*R*)	26±<1	n.d.	26±<1	>99 (*S*)[c]
9	*rac*-**3a**	Aa-ADH[a]+Lbv-ADH[a]	Cv(*S*)	15±1	15±1	n.d.	n.m.
10	*rac*-**3a**	Aa-ADH[a]+Lbv-ADH[a]	At(*R*)	21±5	1±1	20±4	>99 (*S*)[c]
11	*rac*-**3a**	Bs-BDHA[a]+Lbv-ADH[a]	Cv(*S*)	n.c.	n.d.	n.d.	n.m.
12	*rac*-**3a**	Bs-BDHA[a]+Lbv-ADH[a]	At(*R*)	24±<1	n.d.	24±<1	>99 (*S*)[c]

[a]Used in 25 µM. [b]Determined by RP-HPLC analysis after GITC derivatization. [c]Switch of the CIP priority. [d]Reactions were performed in duplicate and results are reported as average of the two samples; n.d. = not detected; n.m. = not measured.

5.2.3.3 One-pot cascade for the conversion of 3a to 5a combining ADHs and ω-transaminases in $HCOONH_4$ buffer

The next step was to investigate the oxidation/transamination cascade, described above, in $HCOONH_4$ buffer (pH 8.5, 1 M); however, the bio-catalytic oxidation of *rac*-**3a** in this buffer system led to lower conversions compared to the screening in Tris-HCl buffer (see figure 5.2). An advantage of performing the reactions in $HCOONH_4$ buffer is the fact that NH_4^+ and $HCOO^-$ required for the recycling of the NAD^+ coenzyme and alanine are directly supplied from the buffer itself.

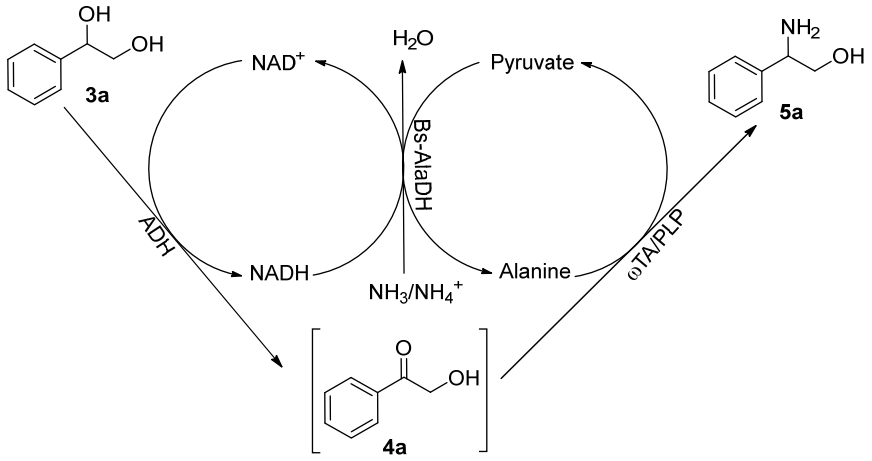

Scheme 5.9. One-pot oxidation/transamination of substrate **3a** in $HCOONH_4$ buffer.

The first screening was performed by using *rac*-**3a** and the same combination of enzymes tested previously in the Tris-HCl buffer system. The results are summarized in **Table 5.10**. Also in this case, Cv(*S*)-ωTA combined with either Aa-ADH, or Lbv-ADH or Bs-BDHA led to mediocre conversions into the desired product **5a** (entry 1, 3, 5 and 7). On the other hand, moderate conversions (considering that we started from *rac*-**3a**) were observed when the (*R*)-selective ωTA (At(*R*)-ωTA) was coupled with either Aa-ADH or Bs-BDHA (entry 2 and 6). Moreover, similar results were obtained when Aa-ADH and Lbv-ADH were combined in the same pot along with At(*R*)-ωTA as well as when Aa-ADH was used alone (entry 2 vs. entry 8). These latter results may be due to the already observed low activity of the recombinant His_6-tagged Lbv-ADH in the multi-enzymatic system. Furthermore, this low conversion may be also due to the inactivation of the Cv(*S*)-ωTA in the one-pot enzymatic system as was also observed in Tris-HCl buffer.

Table 5.10. Screening of two stereocomplementary ωTAs (50 μM) with selected ADHs (50 μM) in $HCOONH_4$ buffer (pH 8.5, 1 M, 30 °C) for the one-pot bioconversion of substrate *rac*-**3a** (10 mM)

Entry	ADH	ωTA	Conv.[%][b]	5a [%][b]	*ee* 5a [%]	4a [%][b]
1	Aa-ADH	Cv(*S*)	6±1	4±<1	n.m.	2±1
2	Aa-ADH	At(*R*)	38±1	38±1	n.m.	<1
3	Lbv-ADH	Cv(*S*)	1±<1	n.d.	n.m.	1±<1
4	Lbv-ADH	At(*R*)	5±<1	5±<1	n.m.	n.d.
5	Bs-BDHA	Cv(*S*)	n.c.	n.d.	n.m.	n.d.
6	Bs-BDHA	At(*R*)	32±<1	31±<1	n.m.	1±<1
7	Aa-ADH[a]+Lbv-ADH[a]	Cv(*S*)	4±<1	3±<1	n.m.	<1
8	Aa-ADH[a]+Lbv-ADH[a]	At(*R*)	40±<1	40±<1	n.m.	n.d.

[a]Used in 25 μM. [b]Reactions were performed in duplicate and results are reported as average of the two samples; n.d. = not detected; n.m. = not measured.

Next, we investigated further the one pot oxidation/transamination by using either substrate (*S*)-**3a** or (*R*)-**3a**. As shown in **Table 5.11**, product **5a** was obtained in only 3% when Lbv-ADH was coupled with the Cv(*S*)-ωTA (entry 1). On the other hand, the conversion increased to 21% when Lbv-ADH was combined with the (*R*)-selective At(*R*)-ωTA (entry 2). Though the moderate conversion, product **5a** was obtained with high enantioselectivity (*ee* >99% (*S*)). These two tests (entry 1 and 2) further demonstrate the inherently low activity of Cv(*S*)-ωTA compared with the At(*R*)-ωTA. Then, the same tests were performed by using substrate (*R*)-**3a** (10 mM) with either Aa-ADH or Bs-BDHA in combination with either Cv(*S*)-ωTA or At(*R*)-ωTA. The results in **Table 5.11** show that low conversion of (*R*)-**3a** to (*R*)-**5a** (11%, *ee* >83%) was obtained when Aa-ADH was coupled with Cv(*S*)-ωTA (entry 3). Furthermore, conversion was not detected at all when Cv(*S*)-TA was combined with Bs-BDHA (entry 5). On the other hand, elevated conversions of (*R*)-**3a** to (*S*)-**5a** (93% and 91%, respectively) were obtained when either Aa-ADH or Bs-BDHA was coupled with At(*R*)-TA (entry 4 and 6). Moreover, the target (*S*)-**5a** product was obtained with perfect enantioselectivity (*ee* >99% (*S*)). Overall, the performance of the cascade in $HCOONH_4$ showed to be higher compared with the results obtained for the cascade in Tris-HCl buffer and using optically pure **3a** as substrate (**Table 5.9** vs. **Table 5.11**). This was unexpected due to the lower observed activity of the ADHs for the bio-oxidation of **3a** in $HCOONH_4$ compared with the Tris-buffer system. This apparent discrepancy might be explained by the fact that the coupling of ADHs and ωTAs in the same pot, along with the AlaDH and the high buffer concentration, could shift the equilibrium towards the formation of the amino alcohol product.

Table 5.11. Bio-oxidation/transamination of optically active **3a** (10 mM) catalyzed by ADHs (50 μM) paired with two stereocomplementary ωTAs (50 μM) in $HCOONH_4$ (pH 8.5, 1 M, 30 °C).

Entry	Substrate	ADH	ωTA	Conv. [%][c]	5a [%][c]	*ee* 5a [%][a]	4a [%][c]
1	(*S*)-**3a**	Lbv-ADH	Cv(*S*)	3±<1	3±<1	n.m.	n.d.
2	(*S*)-**3a**	Lbv-ADH	At(*R*)	21±1	21±1	>99 (*S*)[b]	n.d.
3	(*R*)-**3a**	Aa-ADH	Cv(*S*)	11±3	11±3	>83 (*R*)[b]	n.d.
4	(*R*)-**3a**	Aa-ADH	At(*R*)	93±1	93±1	>99 (*S*)[b]	n.d.
5	(*R*)-**3a**	Bs-BDHA	Cv(*S*)	n.c.	n.d.	n.m.	n.d.
6	(*R*)-**3a**	Bs-BDHA	At(*R*)	92±<1	91±<1	>99 (*S*)[b]	1±<1

[a]Analyzed by RP-HPLC (C18 HD column) after derivatization of the amino group with GITC. [b]Switch of the CIP priority. [c]Reactions were performed in duplicate and results are reported as average of the two samples; n.d. = not detected; n.m. = not measured.

Therefore, according to the results reported in **Table 5.11**, (*S*)-**5a** can be obtained in high conversion and *ee* by using in cascade either Aa-ADH (50 μM) or BDHA (50

µM) combined with At(*R*)-ωTA (50 µM). Nevertheless, based on previous experiments performed on another substrate (e.g., (1*S*,2*S*)-**3**, see chapter 3),[46] full conversion of (*R*)-**3a** may be reached by adjusting the enzymes concentration versus the substrate loading. On the other hand, product (*R*)-**5a** could be obtained in only 11% and moderate enantioselectivity (**Table 5.11**, entry 3) when Aa-ADH was combined with Cv(*S*)-ωTA. Also in this case, there might be possibilities for improvements by performing optimization on the enzymes loading. In summary, the $HCOONH_4$ buffer system (pH 8.5, 1 M) showed to be suitable for performing such one-pot oxidation/transamination cascade.

5.2.3.3.1 Optimization of enzymes loading

To optimize the biocatalytic cascade, different molar ratios of ADH and ωTA were considered at constant substrate concentration (10 mM, either (*S*)-**3a** or (*R*)-**3a**). As reported in **Table 5.12** and according to previous trends, conversion of (*S*)-**3a** into (*R*)-**5a** was not detected when Lbv-ADH was combined with Cv(*S*)-ωTA (entry 1 and 2). Surprisingly, conversion was observed neither when Lbv-ADH (24 µM) was coupled with At(*R*)-ωTA (60 µM). In contrast, product (*S*)-**5a** was obtained in 38% (entry 4) once the concentration of the two enzymes was reversed: Lbv-ADH (70 µM) and At(*R*)-ωTA (35 µM). Furthermore, three other (*S*)-selective ωTAs were tested: Bm(*S*)-ωTA from *Bacillus megaterium* (SC6394)[35] (35 µM), Vf(*S*)-ωTA from *Vibrio fluvialis*[58,59] (20 mg mL^{-1}) and Ac(*S*)-ωTA from *Arthrobacter citreus*[36] (50 µM). While the use of the last two enzymes did not lead to any conversion of (*S*)-**3a** into (*R*)-**5a** (entry 6-7), Lbv-ADH in combination with Bm(*S*)-ωTA led to the formation of the desired product in 38% analytical yield and *ee* >99% (*R*) (entry 5).

Table 5.12. One-pot oxidation/transamination of (*S*)-**3a** (10 mM) catalyzed by Lbv-ADH combined with stereocomplementary ωTAs at different enzymes loading in $HCOONH_4$ buffer (pH 8.5, 1 M, 30 °C).

Entry	ADH [µM]	ωTA [µM]	Conv. [%][d]	5a [%][d]	*ee* 5a [%][b]	4a [%][d]
1	Lbv-ADH [24]	Cv(*S*) [60]	1±<1	n.d.	n.m.	1±<1
2	Lbv-ADH [70]	Cv(*S*)[35]	2±<1	n.d.	n.m.	2±<1
3	Lbv-ADH [24]	At(*R*)[60]	1±<1	n.d.	n.m.	1±<1
4	Lbv-ADH [70]	At(*R*)[35]	38±1	38±1	>99 (*S*)[c]	n.d.
5	Lbv-ADH [70]	Bm(*S*) [35]	38±2	38±2	>99 (*R*)[c]	n.d.
6	Lbv-ADH [70]	Vf(*S*)[a]	n.c.	n.d.	n.m.	n.d.
7	Lbv-ADH [50]	Ac(*S*) [50]	n.c.	n.d.	n.m.	n.d.

[a]Used as lyophilized *E.coli* whole cells (20 mg mL^{-1}). [b]Analyzed by RP-HPLC (C18 HD column) after derivatization of the amino group with GITC. [c]Switch of the CIP priority. [d]Reactions were performed in duplicate and results are reported as average of the two samples; n.d. = not detected; n.m. = not measured.

Similar types of tests were performed on substrate (*R*)-**3a** (10 mM). As reported in **Table 5.13**, in the case of Cv(*S*)-ωTA, the system performed significantly better when an excess of the ωTA was used (60 μM *vs.* 35 μM) combined with a lower Aa-ADH loading (24 μM *vs.* 70 μM) (entry 1-2). These results further prove that Cv(*S*)-ωTA has some limitation in performing such biotransformation as also observed in previous experiments (see Table 5.12). In fact, applying the enzymatic system Aa-ADH:Cv(*S*)-ωTA (24:60 μM) the target product (*R*)-**5a** was obtained in 31% (**Table 5.13**, entry 1; *ee* >99% (*R*)) from substrate (*R*)-**3a**. In contrast, only 2% conversion was obtained when Aa-ADH: Cv(*S*)-ωTA were used in 70:35 (μM) ratio (**Table 5.13**, entry 2). Furthermore, three additional (*S*)-selective transaminases were tested with (*R*)-**3a** substrate. While Vf(*S*)-ωTA and Ac(*S*)-ωTA did not shown any conversion of (*R*)-**3a** into (*R*)-**5a** (**Table 5.13**, entry 4-5), the system Aa-ADH:Bm(*S*)-ωTA (70:35 μM) led to the formation of the desired product (*R*)-**5a** in 70% (**Table 5.13**, entry 3; *ee* >99% *(R)*). On the other hand, elevated conversions to (*S*)-**5a** (95-97%) as well as enantioselectivity (>99% *S*) were observed when (*R*)-**3a** was used as substrate with the (*R*)-selective At(*R*)-ωTA (entry 6-9). In conclusion, the best results were obtained with the enzymatic system Aa-ADH (70 μM) and At(*R*)-ωTA (35 μM) (entry 7).

Table 5.13. One-pot oxidation/transamination of (*R*)-**3a** (10 mM) catalyzed by ADHs combined with stereocomplementary ωTAs at different enzymes loading in $HCOONH_4$ buffer (pH 8.5, 1 M, 30 °C).

Entry	ADH [μM]	ωTA [μM]	Conv. [%][d]	5a [%][d]	*ee* 5a [%][b]	4a [%][d]
1	Aa-ADH [24]	Cv(*S*) [60]	48±12	31±10	>99 (*R*)[c]	17±2
2	Aa-ADH [70]	Cv(*S*) [35]	6±2	2±<1	n.m.	4±2
3	Aa-ADH [70]	Bm(*S*) [35]	71±<1	70±<1	>99 (***R***)[c]	1±<1
4	Aa-ADH [70]	Vf(*S*)[a]	n.c.	n.d.	n.m.	n.d.
5	Aa-ADH [50]	Ac(*S*) [50]	n.c.	n.d.	n.m.	n.d.
6	Aa-ADH [24]	At(*R*) [60]	99±1	96±1	>99 (*S*)[c]	4±1
7	Aa-ADH [70]	At(*R*) [35]	>99	97±<1	>99 (***S***)[c]	3±<1
8	Bs-BDHA [24]	At(*R*) [60]	>99	96±<1	>99 (*S*)[c]	4±<1
9	Bs-BDHA [70]	At(*R*) [35]	>99	95±<1	>99 (*S*)[c]	5±<1

[a]Used as lyophilized *E.coli* whole cells (20 mg mL^{-1}). [b]Analyzed by RP-HPLC (C18 HD column) after derivatization of the amino group with GITC. [c]Switch of the CIP priority. [d]Reactions were performed in duplicate and results are reported as average of the two samples; n.d. = not detected; n.m. = not measured.

In summary, under the optimized conditions, both (*S*)-**5a** (97%, *ee* >99% *S*) and (*R*)-**5a** (70%, *ee* >99% *R*) could be obtained from (*R*)-**3a** by coupling Aa-ADH with stereocomplementary ωTAs as depicted in **Scheme 5.10**.

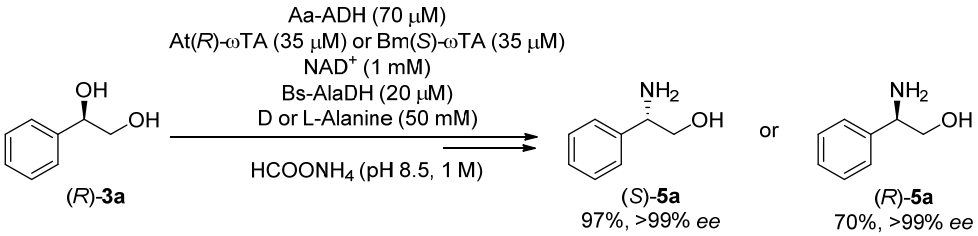

Scheme 5.10. Overview of the one-pot multi-enzymatic cascade for the synthesis of (*S*)-**5a** and (*R*)-**5a** from substrate (*R*)-**3a**

5.2.4 Enzymatic synthesis of optically pure 2-amino-1-phenylethan-1-ol (5a')

5.2.4.1 Testing primary NAD$^+$-dependent ADHs (Ht-ADH vs. HL-ADH)

A first screening for the selective bio-oxidation of the primary hydroxyl moiety of substrate *rac*-**3a** into the correspondent hydroxyl aldehyde **4a'** was performed either by Ht-ADH from *Bacillus stearothermophilus* (LLD-R strain)[60] or by HL-ADH from *Equus caballus* purchased by Sigma Aldrich (product number 9031-72-5, activity 0.52 U mg^{-1}; 20 % protein content). Ht-ADH (50 μM) was used in purified form while HL-ADH (2 mg mL^{-1}) as lyophilized crude cell extract. As for the screening of secondary NAD(P)$^+$-dependent ADHs, the reactions were supplemented with catalytic amount of NAD$^+$ coenzyme; the latter was internally recycled by NOx enzyme. The general reaction scheme is depicted in **Scheme 5.11**.

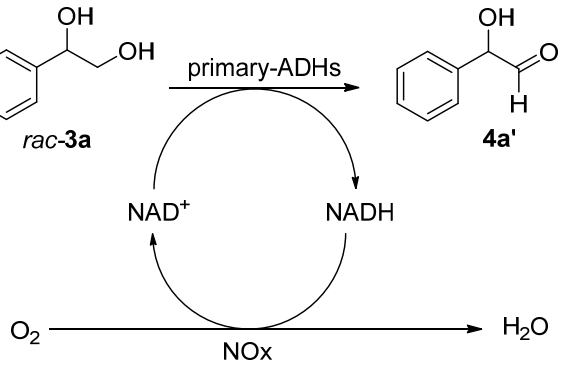

Scheme 5.11. Biocatalytic oxidation of *rac*-**3a** to **4a'**

In both cases, the biocatalytic oxidation of *rac*-**3a** (20 mM) was performed in Tris-HCl buffer (pH 7.5, 50 mM; 1mL final reaction volume) and in the presence of NAD^+ recycling system (1 mM NAD^+; 10 µM NOx). When HL-ADH was used, the formation of the desired product **4a'** was not detected by GC-MS analysis. In contrast, the corresponding hydroxyl ketone isomer **4a** was observed as the only product of the reaction (**Scheme 5.12**); indeed, the hydroxyaldehyde **4a'** can spontaneously rearrange/tautomerize to the most stable isomer **4a**. Nevertheless, substrate *rac*-**3a** was completely consumed which means that the enzyme was active on substrate **3a**. On the other hand, no conversion of substrate *rac*-**3a** was detected by applying the purified Ht-ADH.

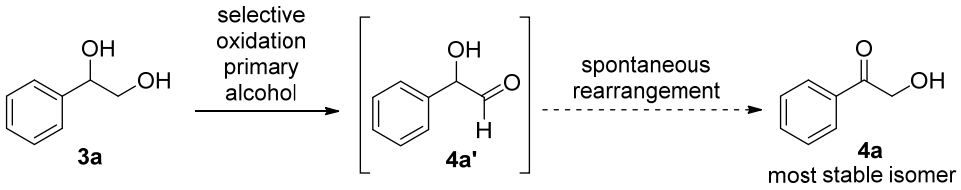

Scheme 5.12. Tautomerization of product **4a'** into its most stable isomeric form **4a**.

A further test was conducted with substrate 2-methoxy-2-phenylethanol (**9**, 20 mM) in which the secondary hydroxyl moiety was protected with a methyl group in order to clarify if compound **4a'** actually forms and then isomerizes to the most stable isomer **4a** (**Scheme 5.13**). As before, both HL-ADH (2 mg mL^{-1}) from Sigma Aldrich and purified Ht-ADH (50 µM) were tested and the biotransformation were carried out in Tris-HCl buffer (pH 7.5, 50 mM; 1 mL final reaction volume) in the presence of NAD^+ recycling system (1 mM NAD^+; 10 µM NOx). No conversion was detected in the case of Ht-ADH, whereas only 3% of product **10** was obtained when HL-ADH was used (GC-MS and GC-FID analysis). This latter result indicates that substrate **9** might not be accepted by the two tested ADHs or some substrate/product inhibition can occur.

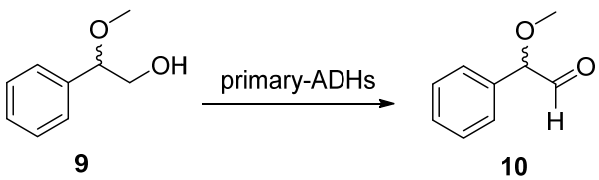

Scheme 5.13. Model reaction for assessing the formation of the aldehyde intermediate by the action of HL-ADH and Ht-ADH.

5.2.4.2 One-pot HB-bioamination cascade from *rac*-3a to 5a' by using HL-ADH/AmDHs system

As described above, it was not possible to isolate the hydroxyl aldehyde **4a'** coming from the oxidation of *rac*-**3a** (5 mM) catalyzed by the two available primary NAD^+-dependent ADH (Ht-ADH or HL-ADH). Therefore, the one-pot HB-bioamination cascade[46,39] was tested in order to try to push the reaction towards the desired product; thus, as soon as compound **4a'** is formed, we can assume that it could be immediately converted into the final product **5a'**, thereby avoiding the spontaneous tautomerization of the hydroxyaldehyde intermediate (**Scheme 5.14**).

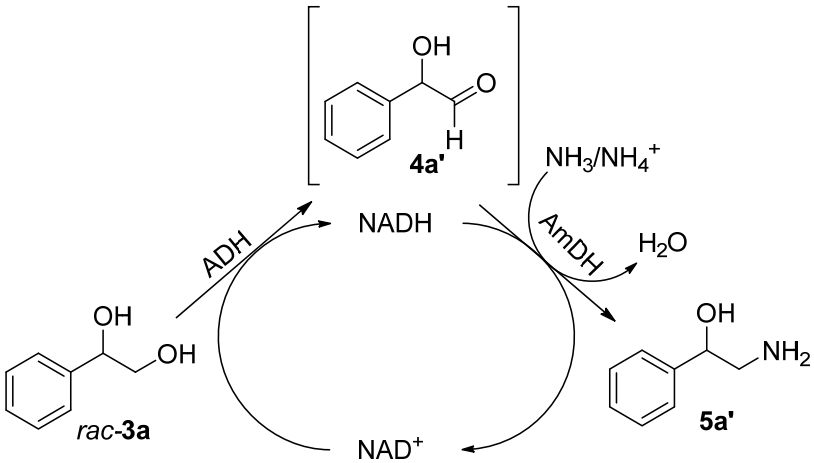

Scheme 5.14. HB-bioamination cascade for the one-pot conversion of *rac*-**3a** to **5a'.**

Lyophilized cell free extract of HL-ADH (2 mg mL^{-1}) was combined in cascade with three (*R*)-selective AmDHs (100 μM), namely Ch1-AmDH,[41] Rs-PhAmDH (variant from *Rhodoccoccus* sp.*)*[55] and Bb-AmDH from *B. badius,*[61] for the bio-conversion of *rac*-**3a** (5 mM) into product **5a'**. The reaction was carried out in $HCOONH_4$ buffer (pH 8.5, 1 M; 0.5 mL final reaction volume) and supplemented with catalytic amount of NAD^+ coenzyme (1 mM). As before, NAD^+ was internally recycled by the ADH/AmDH system itself and the nitrogen source comes from the ammonium/ammonia buffer. As shown in **Table 5.14**, conversion to product **5a'** was observed with both Ch1-AmDH (14%) and Bb-AmDH (6%) (entry 1 and 3). Also in this case, hydroxyaldehyde intermediate **4a'** was not detected while its isomer **4a** was observed in traces. On the other hand, no conversion into the vicinal amino alcohol **5a'** was detected when using Rs-PhAmDH (entry 2). Considering that

substrate **3a** was used in racemic form, the conversion with HL-ADH/Ch1-AmDH showed to be promising.

Table 5.14. Biocatalytic conversion of *rac*-**3a** (5 mM) by the system HL-ADH (2 mg mL^{-1}) combined with AmDHs (100 μM).

Entry	AmDH	Conv.[%]	5a' [%]	4a [%]
1	Ch1-AmDH	15	14	1
2	Rs-PhAmDH	7	n.d.	7
3	Bb-AmDH	7	6	1

n.d. = not detected

5.2.4.3 One-pot cascade from *rac*-3a to 5a' by using HL-ADH/ωTAs system

Additional tests were carried out by combining HL-ADH (2 mg mL^{-1}) with Cv(S)-ωTA (10 mg mL^{-1}). The biotransformation of *rac*-**3a** (5 mM) was carried out in Tris-HCl buffer (pH 7.5, 50 mM; 1 mL). Furthermore, since ADHs are NAD^+-dependent enzymes and pyruvate is the coproduct derived from D-or L-alanine (the amino donor), an internal coenzyme recycling system was introduced (1 mM NAD^+, 25 mM D-or L-alanine, 1 mg mL^{-1} LDH lyophilized crude extract (Codexis LDH-101, activity ca. 60 U mg^{-1})). Moreover, the reaction was supplemented with PLP cofactor (0.5 mM) required for the Cv(S)-ωTA. The whole cascade system is depicted in **Scheme 5.15**.

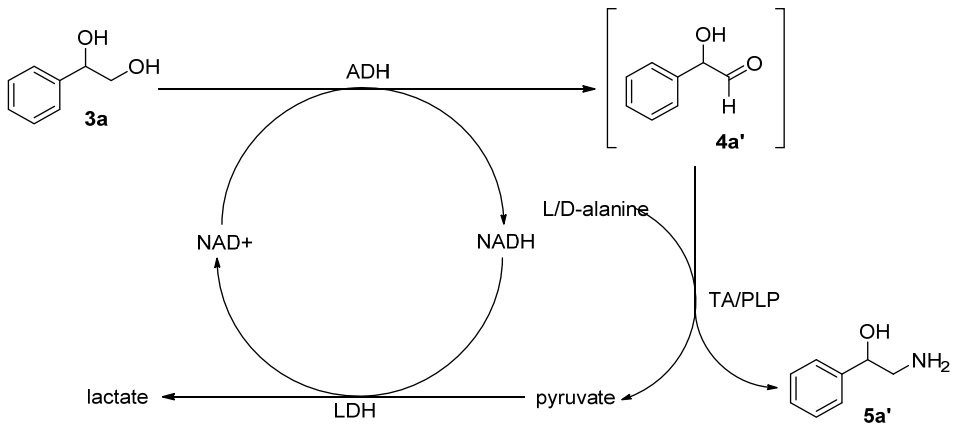

Scheme 5.15. One-pot multi-enzyme cascade for the conversion of *rac*-**3a** to amino alcohol **5a'** by ADH/ωTA system.

As shown in Table **5.15**, in the case of HL-ADH (entry 1), the substrate was fully converted; the target **5a'** was obtained in 76% while the hydroxyaldehyde intermediate **4a'** was not detected. On the other hand, its isomer **4a** was observed

(24%). In contrast, in the case of Ht-ADH, the substrate was not accepted and only a mediocre conversion into the amino alcohol was observed.

Table 5.15. Biocatalytic conversion of *rac*-**3a** (5 mM) catalyzed by either HL-ADH (2 mg mL^{-1}) or Ht-ADH (50 µM) combined with Cv(S)-ωTA (5-15 mg mL^{-1}).

Entry	ADH	Cv(*S*)-ωTA [mg]	Substrate [mM]	Conv. [%]	5a' [%]	4a [%]
1	HL-ADH	10	5	>99	76	24
2	Ht-ADH	15	20	3	3	n.d.

n.d. = not detected

5.2.4.4 Final tests with purified HL-ADH, Ht-ADH and FuCO coupled with either AmDHs or ωTAs

5.2.4.4.1 Expression and optimization of in-house produced HL-ADH

Based on the results obtained above, we continued our studies with the HL-ADH that we expressed and purified in our lab. HL-ADH is a homodimer and NADH-dependent alcohol dehydrogenase from *Equus caballus* that contains two Zn^{2+} ions per monomer.[62,63, 64, 65,66] First, the gene expressing the His_6 tagged HL-ADH was subcloned in *E. coli* BL21 DE3 (pET28b); however, the first expression trial in LB-medium, with induction of enzyme expression performed by 0.5 mM IPTG, led to very low expression levels. Then, the gene expressing the GST-tagged HL-ADH was subcloned in *E. coli* BL21 DE3 (pET28bvar) and different expression conditions were tested. First, the cells were grown in LB medium supplemented with $ZnSO_4$ (100 µM) and expression was induced by three different concentrations of IPTG: 0.5, 1 and 2 mM. In all cases, higher expression levels were detected compared to the His_6-tagged protein. Nevertheless, the highest expression level, though not perfect, was detected when induction was performed with 2 mM IPTG. Moreover, the addition of $ZnSO_4$ seems to have some effects on the protein expression as well as on the folding since almost all of the expressed protein was found in the soluble fraction. We then proceeded with the optimization to be able to further increase the expression level. Thus, the cells were grown in both LB and TB (Terrific Broth) medium without any addition of $ZnSO_4$, and induction of protein expression was performed with 0.5 mM IPTG. Furthermore, the cells were grown in TB-medium supplemented with $ZnSO_4$ (100 µM) and the expression was induced with 0.5 mM IPTG. However, lowering the amount of IPTG was not beneficial for the protein expression at high concentration of $ZnSO_4$. As last attempts, LB medium was supplemented with $ZnSO_4$ (10 µM) and protein expression induced with 0.5 mM IPTG; TB medium was supplemented with $ZnSO_4$ (50 µM) and induction performed

with 2 mM IPTG. In general, both LB and TB medium turned out to be suitable for the enzyme expression. In these cases, a minimum amount of supplemented $ZnSO_4$ (50-100 μM) was beneficial for protein expression and folding. Furthermore, the presence of a GST tag rather than His_6 proved to be beneficial for the protein expression. Nevertheless, comparable results were observed for induction with either 0.5 mM or 2.0 mM IPTG. A summary of the optimized conditions is reported in **Table 5.16**.

Table 5.16. Screening conditions for the optimization of HL-ADH expression.

Entry	Tag	Medium	IPTG [mM]	$ZnSO_4$ [μM]	Expression level[a]
1	His_6	LB	0.5	0	band not visible
2	GST	LB	0.5	100	Low
3	GST	LB	1	100	Medium
4	GST	LB	2	100	Medium/high
5	GST	LB	0.5	0	Very low
6	GST	TB	0.5	0	Medium
7	GST	TB	0.5	100	Medium
8	GST	LB	0.5	10	Low
9	GST	TB	2	50	Medium /high

His_6-tagged HL-ADH, MW = 42.099 kDa; GST-tagged HL-ADH, MW = 66.412 kDa. [a]Analyzed by SDS-PAGE

5.2.4.4.2 One-pot cascades for the conversion of 3a to 5a' by HL-ADH or FuCO with either AmDHs or ωTAs

Based on the preliminary results reported in **Table 5.15**, we proceeded to test both HB-bioamination cascade and the alternative cascade in which ADHs and ωTAs were combined as purified enzymes. GST-tagged HL-ADH was overexpressed in *E. coli* BL21 DE3 in TB medium at 25 °C for 16 h; moreover, the main culture was supplemented with 50 μM of $ZnSO_4$. The protein expression was induced with IPTG (2 mM) and the purification of the GST-tagged protein was then carried out according to the protocol provided by the supplier. Furthermore, another primary NAD^+-dependent ADH namely the lactaldehyde reductase from *E. coli* (FucO, variant D93) has been recently disclosed and engineered for the acceptance of aromatic substrates.[67,68,69] Initially, either purified GST-tagged HL-ADH (25 μM) or purified His_6-tagged FucO-D93 (50 μM) were coupled with two *(R)*-selective AmDHs, namely Ch1-AmDH (50 μM) or Rs-PhAmDH (50 μM), for the conversion of *rac*-**3a** (10 mM) (**Scheme 5.16**). The biotransformations were carried out in $HCOONH_4$ buffer (pH 8.5, 1 M; 0.5 mL reaction volume) supplemented with catalytic amount of NAD^+ coenzyme (1 mM). Nevertheless, conversion was not observed in

any of the tested combinations and the substrate was the only compound detected after extraction.

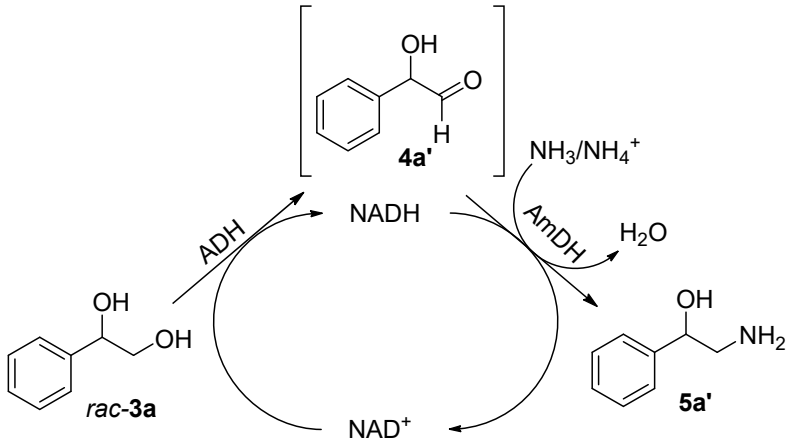

Scheme 5.16. One-pot HB-bioamination of *rac*-**3a** to **5a'**.

Next, we proceeded with testing the one-pot cascade by combining either GST-tagged HL-ADH (25 µM) or His_6-tagged FucO-D93 (50 µM) with either Cv(*S*)-ωTA or At(*R*)-ωTA (50 µM). The biotransformation of *rac*-**3a** (10 mM) was carried out in $HCOONH_4$ buffer (pH 8.5, 1 M; 0.5 mL) supplemented with catalytic amount of NAD^+ (1 mM), L-or D-Alanine (50 mM), PLP (1 mM) and Bs-AlaDH (20 µM) (**Scheme 5.17**).

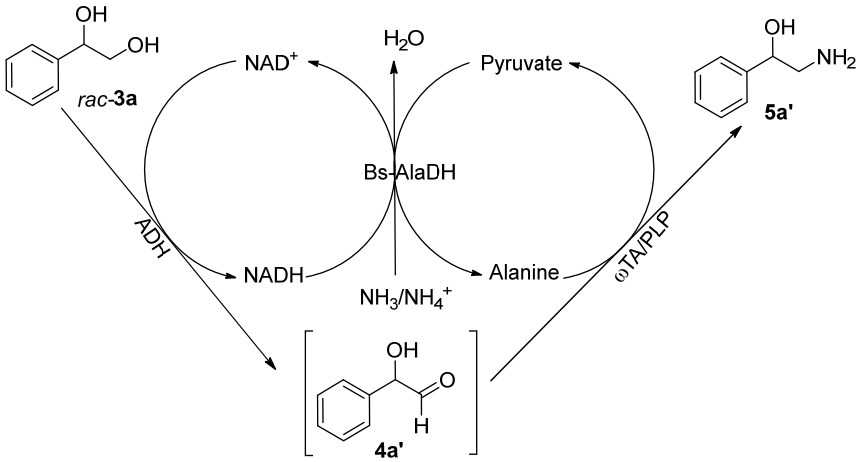

Scheme 5.17. One-pot oxidation/transamination cascade of *rac*-**3a** to **5a'** in $HCOONH_4$ buffer.

As reported in **Table 5.17**, neither conversion was detected when FucO-D93 was applied (entry 3 and 4) nor intermediate formation was observed during the

reaction. On the other hand, when HL-ADH was applied with either Cv(*S*)-ωTA or At(*R*)-ωTA, product **5a'** was formed in 38-39% (entry 1 and 2). Moreover, intermediate **4a'** was not detected while its isomer **4a** was only formed in traces. Considering that racemic substrate was used, the detected conversions look promising for a potential applicability of this one-pot cascade towards the synthesis of **5a'**. However, further tests are needed in order to identify which enantiomer of **3a** is accepted by HL-ADH/ωTAs system as well for assessing the stereochemistry of the desired amino alcohol **5a'**.

Table 5.17. One-pot cascade for the conversion of *rac*-**3a** (10 mM) to **5a'** catalyzed by HL-ADH paired with stereocomplementary ωTAs in $HCOONH_4$ buffer (pH 8.5, 1 M).

Entry	ADH	ωTA	Conv.[%]	4a	5a'
1	HL-ADH	Cv(*S*)-ωTA	38	<1	38
2	HL-ADH	At(*R*)-ωTA	40	1	39
3	FucO	Cv(*S*)-ωTA	n.c.	n.d.	n.d.
4	FuCO	At(*R*)-ωTA	n.c.	n.d.	n.d.

n.d. = not detected

5.2.4.5 Orthogonal bioamination cascade for the synthesis of 5a'

Another elegant cascade for accessing the vicinal amino alcohol **5a'** was envisioned.[38] This involves the combination of an alcohol oxidase from *Arthrobacter chlorophenolicus* (AcCO6, variant of Choline oxidase)[40] in combination with an AmDH (Ch1-AmDH). This is an orthogonal cascade for the bioamination of the diol **3a**, which is supposed to have a more favorable thermodynamic equilibrium. One advantage is that AcCO6 has no NAD-coenzyme dependency, albeit catalase must be added to prevent any possible enzyme deactivation due to the formation of H_2O_2. However, a NADH recycling system is required in the second step of the cascade (formate dehydrogenase from *Candida Boidinii,* Cb-FDH).[42] Moreover, the reactions were performed in $HCOONH_4$ (pH 8.5, 1 M) which provide both nitrogen source for the amination as well as the required hydride for the coenzyme recycling. The one-pot cascade is depicted in **Scheme 5.18**.

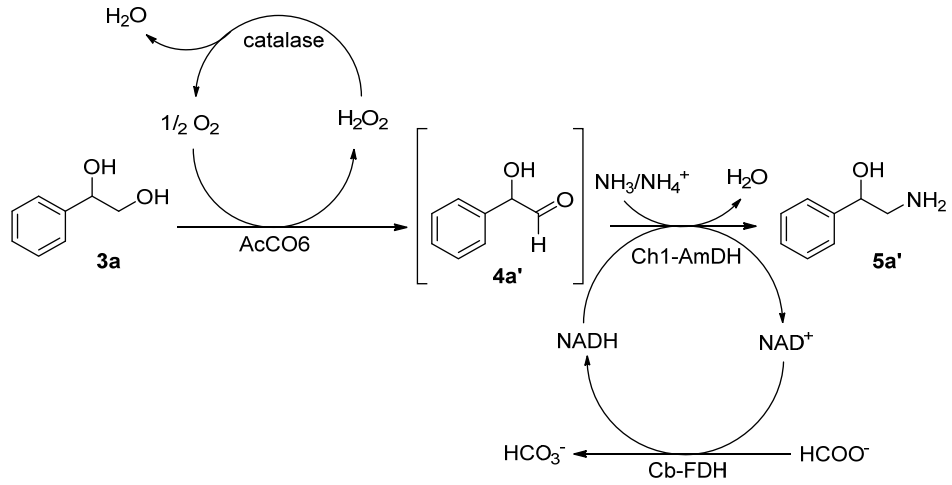

Scheme 5.18. Orthogonal bioamination cascade for the conversion of substrate **3a** to **5a'** in $HCOONH_4$ buffer.

The first screening was carried out by using equimolar ratio of AcCO6 and Ch1-AmDH (50 µM each) in $HCOONH_4$ buffer (pH 8.5, 1 M; 0.5 mL) supplemented with catalytic amount of NAD^+ (1 mM) and catalase (0.1 mg mL^{-1}). **3a** was used as substrate either as racemate or as single enantiomer in *R* or *S* configuration (10 and 20 mM were tested). As shown in **Table 5.18**, quantitative conversion of *rac*-**3a** into the target amino alcohol **5a'** was detected at 10 mM scale (entry 1). Due to the racemic form of the substrate, the enantioslectivity of the product was very low (*ee* 10% (*S*)). Nonetheless, excellent conversion into **5a'** was detected (90%, *ee* 10% (*S*)) using *rac*-**3a** at 20 mM concentration, thus showing that the system tolerates high concentration of substrate (entry 2). Furthermore, these preliminary results demonstrate that the AcCO6 does not discriminate between the two enantiomers of substrate **3a**. Hence, the next step was to investigate the same conditions but using the optically pure substrates in order to obtain chiral **5a'**. Substrate (*S*)-**3a** and (*R*)-**3a** were both tested at 10 and 20 mM scale; (*S*)-**3a** (10 mM) was fully converted thus resulting in 98% of (*S*)-**5a'** (*ee* >98% (*S*)). Lower yield (88%) but still perfect enantioselectivity was obtained at 20 mM substrate concentration (entry 3 and 4). On the other hand, (*R*)-**3a** was converted into the target (*R*)-**5a'** in 92% at 10 mM scale (entry 5) and in 72% at 20 mM substrate loading (entry 6). However, in both cases, (*R*)-**5a'** was obtained with perfect enantioselectivity (*ee* >99% (*R*)). This discrepancy between the conversion of (*S*)-**3a** and (*R*)-**3a** might indicate a slightly higher preference of AcCO6 for the (*S*)-enantiomer of the substrate.

Table 5.18. Orthogonal bioamination of **3a** (10-20 mM) to **5a'** catalyzed by AcCO6 (50 µM) paired with Ch1-AmDH (50 µM) in a one-pot cascade in $HCOONH_4$ buffer (pH 8.5, 1 M; 30 °C)

Entry	Substrate [mM]	Conv. [%][b]	5a' [%][b]	Benzylamine [%][b]	*ee* [%][a]
1	*rac*-**3a** [10]	>99	>99	n.d.	10 (*S*)
2	*rac*-**3a** [20]	92±<1	90±<1	2±<1	10 (*S*)
3	(*S*)-**3a** [10]	>99	98±<1	2±<1	>98 (*S*)
4	(*S*)-**3a** [20]	96±1	88±1	8±<1	>98 (*S*)
5	(*R*)-**3a** [10]	94±<1	92±<1	2±<1	>99 (*R*)
6	(*R*)-**3a** [20]	78±1	72±1	6±<1	>99 (*R*)

[a]Analyzed by RP-HPLC (C18 HD column) after derivatization of the amino group with GITC. [b]Reactions were performed in duplicate and results are reported as average of the two samples

Interestingly, neither intermediate **4a'** nor its more stable isomer **4a** were detected. On the other hand, a side reaction occurred thus forming benzaldehyde that was further converted to benzylamine. As shown in **Table 5.18**, benzylamine formation was observed in all tests with the only exception being *rac*-**3a** at 10 mM concentration for which quantitative conversion of the substrate into the desired product was detected. For reactions with both (*R*)-**3a** and (*S*)-**3a** at 10 mM concentration, traces of benzylamine were detected (2%). On the other hand, at 20 mM substrate concentration, higher amounts of benzylamine were observed (6-8%) due to the lower conversion of both substrates. One possibility is that the unreacted diol undergoes decomposition to benzaldehyde, which is then converted to benzylamine by the Ch1-AmDH. Nevertheless, it might also happen that the intermediate **4a'** undergoes decomposition to benzaldehyde, which is then aminated by Ch1-AmDH (**Scheme 5.19**).

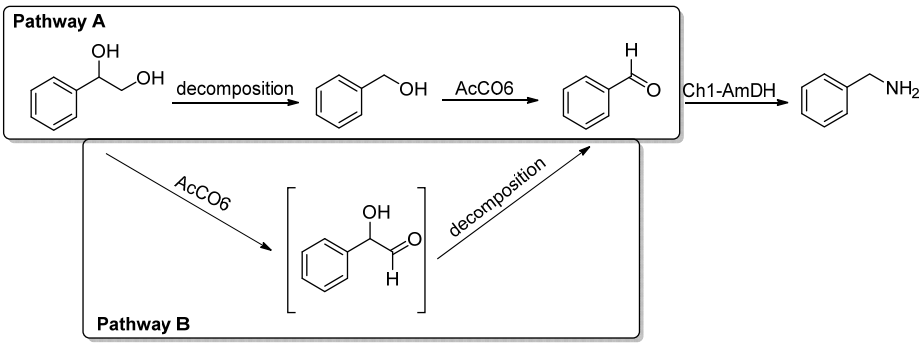

Scheme 5.19. Possible pathways for the formation of benzyalmine side product.

To improve the conversion, especially in the case of (*R*)-**3a**, different enzyme loadings were tested. Three sets of experiments were carried out in which the

AcCO6 was used either in excess or in lower molar ratio compared to the Ch1-AmDH (**Table 5.19**). Surprisingly, the reaction of (*S*)-**3a** (20 mM) at higher AcCO6 loading (entry 1) led to full substrate conversion, although a larger excess of benzylamine was detected (11%); thus (*S*)-**5a'** was formed in 89%. On the other hand, lower AcCO6 loading (entry 2 and 3) led to lower conversion into the desired product (41-77%) as well as lower traces of side products (2-4%). According to these results, it seems that the AcCO6 is also responsible for the side-reaction. However, a higher substrate loading may also affect the magnitude of the side reaction. In fact, for the conversion of (*R*)-**3a** (10 mM), the best results were obtained at higher loading of AcCO6 (70 µM) compared with Ch1-AmDH (35 µM): lower amount of benzylamine (2%) was detected (entry 4). Furthermore, lower conversions into the desired amino alcohol (*R*)-**5a'** were observed by lowering the AcCO6 loading and using 10 mM substrate concentration; as well, the formation of benzylamine side product was also low (entry 5 and 6). This is a further indication that both substrate concentration and AcCO6 loading play a crucial role in the outcome of the reaction. This last hypothesis was further corroborated by testing higher *rac*-**3a** concentration (30 mM) under the same reaction conditions applied on the optically active substrates (entry 7-9, Table 5.19). In fact, at 30 mM substrate concentration and higher loading of AcCO6, higher conversion into the product were observed along with higher production of benzylamine (entry 7). On the other hand, lower conversions were observed when AcCO6 was used in lower amounts compared with the Ch1-AmDH (entry 8 and 9). In these cases, lower amounts of benzylamine were detected as well. The same trend was observed by performing the cascade at 20 mM scale (entry 10-12).

Table 5.19. Optimization of the one-pot orthogonal bioamination cascade of optically active **3a** (10-30 mM) to optically pure **5a'** by varying substrate and enzyme loading.

Entry	Sub. [mM]	AcCO6 [uM]	Ch1-AmDH [uM]	Conv. [%][c]	5a' [%][c]	Benzylamine [%][c]	*ee* [%][b]
1[a]	(*S*)-**3a** [20]	70	35	99±1	89±<1	11±1	>98 (***S***)
2	(*S*)-**3a** [20]	24	60	81±4	77±3	4±1	n.m.
3	(*S*)-**3a** [20]	10	50	43±<1	41±<1	2±<1	n.m.
4	(*R*)-**3a** [10]	70	35	>99	98±<1	2±<1	>99 (***R***)
5	(*R*)-**3a** [10]	24	60	77±<1	76±<1	1±<1	n.m.
6	(*R*)-**3a** [10]	10	50	41±1	40±1	1±<1	n.m.
7	*rac*-**3a** [30]	70	35	94±1	85±1	9±<1	38 (*S*)
8	*rac*-**3a** [30]	24	60	62±1	60±1	2±<1	n.m.
9	*rac*-**3a** [30]	10	50	31±<1	30±<1	1±<1	n.m.
10	*rac*-**3a** [20]	70	35	99±1	96±<1	4±1	33 (*S*)
11	*rac*-**3a** [20]	24	60	75±2	75±2	<1	n.m.

Table 5.19. *(Continued)*

Entry	Sub. [mM]	AcCO6 [uM]	Ch1-AmDH [uM]	Conv. [%][c]	5a' [%][c]	Benzylamine [%][c]	*ee* [%][b]
12	*rac*-**3a** [20]	10	50	42±1	42±1	<1	n.m.

[a]Average of four samples. [b]Analyzed by RP-HPLC (C18 HD column) after derivatization of the amino group with GITC. [c]Reactions were performed in duplicate and results are reported as average of the two samples.

In summary, we could obtain our target products (*S*)-**5a'** and (*R*)-**5a'** with high analytical yields (98%) as well as perfect enantioselectivity (*ee* up to >99%) by tuning both substrates and enzymes loading in order to find a good balance between the formation of the desired products and at the same time limiting the production of benzylamine side product, as summarized in **Scheme 5.20**.

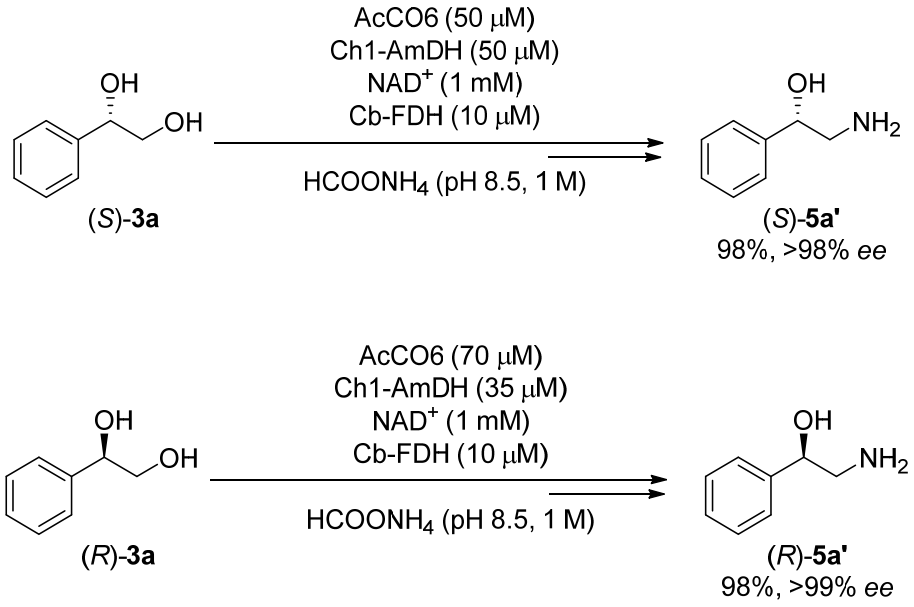

Scheme 5.20. Overview of the one-pot multi-enzymatic cascades for the synthesis of chiral **5a'** from optically active **3a**.

5.3 Conclusions

In conclusion, we have presented the one-pot synthesis of both optically active 2-amino-2-phenylethan-1-ol (**5a**) and 2-amino-1-phenylethan-1-ol (**5a'**) by means of two multi-enzymatic cascades, which convert 1-phenyl-1,2-diols (**3a**) with high conversions and enantioselectivity. Chiral amino alcohols (*R*)-**5a** and (*S*)-**5a** could be obtained in good analytical yields (70-97%) and high selectivity (>99%) starting from substrate (*R*)-**3a**. The strategy was a one-pot bio-oxidation catalyzed by Aa-ADH followed by a transamination of the *in situ* formed hydroxyketone intermediate **4a** catalyzed by two stereocomplementary ωTAs such as Bm(*S*)-ωTA and At(*R*)-ωTA, respectively. Moreover, the NAD^+ coenzyme required for the oxidation step was recycled by the addition of an alanine dehydrogenase (Bs-AlaDH). AlaDH utilizes the ammonia from the buffer, the NADH produced in the first oxidative step and the pyruvate, byproduct of the transamination reaction, to recycle the NAD^+ and the amine donor alanine. Furthermore, due to the lack of suitable primary NAD^+-dependent ADH and the instability of the hydroxyaldehyde intermediate **4a'** that tends to isomerize to **4a**, a different cascade was developed for the one-pot synthesis of optically active **5a'**. This multi-enzymatic cascade consists of the alcohol oxidase AcCO6, which performs the selective bio-oxidation of the primary hydroxyl moiety of either (*S*)-**3a** or (*R*)-**3a**, combined with the amine dehydrogenase Ch1-AmDH. The cascade leads to either (*S*)-**5a'** or (*R*)-**5a'** with high analytical yields and enantioselectivity (>98%; *ee* up to >99%). Furthermore, the multi-enzyme cascades can be implemented into another one-pot cascade for the synthesis of optically active substrates **3a** through the epoxidation/hydrolysis (Fus-SMO/Cb-FDH/EH) of the cheap and readily available styrene **1a** as starting material. These results provide the basis for further extension of the cascades' substrate scope to give access to a diverse range of vicinal amino alcohols. Therefore, the potential of these cascades could be further explored by tuning, engineering and discovery of new enzymes belonging to these families.

5.4 Experimental section

General information: ADHs (Aa, Lbv, Pp, Sy, BDHA, Ls, Te-v1, Te-v2, Te-v3, Lb and Rs), AmDH (Ch1-AmDH and Rs-PhAmDH), Fus-SMO and EHs (Sp(*S*)-EH and St(*R*)-EH) were expressed and in some cases purified according to the procedures described in chapter 3.[46] The ωTAs used in this study were expressed and purified as reported in chapter 4. FuCO and AcCO6 were expressed and purified according to the standard procedures reported in Chapter 3 for His_6-tagged enzymes. A complete list of all the enzymes used in this study together with all the required details is reported in **Table 5.20**. Compounds *rac*-**3a** and **4a** were purchased by TCI while **5a** and **5a'** by Fluorochem.

5.4.1 Enzymes used in this study

Table 5.20. List of enzymes employed in this study

Name	Source/Comment	Plasmid	Tag	Expression/ Purification	Used form	Ref
Fus-SMO	Fused SMO from *Pseudomonas* sp. VLB120	pET28b	N-His_6	Ref. [43]	lyophilized whole cells	43
Fus-SMO (1) + Cb-FDH (2)	Fused SMO coexpressed with Cb-FDH	pET28b/pET21a	N-His_6 (1)/No-Tag (2)	Ref. [43]	lyophilized whole cells	43
Sp(S)-EH	*Sphingomonas* sp. HXN200	pET28b	N-His_6	1 mM IPTG, 25 °C 16 h	lyophilized whole cells	44
St(R)-EH	*Solanum tuberosum*	pET28b	N-His_6	1 mM IPTG, 25 °C 16 h	lyophilized whole cells	44
Rs-ADH	*Ralstonia* sp.	pET28b	N-Strep	0.5 mM IPTG, 25 °C 16 h	lyophilized whole cells	53
Aa-ADH	*Aromatoleum aromaticum*	pET28b	N-His_6	Ref. [70]	purified	32
Pp-ADH	*Paracoccus pantotrophus* DSM 11072	pMS470/ pEamTA	C-His_6	2 mM IPTG, 25 °C, 16 h	lyophilized whole cells	71
Sy-ADH	*Sphingobium yanoikuyae* DSM 6900	pET26b	C-Strep	0.5 mM IPTG, 25 °C 16 h	lyophilized whole cells	48
Te-ADH_{v1}	I86A variant from *Thermoanaerobacter ethanolicus*	pET21a	C-Strep	0.5 mM IPTG, 25 °C 16 h	lyophilized whole cells	38
Te-ADH_{v2}	W110A variant from *Thermoanaerobacter ethanolicus*	pET42a	GST	0.5 mM IPTG, 25 °C 16 h	lyophilized whole cells	38
Te-ADH_{v3}	I86A W110A variant from *Thermoanaerobacter ethanolicus*	pET42a	GST	0.5 mM IPTG, 25 °C 16 h	lyophilized whole cells	38

Table 5.20. *(Continued)*

Name	Source/Comment	Plasmid	Tag	Expression/ Purification	Used form	Ref
Lb-ADH	*Lactobacillus brevis*	pET21a	no Tag	0.5 mM IPTG, 25 °C 16 h	purified	[52]
Lbv-ADH	variant from *Lactobacillus brevis*	pET21a	no Tag	[39]	purified	[47]
Ls-ADH	*Leifsonia* sp.	pET21a	no Tag	0.5 mM IPTG, 25 °C 16 h	lyophilized whole cells and purified	[54]
Bs-BDHA	*Bacillus subtilis* BGSC1A1	pET28b	N-His_6	0.5 mM IPTG, 25 °C 16 h	purified	[50, 51]
Ch1-AmDH	Chimeric AmDH	pET28b	N-His_6	Ref. [39]	purified	[41]
Rs-PhAmDH	variant from *Rhodoccoccus* sp.	pET28b	N-His_6	Ref. [38]	purified	[55]
LE-AmDH	Variant from Ɛ-LysDH		N-His_6	Ref. [56]	purified	[56]
Cb-FDH	*Candida boidinii*	pET28b	N-His_6	Ref. [42]	purified	[42]
YcnD	NAD(P)H-dependent oxidase from *Bacillus subtilis*	pET21a	no Tag	Ref. [38]	purified	[72]
NOx	NADH-dependent oxidase from *Streptococcus* mutans	pET21a	C-His_6	Ref. [73]	purified	[74]
Bs-AlaDH	*Bacillus sphaericus*	pET28b-v	N-$Strep_3$	0.5 mM IPTG, 25 °C 16 h	purified	[37]
HL-ADH	*Equus caballus*	pET28b-v	GST	See paragraph 5.2.4.4.1	purified	[66]
FuCO	Lactaldehyde reductase variant from *E.coli*	pET28b-v	N-His_6	0.5 mM IPTG, 25 °C 16 h	purified	[67-69]
At(R)-ωTA	*Aspergillus terreus*	pET21a	C-His_6	0.5 mM IPTG, 25 °C 16 h	purified	[33, 34]
Cv(S)- ωTA	*Chromobacterium violaceum* DSM 30191	pET28b-v	N-His_6	0.5 mM IPTG, 25 °C 16 h	purified	[57]
Bm(S)-ωTA	*Bacillus megaterium* SC6394	pET28b-v	N-His_6	0.5 mM IPTG, 25 °C 16 h	purified	[35, 36]

Table 5.20. *(Continued)*

Name	Source/Comment	Plasmid	Tag	Expression/ Purification	Used form	Ref
Vf(S)-ωTA	*Vibrio fluvialis*	pET28b-v	N-His_6	0.5 mM IPTG, 25 °C 16 h	lyophilized whole cells	58, 59
Ac(S)-ωTA	*Arthrobacter citreus*	pET28b-v	N-His_6	0.5 mM IPTG, 25 °C 16 h	purified	36
AcCO6	*Arthrobacter chlorophenolicus* Variant of Choline oxidase	pET28b	N-His_6	0.5 mM IPTG, 25 °C 16 h	purified	40

5.4.2 Enzymatic synthesis of chiral substrates 3a

5.4.2.1 Organic solvents screening for the Fus-SMO/Cb-FDH/EHs biocatalytic cascade

Lyophilized *E. coli* cells carrying overexpressed fused-SMO (20 mg mL^{-1}) and EHs (20 mg mL^{-1}) were rehydrated in KPi buffer (pH 8, 50 mM; 0.5-1 mL according to Table 5.1) in a glass vial (4 mL). The buffer already contained NAD^+ (1 mM), HCOONa (100 mM) and FAD (50 µM). Then, Cb-FDH (10 µM) was added followed by substrate **1a** (20 mM, otherwise stated). A second phase, consisting of an organic solvent (2-50 %), was also added in selected experiment (see Table 5.1). The mixture was shaken on an orbital shaker at 30 °C, 180 rpm for 24 h. The aqueous layer was saturated with solid NaCl followed by extraction with MTBE (2 x 500). The organic layer was dried over $MgSO_4$ and analysed by GC-FID and chiral NP-HPLC.

5.4.2.2 Preparative scale enzymatic synthesis of chiral 3a

General remark: The concentrations of coenzymes and co-substrate are always calculated on the volume of the aqueous phase, whereas the concentration of the substrate is referred to the organic phase. Furthermore, the preparative scale reactions were performed under the optimized conditions according to the procedures reported in chapter 3 and 4.

Reaction conditions: Lyophilized *E. coli* cells co-expressing Fus-SMO/Cb-FDH (250 mg, 5 mg mL^{-1}) were rehydrated in KPi buffer (50 mL, 50 mM, pH 8.0) in a baffled Erlenmeyer flask (500 mL). After that, NAD^+ (1 mM), HCOONa (5 eq.), FAD (50 µM) and catalase (0.1 mg mL^{-1}) were added. *n*-Heptane (50 mL; 1:1 volumetric ratio with the buffer) was used as biphasic solvent. Finally, the biocatalytic reactions were initiated by the addition of substrate **1a** (50 mM, 2.5 mmol). The reactions were incubated at 30 °C and 200 rpm on an orbital shaker. After 6 hours, lyophilized *E .coli* cells expressing either Sp(*S*)-EH or St(*R*)-EH (1 g, 20 mg mL^{-1}) were added and the reactions were further incubated at 30 °C and 170 rpm on an orbital

shaker for 30 h. *n*-Heptane was removed, the aqueous phase was saturated with solid NaCl and the organic compounds extracted with MTBE (3 x 25 mL). After drying over $MgSO_4$, the organic phase was removed under reduced pressure. The conversions and purity of the isolated products were determined by GC-FID, while the enantiomeric excess was analyzed by NP-HPLC.

5.4.3 Screening of secondary NAD(P)-dependent ADHs

5.4.3.1 Bio-catalytic reduction of 4a by NAD(P)-dependent ADHs in Tris-HCl buffer

Reaction conditions using lyophilized *E.coli* cells carrying overexpressed NAD^+-dependent ADHs (*Pp*-ADH, *Sy*-ADH, *Bs*-BDHA). Lyophilized *E. coli* cells carrying the required ADH (20 mg mL^{-1}) were rehydrated in an Eppendorf tube (2 mL) in Tris-HCl buffer (pH 7.5, 50 mM; 1 mL) followed by addition of NAD^+ (1 mM), HCOONa (100 mM) and purified *Cb*-FDH (10 µM). Substrate **4a** (20 mM) was added as last. The mixture was incubated at 30 °C, 170 rpm for 24 h on an orbital shaker. After saturation of the aqueous phase with solid NaCl, extraction was performed with EtOAc (2 x 500 µL). The organic layer was dried over $MgSO_4$ and conversion was analyzed by GC-FID**.**

Reaction conditions using purified NAD^+-dependent ADHs (*Aa*-ADH, *Lbv*-ADH). Tris-HCl buffer (pH 7.5, 50 mM, 1 mL final volume) was added to an Eppendorf tube (2 mL) followed by NAD^+ (1 mM), HCOONa (100 mM) and purified Cb-FDH (10 µM). Then, ADH (50 µM) and substrate **4a** (20 mM) were added as last. The mixture was incubated at 30 °C, 170 rpm for 24 h on an orbital shaker. After saturation of the aqueous phase with solid NaCl, extraction was performed with EtOAc (2 x 500 µL). The organic layer was dried over $MgSO_4$ and conversion was analyzed by GC-FID**.**

Reaction conditions using lyophilized *E.coli* cells carrying overexpressed $NADP^+$-dependent ADHs (*Te*-$ADH_{V1,V2,V3}$, *Rs*-ADH). Lyophilized *E. coli* cells carrying the ADH (20 mg mL^{-1}) were rehydrated in an Eppendorf tube (2 mL) in Tris-HCl buffer (pH 7.5, 50 mM, 1 mL final volume) followed by addition of $NADP^+$ (1 mM), glucose (100 mM) and GDH (1 mg mL^{-1}; lyophilized crude extract, Codexis GDH-105, ca. 50 U mg^{-1}). Substrate **4a** (20 mM) was added as last. The mixture was incubated at 30 °C, 170 rpm for 24 h on an orbital shaker. After saturation of the aqueous phase with solid NaCl, extraction was performed with EtOAc (2 x 500 µL). The organic layer was dried over $MgSO_4$ and conversion was analyzed by GC-FID**.**

Reaction conditions using purified $NADP^+$-dependent ADHs (*Lb*-ADH). Tris-HCl buffer (pH 7.5, 50 mM, 1 mL final volume) was added to an Eppendorf tube (2 mL) followed by $NADP^+$ (1 mM), glucose (100 mM) and GDH (1 mg mL^{-1}; lyophilized crude extract, Codexis GDH-105, ca. 50 U mg^{-1}). Then, ADH (50 µM) and substrate **4a** (20 mM) were added as last. The mixture was incubated at 30 °C, 170 rpm for 24 h on an orbital shaker. After saturation of the

aqueous phase with solid NaCl, extraction was performed with EtOAc (2 x 500 µL). The organic layer was dried over $MgSO_4$ and conversion was analyzed by GC-FID**.**

5.4.3.2 Bio-catalytic oxidation of 3a catalyzed by NAD(P)-dependent ADHs in Tris-HCl buffer

Reaction conditions using lyophilized *E. coli* cells expressing one of the following $NAD(P)^+$-dependent ADHs: Sy-ADH, Pp-ADH, Bs-BDHA, Te-ADH-v1, Te-ADH-v2, Te-ADH-v3 and Rs-ADH**.** Lyophilized *E. coli* cells (20 mg mL^{-1}) were rehydrated in an Eppendorf tube (2 mL) in Tris-HCl buffer (1 mL, pH 7.5, 50 mM) containing $NAD(P)^+$ (1 mM). NOx (10 µM) for NAD^+-dependent ADHs or YcnD (10 µM) for $NADP^+$-dependent ADHs, respectively, was also added for cofactor regeneration. Substrate **3a** (10-20 mM) was added as last. The mixtures were incubated at 30 °C, 170 rpm for 24 h on an orbital shaker and, after saturation of the aqueous layer with solid NaCl, the organic compounds were extracted with EtOAc (2 x 500 µL). The organic layers were dried over $MgSO_4$ and analyzed by GC-FID**.**

Reaction conditions using lyophilized *E.coli* cells expressing the NAD^+-dependent Ls-ADH. Lyophilized *E. coli* cells (10 mg mL^{-1}) were rehydrated in an Eppendorf tube (2 mL) in KPi buffer (1 mL, pH 6.5, 100 mM) containing NAD^+ (1 mM). NOx (10 µM) was also used for cofactor regeneration and *rac*-**3a** (10 mM) was added as last. The mixture was incubated at 40 °C, 170 rpm for 24 h on an orbital shaker. After saturation of the aqueous layer with solid NaCl, extraction was performed with MTBE (2 x 500 µL). The organic layer was dried over $MgSO_4$ and analyzed by GC-FID**.**

Reaction conditions using purified ADHs: Lbv-ADH, Aa-ADH and Lb-ADH.
General information: in selected cases, Aa-ADH and Lbv-ADH were combined in the same pot. In these cases, both enzymes were used in 25 µM concentration each.

Tris-HCl buffer (1 mL, pH 7.5, 50 mM) was added to an Eppendorf tube (2 mL) containing either NAD^+ or $NADP^+$ (1 mM, 0.1 eq.); NOx (10 µM) for NAD^+-dependent ADHs or YncD (10 µM) for $NADP^+$-dependent ADHs, respectively, were also added. As last, the tested ADH (50 µM) was added followed by substrate **3a** (10-20 mM). The mixture was incubated at 30 °C, 170 rpm for 24 h on an orbital shaker. After saturation of the aqueous layer with solid NaCl, extraction was performed with EtOAc (2 x 500 µL). The organic layer was dried over $MgSO_4$ and analyzed by GC-FID**.**

5.4.3.3 General procedure for the biocatalytic oxidation of *rac*-3a by purified NAD^+-dependent ADHs in $HCOONH_4$ buffer

General information: in selected cases, Aa-ADH and Lbv-ADH were combined in the same pot. In these cases, both enzymes were used in 25 µM concentration each.

$HCOONH_4$ buffer (0.5 mL, pH 8.5, 1 M) was added to an Eppendorf tube (1.5 mL) containing NAD^+ (1 mM); NOx (10 µM) was also added for coenzyme recycling. As last, the tested ADH (50 µM) was added followed by *rac*-**3a** (10 or 20 mM). The mixture was incubated at 30 °C, 170 rpm for 24 h on an orbital shaker. After saturation of the aqueous layer with solid NaCl, extraction was performed with EtOAc (1 x 500 µL). The organic layer was dried over $MgSO_4$ and analyzed by GC-FID**.**

5.4.4 Enzymatic synthesis of chiral 2-amino-2-phenylethan-1-ol 5a

5.4.4.1 General procedure for the one-pot HB-bioamination of substrate 3a

General information: in selected cases, Aa-ADH and Lbv-ADH were combined in the same pot. In these cases, each enzyme was used in 25 µM concentration.
In an Eppendorf tube (1.5 mL), $HCOONH_4$ buffer (0.5 mL, pH 8.5, 1 M) and NAD^+ (1 mM) were added followed by purified ADH (50 µM) and AmDH (50 µM). Racemic or enantiopure diol **3a** (10 mM) was added as last. The mixture was incubated at 30 °C, 170 rpm for 48 h on an orbital shaker and, after that, quenched with 10 M KOH (100 µL). The aqueous layer was saturated with solid NaCl and the organic compounds extracted with EtOAc (1 x 500 µL). The organic layer was dried over $MgSO_4$ and analyzed by GC-FID to determine the conversion, while the enantiomeric excesses was analyzed by RP-HPLC after derivatization with a chiral reagent (GITC).

General derivatization procedure for the determination of the enantiomeric excess by RP-HPLC [75]
The aqueous reaction mixture (20 µL) was dissolved in acetonitrile (180 µL) to yield a final concentration of 0.5 mM. Then, GITC (2,3,4,6-Tetra-O-acetyl-β-D-glucopyranosyl isothiocyanate) (1.5 mM) and Et_3N (1.5 mM) were added as a solution in acetonitrile (200 µL). The mixture was incubated at room temperature at 1000 rpm for 35 min. Before injection into the RP-HPLC, the samples were centrifuged and filtered if required.

5.4.4.2 One-pot cascade for the conversion of 3a by coupling ADHs with two stereocomplementary ωTAs in Tris-HCl buffer

General information: in selected experiments, either Aa-ADH and Lbv-ADH or Bs-BDHA and Lbv-ADH were combined in the same pot; in these cases, each enzyme was used in 25 µM concentration. In other tests, Aa-ADH, Bs-BDHA and Lbv-ADH were all combined and each enzyme loading was the following: 25:25:50 µM, respectively.

Tris-HCl (pH 7.5, 50 mM; 0.5 mL) was added to an Eppendorf tube (1.5 mL) and supplemented with NAD^+ (1 mM), PLP (1 mM), D- or L-Alanine (50 mM, 5 eq.), Bs-AlaDH (20 µM), $HCOONH_4$ (30 mM). Then, ADH (50 µM) and ωTA (50 µM) were added followed by

substrate **3a** (10 mM). The mixture was incubated at 30 °C, 170 rpm for 48 h on an orbital shaker and, after that, quenched with 10 M KOH (100 µL). The aqueous layer was saturated with solid NaCl and the organic compounds extracted with EtOAc (1 x 500 µL). The organic layer was dried over $MgSO_4$ and analyzed by GC-FID to determine the conversion, while the enantiomeric excesses was analyzed by RP-HPLC after derivatization with a chiral reagent (GITC).

5.4.4.3 One-pot cascade for the conversion of 3a by coupling ADHs with various stereocomplementary ωTAs in $HCOONH_4$ buffer

General information: in selected cases, Aa-ADH and Lbv-ADH were combined in the same pot. In these cases, each enzyme was used in 25 µM concentration.

$HCOONH_4$ buffer (pH 8.5, 1 M; 0.5 mL) was added to an Eppendorf tube (1.5 mL) and supplemented with NAD^+ (1 mM), PLP (1 mM), D- or L-Alanine (50 mM, 5 eq.) and Bs-AlaDH (20 µM). Then, ADH (50 µM otherwise stated in Table 5.12-5.13) and ωTA (50 µ otherwise stated in Table 5.12-5.13) were added followed by substrate **3a** (10 mM). The mixture was incubated at 30 °C, 170 rpm for 48 h on an orbital shaker and, after that, quenched with 10 M KOH (100 µL). The aqueous layer was saturated with solid NaCl and the organic compounds extracted with EtOAc (1 x 500 µL). The organic layer was dried over $MgSO_4$ and analyzed by GC-FID to determine the conversion, while the enantiomeric excesses was analyzed by RP-HPLC after derivatization with a chiral reagent (GITC).

5.4.5 Enzymatic synthesis of chiral 2-amino-1-phenylethan-1-ol 5a'

5.4.5.1 Biocatalytic oxidation of rac-3a catalyzed by primary NAD^+-dependent ADHs

Lyophilized free cell extract of HL-ADH purchased by Sigma Aldrich. Lyophilized free cell extract was rehydrated in an Eppendorf tube (2 mL) in Tris-HCl buffer (1 mL, pH 7.5, 50 mM) followed by addition of NAD^+ (1 mM) and NOx (10 µM). Substrate *rac*-**3a** (20 mM) was added as last. The mixture was incubated at 30 °C, 170 rpm for 24 h on an orbital shaker. Finally, extraction was performed with EtOAc (2 x 500 µL) after saturation of the aqueous phase with solid NaCl. The organic layer was dried over $MgSO_4$ and analyzed by GC-FID.

Purified Ht-ADH. Tris-HCl buffer (1 mL, pH 7.5, 50 mM) was added to an Eppendorf tube (2 mL) followed by NAD^+ (1 mM) and NOx (10 µM). Then, Ht-ADH (50 µM) and substrate *rac*-**3a** (20 mM) were added. The mixture was incubated at 30 °C, 170 rpm for 24 h on an orbital shaker. Finally, the reaction mixture was extracted with EtOAc (2 x 500 µL) after saturation of the aqueous phase with solid NaCl. The organic layer was dried over $MgSO_4$ and analyzed by GC-FID.

5.4.5.2 One-pot cascades for the enzymatic synthesis of 5a'

5.4.5.2.1 Biocatalytic cascade of rac-3a to 5a' by one-pot HL-ADH/AmDHs enzymatic system

Lyophilized cell free extract of HL-ADH (2 mg mL^{-1}, purchased from Sigma Aldrich, product number 9031-72-5, activity 0.52 U/mg; ca. 20 % protein content) was rehydrated in an Eppendorf tube (2 mL) in ammonium formate buffer (0.5 mL, pH 8.5, 1 M) followed by addition of NAD^+ (1 mM) and purified AmDH (100 µM). Substrate *rac*-**3a** (5 mM) was added as last. The mixture was incubated at 30 °C, 180 rpm for 48 h on an orbital shaker. Finally, the reaction mixture was quenched with 10 M KOH (100 µL) ad extracted with EtOAc (1 x 500 µL). The organic layer was dried over $MgSO_4$ and analyzed by GC-FID.

5.4.5.2.2 Biocatalytic cascade for the conversion of *rac*-3a to 5a' by one-pot HL-ADH/Cv(*S*)-ωTA enzymatic system

Lyophilized *E. coli* cells carrying overexpressed Cv(*S*)-ωTA (10 mg mL^{-1}) were rehydrated in an Eppendorf tube (2 mL) in Tris-HCl buffer (1 mL, pH 7.5, 50 mM) followed by addition of L-alanine (25 mM), PLP (0.5 mM), NAD^+ (1 mM), LDH (1 mg mL^{-1}, lyophilized crude extract , Codexis, LDH-101, ca. 60 U mg^{-1}) and HL-ADH (2 mg mL^{-1}). As last, substrate *rac*-**3a** (5 mM) was added. The mixture was incubated at 30 °C, 180 rpm for 48 h on an orbital shaker. The mixture was quenched with 10 M KOH (100 µL) ad extracted with EtOAc (2 x 500 µL). The organic layer was dried over $MgSO_4$ and analyzed by GC-FID.

5.4.5.2.3 Biocatalytic cascade for the conversion of *rac*-3a to 5a' by one-pot Ht-ADH/ Cv(*S*)-ωTA enzymatic system

Lyophilized *E. coli* cells carrying overexpressed Cv(*S*)-ωTA (15 mg mL^{-1}) were rehydrated in an Eppendorf tube (2 mL) in Tris-HCl buffer (1 mL, pH 7.5, 50 mM) followed by addition of L-alanine (100 mM), PLP (0.5 mM), NAD^+ (1 mM), LDH (1 mg mL^{-1}, lyophilized crude extract, Codexis, LDH-101, ca. 60 U mg mL^{-1}) and purified Ht-ADH (50 µM). As last, substrate *rac*-**3a** (20 mM) was added. The mixture was incubated at 30 °C, 180 rpm for 48 h on an orbital shaker. The reaction mixture was quenched with 10 M KOH (100 µL) and extracted with EtOAc (2 x 500 µL). The organic layer was dried over $MgSO_4$ and analyzed by GC-FID.

5.4.5.3 Orthogonal bioamination cascade for the conversion of *rac*-3a to 5a' by one-pot AcCO6/Ch1-AmDH as enzymatic system

In an Eppendorf tube (1.5 mL), $HCOONH_4$ buffer (0.5 mL, pH 8.5, 1 M), NAD^+ (1 mM), catalase (0.1 mg mL^{-1}) and purified Cb-FDH (10 µM) were added followed by purified AcCO6 (50 µM, otherwise stated in Table 5.19) and Ch1-AmDH (50 µM, otherwise stated in Table 5.19). *Rac*-**3a** or enantiopure **3a** (10-20 mM) was added as last. The mixture was incubated at 30 °C, 170 rpm for 48 h on an orbital shaker and, after that, quenched with 10 M KOH (100 µL). The aqueous phase was saturated with solid NaCl and the organic compounds extracted with EtOAc (1 x 500 µL). The organic layer was dried over $MgSO_4$ and analyzed by GC-FID to

determine the conversion, while the enantiomeric excesses was analyzed by RP-HPLC after derivatization with a chiral reagent (GITC).

5.4.6 Analytical methods

GC-FID method A: Column Agilent DB-1701 (30 m, 250 µm, 0.25 µm); injector temperature 250 °C; constant pressure 14.50 psi; temperature program: 80 °C/hold 6.5 min; 160 °C/rate 10 °C min^{-1}/hold 5 min; 200 °C/rate 20 °C min^{-1}/hold 2 min; 280 °C/rate 20 °C min^{-1}/hold 1 min.

NP-HPLC method B: Column chiralcel-OD; Program: constant oven temperature 25 °C; constant pressure 14 bar; eluent composition: Hexane/Isopropanol 95:5, 1 mL min^{-1}; detection at 210 nm.

RP-HPLC method C: Column: Nucleosil C_{18} HD (0.46 cm x 25 cm); program: constant oven temperature 30 °C; eluent composition: isocratic MeOH + 0.1% TFA/MilliQ + 0.1% TFA (50:50); flow rate: 0.7 mL min^{-1}, detection at 248 nm.

Table 5.21. Retention time compounds used in this study associated with the different analytical methods

Compound	Retention time [min]	Method
1a	4.4	A
(*S*)-**2a**	10.3	A
(*S*)-**3a**	19.1	A
	23.1	B
(*R*)-**3a**	19.1	A
	21.9	B
4a	15.8	A
(*S*)-**5a**[a]	17.5	A
	15.1	C
(*R*)-**5a**[a]	17.5	A
	18.8	C
(*S*)-**5a'**[a]	17.4	A
	25.2	C
(*R*)-**5a'**[a]	17.4	A
	23.3	C

[a] After derivatization with GITC

5.5 References

1. T. X. Metro, J. Appenzeller, D. G. Pardo and J. Cossy, *Org. Lett.*, 2006, 8, 3509-3512.
2. I. Cho, C. K. Prier, Z. J. Jia, R. K. Zhang, T. Gorbe and F. H. Arnold, *Angew. Chem. Int. Ed.*, 2019, 58, 3138-3142.
3. J. H. Schrittwieser, F. Coccia, S. Kara, B. Grischek, W. Kroutil, N. d'Alessandro and F. Hollmann, *Green Chem.*, 2013, 15, 3318.
4. D. J. Ager, I. Prakash and D. R. Schaad, *Chem. Rev.*, 1996, 96, 835-876.

5. J. Vicario, D. Badia, L. Carrillo, E. Reyes and J. Etxebarria, *Curr. Org. Chem.*, 2005, 9, 219-235.
6. K. Everaere, A. Mortreux and J.-F. Carpentier, *Adv. Synth. Catal.*, 2003, 345, 67-77.
7. J. A. Bodkin and M. D. McLeod, *J. Chem. Soc., Perkin Trans. 1*, 2002, 2733-2746.
8. D. N. O. Reiser, *Adv. Synth. Catal.*, 2002, 344, 1169-1173.
9. F. D. Klingler, *Acc. Chem. Res.*, 2007, 40, 1367-1376.
10. O. Lohse and C. Spöndlin, *Org. Process Res. Dev.*, 1997, 1, 247-249.
11. N. Azizi and M. R. Saidi, *Org. Lett.*, 2005, 7, 3649-3651.
12. M. Pastó, B. Rodríguez, A. Riera and M. A. Pericàs, *Tetrahedron Lett.*, 2003, 44, 8369-8372.
13. A. Murugan, V. K. Kadambar, S. Bachu, M. Rajashekher Reddy, V. Torlikonda, S. G. Manjunatha, S. Ramasubramanian, S. Nambiar, G. P. Howell and J. Withnall, *Tetrahedron Lett.*, 2012, 53, 5739-5741.
14. H.-T. Chang and K. B. Sharpless, *Tetrahedron Lett.*, 1996, 37, 3219-3222.
15. A. W. Buesking and J. A. Ellman, *Chem. Sci.*, 2014, 5, 1983-1987.
16. O. Reiser, *Angew. Chem. Int. Ed.*, 1996, 35, 1308-1309.
17. R. Lihammar, R. Millet and J.-E. Bäckvall, *Adv. Synth. Catal.*, 2011, 353, 2321-2327.
18. P. Gupta and N. Mahajan, *New J. Chem.*, 2018, 42, 12296-12327.
19. A. Rouf, P. Gupta, M. A. Aga, B. Kumar, R. Parshad and S. C. Taneja, *Tetrahedron: Asymmetry*, 2011, 22, 2134-2143.
20. A. Chaubey, R. Parshad, P. Gupta, S. C. Taneja, G. N. Qazi, C. R. Rajan and S. Ponrathnam, *Biorg. Med. Chem.*, 2009, 17, 29-34.
21. J. Rehdorf, M. D. Mihovilovic and U. T. Bornscheuer, *Angew. Chem. Int. Ed.*, 2010, 49, 4506-4508.
22. J. Rehdorf, M. D. Mihovilovic, M. W. Fraaije and U. T. Bornscheuer, *Chemistry*, 2010, 16, 9525-9535.
23. K. Baer, N. Dückers, W. Hummel and H. Gröger, *ChemCatChem*, 2010, 2, 939-942.
24. T. Sehl, H. C. Hailes, J. M. Ward, R. Wardenga, E. von Lieres, H. Offermann, R. Westphal, M. Pohl and D. Rother, *Angew. Chem. Int. Ed.*, 2013, 52, 6772-6775.
25. S. Matosevic, G. J. Lye and F. Baganz, *J. Biotechnol.*, 2011, 155, 320-329.
26. C. U. Ingram, M. Bommer, M. E. Smith, P. A. Dalby, J. M. Ward, H. C. Hailes and G. J. Lye, *Biotechnol. Bioeng.*, 2007, 96, 559-569.
27. J. Steinreiber, M. Schürmann, F. van Assema, M. Wolberg, K. Fesko, C. Reisinger, D. Mink and H. Griengl, *Adv. Synth. Catal.*, 2007, 349, 1379-1386.
28. J. Steinreiber, M. Schurmann, M. Wolberg, F. van Assema, C. Reisinger, K. Fesko, D. Mink and H. Griengl, *Angew. Chem. Int. Ed.*, 2007, 46, 1624-1626.
29. G. Sello, F. Orsini, S. Bernasconi and P. D. Gennaro, *Tetrahedron: Asymmetry*, 2006, 17, 372-376.
30. Z. B. Sun, Z. J. Zhang, F. L. Li, Y. Nie, H. L. Yu and J. H. Xu, *ChemCatChem*, 2019, 11, 3802-3807.
31. S. Wu, Y. Zhou, T. Wang, H. P. Too, D. I. Wang and Z. Li, *Nat. Commun.*, 2016, 7, 11917.
32. H. W. Hoffken, M. Duong, T. Friedrich, M. Breuer, B. Hauer, R. Reinhardt, R. Rabus and J. Heider, *Biochemistry*, 2006, 45, 82-93.
33. F. G. Mutti, C. S. Fuchs, D. Pressnitz, J. H. Sattler and W. Kroutil, *Adv. Synth. Catal.*, 2011, 353, 3227-3233.
34. A. Lyskowski, C. Gruber, G. Steinkellner, M. Schurmann, H. Schwab, K. Gruber and K. Steiner, *PloS One*, 2014, 9, e87350.
35. R. L. Hanson, B. L. Davis, Y. Chen, S. L. Goldberg, W. L. Parker, T. P. Tully, M. A. Montana and R. N. Patel, *Adv. Synth. Catal.*, 2008, 350, 1367-1375.
36. N. van Oosterwijk, S. Willies, J. Hekelaar, A. C. Terwisscha van Scheltinga, N. J. Turner and B. W. Dijkstra, *Biochemistry*, 2016, 55, 4422-4431.
37. T. Ohashima and K. Soda, *Eur. J. Biochem.*, 1979, 100, 29-30.
38. T. Knaus, L. Cariati, M. F. Masman and F. G. Mutti, *Org. Biomol. Chem.*, 2017, 15, 8313-8325.

39. F. G. Mutti, T. Knaus, N. S. Scrutton, M. Breuer and N. J. Turner, *Science*, 2015, 349, 1525-1529.
40. R. S. Heath, W. R. Birmingham, M. P. Thompson, A. Taglieber, L. Daviet and N. J. Turner, *ChemBioChem*, 2019, 20, 276-281.
41. B. R. Bommarius, M. Schurmann and A. S. Bommarius, *Chem. Commun.*, 2014, 50, 14953-14955.
42. T. Knaus, W. Bohmer and F. G. Mutti, *Green Chem.*, 2017, 19, 453-463.
43. M. L. Corrado, T. Knaus and F. G. Mutti, *ChemBioChem*, 2018, 19, 679-686.
44. S. Wu, Y. Chen, Y. Xu, A. Li, Q. Xu, A. Glieder and Z. Li, *ACS Catal.*, 2014, 4, 409-420.
45. S. Panke, M. Held, M. G. Wubbolts, B. Witholt and A. Schmid, *Biotechnol. Bioeng.*, 2002, 80, 33-41.
46. M. L. Corrado, T. Knaus and F. G. Mutti, *Green Chem.*, 2019, 21, 6246-6251.
47. N. H. Schlieben, K. Niefind, J. Muller, B. Riebel, W. Hummel and D. Schomburg, *J. Mol. Biol.*, 2005, 349, 801-813.
48. I. Lavandera, A. Kern, M. Schaffenberger, J. Gross, A. Glieder, S. de Wildeman and W. Kroutil, *ChemSusChem*, 2008, 1, 431-436.
49. I. Lavandera, A. Kern, V. Resch, B. Ferreira-Silva, A. Glieder, W. M. Fabian, S. de Wildeman and W. Kroutil, *Org. Lett.*, 2008, 10, 2155-2158.
50. J. Zhang, T. Xu and Z. Li, *Adv. Synth. Catal.*, 2013, 355, 3147-3153.
51. J. Zhang, S. Wu, J. Wu and Z. Li, *ACS Catal.*, 2014, 5, 51-58.
52. K. Niefind, J. Muller, B. Riebel, W. Hummel and D. Schomburg, *J. Mol. Biol.*, 2003, 327, 317-328.
53. I. Lavandera, A. Kern, B. Ferreira-Silva, A. Glieder, S. de Wildeman and W. Kroutil, *J. Org. Chem.*, 2008, 73, 6003-6005.
54. K. Inoue, Y. Makino and N. Itoh, *Appl. Environ. Microbiol.*, 2005, 71, 3633-3641.
55. L. J. Ye, H. H. Toh, Y. Yang, J. P. Adams, R. Snajdrova and Z. Li, *ACS Catal.*, 2015, 5, 1119-1122.
56. V. Tseliou, T. Knaus, M. F. Masman, M. L. Corrado and F. G. Mutti, *Nat. Commun.*, 2019, 10, 3717.
57. U. Kaulmann, K. Smithies, M. E. B. Smith, H. C. Hailes and J. M. Ward, *Enzyme Microb. Technol.*, 2007, 41, 628-637.
58. F. G. Mutti, C. S. Fuchs, D. Pressnitz, N. G. Turrini, J. H. Sattler, A. Lerchner, A. Skerra and W. Kroutil, *Eur. J. Org. Chem.*, 2012, 2012, 1003-1007.
59. J. S. Shin, H. Yun, J. W. Jang, I. Park and B. G. Kim, *Appl. Microbiol. Biotechnol.*, 2003, 61, 463-471.
60. R. Cannio, M. Rossi and S. Bartolucci, *Eur. J. Biochem.*, 1994, 222, 345-352.
61. M. J. Abrahamson, J. W. Wong and A. S. Bommarius, *Adv. Synth. Catal.*, 2013, 355, 1780-1786.
62. S. Al-Karadaghi, E. S. Cedergren-Zeppezauer and S. Hovmoller, *Acta Cryst. D.*, 1994, 50, 793-807.
63. D. H. Park and B. V. plapp, *J. Biol. Chem.*, 1991, 13296-13302.
64. H. Eklund, J. P. Samama and T. A. Jones, *Biochemistry*, 1984, 23, 5982-5996.
65. H. Eklund, B. Nordström, E. Zeppezauer, G. Söderlund, I. Ohlsson, T. Boiwe, B.-O. Söderberg, O. Tapia, C.-I. Brändén and Å. Åkeson, *J. Mol. Biol.*, 1976, 102, 27-59.
66. D. Quaglia, M. Pori, P. Galletti, E. Emer, F. Paradisi and D. Giacomini, *Process Biochem.*, 2013, 48, 810-818.
67. C. Blikstad and M. Widersten, *J. Mol. Catal. B: Enzym.*, 2010, 66, 148-155.
68. C. Blikstad, K. M. Dahlström, T. A. Salminen and M. Widersten, *ACS Catal.*, 2013, 3, 3016-3025.
69. C. Blikstad, K. M. Dahlstrom, T. A. Salminen and M. Widersten, *FEBS J.*, 2014, 281, 2387-2398.
70. W. Bohmer, T. Knaus and F. G. Mutti, *ChemCatChem*, 2018, 10, 731-735.

71. I. Lavandera, B. Holler, A. Kern, U. Ellmer, A. Glieder, S. de Wildeman and W. Kroutil, *Tetrahedron: Asymmetry*, 2008, 19, 1954-1958.
72. A. Morokutti, A. Lyskowski, S. Sollner, E. Pointner, T. B. Fitzpatrick, C. Kratky, K. Gruber and P. Macheroux, *Biochemistry*, 2005, 44, 13724-13733.
73. T. Knaus, V. Tseliou, L. D. Humphreys, N. S. Scrutton and F. G. Mutti, *Green Chem.*, 2018, 20, 3931-3943.
74. J. Matsumoto, M. Higuchi, M. Shimada, Y. Yamamoto and Y. Kamio, *Biosci. Biotechnol. Biochem.*, 1996, 60, 39-43.
75. M. S. Malik, E.-S. Park and J.-S. Shin, *Green Chem.*, 2012, 14, 2137.

Chapter 6

Towards the synthesis of valuable chiral vicinal amino alcohols from potential renewable raw materials

6.1 Introduction

Alkenes are highly reactive substrates due to their versatile C-C double bond. However, the origin of these compounds still relies on fossil-based feedstock. Alternative greener raw materials are needed to meet the requirements for a sustainable development towards a circular economy. For instance, a certain class of aromatic olefins can be derived from the decarboxylation of potential renewable substrates, such as caffeic, *p*-coumaric and ferulic acids. These hydroxycinnamic acids are very common in fruits and vegetables.[1] Moreover, they constitute the main units in the various forms of lignin found within different plant species.[2] Decarboxylation of such compounds is usually performed by heating up to reflux a solution of the carboxylic acid in a high boiling organic solvent, e.g., dimethylformamide (DMF).[3, 4] On the other hand, enzymatic systems are known to perform such reaction under milder conditions. Among these methods, ferulic acid decarboxylase from *Enterobacter* sp. (FaDC) was recently applied for the decarboxylation of these type of substrates.[5] In this study, we investigated the potential of the multi-enzymatic cascades developed in this thesis for accessing high valuable vicinal amino alcohols (e.g., adrenaline, *p*-synephrine, normetanephrine)[6, 7] from potential renewable raw materials. Indeed, the aim of this project is to prepare the olefin substrates through the enzymatic decarboxylation of the related carboxylic acids **1b-d** (caffeic, coumaric and ferulic acids) catalyzed by FaDC. In the subsequent steps, the one-pot cascade for the synthesis of the corresponding diols **4b-d** catalyzed by the chimeric styrene monooxygenase (Fus-SMO)[8] and two stereocomplementary epoxide hydrolases (EHs)[9] is implemented (**Scheme 6.1**).[10] Notably, there are no publications about the bio-epoxidation of these aromatic mono- and di-hydroxylated olefin substrates catalyzed by flavin-dependent styrene monooxygenase systems.

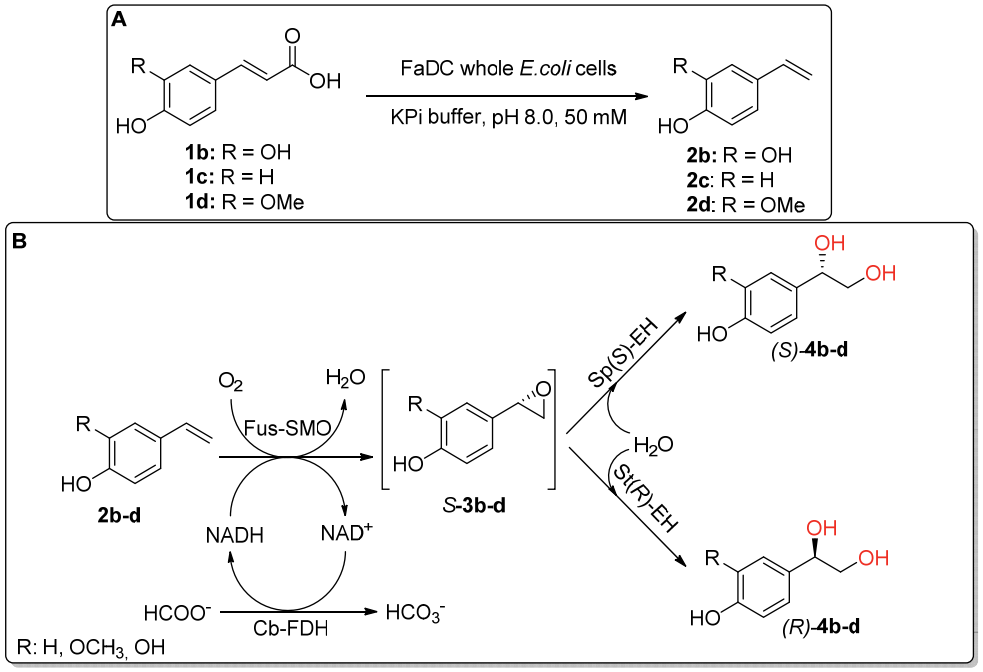

Scheme 6.1. **A)** Decarboxylation of potential renewable carboxylic acid catalyzed by a ferulic acid decarboxylase (FaDC); **B)** one-pot cascade for the dihydroxylation of aromatic olefins catalyzed by a Fus-SMO paired with two EHs.

The next step would be the conversion of these highly functionalized diols **4b-d** to the corresponding vicinal amino alcohols, as depicted in **Scheme 6.2**. This can be accomplished by pairing in a one-pot selected alcohol dehydrogenases (in this case, either Aa-ADH from *Aromatoleum aromaticum*[11] or Bs-BDHA from *Bacillus subtilis* BGSC1A1[12, 13]) with stereocomplementary ω-transaminases (in this case, Cv(*S*)-ωTA from *Chromobacterium violaceum* DSM 30191[14] and At(*R*)- ωTA from *Aspergillus terreus*[15, 16]), as described previously in chapters 4 and 5. On the other hand, another cascade was developed previously for accessing amino alcohols bearing a terminal amino group. This involves the coupling of an alcohol oxidase (AcCO6)[17] with an amine dehydrogenase (Ch1-AmDH).[18]

Overall, this chapter provides a proof-of-concept for the potential application of these routes for the synthesis of this class of amino alcohols. Nevertheless, conclusions cannot be drawn based on these results, yet, because significantly more investigation is required to fairly assess the actual relevance of this approach.

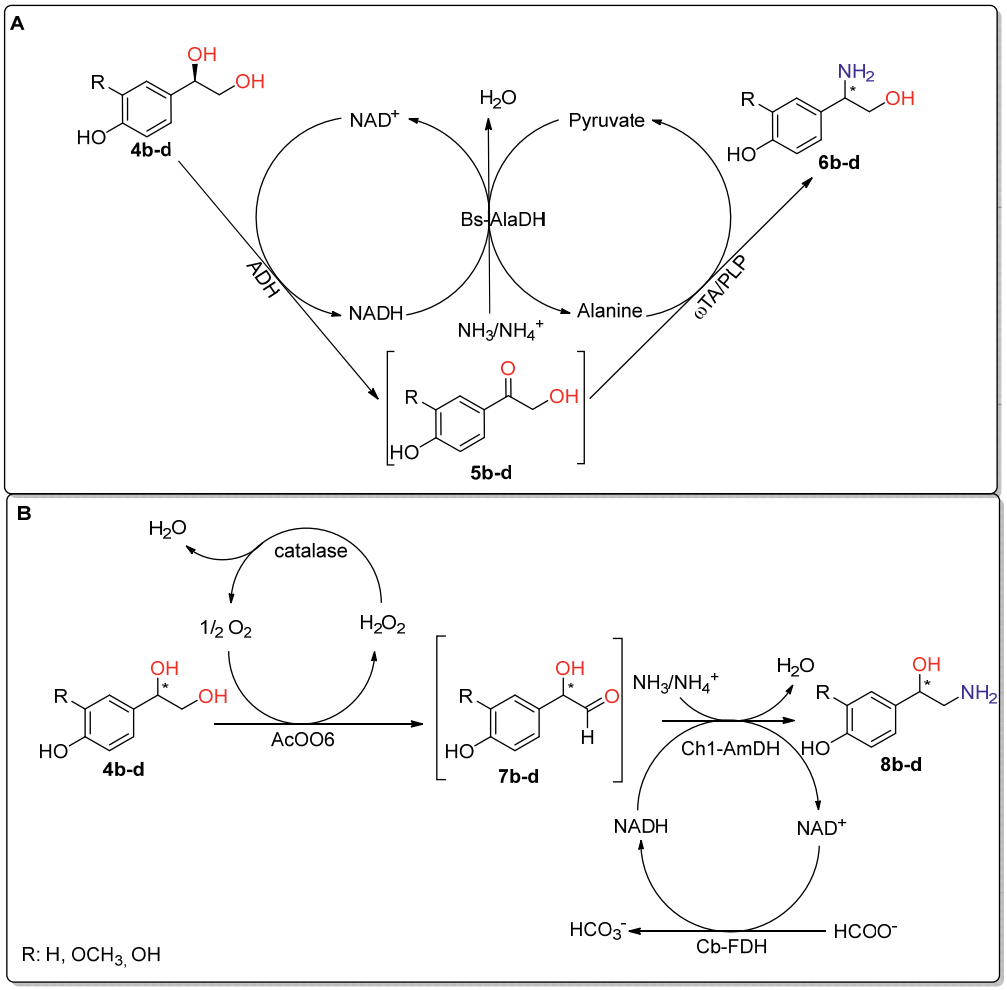

Scheme 6.2. **A)** one-pot cascade approach for the conversion of diols **4b-d** catalyzed by an alcohol dehydrogenase (ADH) paired with stereocomplementary ω-transaminases (ω-TAs) for accessing amino alcohols **6b-d**; **B)** one-pot cascade route for the conversion of diol **4b-d** catalyzed by an alcohol oxidase (AcCO6) paired with an amine dehydrogenase (Ch1-AmDH) for the synthesis of amino alcohols **8b-d**.

6.2 Results and discussion

6.2.1 Testing various conditions for the synthesis of chiral diols from caffeic acid and derivatives

6.2.1.1 Synthesis of olefin substrates by enzymatic decarboxylation of carboxylic acids

Initially, we investigated the decarboxylation step by screening the activity of lyophilized *E. coli* whole cells (20 mg mL^{-1}) carrying overexpressed ferulic acid decarboxylase from *Enterobacter* sp. (FaDC) on three substrates, namely: caffeic acid (**1b**), cumaric acid (**1c**) and ferulic acid (**1d**) at 50 mM concentration (**Scheme 6.3**). The biotransformations were carried out in KPi buffer (pH 8.0, 50 mM) and glass vials were used to prevent (or alleviate) volatility of the olefin products. The decarboxylation of all three substrates proceeded quantitatively into the desired aromatic olefin products in 24 h at 30 °C. We did not perform any further optimization at this stage.

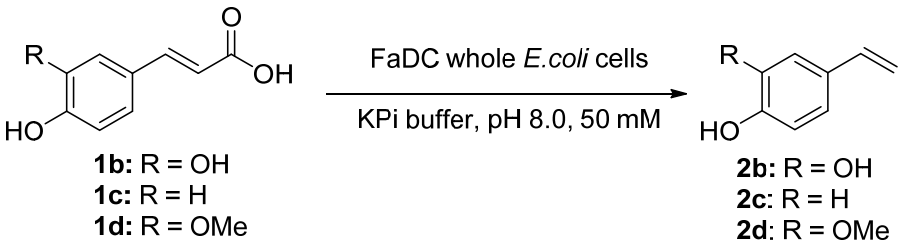

Scheme 6.3. Reaction scheme for the decarboxylation step catalyzed by ferulic acid decarboxylase as lyophilized *E. coli* whole cells

6.2.1.2 Towards the bio-catalytic synthesis of chiral epoxides from caffeic acid substrates

The next step was to investigate the possibility of pairing, in a one-pot fashion, the decarboxylation and the epoxidation steps by adding the fused-styrene monooxygenase (Fus-SMO),[8] thereby obtaining enantiopure epoxides from the correspondent carboxylic acids (50 mM), as depicted in **Scheme 6.4**. The first attempt was to perform the two reactions in a stepwise fashion. Therefore, the decarboxylation step was performed first for 24 h followed by the addition of the reagents required for the bio-epoxidation of the generated olefins. The latter step was performed by using lyophilized *E. coli* whole cells carrying the co-expressed Fus-SMO/Cb-FDH system (10 mg mL^{-1}) for 6 h reaction time. Both steps were carried out in KPi buffer (pH 8.0, 50 mM). However, while the FaDC is a coenzyme-independent enzyme, the Fus-SMO/Cb-FDH system requires the addition of some

reagents, namely: FAD (50 µM), NAD^+ (1 mM), HCOONa (250 mM, 5 eq.) and a catalase (0.1 mg mL^{-1}). Moreover, the epoxidation step is usually performed in a biphasic system by using *n*-heptane as the organic solvent, which was added together with the reagents mentioned above.[8] After a careful analysis of the outcome of this biotransformation, we observed the decarboxylated products. However, no traces of the epoxides were detected. We then proceeded by performing the two steps in a concurrent mode under the same reaction conditions described above. Hence, all the reagents required for both reactions were added in the same pot from the beginning. Surprisingly, in this case, even the decarboxylation of carboxylic acids **1b-d** did not proceed, and the substrates were the only compounds detected after 24 h. Hence, based on these results, we excluded the possibility to perform the two steps in a one-pot cascade because of deactivation and incompatibility of the enzymatic systems.

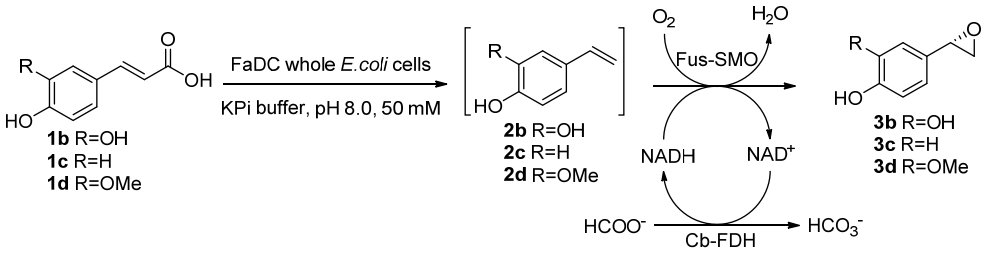

Scheme 6.4. One-pot decarboxylation/epoxidation of carboxylic acid substrates **1b-d** catalyzed by lyophilized *E. coli* whole cells.

The next step was to investigate the bio-epoxidation of aromatic olefins **2b-d** (20 mM), since no epoxides were detected when the biotransformation was carried out in the same pot with the decarboxylase. Thus, we aimed at elucidating whether the lack of epoxidation activity stemmed from the decarboxylation step due to incompatibility with either FaDC or the carboxylic acid substrates. Furthermore, we could examine the activity of the Fus-SMO/Cb-FDH system on these hydroxyl functionalized aromatic olefins, since no data were available in literature for the bio-epoxidation of these types of substrates catalyzed by flavin-dependent styrene monooxygenases. While substrates **2c-d** are commercially available (**2c** as 10% solution in propylene glycol), substrate **2b** was chemically synthesized. Nevertheless, we found out that olefins **2b-d** are not soluble in *n*-heptane, hence, we carried out the bio-epoxidation in KPi buffer only (pH 8.0, 50 mM). Additionally, the reaction depicted in **Scheme 6.5** was tested with whole *E. coli* cells carrying

either the co-expressed Fus-SMO/Cb-FDH system or only the Fus-SMO enzyme. In this last case, purified Cb-FDH (10 µM) was then added separately.

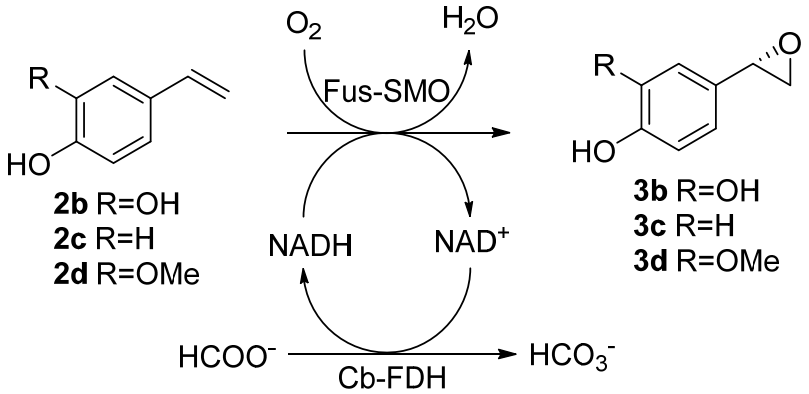

Scheme 6.5. Bio-epoxidation of aromatic olefins **2b-d** catalyzed by a fused-styrene monooxygenase.

The outcome of these biotransformations was examined first by direct analysis of the aqueous phase by RP-HPLC. Unfortunately, the reactions did not proceed as expected and none of the epoxides were detected. Notably, **2b-c** were not observed either, whereas **2d** was the sole substrate that could be recovered back; therefore, it seems that **2d** is not accepted by our enzymatic system at all. Two main hypotheses were raised at this stage: *i)* the targeted epoxides are highly unstable and, once formed, they might undergo spontaneous ring-opening to the corresponding diols; *ii)* substrates **2b-c** are the most polar of the tested series, therefore either the substrates or the corresponding epoxide/diol products might be difficult to extract. In contrast, substrate **2d**, the least polar, is surely not accepted by the Fus-SMO because it is recovered at the end of the reaction. We analyzed the aqueous phase to ascertain the possible presence of diols (e.g., TLC analysis of aqueous and organic layers; extraction of the aqueous layer with a mixture of EtOAc:MeOH (95:5) and analysis by GC-MS; protection of the hydroxyl moieties as acetates for both the organic and aqueous phase). However, none of these analyses and methods could reveal any presence of either substrates **2b-c**, or epoxide, or diol products. Therefore, it might be that either the olefin substrates (**2b-c**), or the epoxides (**3b-c**), or the corresponding diol products cannot be easily extracted from the aqueous buffer containing the lyophilized cells.

6.2.1.3 (Chemo)-enzymatic synthesis of protected 4-vinylbenzene-1,2-diol from caffeic acid

6.2.1.3.1 Chemical synthesis of protected vinyl catechol (2b') from caffeic acid

To evaluate the possibility that the highly polar substrates can interact with our bio-epoxidation system, we focused on testing the protected olefin substrates and caffeic acid **1b** was initially used as the model substrate. The decarboxylation and protection steps were carried out in the same pot by following a literature procedure.[4] Caffeic acid in dimethylformamide (DMF) was refluxed for 6 hours in the presence of potassium carbonate (K_2CO_3) and CH_2Cl_2 yielding the desired product **2b'** (30%).

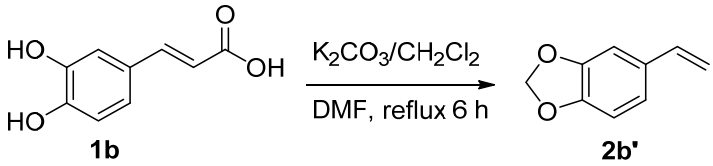

Scheme 6.6. One-pot decarboxylation and protection of caffeic acid.

6.2.1.3.2 One-pot enzymatic cascade for the synthesis of chiral diols 4b'

The next step was to perform the bio-epoxidation by using the Fus-SMO/Cb-FDH (10 mg mL^{-1}) system on the protected vinyl catechol substrate **2b'** (22 mM). The biotransformation was performed under optimized conditions: KPi/heptane buffer (pH 8.0, 50 mM; 1:1 v v^{-1}; 5 mL final reaction volume), NAD^+ (1 mM), HCOONa (110 mM, 5 eq.), FAD (50 µM), catalase (0.1 mg mL^{-1}) as previously reported.[8] The qualitative analysis by GC-MS showed the quantitative conversion of substrate **2b'**. It should be noted that no compounds were detected in the *n*-heptane phase. The EtOAc extract analysis showed the presence of traces of epoxide **3b'** and the main product observed was the hydrolyzed diol product **4b'**, as depicted in **Scheme 6.7**. In an attempt to prevent the spontaneous hydrolysis of the *in situ* generated epoxide, we performed the bio-epoxidation of substrate **2b'** (20 mM) at different pH values of KPi buffer (pH = 6.6, 6.8, 7.0, 7.2, 7.4, 7.6, 7.8, 8.0) under the above-mentioned reaction conditions. From GC-MS analysis, we did not observe any significant influence of the pH on the outcome of the reaction. In fact, under all tested pH values, the substrate **2b'** was completely converted and the diol product **4b'** was the only compound observed after extraction. Nevertheless, slightly acidic and neutral pH values (pH 6.6 and 7.0) afforded slightly better results. At this stage, we also determined the enantiomeric excess of the spontaneously formed diol product by chiral HPLC analysis, which, unfortunately, turned out to be a racemic mixture.

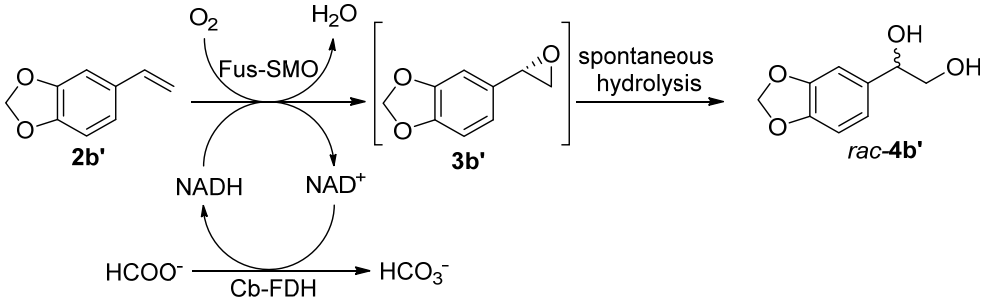

Scheme 6.7. Bio-epoxidation of substrate **2b'** catalyzed by Fus-SMO/Cb-FDH system followed by spontaneous hydrolysis of the *in situ* generated epoxide.

Based on these results, we hypothesized that the presence of the epoxide hydrolase in the same pot of the bio-epoxidation would enable the stereoselective opening of the epoxide intermediate. Thus, we performed the one-pot enzymatic epoxidation/hydrolysis on substrate **2b'** (20 mM) by pairing the co-expressed Fus-SMO/Cb-FDH system (20 mg mL^{-1}) with two stereocomplementary epoxide hydrolases,[9] either Sp(*S*)-EH from *Sphingomonas sp.* HXN200 or St(*R*)-EH from *Solanum tuberosum*, as depicted in **Scheme 6.8**. The biotransformations were carried out under the same reaction conditions described above with the exception that lyophilized *E. coli* whole cells carrying the desired EH (20 mg mL^{-1}) were added in the same pot. Moreover, different pH values (6.6, 7.0 and 8.0; KPi buffer) were tested since slightly better results were observed in the bio-epoxidation step, as described above.

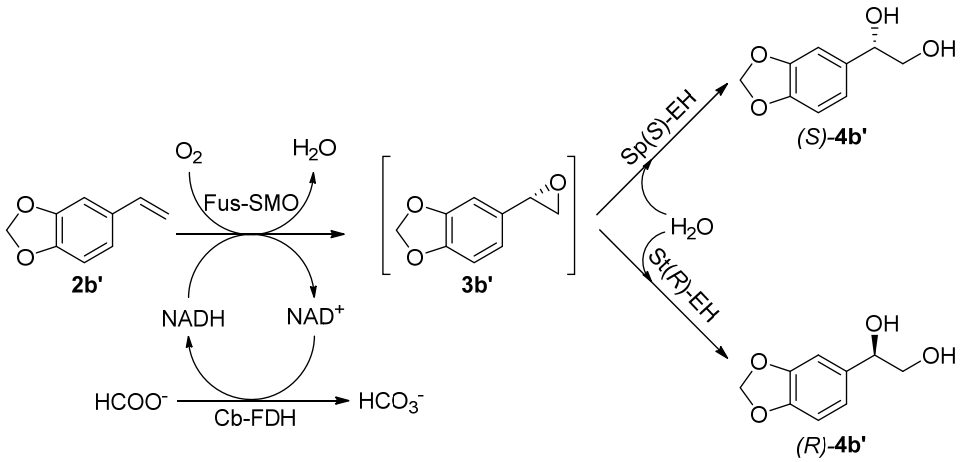

Scheme 6.8. One-pot enzymatic cascade for the epoxidation/hydrolysis of substrate **2b'**.

Based on qualitative GC-MS analysis, the conversion of substrate **2b'** did not proceed to completion. The unreacted substrate was detected only in the *n*-heptane phase, while the diol products were the sole detected compounds after extraction with EtOAc. Next, we determined by chiral HPLC the enantiomeric excess of the diol **4b'** coming from each combination of enzymes. As expected, the presence of the EH in the same pot of the epoxidation reaction enabled the formation of both enantiomers of diol **4b'** with high enantioselectivity, hence showing that the presence of the epoxide hydrolase prevented non-stereoselective ring-opening of the epoxide intermediate. The best results in terms of enantioselectivity were observed at slightly acidic pH (6.6), thereby giving the (*S*)-**4b'** with *ee* 86% and (*R*)-**4b'** with *ee* >98%. In contrast, the enantioselectivity dropped significantly for (*S*)-**4b'** at both pH 7.0 and 8.0 (*ee* 73% and 75%, respectively), while the *R*-enantiomer was still obtained with high enantiomeric excess (92% and 97%, respectively). The low enantioselectivity observed in the case of (*S*)-**4b'** may stem from a combination of two factors: *i*) the intrinsic lower selectivity of Sp(*S*)-EH compared with St(*R*)-EH, as previously observed[10]; *ii*) the higher pH values (7.0 and 8.0) favor the spontaneous non-stereoselective ring-opening of the epoxide intermediate.

6.2.1.3.3 Chemo-enzymatic route to give access to protected (*R*)-4-vinylbenzene-1,2-diol ((*R*)-4b') from caffeic acid (1b)

At this point, we could access both enantiomers of diol **4b'**, albeit we could not perform all of the reactions in one-pot starting from caffeic acid **1b**. Thus, we decided to perform the whole transformation of **1b** to optically active diol **4b'** through two distinct cascade reactions. The first route was the chemo-enzymatic decarboxylation/protection of caffeic acid, followed by a one-pot enzymatic cascade for the conversion of the isolated **2b'** to the chiral *R*-**4b'** (**Scheme 6.9**).

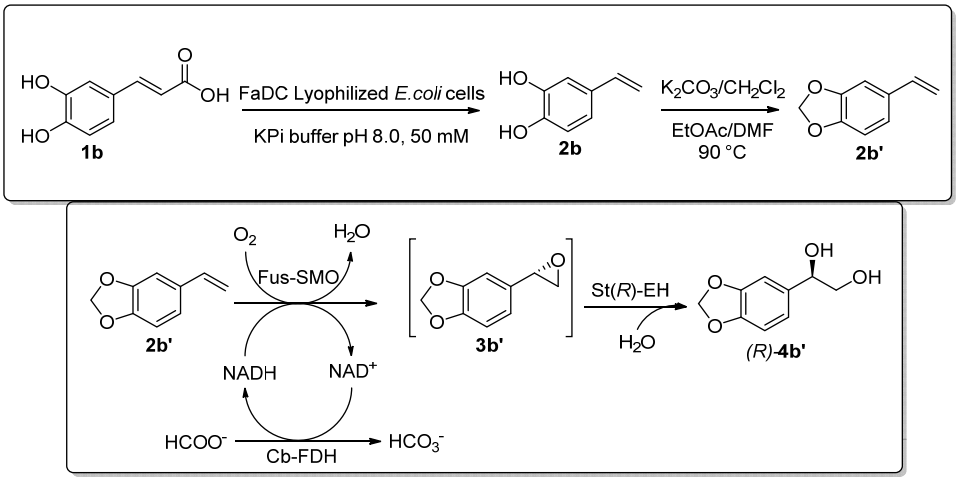

Scheme 6.9. Chemo-enzymatic route for the asymmetric synthesis of diol *R*-**4b'** from caffeic acid **1b**.

The first cascade was performed in a one-pot sequential mode: first, decarboxylation of caffeic acid **1b** (50 mM, 11.1 mmol) was carried out catalyzed by lyophilized *E. coli* whole cells carrying overexpressed FaDC (20 mg mL^{-1}) in KPi buffer (pH 8.0, 50 mM; 222 mL total reaction volume) for 24 h at 30 °C. After removal of the cells debris and extraction of olefin **2b** in EtOAc, the reagents for the protection step were added by assuming quantitative conversion of **1b** into **2b**. The protected vinyl catechol **2b'** was then used as substrate for the follow-up cascade for the synthesis in 100 mg scale of chiral diol (*R*)-**4b'** under the same conditions reported in paragraph 6.2.1.3.2.

6.2.2 Multi-enzymatic cascade for the synthesis of vicinal amino alcohols

With the chiral diol in hands, the next step was to test the one-pot multi enzymatic cascade depicted in **Scheme 6.10** for the synthesis of the targeted vicinal amino alcohol **6b'**. The cascade comprises an alcohol dehydrogenase (50 µM) (either Aa-ADH from *Aromatoleum aromaticum*[11] or Bs-BDHA from *Bacillus subtilis* BGSC1A1)[12, 13] and one between the two stereocomplementary ω-transaminases (50 µM) namely At(*R*)-ωTA from *Aspergillus terreus*[15, 16] and Cv(*S*)-ωTA from *Chromobacterium violaceum* DSM 3019.[14] As described in chapter 5, the cascade was performed in $HCOONH_4$ buffer (pH 8.5, 1 M) supplemented with NAD^+ (1 mM), PLP (1 mM), D- or L-alanine (5 eq.) and Bs-AlaDH[19] (20 µM).

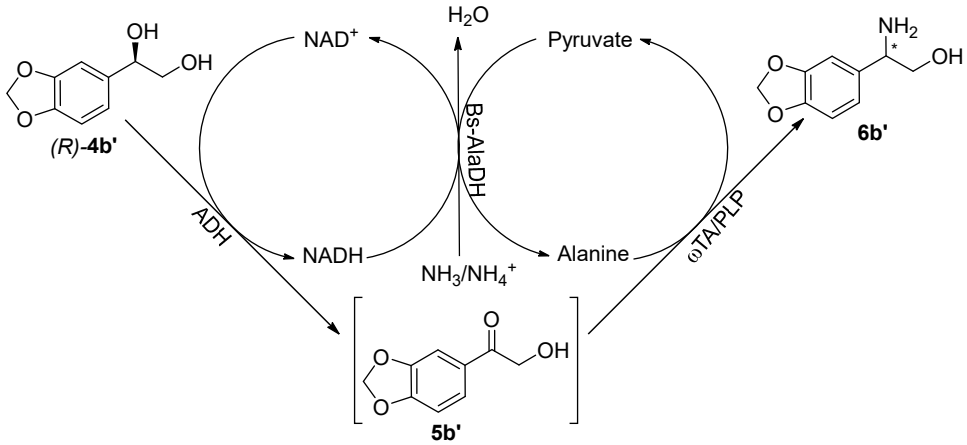

Scheme 6.10. One-pot multi-enzymatic cascade for the conversion of chiral diol **4b'** into the targeted vicinal amino alcohol **6b'.**

As show in **Table 6.1**, the formation of the targeted amino alcohol **6b'** was observed when either one of the two tested ADHs was combined with At(*R*)-ωTA (entry 2 and 4). However, Aa-ADH displayed higher activity compared with Bs-BDHA under the tested reaction conditions. Moreover, in both cases, intermediate **5b'** along with other compounds were detected. Two of them could be identified by GC-MS analysis, namely 2-(benzo[d][1,3]dioxol-5-yl)ethan-1-ol (**9b'**) and 2-(benzo[d][1,3]dioxol-5-yl)ethan-1-amine (**10 b'**), as depicted in **Table 6.1**. Conversely, the third observed compound could not be determined by mass analysis only, however, these reactions were performed in analytical scale, hence we could not analyze at this stage the reaction outcome by ^{1}H-NMR, for instance. On the other hand, conversion into the desired amino alcohol **6b'** was not detected when Cv(*S*)-ωTA was paired with the ADHs (entry 1 and 3). In contrast, in both cases, the main product formed was the intermediate **5b'**. These tests represented a preliminary investigation to assess the potentiality of this cascade; we acknowledge that an in-depth investigation is required to quantitatively determine the formation of the target amino alcohol. Moreover, the enantiomeric excess of the amino alcohol **6b'** was not determined at this stage. In fact, a suitable analytical method for *ee* analysis was still required and must be explained in the next step of this study along with the optimization of the cascade itself (e.g., testing other transaminases; balance enzymes loading; etc.).

Table 6.1. Preliminary results for the conversion of (*R*)-**4b'** (20 mM) catalyzed by ADH coupled with ωTA in a one-pot fashion.

Entry	1st step	2nd step	5b' [%][a]	6b' [%][a]	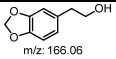 m/z: 166.06 **9b'** [%][a]	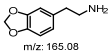 m/z: 165.08 **10b'** [%][a]	Unidentified [%][a]
1	Aa-ADH	Cv(*S*)-ωTA	43±1	n.d.	10±1	14±1	33±3
2	Aa-ADH	At(*R*)-ωTA	12±1	40±2	9±2	12±2	25±4
3	Bs-BDHA	Cv(*S*)-ωTA	33±2	n.d.	46±7	n.d.	21±4
4	Bs-BDHA	At(*R*)-ωTA	31±3	7±2	41±6	n.d.	20±4

[a]Qualitative conversions analyzed by GC-MS; the results reported are the average of two experiments; enantiomeric excess was not determined.

We have performed preliminary tests for synthesizing the regioisomer **8b'** through a one-pot multi enzymatic cascade as previously described in chapter 5. In this case, the alcohol oxidase AcCO6 variant from choline oxidase[17] was paired with the amine dehydrogenase Ch1-AmDH.[18] The cascade was carried out in $HCOONH_4$ (pH 8.5, 1 M) supplemented with NAD^+ (1 mM), catalase (0.1 mg mL^{-1})—for the disproportion of the *in situ* formed H_2O_2—and a formate dehydrogenase (Cb-FDH)[20]—for NADH recycling. Nevertheless, conversion of substrate (*R*)-**4b'** was not observed under the tested conditions and more investigation is needed in order to optimize the cascade and identify the potential issues.

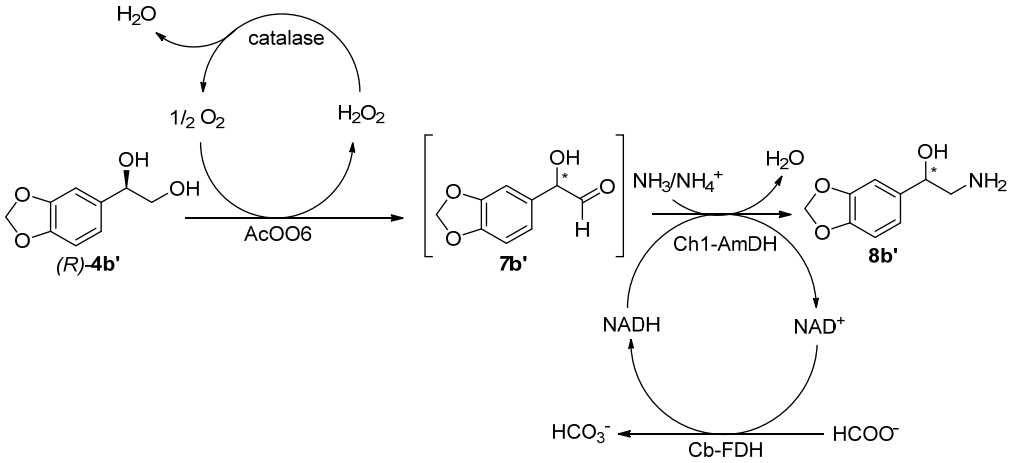

Scheme 6.11. One-pot enzymatic cascade for the conversion of substrate *R*-**4b'** to chiral **8b'**.

6.3 Summary and future prospects

The present study was a proof of concept, which requires further investigation for possible application in the enzymatic synthesis of high valuable vicinal amino alcohols such as adrenaline and derivatives. In summary, we were able to obtain three aromatic olefins from the corresponding carboxylic acids, the latter of which could be sourced from renewable feedstocks. Moreover, we identified a suitable chemo-enzymatic route for the enzymatic synthesis of the high valuable optically active diol **4b'** by two sequential one-pot cascades. First, the olefin substrate was obtained by enzymatic decarboxylation of caffeic acid followed by chemical protection of the catechol moiety. In the second step, the free catechol was identified as the main issue in performing the epoxidation catalyzed by Fus-SMO due to the fact that catechol moieties are prone to further oxidation. This observation aligns with the fact that it is not possible to find in the literature any epoxidation of these types of compounds catalyzed by the styrene monooxygenase system. Thus, we performed the one-pot enzymatic epoxidation of olefin **2b'** by pairing the Fus-SMO with two stereocomplementary EHs in order to form both enantiomers of diol **4b'** ((*S*)-**4b'** 86% *ee*; (*R*)-**4b'** >98% *ee*). Nevertheless, this one-pot cascade requires some further optimization, such as the test of different pH values and types of buffers, and the exact quantification of the system's productivity. It is known that high pH values can lead to faster oxidation of catechols. Moreover, the use of a different buffers might also help to increase the enantiomeric excess of the (*S*)-enantiomer of diol **4b'**. It would also be interesting to investigate the possibility to perform the epoxidation/hydrolysis in an alternative biphasic system by using a "green" organic solvent which is more suitable for these highly polar compounds. Furthermore, the Fus-SMO/EH system could be investigated by using other substrates such as coumaric and ferulic acids. For this purpose, it will be necessary to evaluate different protecting groups for the hydroxyl substituent of the aromatic ring. Nevertheless, other enzymatic systems can be explored for the synthesis of the diol substrates. For example, naphthalene dioxygenase (NDO) is an enzyme that catalyzes the direct dihydroxylation of aromatic alkenes. Hence, the coupling of FaDC and NDO could be a viable alternative route to the one-pot epoxidation/hydrolysis of olefins. Regarding the one-pot cascade for the conversion of diols such as **4b'** to chiral amino alcohol such as **6b'**, more tests are necessary to assess the actual performance of the enzymatic system as well as determine the enantiomeric excess of the final product. Moreover, the combination of other ADHs and TAs could be investigated on both

enantiomers of **4b'** along with system's optimization. Finally, the one-pot cascade to synthesize the regioisomer amino alcohols such as **8b'** did not lead to any conversion of the diol substrate. Indeed, this system needs in-depth studies. An interesting approach would be the identification of other oxidases to perform the oxidation of the diol substrate as well as the use of other amine dehydrogenases or alternative aminating enzymes. Moreover, the use of computational biocatalysis might elucidate what is the actual issue, for instance, by identifying the interaction between the substrate and the enzymes involved. This work would provide the required knowledge to create new variants by protein engineering. This latter point is probably critical for the development of the herein described multi-enzymatic cascades for the synthesis high-value amino alcohols. In fact, the need to expand the substrate scope of these classes of enzymes and discover other enzymes will play a central role towards this aim.

6.4 Experimental section

General information. ADHs and ωTAs used in this study were expressed and purified as reported in chapter 5. FaDC was overexpressed in *E. coli* (50 μg mL^{-1} kanamycin; 0.5 mM IPTG, 25 °C overnight) according to the general enzymes expression protocol reported in chapter 3 and used as lyophilized whole cells.

General procedure for the biocatalytic decarboxylation of 1b-d. Lyophilized *E. coli* cells carrying FaDC (30 mg mL^{-1}) were rehydrated in 1.5 mL KPi buffer (50 mM, pH 8.0) in a 4 mL glass vial. After that, substrate **1b-d** (50 mM) was added. The mixture was shaken at 30 °C and 170 rpm on an orbital shaker for 24 h. Work-up was performed by acidification with HCl (1 M) followed by extraction with EtOAc (2 x 750 μL). Conversion was measured by GC-FID after derivatization or directly by RP-HPLC (100 μL aq. phase diluted with 1 mL H_2O:MeOH (1:1 v v^{-1} + 3% TFA), incubated at room temperature for 15 min, centrifuged and injected in RP-HPLC).

General derivatization procedure for GC-FID analysis. The extract (200 μL) was diluted with MeOH (200 μL) and EtOAc (600 μL) followed by addition of (trimethylsilyl)diazomethane (20 μL). The reaction was shaken at 30 °C, 170 rpm for 1 h. The excess of the derivatization reagent was neutralized by addition of acetic acid (4 μL). The mixture was shaken at 30 °C, 170 rpm for 30 minutes and analyzed by GC-FID.

Procedure for the one-pot reactions to epoxides 3b-d from carboxylic acids 1b-d. Lyophilized *E. coli* cells carrying FaDC (20 mg mL^{-1}) were rehydrated in 1.5 mL KPi buffer (50 mM, pH 8.0) in a 4 mL glass vial. After that, substrate **1b-d** (50 mM) was added. The mixture was shaken at 30 °C and 170 rpm on an orbital shaker for 24 h. The lyophilized *E. coli* whole cells co-expressing Fus-SMO and Cb-FDH (10 mg mL^{-1}) were added together with NAD^+ (1 mM), HCOONa (250 mM, 5 eq.), FAD (50 μM), catalase (0.1 mg mL^{-1}) and *n*-heptane (1.5 mL). The mixture was incubated at 30 °C and 180 rpm on an orbital shaker for 24 h. The organic phase was separated from the aqueous phase; *n*-heptane phase was analyzed by GC-MS, while the aqueous layer was injected in RP-HPLC (100 μL aq. phase diluted with 1 mL H_2O:MeOH (1:1 v v^{-1} + 3% TFA), incubated at room temperature for 15 min, centrifuged and injected in RP-HPLC).

Procedure for the bio-epoxidation of aromatic olefins 2b-d. Lyophilized *E. coli* cells carrying Fus-SMO were rehydrated in KPi buffer (1 mL; 50 mM, pH 8.0, otherwise stated) supplemented with NAD^+ (1 mM), HCOONa (100 mM, 5 eq.), FAD (50 μM), catalase (0.1 mg mL^{-1}) and Cb-FDH (10 μM) in a 4 mL glass vial. As last, substrate **2b-d** (20 mM) was added. The mixture was incubated at 30 °C and 180 rpm on an orbital shaker for 24 h. The aqueous phase was then directly analyzed by RP-HPLC (100 μL aq. phase diluted with 1 mL

H_2O:MeOH (1:1 v v^{-1} + 3% TFA), incubated at room temperature for 15 min, centrifuged and injected in RP-HPLC).

Chemical synthesis of protected vinyl catechol from caffeic acid.[4] To a 100 mL one-neck round bottom flask equipped with a cooling system, CH_2Cl_2 (1.4 mL, 1.8 eq.) and K_2CO_3 (4 g, 2.5 eq) were added to DMF (30 mL); then, a solution of caffeic acid **1b** (2 g, 0.011 mmol) in DMF (20 mL) was dropwise added to the flask. The mixture was refluxed and stirred under magnetic agitation for 18 h; after that, it was cooled down to room temperature and filtered. The filtrate was concentrated, diluted with H_2O, and extracted with EtOAc (3 x 100 mL). The organic layer was washed with 10% NaOH (30 mL), H_2O (25 mL), dried ($MgSO_4$), and evaporated to afford a bark brown oil, which was further filtered over silica (PE:EtOAc 1:1) thus yielding a light orange oil (390 mg, ca. 25%).

General procedure for the one-pot cascade for the synthesis of chiral 4b' from 2b'. Lyophilized *E. coli* cells co-expressing Fus-SMO/Cb-FDH (20 mg mL^{-1}) and lyophilized *E. coli* cells carrying either Sp(S)-EH or St(R)-EH (20 mg mL^{-1}) were rehydrated in KPi buffer (0.5 mL, 50 mM, pH 8.0, otherwise stated) in a 4 mL glass vial. After that, NAD^+ (1 mM), HCOONa (100 mM, 5 eq.), FAD (50 µM) and catalase (0.1 mg mL^{-1}) were added. *n*-Heptane (0.5 mL; 1:1 volumetric ratio with the buffer) was used as biphasic solvent. Finally, the biocatalytic reactions were initiated by the addition of substrate **2b'** (20 mM). The reactions were incubated at 30 °C and 170 rpm on an orbital shaker for 48 h. *n*-Heptane was removed, the aqueous phase was saturated with solid NaCl, and the organic compounds was extracted with EtOAc (1 x 500 µL). After drying over $MgSO_4$, the organic layer was analyzed by GC-MS and the enantiomeric excess determined by chiral HPLC.

General procedure for the chemo-enzymatic synthesis of (*R*)-4b' from 1b. To a 500 mL Erlenmeyer flask, lyophilized *E. coli* whole cells carrying FaDC (20 mg mL^{-1}, 4.4 g) were rehydrated in KPi buffer (222 mL; pH 8.0, 50 mM) and substrate **1b** (50 mM, 2 g) was added. The mixture was incubated at 30 °C, 170 rpm for 24 h. After that, cell debris were removed by centrifugation and the supernatant was extracted with EtOAc (3 x 50 mL). The combined organic layers were concentrated under vacuum up to ca. 17 mL. The EtOAc extract (ca. 9 mL) was used for the follow-up step, considering a hypothetical quantitative conversion of **1b** to vinyl catechol **2b**.
In a 50 mL one-neck bottom flask, CH_2Cl_2 (6 mL) and K_2CO_3 (2.5 g) were added to DMF (15 mL); then, the EtOAc extract (9 mL) was added dropwise to the flask. The mixture was heated up at 90 °C and stirred under magnetic agitation for 18 h. After that, it was cooled down to room temperature and filtered. The filtrate was concentrated, diluted with H_2O, and extracted with EtOAc (3 x 10 mL). The organic layer was washed with 10% NaOH (30 mL), H_2O (30 mL), dried over $MgSO_4$ and evaporated to afford a dark orange oil, which was analyzed by GC-MS.

Lyophilized *E. coli* cells co-expressing Fus-SMO/Cb-FDH (20 mg mL^{-1}) and lyophilized *E. coli* cells carrying St(*R*)-EH (20 mg mL^{-1}) were rehydrated in KPi buffer (39 mL, 50 mM, pH 6.6) in a 250 mL Erlenmeyer flask. After that, NAD^+ (1 mM), HCOONa (100 mM, 5 eq.), FAD (50 µM) and catalase (0.1 mg mL^{-1}) were added. *n*-Heptane (39 mL; 1:1 volumetric ratio with the buffer) was used as biphasic solvent. Finally, the biocatalytic reactions were initiated by the addition of substrate **2b'** (20 mM, 0.675 mmol). The reactions were incubated at 30 °C and 170 rpm on an orbital shaker for 48 h. *n*-Heptane was removed, the aqueous phase was saturated with solid NaCl and the organic compounds extracted with EtOAc (2 x 20 mL). After drying over $MgSO_4$, the organic layer was analyzed by GC-MS and the enantiomeric excess determined by chiral HPLC.

General procedure for the conversion of (*R*)-4b' to chiral 6b'. $HCOONH_4$ buffer (pH 8.5, 1 M; 0.5 mL) was added to an Eppendorf tube (1.5 mL) and supplemented with NAD^+ (1 mM), PLP (1 mM), D-or L-Alanine (100 mM, 5 eq.) and Bs-AlaDH (20 µM). Then, ADH (50 µM) and ωTA (50 µM) were added followed by substrate (*R*)-**4b'** (20 mM). The mixture was incubated at 30 °C, 170 rpm for 48 h on an orbital shaker and, after that, quenched with 10 M KOH (100 µL). The aqueous layer was saturated with solid NaCl and the organic compounds extracted with EtOAc (1 x 500 µL). The organic layer was dried over $MgSO_4$ and analyzed by GC-MS.

General procedure for the conversion of (*R*)-4b' to chiral 8b'. In an Eppendorf tube (1.5 mL), $HCOONH_4$ buffer (0.5 mL, pH 8.5, 1 M), NAD^+ (1 mM), catalase (0.1 mg mL^{-1}) and purified Cb-FDH (10 µM) were added followed by purified AcCO6 (50 µM) and Ch1-AmDH (50 µM). (*R*)-**4b'** (20 mM) was added as last. The mixture was incubated at 30 °C, 170 rpm for 48 h on an orbital shaker and, after that, quenched with 10 M KOH (100 µL). The aqueous phase was saturated with solid NaCl and the organic compounds were extracted with EtOAc (1 x 500 µL). The organic layer was dried over $MgSO_4$ and analyzed by GC-MS.

Analytical methods

GC-FID method A: Column: Agilent DB1701 (30 m, 250 µm, 0.25 µm). Carrier gas: H_2**;** Parameter: T injector 250 °C; constant pressure 6.9 psi; temperature program: 80 °C, hold 6.5 min; gradient 5 °C min^{-1} up to 160 °C, hold 5 min; gradient 20 °C min^{-1} up to 200 °C, hold 2 min; gradient 20 °C min^{-1} up to 280 °C, hold 4 min.

GC-MS method B: Column Agilent DB-1701 (30 m, 250 µm, 0.25 µm); injector temperature 250 °C; constant pressure 71.8 kPa; temperature program: 80 °C/hold 6.5 min; 160 °C/rate 10 °C min^{-1}/hold 5 min; 200 °C/rate 20 °C min^{-1}/hold 2 min; 280 °C/rate 20 °C min^{-1}/hold 1 min.

RP-HPLC method C: Column Shimadzu Shim-pack GIST (4.6 mm x 150 mm); HPLC gradient program: 100% MilliQ (+ 0.1% TFA), down to 40% MilliQ (+ 0.1% TFA) in 20 min.; down to 35% MilliQ (+ 0.1% TFA) in 5 min.; up again to 100% MilliQ (+ 0.1% TFA) in 15 min; oven Temperature 30 °C, 1 mL min^{-1}

Chiral HPLC method D: Column Daicel IC-3 (0.46 cm x 25 cm); HPLC program: constant oven temperature 25 °C; constant pressure 70 bar; eluent composition: *n*-Hexane:Isopropanol 92:8, 1 mL/min

Table 6.2. Retention times of compounds analyzed in this study

Entry	Compound	Retention time [min]	Method
1	**1b**	14.5	C
2	**1c**	34.9	A[a]
		17.1	C
3	**1d**	17.5	C
		35.1	A[a]
4	**2b**	17.2	C
5	**2c**	21.3	A[a]
		20.9	C
6	**2d**	21.4	C
		21.5	A[a]
7	**2b'**	13.01	B
8	**3b'**	16.9	B
9	**4b'**	24.3	B
10	(*S*)-**4b'**	32.6	D
11	(*R*)-**4b'**	33.8	D
12	**5b'**	22.6	B
13	**6b'**	23.4	B

[a]After derivatization with (trimethylsilyl)diazomethane

6.5 References

1. P. Terpinc, T. Polak, N. Segatin, A. Hanzlowsky, N. P. Ulrih and H. Abramovic, *Food Chem.*, 2011, 128, 62-69.
2. R. Tramontina, J. L. Galman, F. Parmeggiani, S. R. Derrington, T. D. H. Bugg, N. J. Turner, F. M. Squina and N. Dixon, *Green Chem.*, 2020, 22, 144-152.
3. H. Takeshima, K. Satoh and M. Kamigaito, *ACS Sustain. Chem. Eng.*, 2018, 6, 13681-13686.
4. M. F. El-Behairy and E. Sundby, *Tetrahedron: Asymmetry*, 2013, 24, 285-289.
5. E. Busto, R. C. Simon and W. Kroutil, *Angew. Chem. Int. Ed.*, 2015, 54, 10899-10902.
6. N. Cabedo, I. Andreu, M. C. Ramirez De Arellano, A. Chagraoui, A. Serrano, A. Bermejo, P. Protais and D. Cortes, *J. Med. Chem.*, 2001, 44, 1794-1801.
7. J. D. Benigni and A. J. Verbiscar, *J. Med. Chem.*, 1963, 6, 607-608.
8. M. L. Corrado, T. Knaus and F. G. Mutti, *ChemBioChem*, 2018, 19, 679-686.
9. S. Wu, Y. Chen, Y. Xu, A. Li, Q. Xu, A. Glieder and Z. Li, *ACS Catal.*, 2014, 4, 409-420.
10. M. L. Corrado, T. Knaus and F. G. Mutti, *Green Chem.*, 2019, 21, 6246-6251.

11. H. W. Hoffken, M. Duong, T. Friedrich, M. Breuer, B. Hauer, R. Reinhardt, R. Rabus and J. Heider, *Biochemistry*, 2006, 45, 82-93.
12. J. Zhang, T. Xu and Z. Li, *Adv. Synth. Catal.*, 2013, 355, 3147-3153.
13. J. Zhang, S. Wu, J. Wu and Z. Li, *ACS Catal.*, 2014, 5, 51-58.
14. U. Kaulmann, K. Smithies, M. E. B. Smith, H. C. Hailes and J. M. Ward, *Enzyme Microb. Technol.*, 2007, 41, 628-637.
15. A. Lyskowski, C. Gruber, G. Steinkellner, M. Schurmann, H. Schwab, K. Gruber and K. Steiner, *PloS One*, 2014, 9, e87350.
16. F. G. Mutti, C. S. Fuchs, D. Pressnitz, J. H. Sattler and W. Kroutil, *Adv. Synth. Catal.*, 2011, 353, 3227-3233.
17. R. S. Heath, W. R. Birmingham, M. P. Thompson, A. Taglieber, L. Daviet and N. J. Turner, *ChemBioChem*, 2019, 20, 276-281.
18. B. R. Bommarius, M. Schurmann and A. S. Bommarius, *Chem. Commun.*, 2014, 50, 14953-14955.
19. T. Ohashima and K. Soda, *Eur. J. Biochem.*, 1979, 100, 29-30.
20. T. Knaus, W. Bohmer and F. G. Mutti, *Green Chem.*, 2017, 19, 453-463.

Summary

The chemical industry still relies largely on fossil carbon. Many of the current manufacturing processes lead to vast amounts of waste. The model for a waste-free circular economy emerged in the last decade and it is at the core of the green chemistry principles. One solution to this problem is the substitution of stoichiometric use of reagents with catalytic alternatives. Furthermore, the shift away from fossil-based feedstocks has brought attention to the valorization of unavoidable waste coming from lignocellulose agricultural residues as alternative renewable raw materials. Nevertheless, this transition requires the development of infrastructure for the treatment of such feedstocks as well as new technologies and processes which must meet the sustainability and greenness requirements. In this context, biocatalysis plays a pivotal role in both lignocellulose biomass treatment and follow-up transformations of the biomass-derived building blocks into high added-value products. Biocatalysts are inherently safe, sustainable and selective as the five green chemistry principles are fulfilled by the intrinsic high chemo-, regio- and stereoselectivity of enzymes. Enzymatic processes are usually performed in aqueous solutions at pH close to neutral, room temperature and pressure. Moreover, biocatalysts are typically biodegradable by nature, biocompatible and sustainable. These aspects are extremely favorable for the development of eco-friendly chemical processes. Furthermore, enzymes with different reactivities are often compatible and therefore can operate simultaneously in the same pot without any physical separation, hence facilitating the combination of multiple steps in a one-pot fashion. All these qualities are highly appreciated in particular in the manufacture of active pharmaceutical ingredients (APIs). Though the transition process to more environmentally friendly and sustainable processes proceeds at lower pace in the pharmaceutical and fine chemicals manufacture compared with bulk chemical industries, various industrial routes have been implemented with enzymatic steps for performing key transformations (e.g., introduction of chiral centers: α-chiral amines by transaminases, chiral alcohols by alcohol dehydrogenases, etc.). Among the functionalities present in biologically active compounds, vicinal amino alcohol moieties constitute the core of several natural products and active pharmaceutical ingredients such as alkaloids, neurotransmitters, HIV protease inhibitors, aminopeptidase inhibitor and antibiotics. In this thesis, we applied several multi-enzymatic cascade reactions for the synthesis of targeted optically active vicinal amino alcohols. Our investigation started with the generation of an engineered styrene monooxygenase (Fus-SMO) in **Chapter 2**. The two units of the bi-enzymatic catalytic system, (StyB, the

reductase domain, and StyA, the epoxidation unit) were genetically fused by a 30 amino acids linker. In this chapter, we evaluated the catalytic performance of lyophilized *E. coli* cells carrying the overexpressed Fus-SMO for the asymmetric epoxidation of styrene **1a** and *trans*-β-methylstyrene **1b** (**Scheme 1**). A further improvement, for a practical applicability of this system, was provided by co-expressing the Fus-SMO with Cb-FDH in the same host organism.

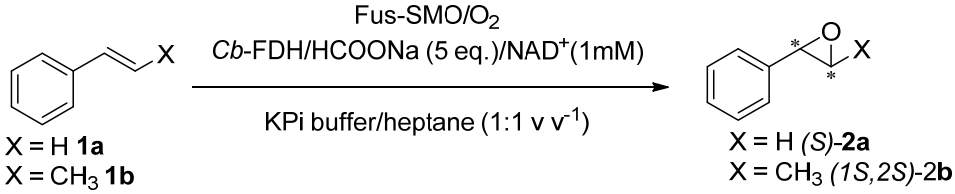

Scheme 1. Whole cell system expressing simultaneously Fus-SMO and Cb-FDH in *E. coli* BL21 DE3 as host organism for the conversion of **1a-b** to optically active epoxides **2a-b**

In **Chapter 3,** we applied our Fus-SMO in a one-pot cascade with stereocomplementary epoxide hydrolases (either Sp(*S*)-EH or St(*R*)-EH) for the synthesis of chiral 1,2-phenylpropanediol isomers **3** (**Scheme 2**). Next, the formal regio-, chemo- and stereoselective synthesis of two isomers of nor(pseudo)ephedrine **5** was accomplished via the biocatalytic hydrogen-borrowing (HB) amination of alcohol, that is a redox-neutral cascade. Optically active diols **3** were converted to the targeted amino alcohols by pairing selected alcohol dehydrogenases (either Bs-BDHA or Ls-ADH) and an amine dehydrogenase (Ch1-AmDH) in a one-pot cascade fashion (**Scheme 3**).

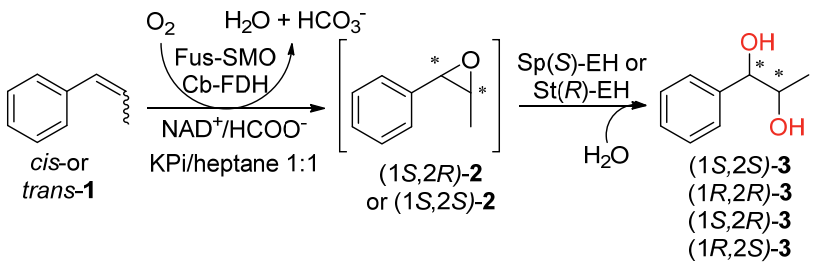

Scheme 2. One-pot multi-enzymatic cascades for the synthesis of optically active diol isomers **3** from olefin **1** by coupling Fus-SMO with two stereocomplementary EHs.

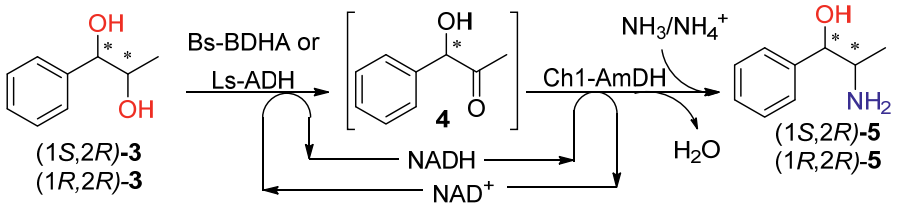

Scheme 3. Formal regio-, chemo- and stereoselective enzymatic synthesis of two isomers of nor(pseudo)ephedrine **5** via the HB-bio-amination cascade.

Due to the lack of (*S*)-selective AmDHs, in **Chapter 4**, we described the enzymatic synthesis of the other two isomers of nor(pseudo)ephedrine **5** by pairing the selected ADHs with stereocomplementary ω-transaminases (ωTAs) in a one-pot cascade for the conversion of chiral diols **3**. The latter compounds were enzymatically synthesized as shown in **Scheme 2.** Similar to the HB-bioamination, the redox-neutral cascade ADH/ωTA system regenerates the required oxidized NAD^+ coenzyme via an alanine dehydrogenase (AlaDH); concurrently, the pyruvate side product is converted back to alanine, the ultimate amino donor for the transamination step (**Scheme 4**).

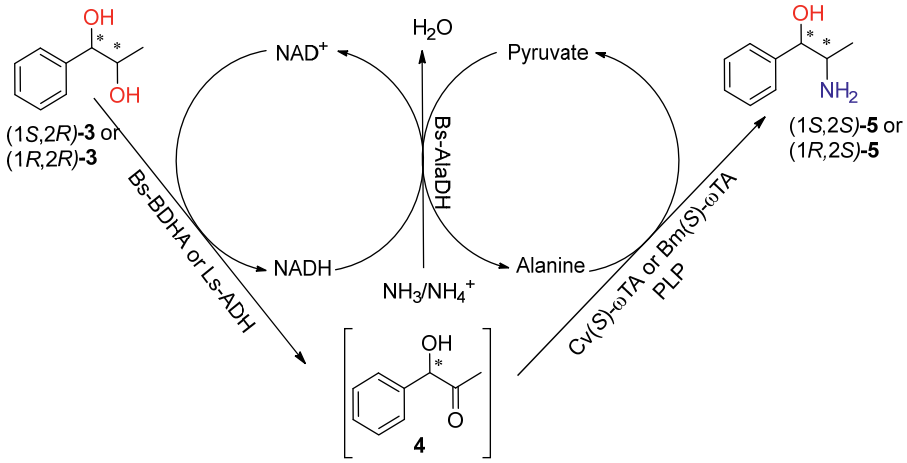

Scheme 4. One-pot cascade reactions for the conversion of optically active diols **3** to two isomers of nor(pseudo)ephedrine **5** by pairing ADH and stereocomplementary ωTAs

Moreover, we could also obtain the regioisomer (1*S*,2*R*)-**5'** with the cascade depicted in **Scheme 4** by choosing a specific combination of diol substrate, ADH and ωTA (**Scheme 5**).

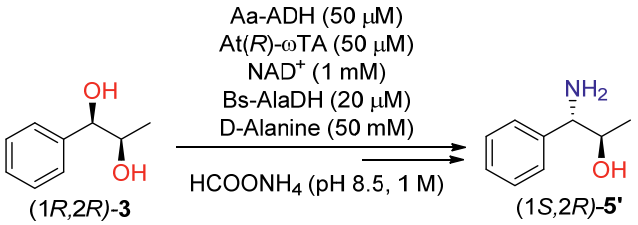

Scheme 5. One-pot cascade reactions for accessing one regioisomer of nor(pseudo)ephedrine

In **Chapter 5,** we have used the one-pot cascade described in **Scheme 4** to synthesize phenylethanolamine isomers **5a** (**Scheme 6, top**). Also in this case, chiral diol substrates **3a** were enzymatically synthesized by the one-pot cascade reported in **Scheme 2**. Styrene **1a** was then used as substrate. Moreover, we designed an orthogonal bioamination cascade for the enzymatic synthesis of amino alcohol **5a'** from optically active diol **3a**. Here, an alcohol oxidase (AcCO6) is paired with an amine dehydrogenase (Ch1-AmDH). The latter enzyme requires an orthogonal enzymatic system for the recycling of the NADH coenzymes (**Scheme 6, bottom**).

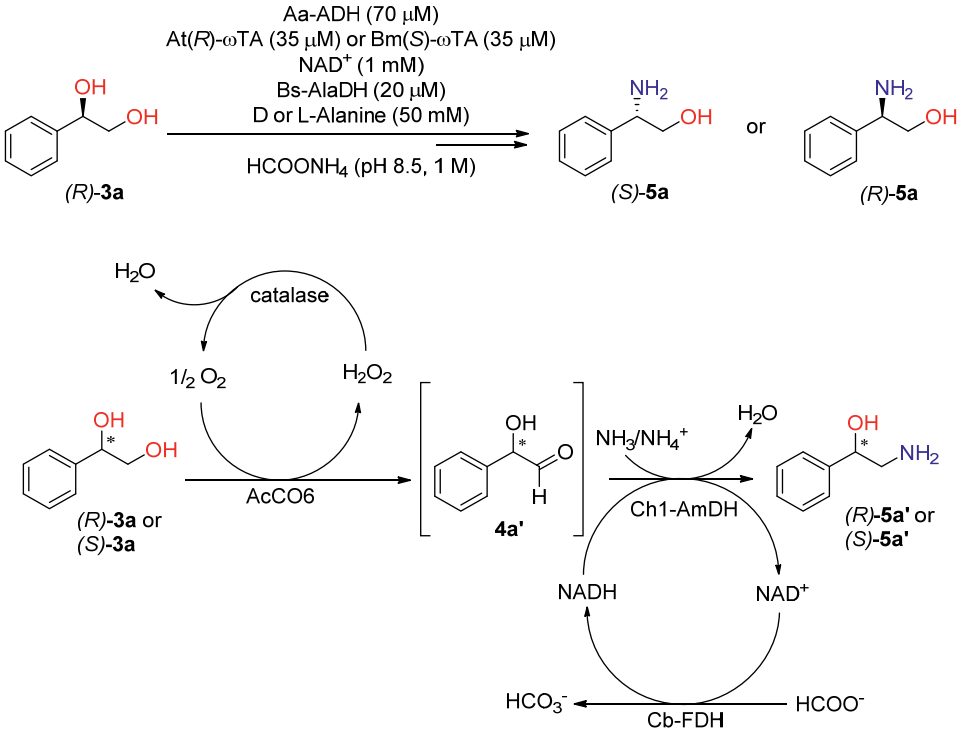

Scheme 6. One-pot cascade for the conversion of (*R*)-**3a** to optically active (*R*)-**5a** and (*S*)-**5a** by pairing selected ADHs with stereocomplementary ωTAs (top); orthogonal bioamination cascade for the conversion of (*R*)-**3a** and (*S*)-**3a** to the corresponding chiral amino alcohols (*R*)-**5a'** and (*S*)-**5a'**, respectively (bottom).

We then decided to extend the multi-enzymatic cascade reactions, described above, for the synthesis of other valuable amino alcohols (e.g., adrenaline and derivatives thereof). Therefore, **chapter 6** deals with a proof-of-principle that exemplifies the high potential of these cascades. An extra enzymatic step was included for the biocatalytic decarboxylation of renewable raw materials, such as caffeic, coumaric and ferulic acids **1b-d,** to obtain the corresponding aromatic olefins **2b-d** (**Scheme 7, top**). Unfortunately, the one-pot dihydroxylation cascade described in **Scheme 2** did not lead to the formation of the related diols. Therefore, the synthesis of substrate **2b'** was proceeded from caffeic acid **1b** as model compound, giving the chiral diols **4b'** (**Scheme 7, middle**). As last, the one-pot cascade described in **Scheme 4** was performed for synthesizing amino alcohol **6b'** (**Scheme 7, bottom**). Nevertheless, more work on this cascade is necessary in order to assess the actual performance of the system as well as to determine the stereochemistry of the amino alcohol product. Moreover, other tests need to be carried out by using all of the substrates described at the beginning of this chapter and find suitable approaches for obtained the targeted amino alcohols (e.g., adrenaline and derivatives). Anyway, the integration of computational biocatalysis and protein engineering is indispensable to expand the enzymatic toolbox required for these cascades.

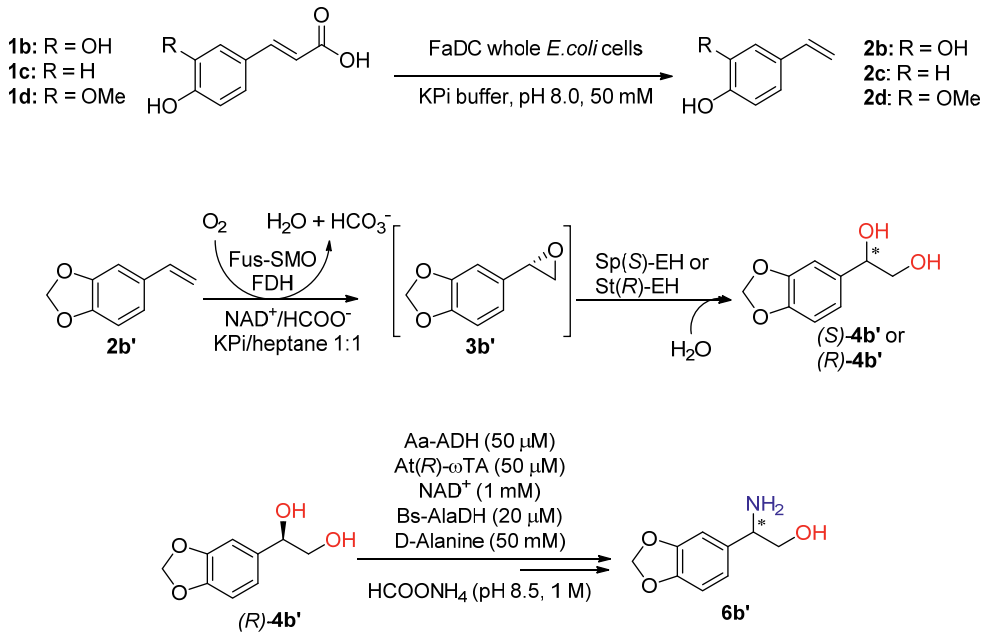

Scheme 7. Preliminary results for the approach described in chapter 6 as proof-of-principle for the potential application of the cascades described in this thesis towards the synthesis of high valuable vicinal amino alcohols.

Samenvatting

De chemische industrie is nog voor een groot deel afhankelijk van fossiele brandstoffen. Vele hedendaagse productieprocessen leiden tot grote hoeveelheden afval. Het model voor in afvalvrije circulaire economie is in het afgelopen decennium opgekomen en bevat de kern van groene energieprincipes. Een oplossing voor dit probleem is de vervanging van het stoichiometrische gebruik van reagentia met katalytische alternatieven. Verder heeft het vermijden van fossiele grondstoffen waardevermeerdering gebracht voor hernieuwbare alternatieven uit plantaardige materialen, zoals lignocellulose, afkomstig van landbouwresiduen. Desalniettemin vraagt deze overgang om de ontwikkeling van de infrastructuur en nieuwe technologieën en processen, die moeten voldoen aan duurzaamheidseisen, voor de behandeling van dergelijke grondstoffen. In deze context speelt biokatalyse een belangrijke rol in de behandeling van lignocellulose uit biomassa en de daaropvolgende omzettingen van uit biomassa verkregen bouwstenen in hoogwaardige eindproducten. Biokatalysatoren zijn inherent veilig, duurzaam en selectief omdat de vijf groene energieprincipes worden vervuld door de intrinsiek hoge chemo-, regio- en stereoselectiviteit van enzymen. Enzymatische processen worden vaak uitgevoerd in waterige oplossingen bij pH dichbij neutraal, kamertemperatuur en druk. Verder zijn biokatalysatoren over het algemeen biologisch afbreekbaar, biocompatibel en duurzaam. Deze aspecten zijn zeer gunstig voor de ontwikkeling van milieuvriendelijke chemische processen. Daarnaast zijn enzymen met verschillende reactiviteiten vaak verenigbaar en kunnen daarom tegelijkertijd in hetzelfde reactievat worden toegepast zonder ze fysiek te hoeven scheiden en dus maken ze de combinatie van meerdere reactiestappen in één pot mogelijk. Al deze kwaliteiten zijn met name van belang bij de vervaardiging van actieve farmaceutische ingrediënten (APIs). Alhoewel de overgang naar milieuvriendelijke en duurzame processen langzamer gaat in de farmaceutische en fijnchemicaliënindustrie, zijn er verscheidene industriële routes geïmplementeerd voor het uitvoeren van belangrijke omzettingen met enzymen (zoals het introduceren van chirale centra: α-chirale amines met transaminases, chirale alcoholen met alcohol dehydrogenases, enz.). Onder de functionaliteiten die zich in biologisch actieve stoffen bevinden, vormen vicinale amino alcoholen de kern van verschillende natuurstoffen en actieve farmaceutische ingrediënten (zoals alkaloïden, neurotransmitters, HIV protease inhibitors, aminopeptidase inhibitor en antibiotica). In deze thesis hebben wij verschillende multi-enzymatische cascadereacties toegepast voor de synthese van gerichte optisch actieve vicinale amino alcoholen. Ons onderzoek start in **hoofdstuk 2** met het genereren van een

zelfontworpen styreen mono-oxygenase enzym (Fus-SMO). De twee units van het katalytische bi-enzymatische systeem (StyB, het reductase domein, en StyA, de epoxidatie unit) zijn genetische gefuseerd m.b.v. een dertig aminozuur lange linker. In dit hoofdstuk hebben wij de katalytische prestatie van gevriesdroogde *E*. coli cellen met Fus-SMO (die tot overexpressie is gebracht) bepaald in de asymmetrische epoxidatie van styreen **1a** in trans-β-methylstyreen **1b** (**Schema 1**). Een verdere verbetering in de praktische toepassing van dit systeem was gemaakt door Fus-SMO en Cb-FDH tot co-expressie te brengen in hetzelfde gastorganisme.

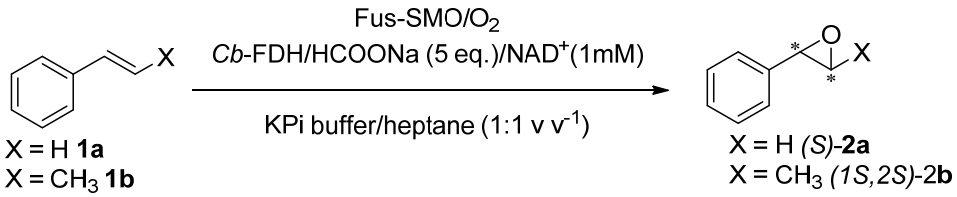

Schema 1. Cell systeem waarbij Fus-SMO en *Cb*-FDH tegelijkertijd tot expressie zijn gebracht in *E*. coli BL21 DE3 als gast organisme voor de omzetting van **1a-b** naar optisch actieve epoxides **2a-b**.

In **hoofdstuk 3** hebben we onze Fus-SMO toegepast in een een-pots cascade met stereocomplementaire epoxide hydrolases (Sp(*S*)-EH of St(*R*)-EH) voor de synthese van chirale 1,2-fenylpropaandiol isomeren **3** (**Schema 2**). Vervolgens werd de formele regio-, chemo- en stereoselectieve synthese van twee isomeren van nor(pseudo)efedrine **5** behaald m.b.v. de biokatalytische hydrogen-borrowing (HB) aminering van het alcohol; dit is een redox neutrale cascade. Optisch actieve diolen **3** werden omgezet naar de desbetreffende amino alcoholen door het combineren van geselecteerde alcohol dehydrogenases (Bs-BDHA of Ls-ADH) en een amine dehydrogenase (Ch1-AmDH) gebruikmakende van wederom een een-pots cascade (**Schema 3**).

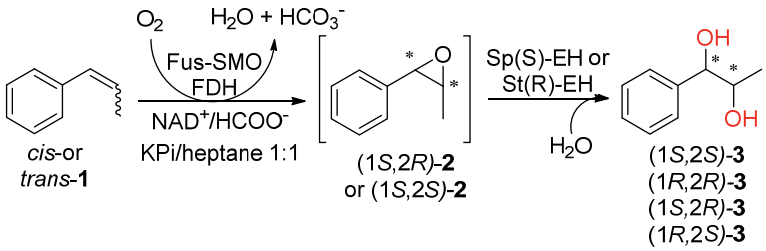

Schema 2. Een-pots multi-enzymatische cascades voor de synthese van optisch actieve diol isomeren **3** van olefine **1** d.m.v. een koppeling van Fus-SMO met twee stereocomplementaire EHs.

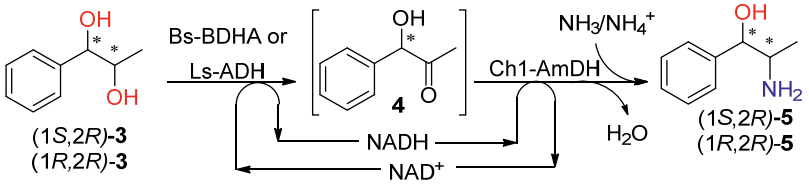

Schema 3. Formeel regio-, chemo- en stereoselectieve enzymatische synthese van twee isomeren van nor(pseudo)efedrine **5** via de HB bio-aminering cascade.

Vanwege het ontbreken van (*S*)-selectieve AmDHs, beschrijven we in **hoofdstuk 4** de enzymatische synthese van de twee andere isomeren van nor(pseudo)efedrine **5** door een combinatie van de geselecteerde ADHs met stereocomplementaire ω-transaminases (ωTAs) in een een-pots cascade voor de omzetting van chirale diolen **3**. Deze laatstgenoemde stoffen werden enzymatisch gesynthetiseerd, zoals geïllustreerd in Schema 2. Net als de HB bio-aminering, re-genereerd de redox-neutrale ADH/ωTA cascade het vereiste en geoxideerde NAD^+ co-enzym m.b.v. een alanine dehydrogenase (AlaDH). Gelijktijkig wordt het pyruvaat bijproduct terug omgezet naar alanine: de ultieme amino donor voor de transaminering (**Schema 4**).

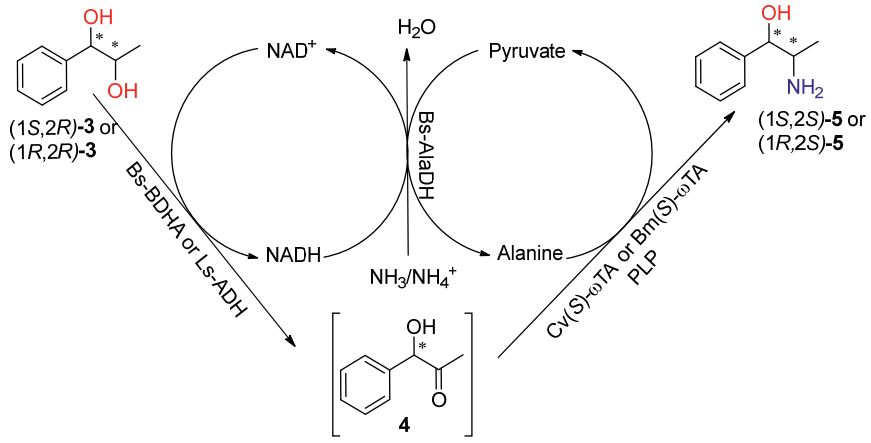

Schema 4. Een-pots cascade voor de omzetting van optisch actieve diolen **3** naar twee isomeren van nor(pseudo)efedrine **5** door een combinatie van ADH en stereocomplementaire ωTAs.

Verder zijn we in staat geweest om regio-isomeer (1*S*,2*R*)-**5'** te verkrijgen met de cascade uit **Schema 4** door een specifieke combinatie van diol substraat, ADH en ωTA te kiezen.

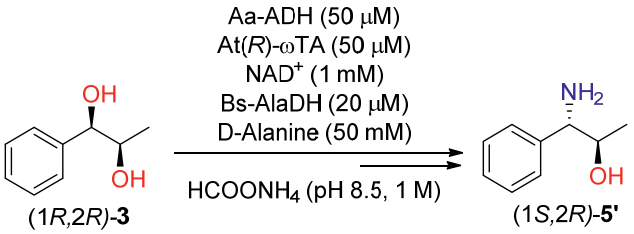

Schema 5. Een-pots cascade reacties voor het verkrijgen van een specifiek regio-isomeer van nor(pseudo)efedrine.

In **hoofdstuk 5** hebben we gebruik gemaakt van de een-pots cascade uit Schema 4 voor de synthese van fenylethanolamine isomeren **5a** (**Schema 6, boven**). Ook in dit geval zijn chirale diolen **3a** enzymatisch gesynthetiseerd m.b.v. de een-pots cascade uit Schema 2. Styreen **1a** is daar als substraat gebruikt. Daarnaast hebben we een orthogonale bio-amineringscascade ontwikkeld voor de enzymatische synthese van amino alcohol **5a'** vanuit optisch actieve diol **3a**. Hier is een alcohol oxidase (AcCO6) gekoppeld met een amine dehydrogenase (Ch1-AmDH). Het laatstgenoemde enzym vereist een orthogonaal enzymatisch systeem voor de recycling van de NADH co-enzymen (**Schema 6, onder**).

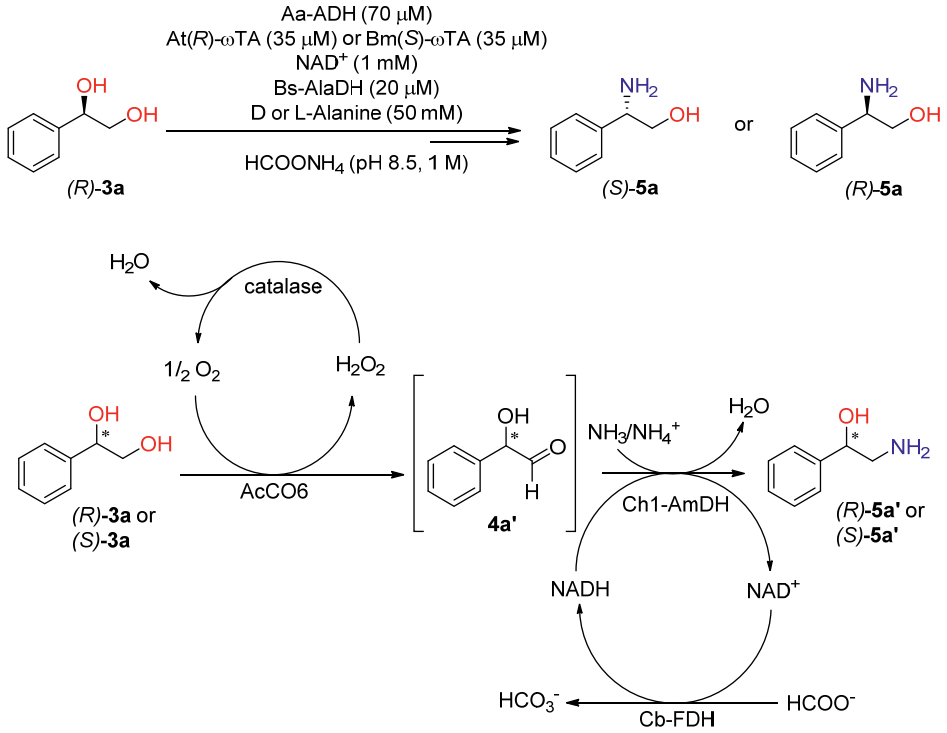

Schema 6. Een-pots cascade voor de omzetting van (*R*)-**3a** naar optisch actief (*R*)-**5a** en (*S*)-**5a** d.m.v. koppeling van geselecteerde ADHs met stereocomplementaire ωTAs (boven); orthogonale bio-amineringscascade voor de omzetting van (*R*)-**3a** en (*S*)-**3a** naar de corresponderende chirale amino alcoholen (*R*)-**5a'** en (*S*)-**5a'** respectievelijk (onder).

We hebben vervolgens besloten de multi-enzymatische cascade reacties, zoals bovenstaand beschreven, uit te breiden voor de synthese van andere waardevolle amino alcoholen (i.e., adrenaline en derivaten daarvan). **Hoofdstuk 6** behandelt een principebewijs dat als voorbeeld dient voor de hoge potentie van deze cascades. Een extra enzymatische stap was geïntroduceerd voor de biokatalytische decarboxylatie van hernieuwbare grondstoffen zoals caffeïnezuur, cumaarzuur en ferulinezuur **1b-d**, voor het verkrijgen van de corresponderende aromatische olefines **2b-d** (**Schema 7, boven**). Echter leidde de een-pots dehydroxylatiecascade uit Schema 2 niet tot de vorming van gerelateerde diolen. Mede daarom waas de synthese van substraat **2b'** voortgezet met caffeïnezuur **1b** als uitgangsstof wat leidt tot chirale diolen **4b'** (**Schema 7, midden**). Als laatste is de een-pots cascade uit Schema 4 toegepast voor de synthese van amino alcohol **6b'** (**Schema 7, onder**). Desalniettemin is er meer werk nodig aan deze cascade om de daadwerkelijke prestatie van het systeem te bepalen alsmede de stereochemie van het amino alcohol product te bepalen. Verder zullen andere tests moeten worden uitgevoerd met alle substraten die aan het begin van dit hoofdstuk zijn beschreven en zullen passende routes gevonden moeten worden om de gewenste amino alcoholen te verkrijgen (i.e., adrenaline en derivaten). De integratie van computationele biokatalyse en eiwitengineering is essentieel voor uitbreiding van de enzymatische systemen die nodig zijn voor deze cascades.

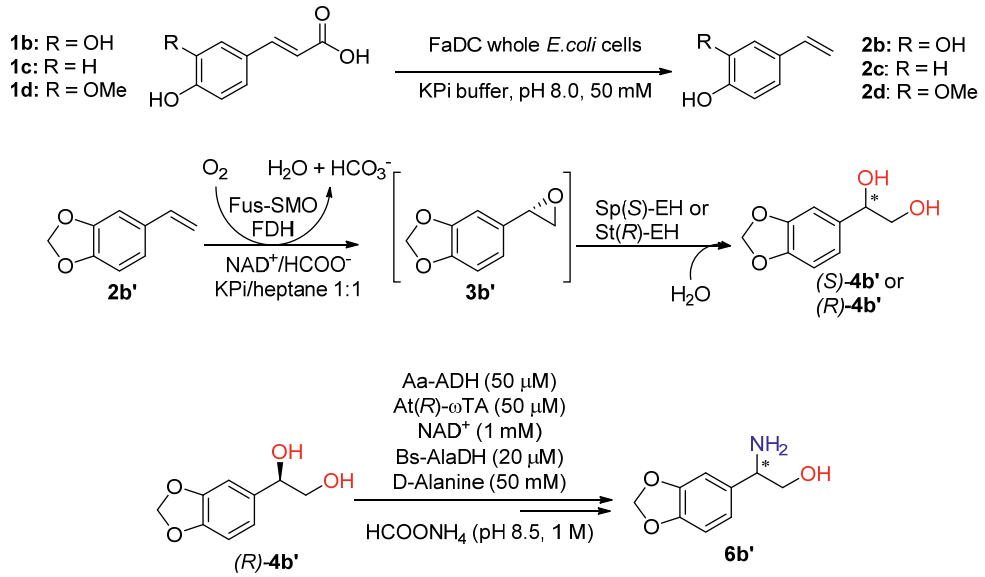

Schema 7. Voorlopige resultaten van de aanpak beschreven in hoofdstuk 6 als principebewijs voor de potentiële toepassing van de cascades voor de synthese van hoogwaardige vicinale amino alcoholen, zoals beschreven in deze thesis.

Acknowledgements

The time has come! It is an indescribable feeling to finally see the hard work of these last four years coming to an end in this thesis. It has been an intense period of my life, with a lot of challenges but many (and mostly) good moments. I have met so many people who contributed to this journey and I would like to thank you all. First of all, big thanks to my promotors and supervisors.

Francesco, I would like to thank you for giving me the opportunity to join your research group and the chance to undertake this exciting project. Your constant scientific support, together with **Tanja**, made all the hard work to be recognized with many publications. The past five years were very intense, a new group to start and new labs to be organized. But you both have succeeded to build it up and carry out high level research. Apart from science, we also had some relaxing moments. I will never forget Tanja's delicious osterjause and glühwein celebrations, with nice chats and a lot of fun. Thanks for your support and I wish you both all the best for the future.

Jan (van Maarseveen), you have been a source of inspiration! I still remember the first time I talked to you. I was a master student and you were the coordinator of my master track. Since then, I already understood the wonderful and amazing professor (and person) you are. You were my inspirational source in pursuing my academic career and yes, I am here to defend my PhD work also thanks to you and your positivity.

I would like to thank all the members of my PhD committee, **Prof. dr. H.J. Bouwmeester**, **Prof. dr. P. Timmerman**, **Prof. dr. W.J.H. van Berkel**, **Prof. dr. F. Hollmann**, **dr. M.A. Fernández Ibáñez** and **dr. J.C. Slootweg,** for their dedication in evaluating my thesis.

I wish to thank emeritus Prof. dr. **Henk Hiemstra** for his wisdom and deep knowledge. You always gave me great tips and suggestions both during my master and PhD.

Steen, **Tati**, **Chris**, thanks for the good scientific discussions during our weekly group meeting. And of course, we also enjoyed the long and the delicious Christmas lunches.

Gaston, thanks for accepting the task of being my paranymph. I knew you would be the chosen one since I started my PhD. I was your first master student (back to 2015) and since then we have never lost contacts! And I hope that this will continue.

Though in the last years we took different directions (workwise), I have so many amazing and unforgettable memories: our Friday borrels and parties with lots of drinks and singing, poker nights where nobody wanted to give up until the last chip and many other moments that of course I made sure to document with photos and videos! Good luck with the next steps in your life and scientific career.

Roel, I could not choose anybody else then you as my paranymph. Thanks for accepting this "job". We know each other since quite some years. I will never forget our chats, Friday afternoons, parties, the rides to the train station (and not only) on the back of your bike. And so many funnier moments that I will carry in my baggage with lots of pictures and videos. I wish you all the best in your scientific career and life.

Vasilis, we are so similar (culturally) but so different in personality. And this made our bond stronger. Our amazing discussions, talks, house parties and a lot of laughing will remain forever in my memory. Our daily collaboration turned in an amazing publication! I will never stop thanking you for your support during the past years. I am sure you will succeed in everything in your next career.

Jan (Vilim), my dear colleague! You have been the "jolly" of the group. Your amazing jokes will remain forever in the history! I have so many good memories of these years, nice parties and borrels but also interesting discussions, with you having always a different perspective of seeing things around us. Apart from the funny moments, we were always ready to collaborate and help each other in the lab. I wish you best of luck with your next steps.

Wesley, the dutch of the group! It took a while to set each other on the same wavelength but after that we were always ready to support each other. Though we come from a different cultural background, you have always accepted me for who I am. Thanks for being always there and I wish you all the best for your future career.

Marcelo, what to say to you. You are a special person and an excellent scientist! Thanks for all the support and constructive discussions we had together. My book cover is stunning and this is only because of you and your creativity. I hope we will stay in touch and I wish you all the best with your career.

I want also to thank previous members and students of the Biocat group. **Joseline**, it has been a pleasure to meet you. **Magda**, **Martina**, **Don**, **Sam**, **Tim**, **Sheetal,**

Sophie, thank you all for your contribution to my PhD experience. And **Gabriele**, my only and last student. Unfortunately, our lab experience lasted only 2 weeks, then the covid-19 did the rest. But these two weeks were already enough to exchange some ideas and opinions. Good luck to all of you with your future career!

I would like to thank so many people that I have met in these years, but I know it would be impossible! SOC members&Co., **Yolanda**, **Kananat**, **Simone**, **Weng-Lian**, **Luuk**, **Marissa**, **Andy**, **Vivi**, **Sergei**, **Evi**, **Piotr**, **Agnieska**, **Flip**, **Cat**, **Dieuwertije**, **Arnout,** we had delicious Christmas lunches (and parties) and interesting scientific meetings. The office neighbors, **Marta**, **Alan**, **Dorina**, **Liana**, **Noor** we had very nice and long chats, but playing "briscola" was the top! Thank you all! For sure I have learnt something from each of you and I wish you best of luck for your next steps.

My childhood friends, **Olimpia e Caterina**. We have been through so many things that a book will not be enough to describe them all. Even though we do not meet for long periods, every time we come together it's like nothing has changed. Thanks for being the special persons you are! And **Frank**, I can say we were born together and since then we never lost our bond even after I left our village (12 years ago). Thanks for being always there!

Paola, my second sister! I still remember the first time we met. You were in your last year of high school and ready to take the driving license. We have spent a lot of time together (though it is never enough) and it was amazing to hear few years ago that you were coming to Amsterdam. Also here, I have lots of memories that I will not be able to tell them all: our Easter lunch on the canal next to your house, our parties and borrels, bbq at Science Park and the cozy evenings at home. Now you are in Malta, for a new adventure and I am sure you will realize all your dreams.

Pompeo e Diana, my second family! You are always ready to support us and I will never forget all the amazing moments we had together (and many more to come). The trip to Turkey, our winter holiday, the virtual birthdays' lunches and all the trips here in the Netherlands. Grazie di essere sempre presenti.

Un grazie a **zio Michele**, **zia Mariolina** e i miei cugini **Domenico**, **Romina**, **Corrado**, **Katia**, **Antonio**, **Angelina** e tutti i piccoli cuginetti. Anche se abbiamo attraversato momenti difficili, noi siamo ancora tutti qui, come una grande e bella famiglia.

Vincenzo (Cecio), il mio fratellone! Quante cose abbiamo passato durante la nostra infanzia. Mi hai anche rotto un dente (quello davanti!) correndo nel corridoio di

casa e mi sono quasi spaccata la testa in giro in bici (tu alla guida ed io in piedi sul "sedile posteriore") al villaggio dove andavamo sempre in estate. Poi siamo diventati "grandi". Abbiamo attraversato momenti difficili ma ci siamo sempre rialzati piu' forti di prima. Anche se la distanza fa da padrone, il nostro legame rimarra' per sempre indelebile. **Francesca** la mia cognatina! Hai attraversato un periodo molto particolare ma ti sei rialzata a gran voce e 7 mesi fa hai dato alla luce il gioiello della famiglia, il mio piccolo nipotino **Alberto.** Grazie per il vostro supporto!

Francesca, la mia sorellina! Da quando sei nata sei diventata la mia bambolina di giochi preferita. Ti preparavo da mangiare (con le pentoline finte!), ti coccolavo e quando capitava ti sferravo anche qualche "pizza". Poi sei diventata un po piu grande e direi che abbiamo perso abbastanza tempo a litigare. Ora sei diventata una piccola donna, responsabile e la voglia di intraprendere nuove avventure non ti manca affatto. Ti auguro di realizzare tutti I tuoi sogni e io saro' sempre al tuo fianco. Ti voglio bene zazzolina del mio cuore.

Zia (nonna) Maria, la nostra ancora, il nostro faro! Sei la persona piu forte che conosca. Ed un pensiero al mio caro **zio (nonno) Nicola** che sono sicura sarebbe stato molto fiero ed orgoglioso di me.

Mamma e Papá, cosa farei senza di voi! Siete il mio esempio di vita. Avete superato ostacoli insormontabili e nonostante cio siete sempre andati avanti, fatti forza l'uno con l'altro per sostenere noi, i vostri figli. Non avete mai esitato nell'accettare le mie scelte e alla fine la perseverenza ha dato i suoi risultati. Non smetterò mai di ringraziarvi per tutto quello che avete fatto e continuate a fare per me. E se oggi sono qui è sicuramente anche merito vostro. Grazie di tutto e non dimenticate mai che vi voglio un bene infinito ed indescrivibile.

E te **Marco**! La persona piu importante della mia vita. Possiamo dire che siamo e stiamo crescendo insieme. Appena arrivata a Roma, da un paesino in mezzo alle montagne calabresi, sei apparso te, un timido raggio di sole. Ricordo ancora come se fosse ieri (ma in realta' sono passati ben 11 anni e 2 mesi!) il giorno in cui ci siamo parlati per la prima volta nei laboratori di chimica analitica 1. E da allora non abbiamo piu smesso di parlarci. Grazie per avermi supportato (e sopportato) in tutti questi anni e che so continuerai a fare ancora per un po! Se sono qui oggi e' anche merito tuo.

List of publications

Papers

1) **Maria L. Corrado**, Tanja Knaus and Francesco G. Mutti, A Chimeric Styrene Monooxygenase with Increased Efficiency in Asymmetric Biocatalytic Epoxidation, C*hemBioChem,* **2018,** 19 (7), 679-686 (Front Cover)

2) Vasilis Tseliou, Tanja Knaus, Marcelo F. Masman, **Maria L. Corrado** and Francesco G. Mutti, Generation of amine dehydrogenases with increased catalytic performance and substrate scope from ε-deaminating L-Lysine dehydrogenase, *Nature Communications*, **2019**, 10, 3717

3) **Maria L. Corrado**, Tanja Knaus and Francesco G. Mutti, Regio- and Stereoselective Multi-enzymatic Aminohydroxylation of β-methylstyrene using Dioxygen, Ammonia and Formate, *Green Chemistry*, **2019,** 21(23), 6246-6251

4) **Maria L. Corrado**, Tanja Knaus, Wesley Böhmer and Francesco G. Mutti, One-pot cascade for the synthesis of chiral phenylpropanolamines by pairing alcohol dehydrogenases with stereocomplementary ω-transaminases, *manuscript in preparation*.

5) **Maria L. Corrado**, Tanja Knaus, Jan Vilím and Francesco G. Mutti, Multi-enzymatic cascades for the synthesis of optically active phenylethanolamine isomers, *manuscript in preparation.*

6) Jan Vilím, Tanja Knaus, **Maria L. Corrado**, Marcelo F. Masman and Francesco G. Mutti, One pot multi-enzymatic cascade for the synthesis of nylon monomer from cyclohexanol, *manuscript in preparation*.

7) Tanja Knaus, **Maria L. Corrado** and Francesco G. Mutti, One-pot enzymatic synthesis of chiral amines by ene-reductase/imine reductase catalytic system, *manuscript in preparation*.

8) Tanja Knaus, **Maria L. Corrado**, Marcelo F. Masman and Francesco G. Mutti, Te-ADH variants for the bio-oxidation of racemic alcohols, *manuscript in preparation*.

Book Chapters

9) Vasilis Tseliou, Wesley Böhmer, **Maria L. Corrado**, Marcelo F. Masman, Tanja Knaus and Francesco G. Mutti, Asymmetric reductive amination of ketones catalysed by amine dehydrogenases, *Applied Biocatalysis: The Chemist's Enzyme Toolkit*, Wiley, **2020**, in press.

10) **Maria L. Corrado**, Vasilis Tseliou, Joseline H. Houwman, Wesley Böhmer, Jan Vilím, Marcelo F. Masman, Tanja Knaus and Francesco G. Mutti, Hydrogen-borrowing conversion of alcohols into optically active primary amines by combination of alcohol dehydrogenases and amine dehydrogenases, *Applied Biocatalysis: The Chemist's Enzyme Toolkit*, Wiley, **2020**, in press.